Titre: Title:	Seismic Response and Design of Steel Multi-Tiered Concentrically Braced Frames
Auteur: Author:	Ali Imanpour
Date:	2015
Type:	Mémoire ou thèse / Dissertation or Thesis
Référence: Citation:	Imanpour, A. (2015). Seismic Response and Design of Steel Multi-Tiered Concentrically Braced Frames [Ph.D. thesis, École Polytechnique de Montréal]. PolyPublie. https://publications.polymtl.ca/1938/

UNIVERSITÉ DE MONTRÉAL

SEISMIC RESPONSE AND DESIGN OF STEEL MULTI-TIERED CONCENTRICALLY BRACED FRAMES

ALI IMANPOUR

DÉPARTEMENT DES GÉNIES CIVIL, GÉOLOGIQUE ET DES MINES

ÉCOLE POLYTECHNIQUE DE MONTRÉAL

THÈSE PRÉSENTÉE EN VUE DE L'OBTENTION

DU DIPLÔME DE PHILOSOPHIAE DOCTOR

(GÉNIE CIVIL)

NOVEMBRE 2015

UNIVERSITÉ DE MONTRÉAL

ÉCOLE POLYTECHNIQUE DE MONTRÉAL

Cette thèse intitulée :

SEISMIC RESPONSE AND DESIGN OF STEEL MULTI-TIERED CONCENTRICALLY BRACED FRAMES

présentée par : IMANPOUR Ali

en vue de l'obtention du diplôme de : Philosophiae Doctor

a été dûment acceptée par le jury d'examen constitué de :

Mme KOBOEVIC Sanda, Ph. D., présidente

M. TREMBLAY Robert, Ph. D., membre et directeur de recherche

M. ROGERS Colin, Ph. D., membre

M. UANG Chia-Ming, Ph. D., membre

DEDICATION

Dedicated to my parents,

Sorayya Hejrati and Rostam Imanpour

ACKNOWLEDGEMENTS

I wish to gratefully thank a few of the many people who have helped me to complete this research at Polytechnique Montréal. I owe my sincere gratitude to Professor Robert Tremblay for his continuous support of my Ph.D. study. I have had the privilege to work under his brilliance for the past five years. I hope to continue our collaboration not only as colleagues but also as friends.

Besides my advisor, I would like to express my great thanks to Professor Larry Fahnestock and Professor Ali Davaran, who both guided me in my work. Rafael Sabelli, Dr. Christopher Stoakes, and Professor Dimitrios Lignos are really appreciated for their precious advices. The input from AISC Task Committee 9 – Seismic Design has had a strong influence on the development of the design method and is greatly appreciated.

Parts of the works related to the development of hybrid simulation and numerical analysis of braced frames with contribution from gravity columns were carried out in collaboration with Guillaume Toutant and Karl Auger, M.Sc. students at Polytechnique Montréal. I am very thankful for their friendship and I wish them the success in their career. Yan Jiang and Morteza Dehghani are also acknowledged for their thoughts and input throughout the numerical simulation process.

I am grateful to Dr. Andreas Schellenberg for his assistance in the development of the computational substructure for the hybrid simulation. Sincere appreciation is given to Martin Leclerc and Romain Siguier at the Structural Engineering Laboratory of Polytechnique Montréal for their assistance and patience in the development of hybrid testing. Also, the help of the undergraduate students working at the laboratory is thanked.

I wish to thank the external jury, Professor Chia-Ming Uang from the University of California at San Diego, Professor Colin Rogers from McGill University, and Professor Sanda Koboevic from Polytechnique Montréal to have read and evaluated this Ph.D. dissertation.

The financial support provided by the Natural Sciences and Engineering Research Council of Canada (NSERC) is acknowledged.

Finally, I would like to express my deepest gratitude to my wife, Yasaman, for her continued support for the past five years. She has always been an inspiration to me to pursue my goals. I wish to thank my sister, Sara, who has always supported me during difficult times of my life.

RÉSUMÉ

Les contreventements concentriques en treillis à multiples segments (CCMS) sont des contreventements constitués de diagonales formant deux ou plusieurs panneaux qui sont superposés sur la hauteur du contreventement. Les CCMS sont couramment utilisés en Amérique du Nord afin d'offrir une résistance latérale pour les bâtiments d'un seul étage de grande hauteur, comme les bâtiments industriels, les installations sportives, les centres de congrès ou les hangars d'avion. Dans ces structures, la configuration CCMS est préférable puisque l'utilisation de diagonales de contreventement simples partant des fondations jusqu'au niveau du toit n'est plus pratique. Dans les CCMS, la longueur et la taille des diagonales sont réduites de manière significative, ce qui est favorable pour rencontrer les limites d'élancement prescrites dans les normes parasismiques. De plus, les colonnes peuvent être considérées comme contreventées latéralement dans le plan du cadre à niveau intermédiaire entre deux panneaux, ce qui contribue également à réduire la taille des poteaux et la quantité requise d'acier. Les colonnes de gravité adjacentes qui sont situées dans le même plan qu'un CCMS peuvent aussi être considérées comme contreventées latéralement en ajoutant des membrures horizontales aux niveaux intermédiaires entre les panneaux. Dans les CCMS, les colonnes sont en général des sections en W orientées de telle sorte que la flexion hors-plan se produise selon l'axe fort de la colonne, permettant ainsi à la colonne de résister au flambement hors plan sur toute la hauteur du cadre.

Des exigences et des règles de calcul spéciales en matière de conception parasismique ont été introduites pour les CCMS dans l'édition 2009 de la norme CSA S16 pour la conception des structures ne acier au Canada. Ces exigences comprennent la vérification de la résistance des poteaux sous des moments de flexion dans le plan et hors du plan du contreventement en supposant que les déformations élastiques sont concentrées dans un seul panneau. On exige également de placer des barres horizontales entre chaque panneau. Toutefois, aucune disposition n'est spécifiée pour la conception parasismique des cadres CCMS dans les normes parasismiques de l'AISC aux États-Unis.

Le premier objectif poursuivi dans cette étude était d'examiner la réponse sismique des contreventements CCMS conçus en conformité avec les normes CSA S16 et les dispositions parasismiques de l'AISC. Pour les applications canadiennes, l'évaluation de la réponse sismique a été réalisée afin d'évaluer l'adéquation des exigences spéciales de conception spécifiées pour les

CCMS dans la norme CSA S16-09 et de vérifier si une amélioration des dispositions de conception était nécessaire. Sur la base de ces travaux, les règles ont été ajustées dans la norme CSA S16-14, permettant d'élargir l'utilisation des contreventements de type CCMS et de réduire les moments de flexion hors-plan dans les poteaux. Pour les contreventements conçus à l'aide des normes de conception des États-Unis, l'évaluation parasismique visait à vérifier la nécessité d'introduire de nouvelles dispositions de conception parasismique pour les CCMS. Le second objectif de cette étude consistait à développer et présenter une stratégie de conception parasismique améliorée compatible avec les normes nord-américaines existantes.

Pour les États-Unis, une série de contreventements en acier avec diagonales disposées en X a été conçue selon les dispositions et les normes parasismiques courantes de l'AISC. La réponse sismique de quelques cadres prototypes, simulés aen utilisant des éléments de fibres dans le logiciel *OpenSees*, a été validée à l'aide de modèle d'éléments finis 3D. Une attention particulière a été accordée au flambement des colonnes. Des analyses dynamiques non-linéaires ont ensuite été réalisées pour étudier un large éventail de CCMS conçus selon les dispositions pour les contreventements concentriques spéciaux (*SCBFs*). Les résultats des analyses ont montré que les déformations inélastiques dans les diagonales ont tendance à se concentrer à l'étage présentant une résistance au cisaillement relativement plus faible, et qu'une forte demande de flexion en plan est induite dans les colonnes. En outre, il a été montré que la plastification en flexion et l'instabilité de la colonne causée par une distribution non-uniforme des déformations latérales des panneaux peuvent affecter la réponse des contreventements sous un chargement sismique. Des stratégies de conception alternatives telles que l'utilisation de diagonales confinées ductiles dans les CCMS au lieu des diagonales classiques, et la contribution des colonnes gravitaires dans la résistance aux moments de flexion sismiques imposés sur les colonnes du CCMS ont été introduites et leur adéquation a été examiné en utilisant des analyses temporelles non-linéaires de structures prototypes. Pour la contribution des poteaux de gravité, différentes approches de conception parasismique ont été proposées dans le cadre des normes parasismiques AISC pour concevoir le cadre et les colonnes gravitaires. Pour les contreventements concentriques en acier, une analyse sismique et une procédure de dimensionnement a été proposée qui permet de déterminer les moments de flexion dans les colonnes résultant d'une distribution inégale des déformations inélastiques dans les diagonales sur la hauteur du bâtiment et de vérifier les poteaux en considérant l'action combinée des efforts axiaux et de flexion. Différentes analyses et

méthodes de conception, qui sont destinés à être mis en œuvre dans le cadre des normes parasismiques AISC, ont été introduites pour répondre aux exigences proposées. Les méthodes ont été validées pour les cadres prototypes en comparant la sollicitation sismique considérée dans la conception à celle obtenue à partir des analyses dynamiques non-linéaires. Il a été montré que la demande sismique dans le plan de flexion des colonnes peut être très bien prédite dans la phase de conception.

L'évaluation de la réponse sismique des cadres conçus à l'aide de la norme canadienne révisée CSA S16-14 a été réalisée en étudiant la réponse sismique non-linéaire de contreventements CCMS de 3 et 5 panneaux des catégories MD et LD, respectivement. L'analyse a montré que les moments de flexion dans le plan des colonnes du CCMS est abordée de façon réaliste par les exigences courantes de la norme CSA S16. La recherche a permis de proposer une méthode permettant de prédire les moments de flexion et les déplacements pour des contreventements ayant un nombre de panneaux plus grand que les limites de la norme CSA S16-14. La méthode permet de tenir compte de la propagation des déformations inélastiques sur la hauteur de la structure, une hypothèse plus réaliste pour ces contreventements. La méthode proposée a été illustrée et validée au moyen d'analyses dynamiques non linéaires pour un contreventement de Type MD ayant 5 panneaux.

Une étude préliminaire a été réalisée pour répondre à certains des défis attendus dans la réalisation d'une simulation hybride prévu pour être réalisée à l'aide du système à 6 degrés de liberté situé au laboratoire de structures de Polytechnique Montréal. La simulation hybride vise à étudier la stabilité de colonnes de profilé W en acier, dans des cadres CBFs ou CCMS, soumis à des efforts combinés de compression axiale et de moment de flexion dans l'axe faible ou des moments de flexion bi-axiale.

ABSTRACT

Steel multi-tiered braced frames (MT-BFs) are commonly used in North America to provide lateral resistance for tall single storey buildings such as industrial buildings, sport facilities, convention centers, or airplane hangars. In these structures, MT-BF configuration is preferable, as the use of single bracing members extending from the foundation to the roof level is no longer practical. MT-BFs consist of tall steel braced frames built with multiple bracing panels stacked over the height of the frame. In MT-BFs, brace lengths and sizes are reduced significantly, which is favourable to satisfy the slenderness limits specified in the seismic provisions. Additionally, the columns can be considered as laterally braced in the plane of the frame at every tier point, which also contributes to reducing the steel tonnage. Adjacent gravity columns located along MT-BF lines can similarly be laterally braced by adding horizontal struts at tier levels. In MT-BFs, columns are typically I-shaped members oriented such that strong axis bending develops out-of-plane, so the column can resist out-of-plane buckling over the full building height.

Special seismic design requirements have been introduced for MT-BFs in the Canadian steel standard (CSA S16). These requirements include column in-plane and out-of-plane demands and the need to place struts between tiers. However, as of now, there is no seismic design provision available in the AISC Seismic Provisions for this framing configuration.

The first objective pursued in this study was to examine the seismic response of the MT-BFs designed in accordance with the CSA S16 design standard for steel structures and 2010 AISC Seismic Provisions for Structural Steel Buildings. For Canadian applications, a seismic response evaluation was performed to assess the adequacy of the 2009 design requirements specified for MT-BFs and to verify whether improved design provisions were required. The 2014 CSA S16 provisions were adjusted on the basis of these studies, allowing a wider range of frames where MT-BFs can be used and reducing out-of-plane design moments in columns. For the frames designed based on U.S. design standards, the seismic evaluation aimed at verifying the necessity of introducing new seismic design requirements for MT-BFs. The second objective of this study was to develop and present an enhanced seismic design strategy that is consistent with the current North American design provisions. A hybrid test program was also developed for MT-BF columns using the Multi-Directional Hybrid Testing System (MDHTS) at Polytechnique Montréal.

A series of X-braced frames was designed according to the 2010 AISC Seismic Provisions. The seismic response of the prototype frames, simulated using fiber elements in the *OpenSees* program, was validated against the 3D finite element model. Special attention was paid to the buckling response of the columns. Then, nonlinear dynamic analyses were performed to study a wide range of MT-BFs designed with the special concentrically bracing system. The results of the analyses showed that inelastic brace deformations tend to concentrate in the tier(s) exhibiting relatively lower storey shear resistance, which induce excessive drift in these weaker tier(s) and increase the potential for low-cycle fatigue fracture of the bracing members. Also, high in-plane bending demands are induced in the columns due to non-uniform tier drift demand, which cause flexural yielding and column instability under seismic loading. For two-tiered steel concentrically braced frames, a seismic analysis and design procedure was proposed in which the in-plane flexural demands of the columns resulting from uneven distribution of brace inelastic deformations over the frame height are determined and the columns are designed to resist the combined axial loads and the in-plane flexural moments. Alternative design strategies such as using buckling restrained bracing members and mobilizing gravity columns in the resistance of seismic in-plane bending moments imposed on the MT-BF columns were introduced, and their adequacy was verified using a nonlinear response history analysis of prototype structures. For the latter, three design approaches were proposed in the framework of the AISC Seismic Provisions to design the braced frame and gravity columns. Two analysis procedures, a sub-structuring technique and a stiffness analysis method, consistent with the AISC Seismic Provisions, were proposed for the design of MT-BFs with three or more tiers for in-plane seismic demand. The methods are used to determine the seismic induced in-plane bending demands of columns as well as tier drifts. The columns are then sized with sufficient strength and stiffness to avoid column buckling and excessive drift in tiers. The methods have been validated for prototype frames by comparing the seismic demand considered in design to that obtained from nonlinear dynamic analysis. It was shown that the seismic in-plane bending demand of the columns could be very well predicted using the proposed methods.

A seismic response evaluation of the frames designed based on the Canadian standard was performed by studying the nonlinear seismic response of a series of 3- and 5-tiered X-braced frames respectively of the moderate and limited ductility categories. An analysis method was proposed to apply the revised seismic design requirements specified in CSA S16-14. The results

of nonlinear time history analyses showed that the in-plane flexural seismic bending demand on MT-BF columns can be properly predicted by the CSA S16-14 requirements. A design method was also proposed, in the framework of CSA S16, for frames exceeding CSA S16 limits on the number of tiers. This method accounts for the distribution of the seismic inelastic demand between tiers. The application of the proposed method was demonstrated for a 5-tiered Type MD concentrically braced frame and validated using nonlinear dynamic analysis.

A hybrid test program was developed for MT-BF columns using the new Multi-Directional Hybrid Testing System (MDHTS) at the Structural Engineering Laboratory at Polytechnique Montréal. Additionally a preliminary study was performed to verify the MDHTS and to compensate for the frictional force in the hybrid simulation. The hybrid simulation aims at studying the stability of steel W-shape columns, as part of steel MT-BFs, subjected to combined axial compression forces and weak axis or biaxial bending moments.

TABLE OF CONTENTS

LIST OF TABLES

LIST OF FIGURES

LIST OF SYMBOLS AND ABBREVIATIONS

Symbols

A	Column cross-sectional area
A_g	Brace cross-sectional area
B_1	Multiplier for P-δ effects (AISC 360)
b	Width of flange
C_d	Deflection amplification factor (ASCE 7)
C_{exp}	Brace expected strength in compression (AISC 341)
C'_{exp}	Brace expected post-buckling strength (AISC 341)
C_m	Equivalent moment coefficient (AISC 360)
C_r	Compressive resistance of a member (CSA S16)
C_s	Seismic response coefficient (ASCE 7)
C_u	Probable brace resistance in compression (CSA S16); coefficient for upper limit on calculated period (ASCE 7)
C'_u	Probable brace post-buckling resistance (CSA S16)
d	Depth of the section
F_a	Acceleration-based site coefficient
F_{cr}	Column inelastic buckling stress (AISC 360)
F_e	Column elastic buckling stress (AISC 360)
F_{cre}	Inelastic buckling stress for brace flexural buckling using expected yield strength (AISC 360)
F_v	Velocity-based site coefficient
F_y	Yielding stress of steel
h	Height of column or frame; distance between flanges less the corner radius

h_n	Frame total height
I_E	Earthquake importance factor of the structure (NBCC)
I_e	Importance factor of the structure (ASCE 7)
K	Effective length of column
Kl	Effective length
Kl/r	Effective slenderness ratio or Brace slenderness limit
M_c	Column seismic induced in-plane flexural bending moment
M_{ny}	Column weak-axis nominal flexural strength
M_{pbr}	Brace flexural strength
M_{uy}	Column weak-axis required flexural strength
M_v	Higher mode effect factor
M_1	The smaller moment at the end of the column segment in each tier calculated from a first-order analysis (AISC 360)
M_2	The larger moment at the end of the column segment in each tier calculated from a first-order analysis (AISC 360)
P	Column axial force
P_{e1}	Column elastic buckling strength in the plane of bending (AISC 360)
P_n	Column nominal compressive strength
P_u	Column required axial strength, or brace required axial strength
P_y	Column nominal axial yield strength
R	Response modification factor (ASCE 7)
r	Radius of gyration
R_d	Ductility related force modification factor (NBCC)
R_o	Overstrength-related force modification factor (NBCC)
S_{DS}	Design spectral response acceleration parameter for short periods (ASCE 7)

S_{D1}	Design spectral response acceleration parameter at 1 s (ASCE 7)
S_{MS}	MCE_R spectral response acceleration parameter for short periods (ASCE 7)
S_{M1}	MCE_R spectral response acceleration parameter at 1 s (ASCE 7)
$S(T_a)$	5% damped spectral response acceleration (NBCC)
T_{exp}	Brace expected strength in tension (AISC 341)
T_a	Fundamental lateral period of vibration of the structure; approximate fundamental period
t_f	Thickness of the flange
T_u	Probable brace resistance in tension (CSA S16)
t_w	Thickness of the web
U_{1y}	Factor to account for moment gradient and for second-order effects of axial force acting on the deformed member (CSA S16)
V	Design Storey shear
V_c	Column shear force
W	Seismic weight
Z	Plastic section modulus of the column
β	Coefficient for bending in beam-columns
λ	Slenderness parameter
ν	Column lateral deflection at its mid-height
φ	Resistance factor

Abbreviations

3D	3-Dimensional
AISC	American Institute of Steel Construction
ASCE	American Society of Civil Engineers

BFCs	Braced Frame Columns
BFs	Braced frames
BRBF	Buckling restraint braced frames
CBFs	Concentrically braced frames
CHS	Circular Hollow Section
CSA	Canadian Standards Association
DAQ	Data acquisition system
DBE	Design basis earthquake
EBFs	Eccentrically braced frames
GCs	Gravity columns
HCC	Hydraulic control and configuration
HSS	Hollow Square Section
LD	Limited ductility
MD	Moderately ductile
OCBF	Ordinary concentrically braced frames
MCE_R	Maximum considered earthquake
MDHTS	Multi-Direction Hybrid Testing System
MPa	Mega Pascal
MRFs	Moment resisting frames
MT-BFs	Multi-tiered braced frames
MT-BRBFs	Multi-tiered buckling restraint braced frames
MT-CBFs	Multi-tiered concentrically braced frames
MT-OCBFs	Multi-tiered ordinary concentrically braced frames
MT-SCBFs	Multi-tiered special concentrically braced frames

NBCC	National Building Code of Canada
NLRH	Nonlinear response history
OpenFresco	Open framework for experimental setup and control
OpenSees	Open system for earthquake engineering simulation
RHS	Right Hand Side; Rectangular Hollow Section
SCBF	Special concentrically braced frames
SDC	Seismic Design Category
SDOF	Single-Degree-Of-Freedom
SMF	Special moment frame
UHS	Uniform hazard spectrum

LIST OF APPENDICES

CHAPTER 1 INTRODUCTION

1.1 Background

Tall single-storey steel buildings are commonly used in North America for the purpose of commercial, sport and industrial facilities. Concentrically braced frames (CBFs) are very effective for providing lateral resistance to these buildings. Multi-tier bracing configuration with two or more bracing tiers is commonly used in building applications that require tall open spaces, when long single bracing members extending from the foundations to the roof level are no longer practical. Figure 1.1 shows four examples of multi-tiered braced frames (MT-BFs) with various ranges of height and number of tiers. Compared to one continuous bracing from the ground to the roof level, the application of an MT-BF arrangement generally leads to an economical design. In MT-BF configuration, brace sizes can be significantly reduced, which leads to easily satisfying the stringent cross-section and overall member slenderness limitation for seismic applications. Furthermore, as required by seismic design provisions, beams and columns of CBFs must be designed for the forces that develop upon brace yielding and buckling. Smaller bracing members as typically required in MT-BFs may result in smaller beams, columns and connections and, therefore, reduce the overall costs of the structure.

In MT-BFs, columns can be considered as laterally braced in the plane of the frame at every tier point, which also contributes to reducing the steel tonnage. Adjacent gravity columns located in the exterior wall of the building can similarly be laterally braced by adding horizontal struts at the tier levels (Figure 1.1b).

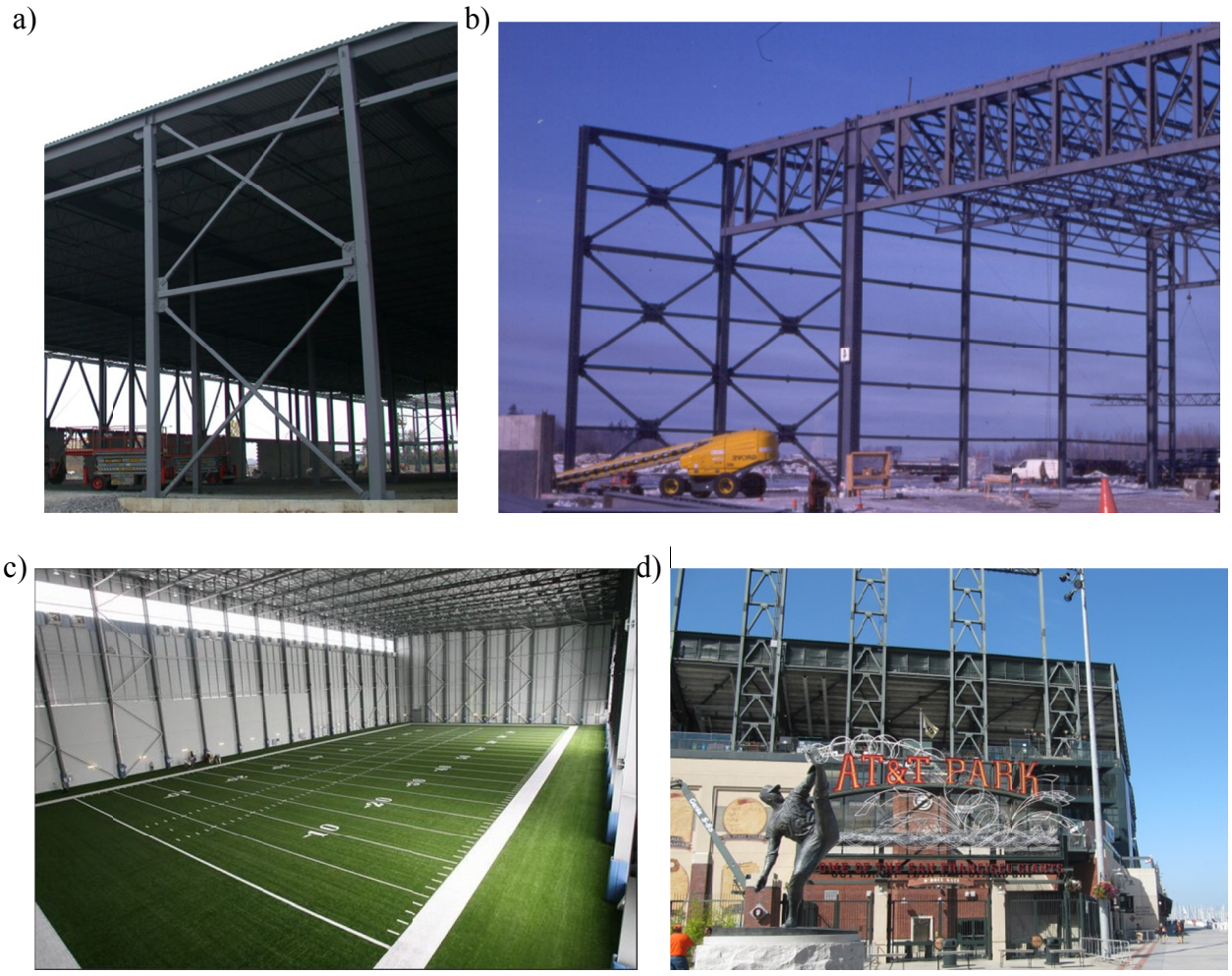

Figure 1.1: a) 2-tiered CBF in a medium-rise building; b) 3-tiered CBF in a tall single-storey steel building; c) 5-tiered Buckling Restraint Braced Frame (BRBF), Seahawks indoor practice facility, Seattle, WA (https://www.google.ca); and d) 8-tiered chevron-braced frame, AT&T Park sport center, San Francisco, CA (https://anotherheader.wordpress.com/2010/05/06/att-park/).

Multi-tiered bracing can be designed with X-, chevron, V- or single diagonal bracing panels. Bracing tiers are typically chosen to be uniform over the frame height, but project-specific constraints may require different tier heights and different bracing arrangements along the frame height. For seismic applications, struts are typically provided at tier levels to resist the unbalanced brace loads that can develop at the tier points without imposing unbalanced lateral loads on the columns; these loads are induced in the struts due to the difference between tension and compression brace forces after the compression braces have buckled. The presence of struts

allows the transfer of the unbalanced brace forces down to the foundations by truss action in the braced frame, rather than by flexure of the columns as is the case in K-type braced frames (Figure 1.2). Additionally, struts may be employed to install the wall cladding for the frames located in the exterior wall of the building. Braces and struts can be made from a variety of shapes including angles, pipes, tubes or I-shapes. Columns are typically I-shaped members oriented such that strong axis bending develops out-of-plane so that the column can resist out-of-plane buckling over the full building height. This column orientation is also preferred for MT-BF columns subjected to out-of-plane flexure resulting from wind loading, crane loading, and/or moment frames spanning perpendicular to the braced frame plane.

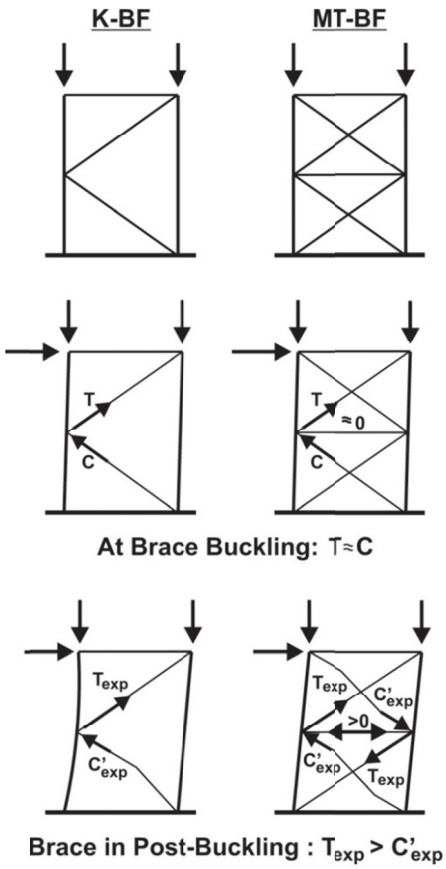

Figure 1.2: Seismic induced brace forces in K-type braced frames and multi-tiered braced frames with struts.

In view of the above, MT-BFs feature two main aspects that result in a markedly different behaviours when compared to multi-storey braced frames. First, MT-BF columns lack out-of-plane

support at the tier levels, whereas multi-storey braced frames do have out-of- plane support at the floor levels. Second, MT-BFs are single-degree-of-freedom systems and do not develop inertial forces at the tier levels, so all inelastic force redistribution must happen within the braced frame. In contrast, multi-storey braced frames develop inertial forces at the floor levels, which can help equilibrate unbalanced horizontal forces that develop after brace buckling and yielding. These differences between multi-tiered and multi-storey braced frames raise concerns regarding the application of the current seismic design procedures developed for single bracing panels between adjacent levels to braced frames with multiple bracing panels stacked between floors. Thus, the questions that must be addressed are how - and to what extent - does the seismic response of MT-BFs differ from standard multi-storey CBFs? Is there a need for special requirements to analyze and design MT-BFs under seismic loading?

Under seismic ground motions, inelastic response may not distribute evenly along the MT-BF height, leading to variations in tier drifts. The reason for this behaviour is that brace buckling in compression is likely to occur first in one of the tiers due to unavoidable inherent differences in brace boundary conditions, brace out-of-straightness, and material properties. Due to the softening response following brace buckling, further frame lateral deformations then tend to concentrate in that same critical tier. Brace tension yielding develops in the critical tier, which leads to plastic elongation of the braces in that tier, even after brace buckling has occurred in the other tiers. This response induces in-plane flexural demand on the columns that may compromise the stability of the columns. Furthermore, drift concentration may impose excessive ductility demand on braces, which can cause brace premature low-cycle fatigue fracture.

No experimental data is available on the seismic response of MT-BFs to verify the concerns mentioned above. However, a full-scale experimental program performed by Uriz (2005) on a 2-storey chevron braced frame with identical storeys represents the conditions of a 2-tiered CBF because the lateral displacement is applied at the roof level only. Figure 1.3 shows the test specimen loaded in the second storey beam level. The results of this study confirmed the concerns raised for MT-BFs as the frame inelastic deformations concentrated in the lower level (Figure 1.4), which imposed flexural demands on the columns. Figure 1.5 shows the hysteresis loops for the frame and the first storey. The complete fracture of braces was observed in the first storey due to the concentration of the damage in this storey as the lateral load was applied. The maximum storey drift that developed in the lower storey before brace fracture is 2.5%, which corresponds to 1.3%

storey drift. The full-scale experimental observations and results verify the non-uniformity of the lateral response and its possible consequences on the seismic performance of MT-BFs.

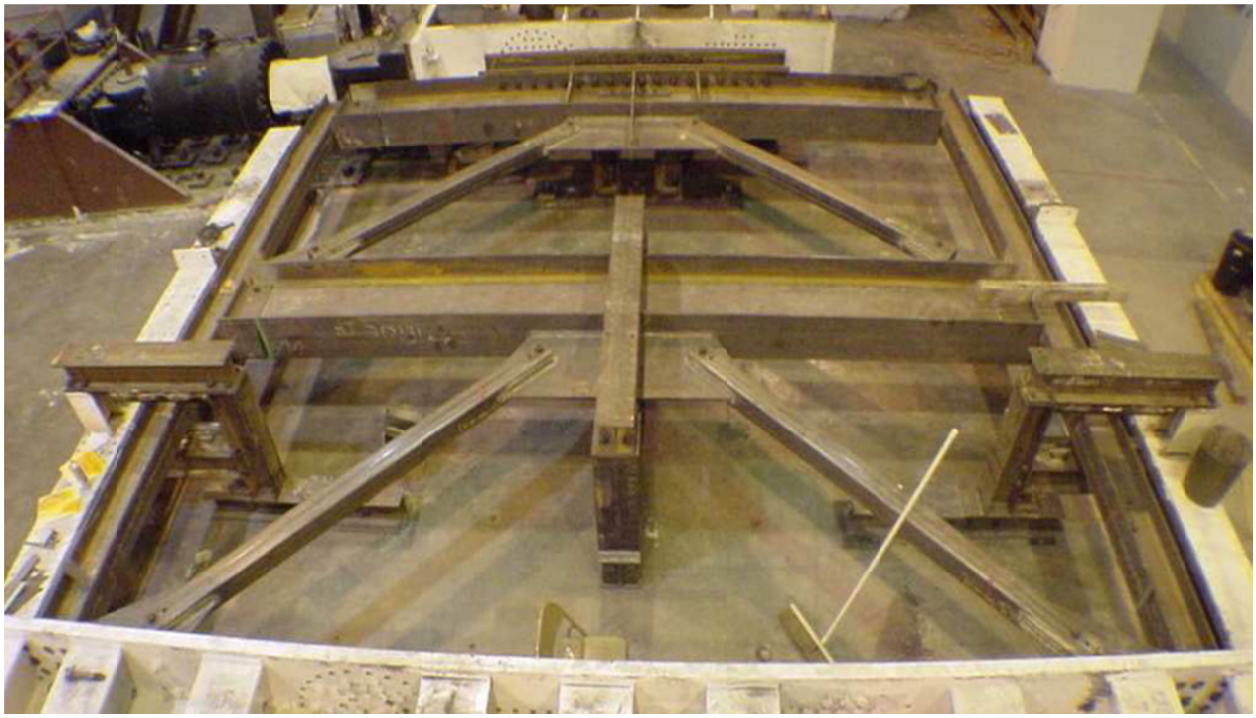

Figure 1.3: 2-storey chevron braced frame specimen (Uriz 2005).

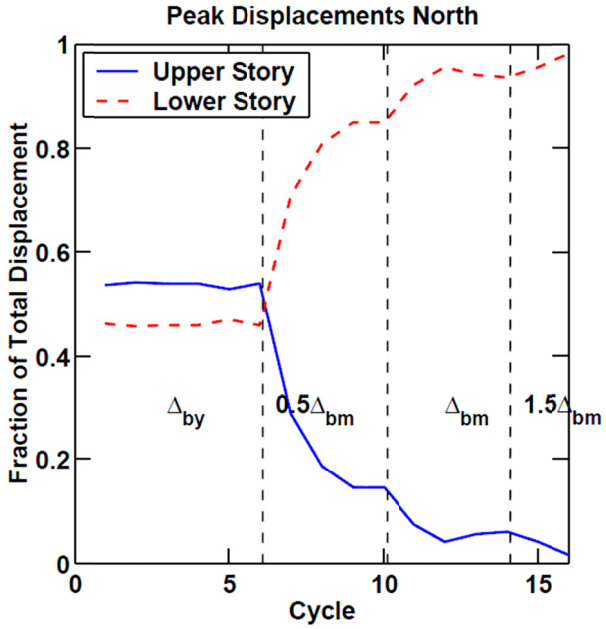

Figure 1.4: Concentration of drift in the first storey of the 2-storey chevron braced frame (Uriz 2005).

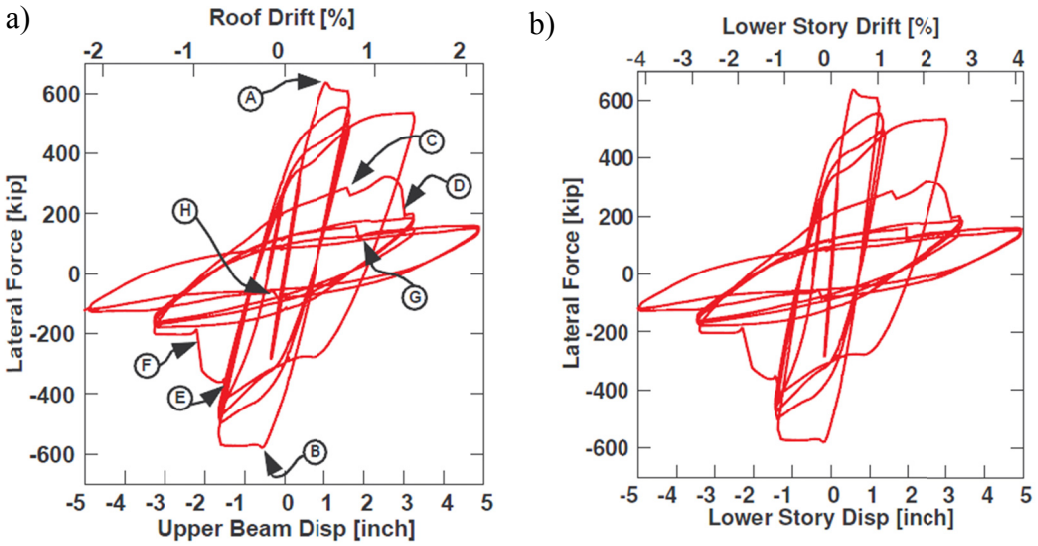

Figure 1.5: Hysteretic of displacement vs. base shear for the a) 2-storey frame; and b) First storey (Uriz 2005).

In 2009, special provisions for the seismic design of MT-BFs were introduced for the first time in the CSA S16 Canadian steel design standard (CSA 2009). In these provisions, horizontal struts must be provided between each tier to prevent a K-braced frame response shown in Figure 1.2. Column axial forces and in-plane bending moments must be determined for the brace loading scenarios where brace tension yielding and brace significant buckling concentrate in any one of the tiers when the design storey drift is reached. In the remaining tiers, the compression braces have reached their buckling strength but the tension braces have not yielded. Notional out-of-plane transverse loads equal to 10% of the compression load carried by the members meeting at the brace-to-column intersecting points must be applied at these points. These loads account for the out-of-plane forces and deformations that may develop in MT-BF columns, such as the demands due to brace buckling and hinge forming in brace gusset plates. In CSA S16-09, MT-BFs were limited to Type LD (Limited Ductility) braced frames (CBFs designed with a ductility-related force modification factor $R_d = 2.0$) to limit the inelastic deformation demand on the bracing members.

At the beginning of this project, numerical investigations were performed to evaluate the seismic response of the MT-BFs designed in accordance with the requirements of CSA S16-09 (Imanpour et al. 2012a; Imanpour and Tremblay 2012; Imanpour et al. 2012b). The results verified that brace yielding essentially concentrates in one tier along the frame height, which

induces in-plane flexural demands on the columns of the braced frame. The study also included Type MD (Moderately Ductile) and Type LD (Limited Ductility) MT-BFs. It was found that the in-plane bending moments in Type LD frames are lower than those observed in ductile frames. The performance of Type MD MT-BFs was also adequate for frames with a limited number of tiers. The results of the numerical studies confirmed that column in-plane bending demands can be appropriately predicted by the S16 requirements. The out-of-plane flexural demand was significantly lower than specified in CSA S16-09. Changes were introduced in the 2014 edition of CSA S16 (CSA S16-14) to reflect these findings. For Type LD braced frames, the limitation on the number of tiers was introduced, which limited the bracing panels to five. Type MD MT-BFs were also allowed to be used for frames up to three tiers. Moreover, the notional out-of-plane transverse loads for the columns were reduced to 2% of the factored axial compression load in the columns below the brace-to-column intersecting points.

In contrast, seismic design provisions for MT-BFs are not available in the U.S. design standards for steel structures. In the 2010 AISC Seismic Provisions for Structural Steel Buildings (AISC 2010a), this configuration is assigned to the K-type braced frame category and is therefore prohibited for the OCBF (ordinary concentrically braced frame) and SCBF (special concentrically braced frame) systems. However, Chapter 15 of ASCE 7-10 (ASCE 2010) allows engineers to design MT-BFs as non-building structures. According to Table 15.4-1 of ASCE 7-10, no seismic design requirement is required for ordinary CBFs designed with a response modification factor, $R = 1.5$, and deflection amplification factor, $C_d = 1.5$. No height limit is specified for this type of CBF and only the requirements of the AISC 360-10 Specifications (AISC 2010b) must be followed. This means that the MT-BF configuration is permitted only when a very limited seismic ductility demand is expected. Thus, considering the wide use of MT-BF configuration in sport facilities, convention centers, or industrial plants (Figure 1.1), engineers have a limited choice of lateral load resisting systems for such buildings in the U.S. Additionally, since more ductile braced frame systems are allowed in the U.S. design standards and design seismic load is defined based on the design basis earthquake (DBE) with a 10% probability of exceedance in 50 years, it was expected that the seismic demands on MT-BFs designed in accordance with the U.S. standards would be more pronounced compared to the Canadian applications. It was therefore believed that similar design requirements would be needed for MT-BFs in the U.S.

MT-BF columns are subjected to combined axial compression and flexural bending demands that can lead to column buckling. Tests performed by Newell and Uang (2006) on stocky square columns with a low width-to-thickness ratio showed that the columns could maintain axial strength for large inelastic drift demands without experiencing any global buckling. However, no such tests had been conducted on deep slender columns as used in MT-BFs. Therefore, there was a need to perform large-scale physical tests on these columns. A new Multi-Direction Hybrid Testing System (MDHTS) recently installed at Structural Laboratory of Polytechnique Montréal can be used to perform hybrid simulation of MT-BFs. In this testing, a steel column part of an MT-BF is experimentally tested in the laboratory whereas the rest of the frame is simulated using the *OpenSees* program (McKenna and Fenves 2004). The hybrid simulation is an appropriate testing method for this application, as the columns in MT-BFs are prone to instability, which may lead to frame collapse. The MDHTS (Figure 1.6) is capable of applying any combination of forces and deformations along six degrees-of-freedoms to full scale column specimens.

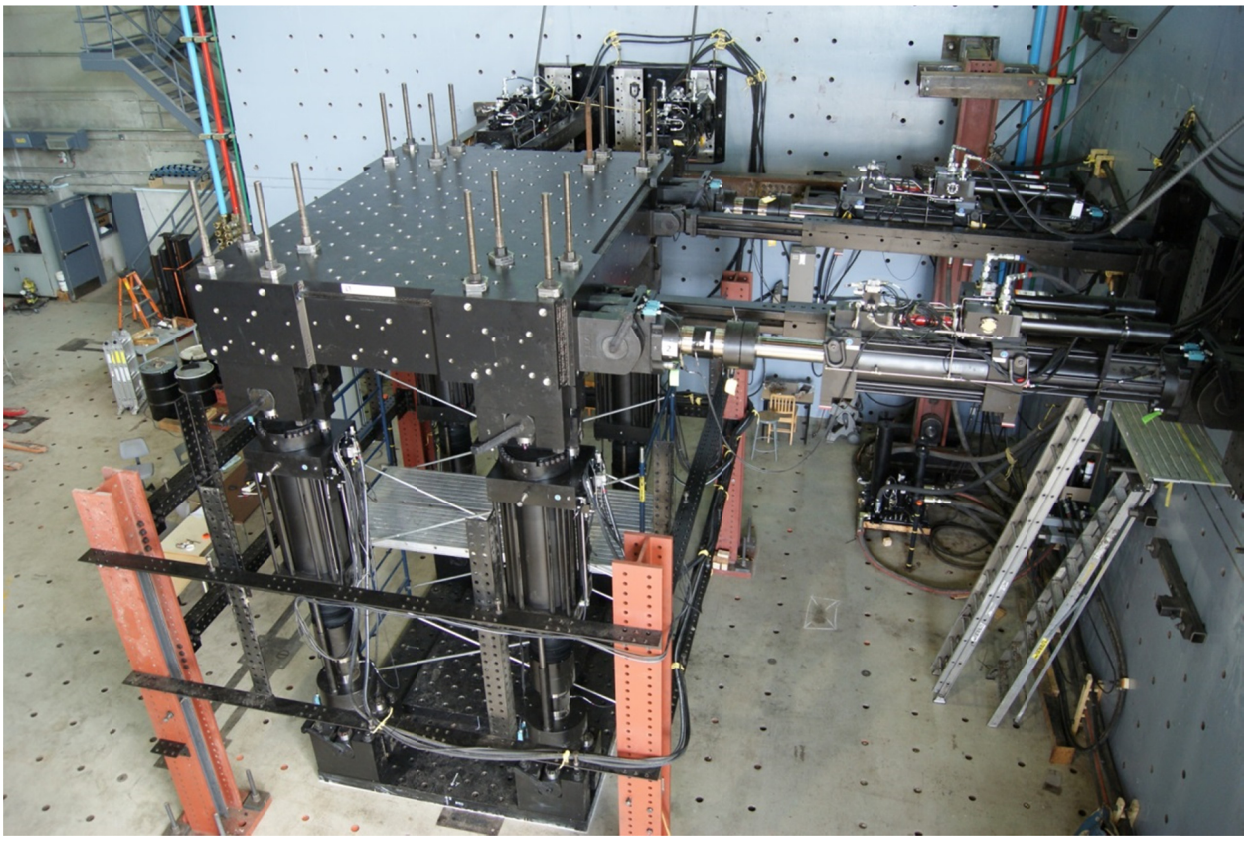

Figure 1.6: Multi-Directional Hybrid Testing System at Polytechnique Montréal.

1.2 Objectives

This PhD thesis aimed to: 1) assess the seismic response of steel multi-tiered braced frames, and 2) develop analysis and seismic design methods to achieve safe and economical MT-BF designs in North America. The study was limited to single-storey buildings with steel braced frames. The objectives can be detailed as follows:

- Since the seismic response of the MT-BFs had not been studied extensively and several concerns had been raised by engineering communities in the U.S. and Canada regarding the application of this framing configuration in seismic areas, the first objective of the research was to develop a better understanding of the seismic behaviour of MT-BFs by studying the distribution of inelastic demands along the height of frame as well as in-plane and out-of-plane flexural bending demands on columns. The influence of various parameters including frame geometry (height, number of tiers, relative tier heights), seismic region and design standards (the U.S. and Canada), braced frame systems (CBFs and BRBFs for the U.S. and CBFs for Canada), design seismic load (Response modification factor, R, for the U.S. and Ductility related factor, R_d for Canada) had to be considered.
- The second objective of this research was to propose analysis and design methods to predict the in-plane flexural demands on columns and tier drift distributions along the frame height. The methods had to be suited to the two design environments in Canada and the U.S. and take into consideration the expected differences in demand and design guidelines. For the U.S. applications, the method had to cover frames with small and large number of tiers and consistent with the analysis cases for SCBFs implicit in the 2010 AISC Seismic Provisions. For the Canadian applications, however, the 2009 special design requirements for MT-BFs had to be revisited and improved as necessary.

1.3 Research methodology

The main activities of this research are summarized as follows:

- At the beginning of the study and during the course of the work, a literature review of design provisions for concentrically braced frames in Canada and the U.S. was carried out with focus on past studies on the inelastic response of the CBFs and column buckling response.

– For the first objective of developing a better understanding of MT-BF seismic response, the following tasks were completed:
  - Design of prototype MT-BFs in accordance with current design provisions, i.e. CSA S16-09 in Canada and AISC 341-10 and AISC 360-10 in the U.S. The frames selected covered a wide range of geometries, braced frame systems and ductility. The frames in Canada were located in Vancouver and Montréal; the frames in the U.S. were located in Coastal California.
  - Development of numerical models using the *OpenSees* programs. Special attention was devoted to properly model the buckling response of the bracing and column members. Two models were developed: a simple model with simplified brace connection details, and a second model with refined connection details.
  - NonLinear Response History (NLRH) analysis of the prototype structures under an ensemble of ground motions that are representative of the design level earthquake (probability of exceedance of 2% in 50 years) in Canada and Maximum Considered Earthquake (MCE_R) level in the U.S.
  - Nonlinear static (pushover) analysis performed on selected MT-BFs to better understand the sequence of brace buckling and yielding leading to the in-plane flexural demand on columns and subsequent column buckling.
  - Collaboration with U.S. researchers who performed detailed finite element analysis of isolated MT-BF columns subjected to in-plane rotation and axial compression load demands obtained from *OpenSees* analyses and entire MT-BFs subjected to seismic ground motions. Similar, although limited, finite element analysis were also conducted in this thesis work to validate *OpenSees* results and confirm the findings from collaborators.
  - Examination of the analysis results with emphasis on the sequence of brace buckling and yielding along the frame height, column buckling response, in-plane flexural demand on columns, and tier drifts. Statistics of these response parameters were generated. In some studies, out-of-plane demand was also examined.
– For the second objective of developing seismic analysis and design methods for MT-BFs, the following tasks were accomplished:

- Close examination of the time history response of the prototype MT-BFs to understand the relationships between the bending moment demand in columns, the axial loads acting in the bracing members, storey drift and tier drifts.
- Close examination of the buckling mode of the columns to understand how buckling develops under the seismic demand.
- Development of an analysis and design method for simpler, 2-tiered SCBF systems in the U.S. The design approach was verified through nonlinear static and dynamic analysis.
- Use of nonlinear static (pushover) analysis to predict the flexural demand on columns and tier drift response.
- Development of guidance for the design of gravity columns along braced lines that are used to distribute and limit seismic induced column flexural demands and tier drifts in MT-BFs.
- Development of more comprehensive analysis and design methods for SCBFs with three or more tiers.
- Validation of the current Canadian design method and development of a modified analysis and design method for frames having a number of tiers in excess of CSA S16-14 limits.

– In addition, an experimental program including hybrid column testing was initiated to verify the buckling response of the steel W-shape columns as part of MT-BFs and validate the seismic design requirements proposed using the MDHTS at Polytechnique Montréal. Note that this test program has been only partially completed because of issues regarding the testing machine. For this test program, the following tasks have been accomplished so far:
  - Review of the MDHTS at Polytechnique Montréal
  - Selection of representative MT-BF column test specimens and development of a test program for MT-BF columns
  - Development of a preliminary column test program on smaller specimens
  - Preliminary hybrid testing including development of *OpenFresco* models
  - Characterization of the frictional forces developing in the experimental setup and development of numerical models and techniques to compensate for these forces.

Since this thesis is presented by relevant articles, parts of the presented tasks have been conducted more than once and at different periods of time, as each of the individual articles required that all steps performed during the course of this thesis be presented. Other tasks presented in only one article were accomplished only once.

1.4 Organization

This dissertation consists of relevant articles and is divided into 10 chapters and two appendices. Chapter 1 is the introduction chapter. It presents background information, the main objectives of the research, and the methodology that has been adopted. A literature review on the seismic behaviour of steel concentrically braced frames and column buckling response is presented in Chapter 2. Chapter 3 concentrates on the methodology of the research. In Chapters 4 to 8, five articles that include the main findings of the research project and have been submitted for publication in scientific journals are presented. These articles are as follows:

1) Seismic Performance Assessment of Multi-Tiered Steel Concentrically Braced Frames Designed in Accordance with Current AISC Seismic Provisions; Ali Imanpour, Robert Tremblay, Ali Davaran, Christopher Stoakes, and Larry A. Fahnestock; submitted to the *Journal of Structural Engineering, ASCE* on August 16, 2015.
2) Analysis and Design of Two-Tiered Braced Frames under In-Plane Seismic Demand; Ali Imanpour, Robert Tremblay, Larry A. Fahnestock, and Christopher Stoakes; submitted to the *Journal of Structural Engineering, ASCE* on November 2, 2014 (initial version) and May 13, 2015 (revised version).
3) Seismic Design and Performance of Multi-Tiered Steel Braced Frames Including the Contribution from Gravity Columns under In-plane Seismic Demand; Ali Imanpour, Karl Auger, and Robert Tremblay; submitted to the *Journal of Advances in Engineering Software* on July 10, 2015.
4) Analysis Methods for the Design of Special Concentrically Braced Frames with Three and More Tiers for In-Plane Seismic Demand; Ali Imanpour and Robert Tremblay; submitted to the *Journal of Structural Engineering, ASCE* on September 11, 2015.
5) Seismic Design and Response of Steel Multi-Tiered Concentrically Braced Frames in Canada; Ali Imanpour and Robert Tremblay; submitted to the *Canadian Journal of Civil Engineering* on September 15, 2015.

Chapter 9 presents a discussion on the main findings of this research. The conclusions and recommendations for future studies are summarized in Chapter 10. Appendix A presents the work performed to initiate the testing machine and develop a hybrid test program on MT-BF columns. In Appendix B, detailed derivation of the equation used to determine the number of yielding tiers in Chapter 7 is presented.

CHAPTER 2 LITERATURE REVIEW

2.1 General

A literature survey is provided in this chapter on the inelastic response of the steel concentrically braced frames (CBFs) and buckling response of steel W-shape columns. Considerable experimental and numerical research has been conducted on the behaviour of steel braced frames and their connections under loading protocols that are representative of strong earthquake loading. The influence of several parameters on the elastic and inelastic response of CBFs has been investigated. The information provided in these studies is necessary to understand the response of MT-BFs and validate the numerical models used in the analyses. Since there has been extensive research on the behaviour and design of CBFs, a review of the most relevant research work is summarized in the first part of this chapter. References are also made to previous works that include information on the inelastic seismic response of steel braced frames. Additionally, a brief review of the research that has been recently performed on the steel multi-tiered braced frames is presented. In the second part of this chapter, the seismic design requirements for steel concentrically braced frames designed in accordance with the Canadian and the U.S. standards are summarized.

Limited research, however, has been performed on the buckling response of the steel W-shape column part of seismic force resisting systems. This research consists of numerical investigations as well as experimental validations on the column buckling and failure modes. In the third part of this chapter, a review of the related publications is provided to help understand the behaviour of the MT-BF columns under seismic loading and, in particular, the instability mode of the columns.

2.2 Behaviour of steel CBFs

The literature review on CBFs is divided into the following categories:

- Brace inelastic response;
- Effective length and connection effects on brace resistance;
- Prediction of fracture life;
- Inelastic demand on steel CBFs;
- Numerical modeling of brace cyclic response.

2.2.1 Brace inelastic response

Extensive experimental studies have been performed on the inelastic response of bracing members for steel CBFs in the past three decades (Kahn and Hanson 1976; Jain et al. 1980; Popov and Black 1981; Lee and Goel 1987; Bertero et al. 1989; Fukuta et al. 1989; Shaback 2001; Tremblay et al. 2003). This research revealed that bracing members typically exhibit non-symmetrical and stable hysteretic behaviour under loading that is representative of seismic ground motion. The typical hysteretic response of a single bracing member tested under cyclic loading is illustrated in Figure 2.1. Non-symmetrical hysteretic response of the diagonal is associated to the difference between brace resistances in tension and compression. For the compression loading, strength degradation of the diagonal occurs with cycles or when increasing the imposed axial deformations; however, permanent deformation accumulates when the brace is stretched in the inelastic range in tension. Due to the pinched hysteretic response, the studies revealed a limited energy dissipation capacity for steel braces under seismic loading.

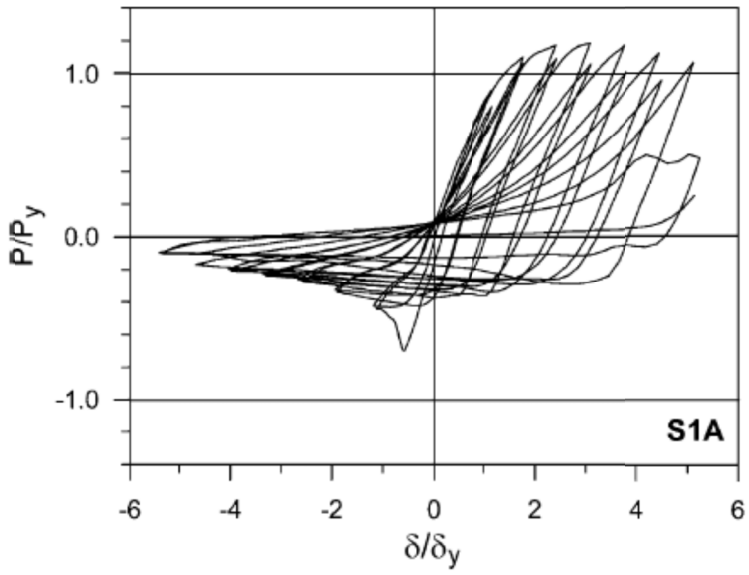

Figure 2.1: Brace hysteretic response under symmetrical cyclic loading (Tremblay 2002).

Tremblay (2002) reviewed the results of several cyclic experimental tests on diagonal steel bracing members made of various cross-sections including rectangular hollow sections (RHS), W-sections, and pipes. Several parameters were investigated including the brace buckling and

post-buckling resistances, brace maximum tensile resistance, and lateral deformations of the braces upon buckling. The identification of the brace buckling strength together with the strength reduction in the post-buckling range was also discussed in this paper, and equations were proposed based on the experimental data to predict the brace tension, buckling, post-buckling resistances, and maximum out-of-plane deformation of the compression braces. As reported in this study, the energy dissipation capacity of a bracing member increases when the brace slenderness decreases. As will be discussed later on, brace fracture life was found to decrease when the brace slenderness is reduced.

The main characteristics of the inelastic seismic response of CBFs were presented in Tremblay (2001). This document summarizes provisions for ductile response of bracing members such as the effect of the brace slenderness on the fracture life, brace overstrength, and ability of the brace to dissipate seismic energy. Additionally, the results of a series of quasi-static cyclic tests on CBFs were reported in Tremblay et al. (2003). This test program aimed at evaluating the seismic performance of the CBFs made with cold-formed RHS bracing members and by comparing the response of X-bracing and single diagonal bracing.

2.2.2 Effective length and connection effects on brace resistance

Several experimental and numerical studies have been performed to verify the concept of the effective length factor for steel bracing members in the inelastic range. Based on these studies, the effect of the connection detail is one of the most important factors that should be considered. Additionally, the support provided by the tension-acting member in the cross diagonals plays a key role in determining the brace's effective length. One of the earliest works to define the effective slenderness ratio of the single diagonal bracing and X-bracing configuration was performed by Wakabayashi et al. (1980). In this study, the effective length factor was estimated for the buckling of the braces, taking into account the rotational rigidity of the connected members. The effective slenderness ratio was proposed for the brace post-buckling and hysteretic response provided that the braces are rigidly connected at their ends.

Wakabayashi et al. (1974; 1977) conducted another experimental study on a series of X-bracing taking into account brace end conditions. These researchers concluded that the effective length factor depend on the connection type and plane of buckling. They proposed an effective length factor of 0.6 for in-plane and 0.7 for out-of-plane buckling. A theoretical model was proposed by

El-Tayem and Geol (1986) based on an experimental study on X-bracing made with single and double angle braces to estimate the effective length factor of the compression brace for in-plane and out-of-plane buckling modes. Similar recommendations were proposed by Tremblay et al. (2003) based on the test results to determine the compression strengths of the brace for single diagonal bracing and X-bracing. This study also confirmed that the tension brace in the X-bracing configuration can provide an appropriate out-of-plane support to the member acting in compression except at a storey drift close to zero. Palmer et al. (2012) proposed an effective length factor of 0.5 based on the experimental study performed on a single-story X-configuration with center-splice connection. The brace length was set equal to actual total brace length. Also, it was shown that the tension-acting brace can provide sufficient out-of-plane support for the compression member. The results of an experimental study by Tremblay et al. (2003) showed that the slenderness of bracing members of X-bracing systems could be determined with a K factor of 0.5 as X-bracing could provide similar hysteretic response and energy dissipation characteristics compared to single bracing, with the same effective slenderness ratio.

Furthermore, several theoretical studies addressed the effective length factor and buckling load of CBFs with an X-bracing configuration. Picard and Beaulieu (1987) proposed an equation to determine the effective length factor of X-bracing, which depends on the tension and compression forces in the braces. Based on this equation, for the ratio of compression brace force to tension brace force smaller than 1.6, the effective length of the compression diagonal is 0.5 times the length of the brace. The stability criteria of bracing members in X-bracing system were formulated using the energy approach by Stoman (1988) and Wang and Boresi (1992). The Raleigh-Ritz method was used to obtain the critical load of the compression brace in the presence of tension acting members and brace effective length was proposed for design purpose. Stoman (1989) showed that the effective length of the compression brace is sensitive to the relative stiffness of the two cross diagonals as well as the brace end conditions. Various parameters were investigated by Segal et al. (1994) to obtain the compression buckling loads of the braces in the X-braced frame subjected to out-of-plane buckling, including the end conditions (rigid, pinned, and semi rigid), the length of the members, the flexural stiffness of the boundaries, and the relative axial loads in the tension and compression members. They proposed closed-form relationships to determine the brace buckling loads. A similar study was performed by Sabelli and Hohbach (1999), where a relationship was derived between brace buckling strength and end-

rotational stiffness. This study provides design value for effective length factor of the X-bracing for in-plane and out-of-plane buckling modes.

A closed formed solution was proposed by Davaran (2001) for the effective length factor in the elastic range of the discontinuous member part of an X-bracing system to estimate the effect of the mid-span connection on the brace buckling resistance. Buckling analysis was solved for two mid-connection details: pinned and semi-rigid. The results showed that the rotational stiffness of the mid-connection should be increased to achieve higher load capacity for the bracing system. A complementary study by Davaran and Hoveidae (2009) using nonlinear 3-Dimensional (3D) finite element analysis confirmed that the buckling strength and ductility of the X-braced configuration is improved by using a new mid-connection detail. Davaran et al. (2014) performed an experimental study on X-bracing systems with bolted single shear splice connections to evaluate the compressive resistance of discontinuous bracing members. An analytical method was proposed based on the test data to predict the compressive resistance of these members. One of the main findings of this study was that the current AISC design procedure for Hollow Structural Section (HSS) connections overestimates the buckling strength. An equation was proposed to predict the effective length factor of these members, taking into account the formation of three plastic hinges over the length of the discontinuous member.

2.2.3 Prediction of fracture life

Cold formed Rectangular Hollow Sections (RHSs) are commonly used in steel CBFs as they offer an effective cross-section to resist compression forces. Low-cycle fatigue fracture of these members at the plastic hinge location has been known as an unsatisfactory limit state for the brace frames. The observations of the Northridge 1994 and Kobe 1995 earthquakes (Tremblay et al. 1995; Tremblay et al. 1996) also confirmed that the braces made of RHSs are prone to premature fracture resulting from the local buckling at the plastic hinge regions. So far, extensive research studies have been performed to investigate the brace fracture, especially on the braces made of cold-formed square or rectangular steel tubing (Tang and Goel 1987; Archambault et al. 1995; Shaback 2001; Tremblay 2003; Hsiao 2013).

Tremblay (2002) proposed an empirical equation to predict ductility at brace fracture as a function of brace slenderness. In their experimental study, Tremblay et al. (2003) showed that brace fracture generally occurs when the brace is in tension after developing local buckling of the

tube in the previous compressive cycle. An empirical model was proposed in this study to predict the fracture life of braces made of RHSs. Maximum end rotation was used in this model to characterize the deformation demand at brace fracture initiation. Based on this model, the resistance to fracture increases by reducing the width-to-thickness (b/t) of the tube wall and when the effective brace slenderness ratio (Kl/r) increases. It was confirmed that local buckling of the walls of the HSS members play an important role in resistance to fracture.

Fell et al. (2009) reported the results of 18 large-scale tests of bracing members made of HSS, pipe, and W-sections. The study aimed at examining the fracture behaviour of these braces under cyclic loading. The results of the experimental study showed that the brace width-to-thickness ratio has the largest impact on the brace fracture ductility as the section local buckling results in developing large plastic strain in the section, and in turn, leads to fracture initiation near the corners of the HSS member. However, member slenderness ratio and loading parameters have lesser impact on the brace fracture ductility. Figure 2.2 shows the variation of fracture drift with brace width-to-thickness ratio and slenderness ratio for the specimens tested in this study. The results revealed that resistance to fracture increases for more compact HSS sections and more slender members.

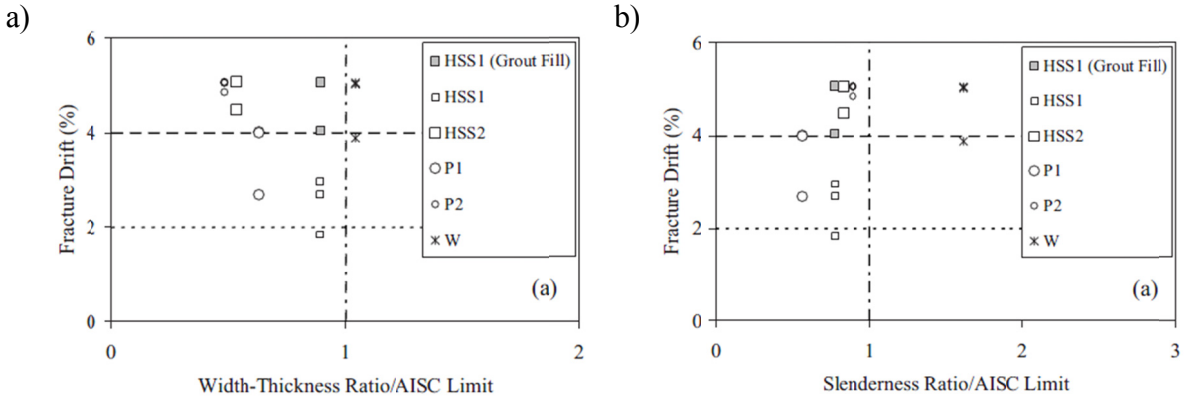

Figure 2.2: Maximum drift at fracture initiation versus a) brace width-to-thickness ratio; and b) brace overall slenderness ratio (Fell et al. 2009).

Several experimental studies have also been performed on fracture ductility of the bracing members by researchers at University of California at Berkeley (Uriz 2005; Uriz and Mahin 2008; Yang and

Mahin 2005; Chen et al. 2008; Lai et al. 2010; Lai and Mahin 2014). These studies include cyclic experimental testing of braced frames with braces made of square HSS, round HSS, pipe, and W-section. Uriz (2005) performed an experimental study on a 2-storey Special Concentrically Braced Frame (SCBF) with HSS braces in a chevron bracing configuration. The two storeys were identical and the horizontal displacement was applied at the top of the second level, similar to a multi-tiered braced frame except that the columns were subjected to strong-axis bending moment in the plane of the frame. In the test, lateral deformations concentrated in the lower storey and brace fracture occurred at a storey drift of 2.5%. Figure 2.3 shows the fraction of roof drift distributed in each storey until the fracture. Also, a fatigue model based on strain accumulation was developed to predict the fracture life for the HSS braces. Yang and Mahin (2005) performed tests on individual square HSS braces and showed that fracture occurred at storey drifts equal to 2.5%; however, circular braces made from pipes resulted in better resistance to fracture than the square HSS braces. Similar conclusions were made by Lai and Mahin (2014) based on the results of an experimental study on two 2-storey full-scale steel braced frame specimens with RHS and CHS braces tested under cyclic loading.

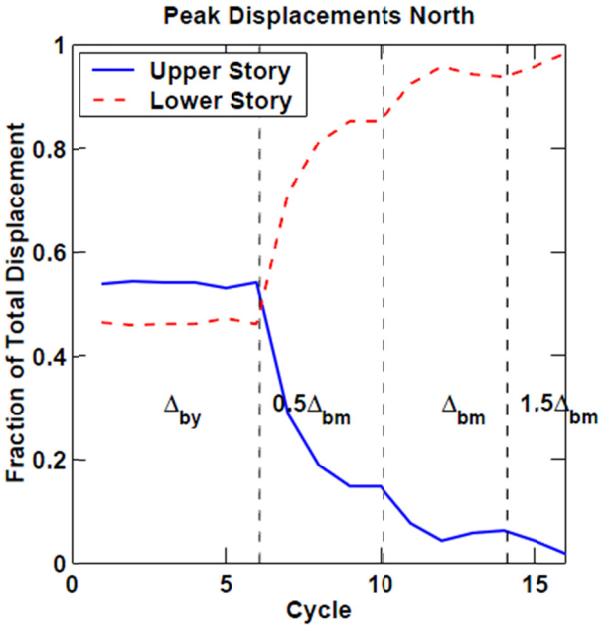

Figure 2.3: Concentration of drift in the first storey of a 2-storey CBF (Uriz 2005).

Recently, Tsai et al. (2010; 2013) conducted experimental studies on braces and full-scale three storey CBFs with W-section braces subjected to out-of-plane and in-plane buckling. Braces were tested under cyclic displacement, whereas pseudo-dynamic technique was used to perform frame test. This study concluded that the maximum storey drift that leads to tensile fracture of the braces in multi-storey frames is equal to 3% and 5% for out-of-plane and in-plane buckling, respectively. A similar study was performed by Roeder (2011) on three full-scale, two-storey SCBFs with an X-braced configuration. Two specimens included rectangular HSS brace members and the third specimen had wide-flange braces. Different gusset plate details were studied. The experimental study showed that the HSS braces achieved maximum storey drift of 2% before brace fracture, whereas the corresponding drift for wide flange braces was 2.5%; however, the loss of brace strength after buckling was more significant for the braces made of wide flange sections.

A team of researchers at University of Washington (Hsiao et al. 2013) used the fracture data from over 40 steel braced frame tests to propose a fracture model for nonlinear modeling of SCBFs with HSS braces. This model accounts for the width-to-thickness ratio of the cross-section, overall slenderness ratio of the brace, and yield strength of the bracing members. Hsiao et al. proposed that the maximum strain can be used as the best variable to predict brace fracture (Figure 2.4). Using the model proposed in this study, it is found that the maximum storey drift before fracture for square HSS braces satisfying the 2010 AISC Seismic Provisions limit for a highly ductile member is approximately 2%.

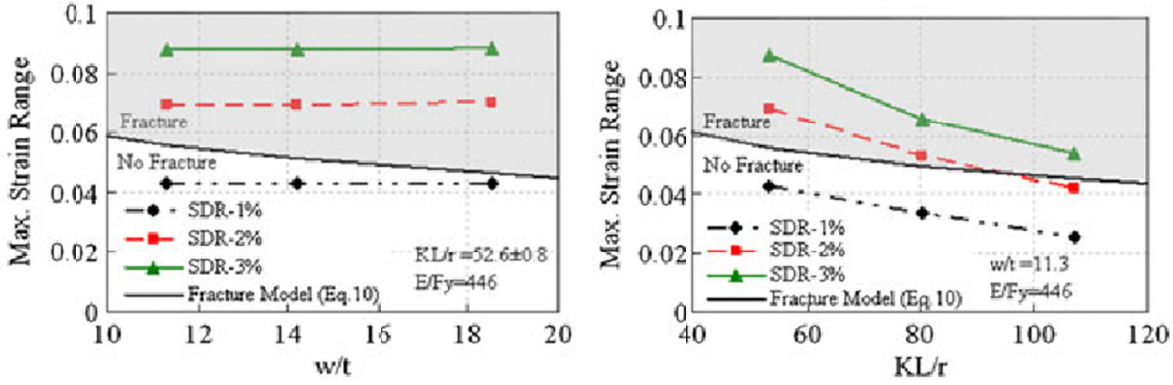

Figure 2.4: Brace fracture limit varying with a) brace width-to-thickness ratio (KL/r =52.6 and E/F_y = 446 MPa); and b) brace slenderness ratio (b/t =11.3 and E/F_y = 446 MPa) (Hsiao et al. 2013).

2.2.4 Inelastic demand on steel CBFs

In steel CBFs, uneven distribution of seismic demand along the height of CBFs may affect the performance of the structure while responding to seismic shaking. Concentration of inelastic demands in multi-storey steel frames that may lead to soft-storey mechanism have been widely investigated previously. As stated by Tremblay (2000; 2003) and Tremblay and Merzouq (2004), dynamic instability of multi-storey CBFs is mainly developed due to the non-uniform distribution of inelastic seismic demand, which itself results from the reduction of the storey shear resistance in the storey (or storeys) where brace buckling first occurs (Uriz 2005). This response induces in-plane flexural bending demands in the CBF columns. The intensity of this behaviour depends on various parameters, including hysteretic response of the bracing member, braced frame configuration, number of storeys, and the characteristics of the ground motion. Also, non-uniform distribution of inelastic demand over the height of steel braced frames contributes to reducing the seismic induced axial force demands in the columns. This is because brace yielding does not occur simultaneously over the entire height under seismic loading. However, this behaviour imposes high rotational demands on the CBF columns (Tremblay and Stiemer 1994; Tremblay 2000; Tremblay 2003; Richards 2009). Extensive research (Uetani and Tagawa 1998; Krawinkler and Gupta 1998; Moghadam et al. 2004; Uriz 2005; Chen et al. 2008; Richards 2009; Lai and Mahin 2014) has been conducted to recognize the causes of drift concentration in CBFs and propose cost-effective and simple solutions; however, no practical solution has yet been developed to mitigate this unsatisfactory response in the CBFs. Note that past studies have not examined the seismic response of multi-tiered braced frames. The following ideas were among those proposed by some researchers to avoid dynamic instability, distribute inelastic demand over the building height, and achieve more stable braced frame response in steel CBFs:

- Use of elastic members (or truss) together with the CBF
- Proper detailing of the bracing members
- Application of BRBFs instead of conventional CBF

The schematics of elastic vertical truss attached to the main frame are shown in Figure 2.5. In this system, the high rigidity provided by the elastic truss helps to distribute drift between the storeys by triggering the brace yielding and buckling (Tremblay et al. 1997; Tremblay 2003; Tremblay and Merzouq 2004).

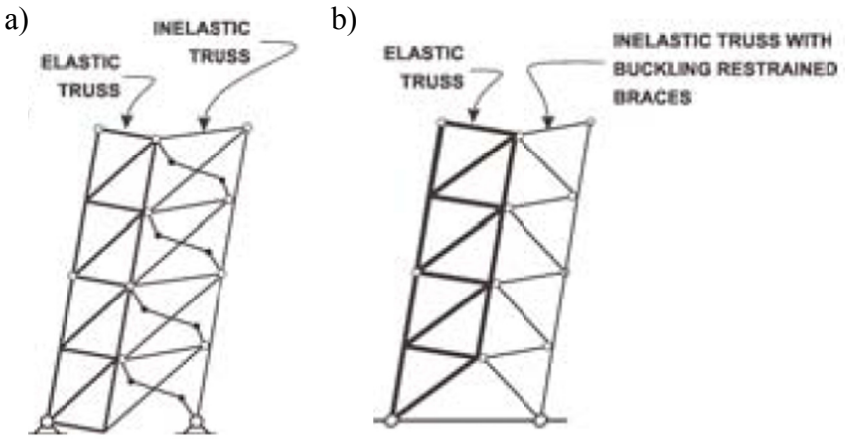

Figure 2.5: Elastic vertical truss attached to a) a conventional X-braced frame; and b) a buckling restrained braced frame (Tremblay 2003).

In braced frames with elastic truss, all the braced storeys undergo the same drift when the frame responds in inelastic region because the vertical truss has enough flexural stiffness to force yielding in all of the storeys attached. The elastic vertical truss concept was used for the construction of a 19-storey building in Japan (Aoki et al. 1998). In recent research by Wada et al. (2009), the implementation of rocking walls and steel dampers was studied to increase the strength and energy dissipation of an 11-storey reinforced concrete frame in Japan. An example of using this system together with a steel moment resisting system is shown in Figure 2.6. The results of this study confirmed that using the rocking system can improve the seismic performance of the frame by controlling the global behaviour of the structure and reducing the possibility of damage in deficient structural members.

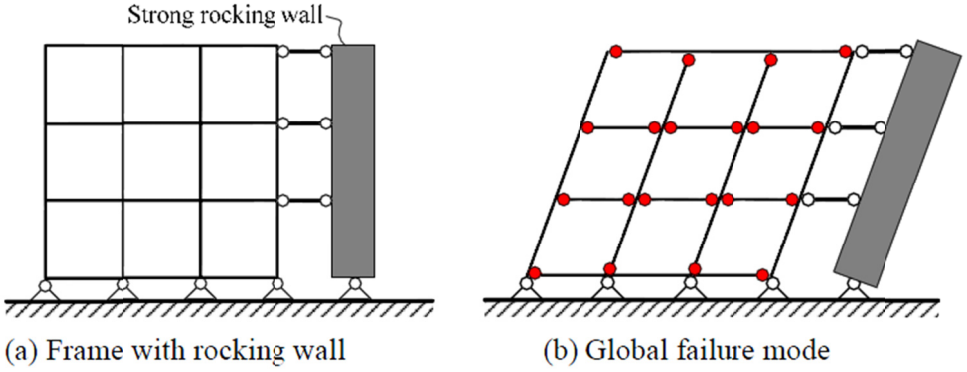

Figure 2.6: Strong rocking wall attached to a steel moment resisting frame (Wada et al. 2009).

Lai and Mahin (2014) proposed a new seismic force resisting system named the strongback system. This system is similar to the vertical truss member proposed by Tremblay (2003) and aims at promoting uniform storey drift over the heigth of the structure and prevent the occurance of soft storey mechanism. A design strategy was also proposed to prevent deformation concentration in steel braced frames. The results of nonlinear dynamic analysis showed that this system is capable of preventing soft-storey mechanism. Pollino et al. (2013) and Qu et al. (2014) also proposed a similar idea (vertical truss) to enhance the seismic performance of the existing CBFs using one or multiple rocking cores added to the main frame in order to engage all the braces over the frame height and redistribute the seismic forces. Pollino et al. (2013) also listed the number of reasons that may cause non-uniform distribution of the seismic demand or capacity over the building height. These reasons include non-uniform overstrength over the frame height, uncertainties in mass distributions, differences in the structural properties, and uncertainties in the magnitude and frequency content of the earthquake. A design example together with performance evaluation of new technique was presented in Qu et al. (2014). The results of this research revealed that this technique can effectively reduce the excessive storey drift demands for the rehabilitated CBF.

As an alternative solution to minimize the concentration of the inelastic demand along the height of the structure, Tremblay et al, (1994) Tremblay (2000) and MacRae et al. (2004) proposed making use of the continuity of the columns to reduce drift concentration and promote uniform drift along the height of CBFs, which would result in simultaneous brace yielding and increase column axial demands. Minimum column continuity requirements have been introduced in CSA S16 in 2001: minimum of two storeys for tension-compression CBFs and over the full building height for tension-only CBFs. MacRae et al. (2004) developed relationships between the drift, column strength, and stiffness for two-storey CBFs. Column bending demands were related to the column stiffness, the ratio of displacement at top of the frame to the roof displacement at yield, and storey shear force developed by the braces. Empirical relationships were proposed for multi-storey CBFs. In multi-storey structures, gravity columns are also attached to the lateral load resisting systems through the floor; therefore, one can make use of the continuity of the gravity columns to help prevent concentration of seismic ductility demand. Flores et al. (2014) showed that the additional stiffness provided by continuous (without splice) gravity columns can help to improve seismic performance of Special Moment Frames (SMFs).

In addition to the idea of the elastic stiff member, several other methods were proposed to mitigate drift concentration, prevent dynamic instability, and improve seismic response of CBFs. Among those methods, a design method was proposed by Lacerte and Tremblay (2006), where slender braces are selected with post-buckling storey shear resistance sufficient to trigger buckling of the compression brace in the adjacent top or bottom storey. The results of the numerical simulation of a 12-storey CBF verified the method to achieve stable and satisfactory seismic performance in the 2-storey X-configuration. Recently, European researchers Merczela et al. (2014) introduced a plasticity-based method, where the structure is designed first in accordance with the Eurocode requirements. Then, braces and columns are modified such that the load parameters, which cause localized plastic storey mechanism, are always larger than load parameter that results in a distributed yielding along the height of the structure. This methodology is illustrated schematically in Figure 2.7.

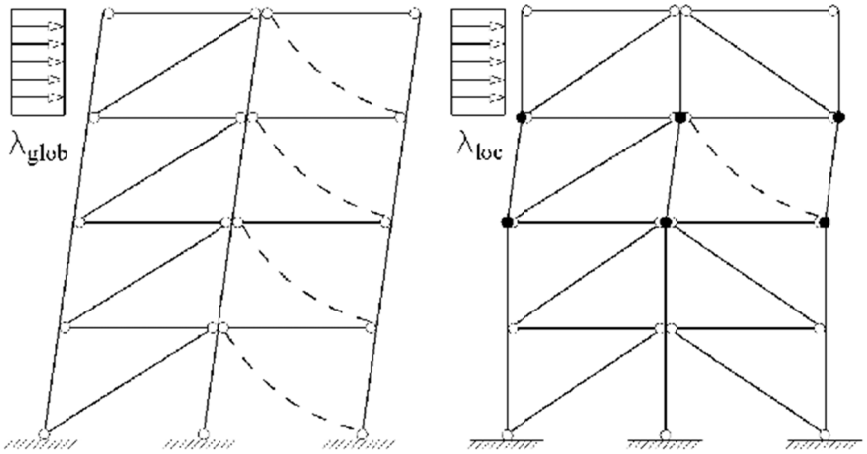

Figure 2.7: Global plastic and soft storey mechanisms (Merczela et al. 2014).

2.2.5 Numerical modeling of brace cyclic response

A significant amount of research has been performed on numerical modeling of braces, as an accurate model of brace inelastic response is essential to achieve meaningful results. Since a fiber-based model was extensively used in this study, an overview of landmark studies that were

used as the basics to develop the numerical model in *OpenSees* program (McKenna and Fenves 2004) is presented.

Force-based beam-column model used in *OpenSees* program was developed by Spacone et al. (1996) for the nonlinear analysis of reinforced concrete frames. In this model, a flexibility-based formulation was used and it was assumed that the plane section remain plane. Bending moment and axial force were employed to satisfy element equilibrium using force interpolation functions. The main advantages of this model include: 1) exact force interpolation functions with reduced number of elements; 2) robustness and reliability of the model to simulate the strength degradation and softening; and 3) ability to incorporate distributed element loads. So that the force-based formulation offers higher accuracy; additionally, post-bucking axial compressive strength degradation, such as brace or column buckling, can be appropriately predicted from the equilibrium of force field at any level of inelastic deformation (Spacone et al. 1996; Calabrese 2010; D'Aniello et al. 2013; Wijesundaraet al. 2014). Force-based beam-column element with fiber discretization of the cross-section was validated by Uriz et al. (2008) for single-plane flexural buckling of braces. Uriz et al. showed that this element is able to accurately predict the brace hysteretic response including tension and buckling resistances, and post-buckling behaviour. Additionally, it was found that local buckling has an insignificant impact on the overall hysteretic force-displacement response of steel braces with compact sections; however, using a smooth transition from the elastic to inelastic region of material stress-strain response indirectly compensates for this minor effect (D'Aniello et al. 2013). In another validation study, Agüero et al. (2006) investigated the influence of the various parameters including the type of elements (force-based and displacement elements), number of elements along the brace length, number of integration points along the element length, number of fibers required to define brace section, material model, and amplitude and number of displacement increments required to simulate cyclic response of bracing members. Test results were used to validate predictions from numerical models. It was concluded that the elements with force-based formulations result in more accurate predictions, even though more computational time is required when using force-based elements. Furthermore, the uniaxial Giuffré-Menegotto-Pinto material model (Menegotto and Pinto 1973) was found to be an appropriate steel material for modeling cyclic response of braces.

Agüero et al. (2006) also reported that the number of integration points has no significant impact on brace response; three integration points was recommended in this study; Scott and Fenves

(2006) and D'Aniello et al. (2013) recommended four integration points per element. Based on Agüero et al. (2006), sufficient accuracy is achieved in predicting the brace response if eight elements per brace with 16 fibers for cross-section discretization were used. Error is increased by reducing the number of elements or the number of fibers.

In addition to an accurate nonlinear model for the bracing members, a realistic and sophisticated modeling approach is needed to assess the buckling and post-buckling response of steel CBFs. According to Agüero et al. (2006), using a brace connection model with rotational spring (Figure 2.8), which reproduces the hysteretic response of the gusset plates, was found to offer a good match between prediction and test results for the cases studied. In a research study by Hsiao et al. (2012), an accurate yet practical modeling approach was proposed for gusset plate connection, which includes nonlinear rotational springs with multiple rigid zones. This spring is able to simulate the hysteretic flexural response of the gusset plates. One example of this connection model is shown in Figure 2.9.

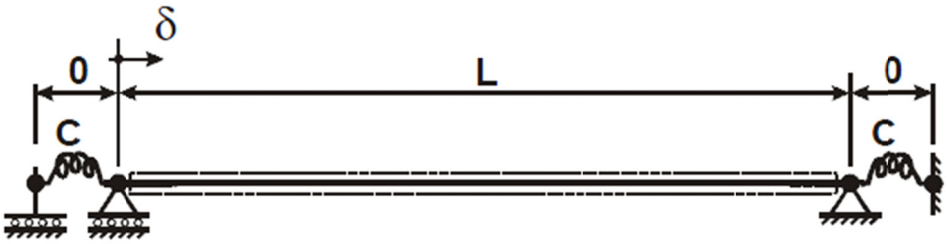

Figure 2.8: Brace connection model with zero-length rotational spring (Agüero et al. 2006).

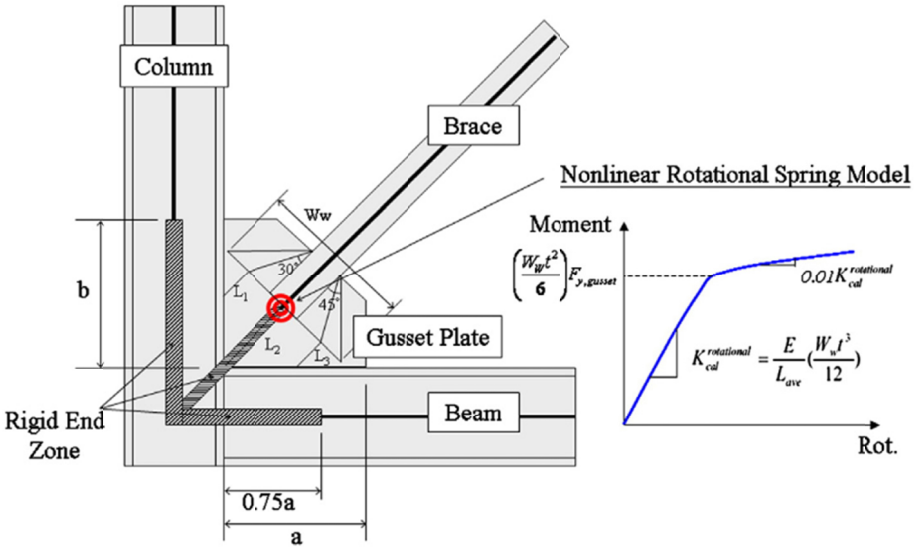

Figure 2.9: Brace connection model with zero-length rotational spring and rigid links (Hsiao et al. 2012).

2.2.6 Multi-tiered braced frames

Very few research studies were found in the literature that investigate the seismic response of steel multi-tiered braced frames. The research performed by the collaborators of the current study is reported here; although part of that work is presented in the journal articles accompanying this thesis. Stoakes and Fahnestock (2012; 2013) investigated the influence of weak-axis flexural yielding on strong-axis stability of isolated W-shape columns part of steel MT-BFs designed in accordance with the 2010 AISC Seismic Provisions. The study aims at characterizing the inelasticity effect on the column compression strength, as the current column strength curve such as the one specified in the AISC Specifications (2010b) does not account for the yielding of the column when verifying the limit state of strong-axis out-of-plane buckling. 3D finite element analyses were performed on the columns subjected to combined compression loads and weak-axis flexural bending. The flexural bending was increased such that yielding initiates in columns. The results of the finite element analyses showed that the strong-axis buckling strength of isolated MT-BF columns can be reduced under monotonic loading due to the presence of weak-axis flexure provided that the weak-axis rotation is large and torsional restraint is not provided at the tier levels. As shown in Figure 2.10, a biaxial buckling mode, which involves a combination of strong-axis

and weak-axis deformations, was observed for the columns loaded with distributed axial loads along the height, as is the case for MT-BF columns being loaded at tier levels by the vertical components of the brace axial forces. This study raised concerns regarding the possibility of coupled in-plane and out-of-plane buckling of MT-BF columns under in-plane seismic demand induced by brace nonlinear response and the lack of suitable interaction equations to address this response.

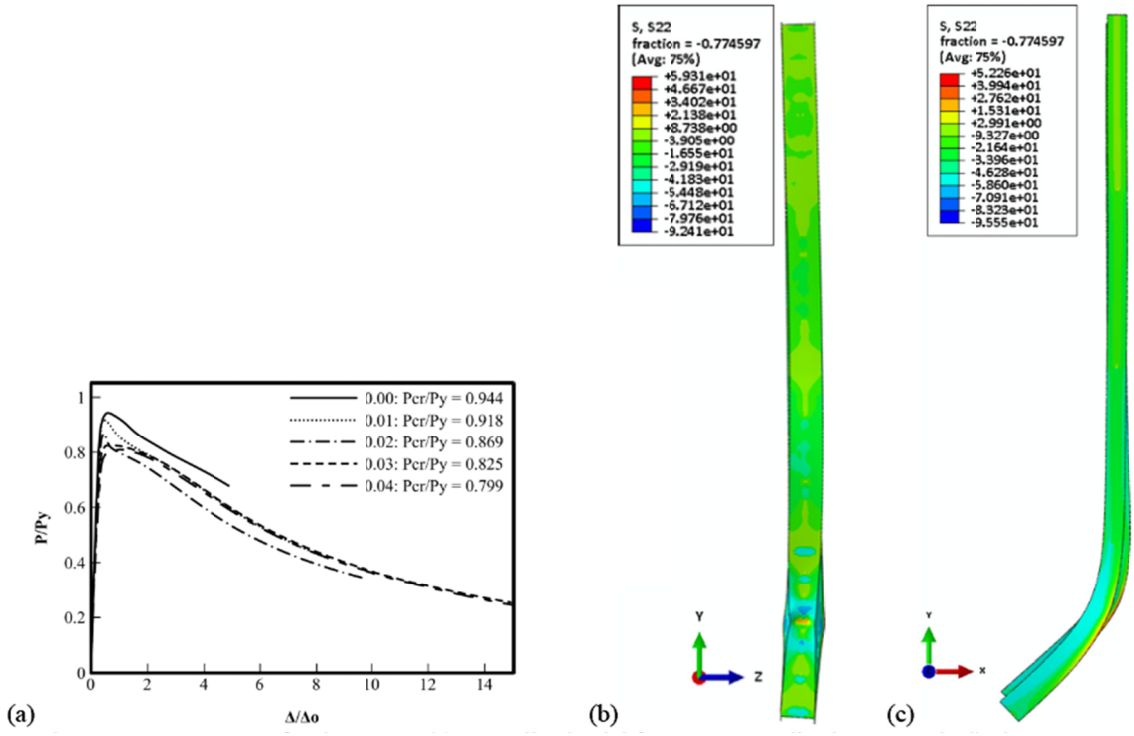

Figure 2.10: 4-tiered isolated W610x195 column with total height of 40 ft: a) Normalized axial force vs normalized strong-axis displacement; b) Buckled shape with normal stress contours (ksi) at 0.02 rad.; and c) Buckled shape with normal stress contours (ksi) at 0.03 rad. (Stoakes and Fahnestock 2013).

MT-BF columns are subjected to varying axial loads along their height due to the vertical components of brace axial loads at tier levels. This loading condition affects the buckling length of the column in the plane and out of the plane of the frame and should be accounted for in the stability analysis when defining the effective length factor. In industrial applications, MT-BF

columns are referred to as stepped (or crane) columns because the column member provides a support for the crane runway girder installed between the ground and roof levels; also the column section is generally reduced between the crane runway girder and roof level. Stepped columns are typically unsupported over their entire height for buckling about strong-axis, whereas for buckling about weak axis, the lateral support is provided by the crane runaway girder and/or intermediate struts. Extensive research was carried out in the past four decades to define the bucking length of stepped columns using elastic stability analysis (Huang 1968; Dalal 1969; Anderson and Woodward 1972; Lay 1973; Agrawal and Stafiej 1980; Moore 1986; Fraser 1987, 1989, 1990; Fraser and Bridge 1990; Bendapudi 1994; Lui and Sun 1995; Simão et al. 2012). Some of these studies are summarized below:

Huang (1968) presented the slenderness ratio of heavy mill building stepped columns with two tiers. In this study, a practical method was introduced to design columns in mill building for out-of-plane buckling. It was concluded that the ratio of the moment of inertias, the tier height ratio, and the axial loads applied at tier as well as roof levels affect the buckling length of the columns. Design curves were presented for practical values. The effective length factor of the bottom column segment increases by increasing the moment of inertia as well as the height of the top tier, and decreasing the axial load at the roof level. The effective length factor of the top column segment increases by decreasing the moment of inertia of the bottom tier and increasing the axial load at the roof level.

Dalal (1969) solved the elastic buckling equation for out-of-plane buckling of several non-conventional cases including: symmetrically and unsymmetrically stepped columns with axial loads at the roof level, prismatic columns with distributed axial loads, prismatic columns with intermediate axial loads, prismatic columns with axial loads at the roof level, and unsymmetrically stepped columns with intermediate and end axial loads. Design tables were given as a function of the parameters affecting the buckling length including the axial loads, the ratio of the moment of inertia, and the tier height ratio. Figure 2.11 shows the critical load for a stepped column subjected to end and intermediate axial loads. The buckling load increases when the intermediate axial load is increased.

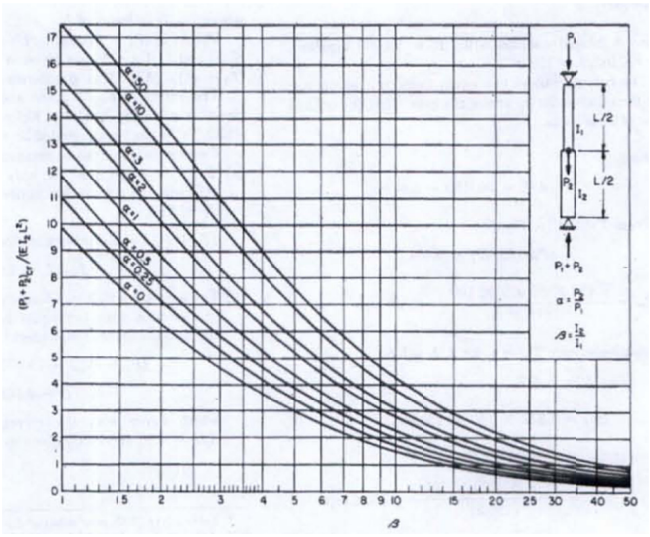

Figure 2.11: Stepped column critical load with end and intermediate axial loads (Dalal 1969).

Agrawal et al. (1980) performed a similar study for in-plane buckling of the stepped columns. They concluded that the buckling length depends on the end fixities, the tier height ratio, the ratio of the moment of inertia, and the ratio of the applied axial loads. Effective length factors were presented for various end conditions of the stepped column. In a similar study, Anderson and Woodward (1972) solved the stability equation for the stepped column with different end conditions.

Fraser and Bridge (1990) investigated the buckling load of stepped columns within rigid frames. These researchers included the flexural stiffness of the roof beam in addition to the above-mentioned parameters and proposed practical design curves to determine the effective length factor.

Simão et al. (2012) proposed a geometrically nonlinear model for stability analysis of sway and sway-prevented stepped columns for out-of-plane strong-axis buckling. Comprehensive design tables were given to define effective length factors for practical range of the following parameters: the ratio of the end axial load to the intermediate axial load, the tier height ratio, end fixities, the ratio of moment of inertia of the column segments, and the stiffness of the column splice. Column end conditions for which design values were presented in the paper are shown in Figure 2.12. Figure 2.13 presents buckling loads for sway and sway-prevented columns varying with the height ratio ($L_I = \alpha L$, where L_I is the height of bottom column segment and L is the total height), the ratio of the end axial load to intermediate axial load (γ), the ratio of moment of inertia of the column segments (I_I / I_{II}), and the stiffness of the column splice.

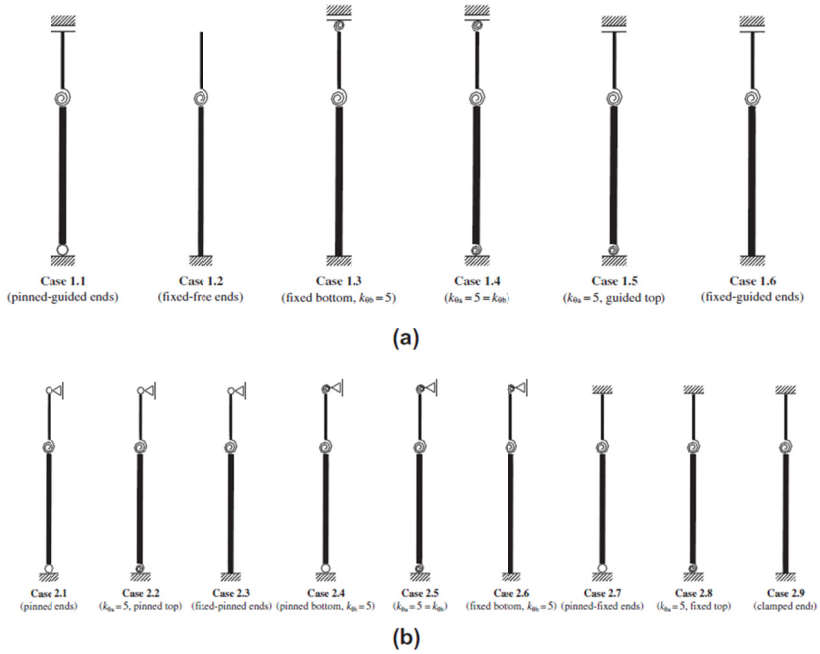

Figure 2.12: Column end conditions: a) Sway column; and b) Sway-prevented column (Simão et al. 2012).

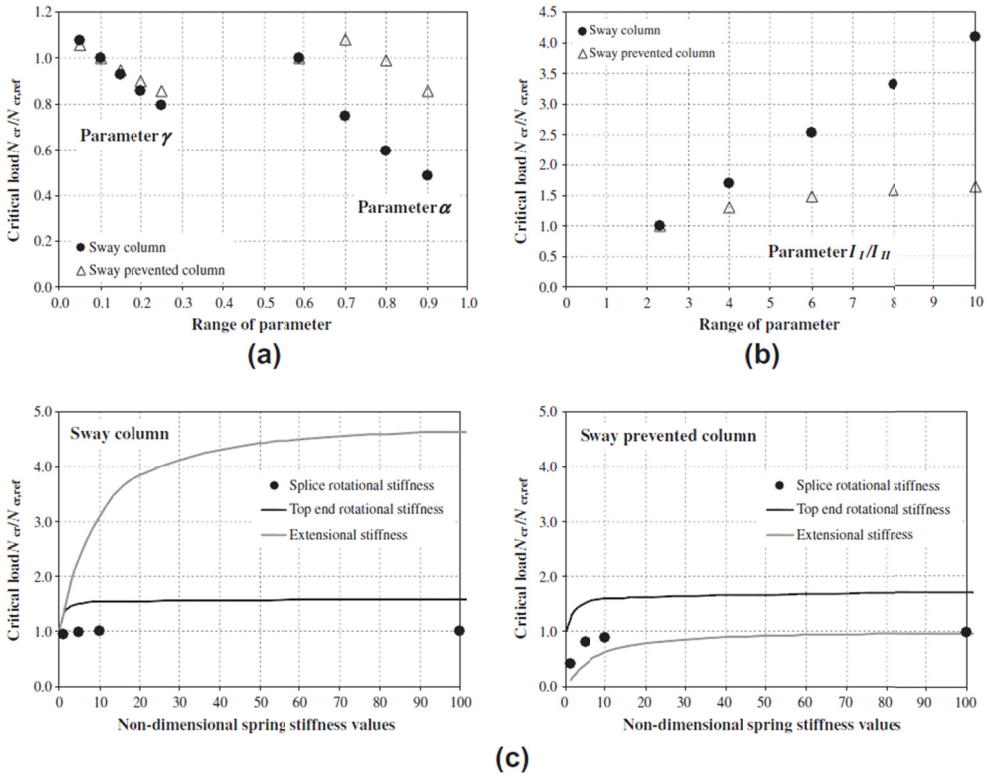

Figure 2.13: Buckling loads varying with: a) α and γ; b) I_I / I_{II}; and c) Spring stiffness (Simão et al. 2012).

2.3 Seismic design requirements for steel CBFs

In view of the extensive use of the CSA S16-14, AISC 341-10 and AISC 360-10 seismic design provisions in this study, a review of the requirements specified in these standards are summarized for Type MD and LD CBFs (in CSA S16) and SCBFs (in AISC 341).

2.3.1 Type MD (moderately ductile) concentrically braced frames in CSA S16-14

- Brace frame configuration: tension-compression, tension-only bracing, and other systems if stable inelastic response can be verified. Knee bracing and K-bracing are not permitted.
- Height limit: 40 m for the tension-compression configuration if $I_E F_a S_a(0.2) > 0.35$ or $I_E F_v S_a(1.0) > 0.30$ and factored seismic forces should be increased by 3% per metre for the height above 32 m; 20 m for the tension-only configuration if $I_E F_a S_a(0.2) > 0.35$ or $I_E F_v S_a(1.0) > 0.30$ and factored seismic forces should be increased by 3% per metre for a height above 16 m.
- Fundamental lateral period, T_a: $0.025h_n$ where h_n is the frame total height. T_a should not exceed 2.0 times the period obtained from analysis of the structural model. For the calculation of the deflection, this upper limit is not considered and computed fundamental period can be used.
- Ductility-related force modification factor, R_d : 3.0
- Overstrength-related force modification factor, R_o : 1.3
- Earthquake importance factor of the structure within Importance Category Normal, I_E: 1.0
- Higher mode effect factor M_v: 1.0
- 5% damped spectral response acceleration, $S(T_a)$: it is obtained from design spectral response acceleration based on a 2% probability of exceedance in 50 years for a given Site Class.
- Seismic weight, W: calculated using the dead load plus 25% of the snow load plus 60% of the storage load for areas used for storage.
- Design storey shear, V: $S(T_a) M_v I_E W / (R_d R_o)$
- Brace slenderness (KL/r) limit: less than 200. If $I_E F_a S_a (0.2) > 0.75$ or $I_E F_v S_a(1.0) > 0.30$, KL/r for the HSS members should not be less than 70.
- Section compactness limit for HSS braces: If $I_E F_a S_a (0.2) > 0.35$ and $KL/r < 100$, for rectangular and square HSS: width to thickness ratio $< 330 / (F_y)^{0.5}$ and for circular HSS:

diameter to thickness ratio < 10000 / F_y. If $I_E F_a S_a$ (0.2) > 0.35 and KL/r = 200: Class 1, where F_y is the yielding stress.

- Probable brace resistances: in tension, T_u, is equal to $A_g R_y F_y$; in compression, C_u, is equal to the lesser of $A_g R_y F_y$ and $1.2C_r / \phi$; and in the post-buckling range, C'_u, is equal to the lesser of 0.2 $A_g R_y F_y$ and C_r / ϕ, where C_r is the factored compressive resistance of the brace and computed using $R_y F_y$, ϕ is the resistance factor, and A_g is the brace cross-sectional area.
- Brace connections: ductile hinge should be provided in the brace or connection for in-plane or out-of-plane buckling of the brace. The resistance of the connections should be larger than T_u and C_u.
- Columns and beams design loads: the gravity load plus the seismic load corresponding to two brace loading scenario 1) when the tension braces reach T_u while the compression braces reach C_u; and 2) when the tension braces reach T_u while the compression braces reach C'_u. Additional bending demand equal to 0.2 $Z F_y$ should be considered in the plane of the frame for column design, where Z is the plastic section modulus of the column in the plane of the frame.
- Section compactness limit for columns: Class 1 or 2 beam-columns.
- Columns with braces intersecting between horizontal diaphragms (MT-BFs):
  - Maximum number of tiers: 3
  - Horizontal struts should be provided between tiers.
  - Column design loads: the axial loads, shear forces, and in-plane bending moments induced when braces reach T_u and C'_u in any one of the tiers at design storey drift; out-of-plane bending moments induced by transverse loads at each brace-to-column connection equal to 2% of the factored axial compression load in the columns below the connection.

2.3.2 Type LD (limited ductility) concentrically braced frames in CSA S16-14

- Brace frame configuration: tension-compression, tension-only bracing, and other systems if stable inelastic response can be verified. Knee bracing and K-bracing are not permitted.
- Height limit: 60 m for the tension-compression configuration if $I_E F_a S_a(0.2)$ > 0.35 and factored seismic forces should be increased by 2% per metre for the height above 48 m; 40 m for the tension-only configuration if $I_E F_a S_a(0.2)$ > 0.35 factored seismic forces should be increased by 3% per metre for a height above 32 m.

- Fundamental lateral period, T_a: $0.025h_n$. T_a should not exceed 2.0 times the period obtained from analysis of the structural model. For the calculation of the deflection, this upper limit is not considered and computed fundamental period can be used.
- Ductility-related force modification factor, R_d : 2.0
- Overstrength-related force modification factor, R_o : 1.3
- Earthquake importance factor of the structure within Importance Category Normal, I_E: 1.0
- Higher mode effect factor M_v: 1.0
- 5% damped spectral response acceleration, S(T_a): it is obtained from design spectral response acceleration based on a 2% probability of exceedance in 50 years for a given Site Class.
- Seismic weight, W: calculated using the dead load plus 25% of the snow load plus 60% of the storage load for areas used for storage.
- Design storey shear, V: S(T_a) M_v I_E W / (R_d R_o)
- Brace slenderness (KL/r) limit: less than 200 except in single- and two-storey structures should not exceed 300. If I_E F_a $S_a(0.2)$ > 0.75 or I_E F_v $S_a(1.0)$ > 0.30, KL/r for the HSS members should not be less than 70.
- Section compactness limit for HSS braces:
  - If I_E F_a $S_a(0.2)$ > 0.35 and KL/r < 100, for rectangular and square HSS: width to thickness ratio < 330 / $(F_y)^{0.5}$ and for circular HSS: diameter to thickness ratio < 10000 / F_y. If I_E F_a $S_a(0.2)$ > 0.35 and KL/r = 200: Class 1.
  - Class 2 for structures less than 40 m in height and I_E F_a $S_a(0.2)$ < 0.45
  - There is no limit if the brace slenderness ratio exceeds 200.
- Probable brace resistances: in tension, T_u, is equal to A_g R_y F_y; in compression, C_u, is equal to the lesser of A_g R_y F_y and $1.2C_r$ / ϕ; and in the post-buckling range, C'_u, is equal to the lesser of 0.2 A_g R_y F_y and C_r / ϕ.
- Brace connections: ductile hinge should be provided in the brace or connection for in-plane or out-of-plane buckling of the brace except if I_E F_a $S_a(0.2)$ < 0.55 and KL/r > 100. The resistance of the connections should be larger than T_u and C_u.
- Columns and beams design loads: the gravity load plus the seismic load corresponding to two brace loading scenario 1) when the tension braces reach T_u while the compression braces reach C_u; and 2) when the tension braces reach T_u while the compression braces reach C'_u.

Additional bending demand equal to 0.2 $Z F_y$ should be considered in the plane of the frame for column design.

- Section compactness limit for columns: Class 1 or 2 beam-columns.
- Columns with braces intersecting between horizontal diaphragms (MT-BFs):
  - Maximum number of tiers: 5
  - Horizontal struts should be provided between tiers.
  - Column design loads: the axial loads, shear forces, and in-plane bending moments induced when braces reach T_u and C'_u in any one of the tiers at design storey drift; out-of-plane bending moments induced by transverse loads at each brace-to-column connection equal to 2% of the factored axial compression load in the columns below the connection.

2.3.3 Special concentrically braced frames in AISC 341-10

- Brace frame configuration: tension-compression. Tension-only bracing and K-type bracing are not permitted.
- Height limit: there is no limit for Seismic Design Category B and C. 49 and 30 m for Seismic Design Category D & E and F respectively.
- Approximate fundamental period, T_a: $0.0488 h_n^{0.75}$.
- Fundamental period, T: it should be less than upper limit ($C_u T_a$), where C_u is the coefficient for upper limit on calculated period. For computing storey drift, it is permitted to use the computed fundamental period of the structure without the upper limit.
- Response modification factor, R: 6.0
- Importance factor of the structure for Risk Category II, I_e: 1.0
- Design spectral response acceleration parameters, S_{DS} and S_{D1}: 2 / 3 S_{MS} and 2 / 3 S_{M1} respectively, where S_{MS} and S_{M1} are the Maximum Considered Earthquake (MCE_R) spectral response acceleration parameter for short periods and at 1 s respectively.
- The effective seismic weight, W: calculated using the dead load plus 25% of the live load.
- Seismic response coefficient, C_s: $S_{DS} I_e / R$
- Seismic base shear, V: $C_s W$
- Brace slenderness (KL/r) limit: less than 200.
- Section compactness limit for HSS braces: highly ductile members.

- Expected brace strength: in tension, T_{exp}, is equal to $R_y F_y A_g$; in compression, C_{exp}, is equal to the lesser of $R_y F_y A_g$ and 1.14 $F_{cre} A_g$; and in the post-buckling range, C'_{exp}, is equal to 0.3 C_{exp}, where F_{cre} is the critical stress for flexural buckling of the brace and computed using $R_y F_y$.
- Required tensile strength of brace connections: the lesser of T_{exp} and the maximum load effect that can be transferred to the brace system.
- Required compressive strength of brace connections: 1.1 times C_{exp}.
- Buckling requirements for brace connections: the connections should be designed to resist the flexural forces or rotations imposed by brace buckling.
- Required flexural strength or rotation of brace connections: tequired flexural strength is equal to 1.1 times the expected brace flexural strength, $R_y M_{pbr}$. Required rotation corresponds to the rotation at the design storey drift.
- Required strength of columns, beams, and connections: the gravity load plus the seismic load including the amplified seismic load effects. The amplified seismic load effect include the larger force of the two brace loading scenarios: 1) when the tension braces reach T_{exp} while the compression braces reach C_{exp}; and 2) when the tension braces reach T_{exp} while the compression braces reach C'_{exp}.
- Section compactness limit for columns: Highly ductile members.
- Section compactness limit for beams: Moderately ductile members.

2.4 Column buckling response

Although columns are the most critical components of the structure to maintain the integrity of the gravity load carrying system under seismic load effects, limited research has focused on the buckling response of steel columns subjected to seismic demands. One of the landmark research studies on steel columns is the study performed by Newell and Uang (2006) to evaluate the ductility capacity of steel W-shape columns under axial load and large storey drifts. These researchers conducted an extensive experimental study, which involved cyclic testing of steel columns subjected to various levels of axial loads (equal to 35, 55, and 75% of nominal axial yield strength, P_y) and large drifts. The tested specimens represent the columns in the first storeys of multi-storey steel braced frames. Stocky columns with low width-to-thickness ratio were tested in this program. Loading protocol representing maximum storey drift and axial load demands of the

columns part of multi-storey steel BRBF structure was used to test the specimens. The results showed that columns can maintain axial strength for drifts of 7.0– 9.0% without experiencing any global buckling. The dominant buckling mode was the flange local buckling. This study concluded that columns can exhibit significant rotational capacity, even under high axial force demands. Additionally, the test data corresponds well to the AISC P-M interaction curve as shown in Figure 2.14 for W360x196 specimen with maximum axial force equal to 0.75 P_y; a noticeable overstrength was also observed due to strain hardening effect in large deformation levels.

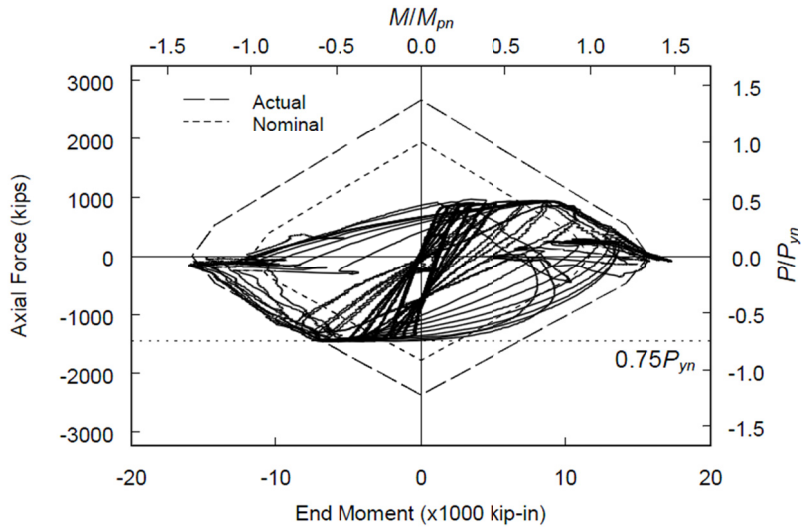

Figure 2.14: P-M Interaction for W360x196 specimen under axial load equal to 0.75 P_y (Newell and Uang 2006).

Buckling response of steel columns in multi-storey braced frames was investigated experimentally by Lamarche and Tremblay (2011). Four full-scale W310x129 specimens were tested under monotonic (one specimen), cyclic loadings (two specimens) and cyclic loading with eccentricity (one specimen). The cyclic tests aimed at examining the seismic buckling of the columns. Initial static axial load corresponding to 60% of the column nominal compressive resistance was applied to reproduce the gravity induced axial load. Cyclic axial displacements were then applied to simulate the seismic demands expected in the braced frame columns. Weak axis buckling of the columns was observed in the tested specimens with the formation of a flexural plastic hinge at the mid-height of the specimens. An example of this buckling mode is shown in Figure 2.15.

Figure 2.15: Weak axis buckling of W-shape column: deformed shape at the end of test (Lamarche and Tremblay 2011).

This study also included a numerical validation using force-based element capable of reproducing residual stresses in the *OpenSees* program. The results of the numerical study confirmed that this program can appropriately reproduce the buckling and post-buckling response of the steel W-shape columns under monotonic and cyclic loadings. Figure 2.16 shows the comparison between the test results and numerical prediction with and without inclusion of residual stresses in the model. As shown, residual stresses have higher effect on the buckling load and the effect diminishes in the post-buckling range.

The comparison between the experimental and numerical results showed that local bucking did not significantly impact the column post-buckling axial resistance for the centrally loaded specimens; however, local buckling occurred before global buckling when the column buckled under eccentric loading. The results of numerical investigations by Fogarty and El-Tawil (2013) and Fogarty et al. (2013) verified the findings by Lamarche and Tremblay (2011) concerning the effect of the flange local buckling on the capacity of braced columns.

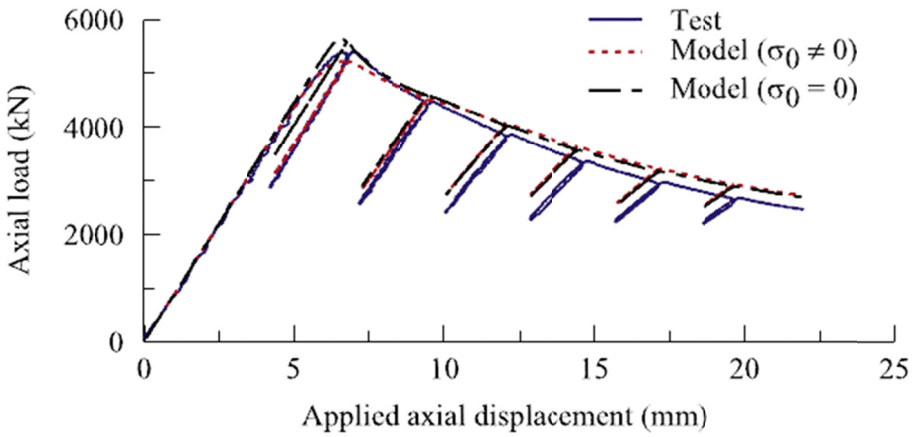

Figure 2.16: Weak axis buckling of W-shape column: axial load-axial displacement response (Lamarche and Tremblay 2011).

CHAPTER 3 METHODOLOGY AND RESEARCH ACTIVITIES

3.1 General

In this chapter, the key accomplishments of the research to achieve the specific objectives are presented. In the first part, the research methodology is explained by presenting some of the main findings obtained in the various phases of the study. The main activities performed in the course of this study are discussed in the second part of this chapter.

3.2 Methodology

3.2.1 Design and nonlinear analysis

MT-BFs are commonly used in North America as lateral load resisting system of tall single storey buildings; however, there has been no research into the seismic response of this framing configuration. The seismic design requirements specified for this framing configuration in Canadian design standard for steel structures (CSA S16-14) lacks sufficient background research. Moreover, no design requirements are available for MT-BFs in the current AISC Seismic Provisions for Structural Steel Buildings (AISC 2010a). Note that, in this thesis, when the "current AISC Seismic Provisions" or "AISC 341" is used, it refers to 2010 edition of this standard. In this regard, it was felt that a seismic evaluation of these frames would be the first step to understand their seismic response and would pave the way to proposing new seismic design guidelines. Therefore, to achieve the first objective, assessing the seismic response of steel multi-tiered braced frames, typical prototype braced frames were selected as part of single storey industrial buildings. These frames were designed based on the Canadian and the U.S. design standards. Then a 3-Dimensional (3D) numerical model of the frame was created using the *OpenSees* program (McKenna and Fenves 2004). The connection details, residual stresses, out-of-straightness, and geometric nonlinearities were included in the model. The model was calibrated against quasi-static cyclic test performed on single-storey steel braced frame using quasi-static cyclic analysis. A number of ground motions were selected and scaled to match the design spectra for Vancouver, BC, in Canada and for Coastal California, CA, in the U.S. A lateral response evaluation of the MT-BFs started with running nonlinear incremental static (pushover) analysis, as this offers a faster and easier way to examine the global and local

response of frames. Additionally, since MT-BFs are Single-Degree-Of-Freedom (SDOF) systems, their seismic response can be predicted well by using pushover analysis. Afterwards, extensive numbers of NonLinear Response History (NLRH) analyses were performed to examine the seismic response of the MT-BFs under seismic ground motions. Several parameters of the braces frames were changed to cover a wide range of situations; these parameters include the frame geometry (total height, number of tiers, and the ratio of Tier 1 height to the height of the other tiers (tier height ratio)), frame ductility (R or R_d factor), and bracing system (Types MD and LD in Canada, and SCBFs, OCBFs, and BRBFs in the U.S.). The influence of the variable parameters on the seismic response of the frames was assessed. Two main criteria were considered to assess the seismic performance of the frames:

1) Column demands and stability conditions: due to the importance of columns as gravity load carrying elements of MT-BFs, special attention was given to this member by evaluating the seismic induced in-plane flexural demand and examining the stability condition of the columns under combined axial compression forces and in-plane bending demands.

2) Tier drift demands: non-uniform brace tension yielding along the frame height may induce large inelastic deformations in the tier(s) where brace tension yielding takes place. The influence of this demand on the braces and their adjacent connections was evaluated.

The pushover analysis is discussed first and NLRH analyses will be presented later. Figure 3.1 shows the results of the pushover analysis for a 2-tiered BF designed in accordance with the AISC 341-10. Two column sizes were studied: W250x115 and W360x196. Smaller columns were designed based on the 2010 AISC Seismic Provisions for axial load only. Larger W360x196 columns were chosen to illustrate the effect of column flexural stiffness on the MT-BF response. The results are first discussed for the smaller W250x115 section. As shown, tier drifts increase nearly linearly in both tiers until brace tension yielding initiated in Tier 2 at approximately 0.5% storey drift. Tier 2 is referred to as the critical tier, as the tension yielding is first initiated in the brace of this tier. The difference between the brace tension forces relative to their expected yield tensile strengths in the two tiers are shown in Figures 3.1b and 3.1c. By further increasing the roof displacement, the compression brace resistance in the critical Tier 2 is reduced as it approaches its post-buckling resistance. This reduces the storey shear resistance in that tier and prevents tension yielding of the brace in Tier 1. Hence, the frame's lateral deflection developed

almost exclusively in Tier 2 as the roof displacement increases (Figure 3.1a) and brace in Tier 1 remained elastic until the end of the analysis. This result confirmed that tier drift is not evenly distributed along the height of the frame. The response shown in Figure 3.1 is typical of MT-BFs with columns designed for axial load only.

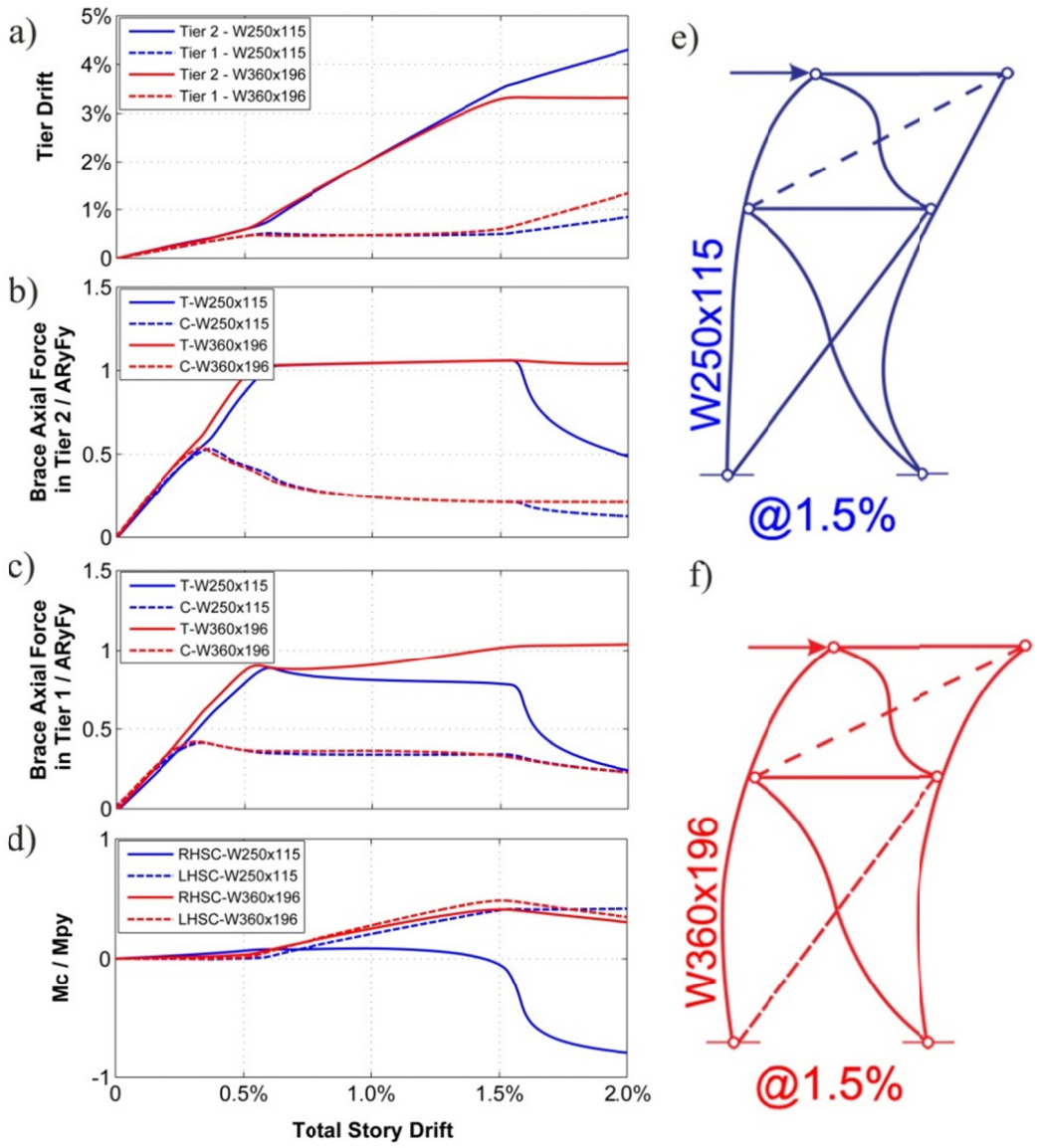

Figure 3.1: Pushover analysis of a 2-tiered braced frame: a) Tier drifts; b) Brace axial forces in Tier 2 (brace compression forces are plotted positive); c) Brace axial forces in Tier 1; d) Column in-plane bending moments at the top of Tier 1; e) Deformed shape of the frame with W250x115 columns at storey drift of 1.5% *h*; and e) Deformed shape of the frame with W360x196 columns at storey drift of 1.5% *h*.

The flexural demands induced in the columns are also shown in Figure 3.1d. The demand is induced by the difference in tier drifts and steadily increased after 0.5% storey drift. At a storey drift of 1.2%, a plastic hinge started to form in the Right Hand Side (RHS) column near the mid-height of Tier 1 due to the moment, amplified by the large axial load from the braces and gravity loads acting on the deformed column. Then, the bending moment at the top of Tier 1 gradually reduced as the curvature of the column was affected by the formation of the plastic hinge and the reduction in the column effective flexural stiffness. In-plane flexural buckling of the RHS column eventually occurred in that tier at a roof displacement of 1.5% h, where h is the total height of the column. After initiation of in-plane buckling, the buckling mode progressively changed to bi-axial buckling. However, this buckling mode is not visible in Figure 3.1 and is discussed for another 2-tiered frame analyzed using the *OpenSees* and *Abaqus* (Simulia 2011) programs in Figure 3.2.

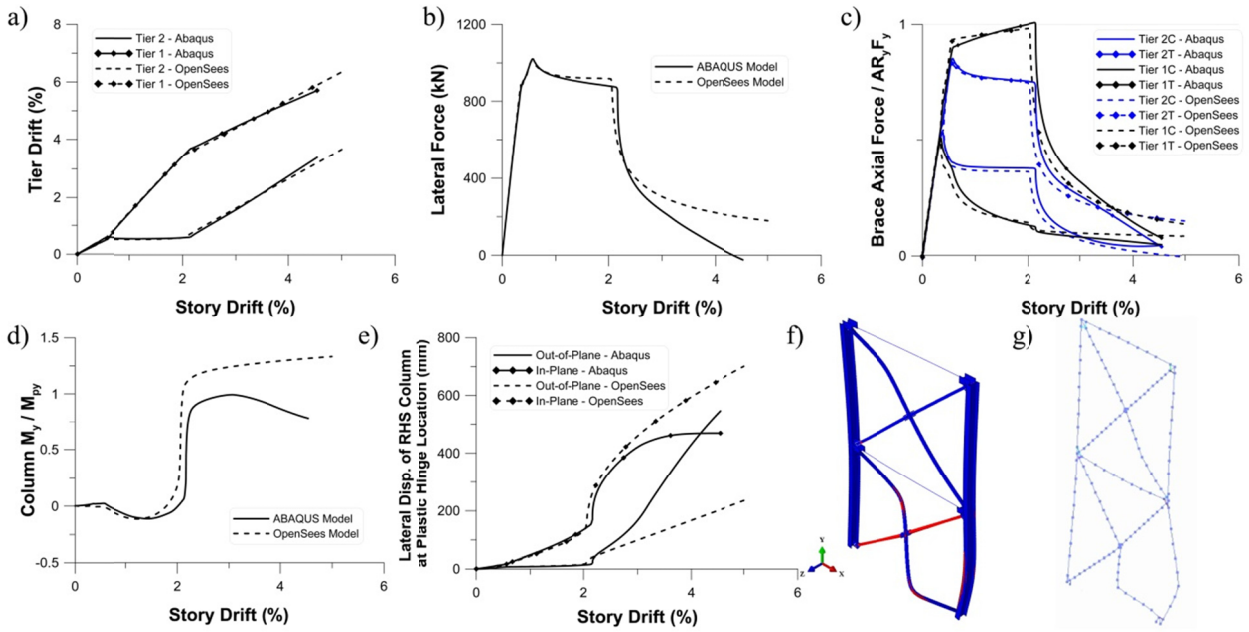

Figure 3.2: Response of a 2-tiered CBF from nonlinear static analysis: a) Tier drifts; b) Lateral load; c) Brace axial forces (both tension and compression forces shown positive); d) In-plane bending moment in the compression (RHS) column; e) RHS column lateral displacement at 40% of Tier 1 height; f) frame deformed shape in *Abaqus*; and g) frame deformed shape in *OpenSees*.

For the frame of Figure 3.2, at a storey drift of 2.0%, the column axial strength suddenly dropped due to in-plane flexural buckling of the compression (RHS) column in Tier 1. Column in-plane

buckling developed first as the column in-plane lateral displacement increased rapidly (Figure 3.2e). This instability mode occurred as a result of plastic hinges forming in the column at the top of and within Tier 1. As shown in Figure 3.2e, complete plastic hinge forming at mid-height of the first tier associated to in-plane buckling mode triggered an out-of-plane buckling response of the RHS column over full height due to the lack of lateral support at the tier level. As a result of this buckling mode, large out-of-plane deformations developed in the column of Tier 1 (Figure 3.2e).

The similar column buckling response was observed for some of the prototype frames studied in this research. This behaviour suggested that the MT-BF response could be improved by increasing the column flexural stiffness, as stiffer columns could contribute to triggering sooner brace tension yielding in the non-critical tier(s), leading to more uniform tier drifts and brace inelastic deformations along the frame height as shown in Figure 3.1 for the frame with the larger W360x196 columns. The stiffer columns were able to initiate yielding of the tension brace in Tier 1 at a storey drift of 1.5%. After this point, the difference between the tier drifts started to reduce, as well as the bending moments and shears in the columns, as the columns gradually straightened up. The higher strength of the stiffer columns also contributed to preventing column plastic hinging and buckling. It was concluded that the variations in tier drifts and brace inelastic demands over the frame height can be controlled and that better column behaviour can be achieved by selecting larger columns with sufficient in-plane flexural stiffness and strength. This observation inspired the proposed design methods that will be discussed later.

3.2.2 Validation of the OpenSees model

Column instability in MT-BFs directed the author to conduct a literature review on column buckling and ductility, and then investigate the buckling response of W-shape steel columns as part of the multi-tiered braced frame. The model of the column was first validated against the data obtained from the experimental study. As described in Chapter 2, Lamarche and Tremblay (2011) performed an experimental study on steel W-shape columns to examine the buckling response of these columns under various loading conditions. A similar test program was developed to perform full-scale column testing at the Structural Engineering Laboratory of Polytechnique Montréal. Detailed information regarding this test program is given in Appendix A. As part of this program, several W250x101 columns were tested under various loading conditions to verify the capability of the new MDHTS apparatus. The experimental data presented here was obtained from tests

conducted by collaborators of this experimental study, Karl Auger (2015) and Yasaman Balazadeh-Minouei (2015). The height of specimens is 4.0 m. The specimens are rigidly connected at their top and bottom ends. The measured column yield strengths were 402 MPa and 398 MPa for the web and the flanges, respectively. In the first test, the column was subjected to cyclic axial displacement. In the other two tests, a constant axial load and a storey drift were applied at the specimens' top end.

In *OpenSees*, the column was modelled using 10 force-based beam-column elements. Gauss-Lobatto integration was used with 5 integration points per element. The web was modelled using 10 fibers while 20 fibers were used for the flanges. The measured column dimensions were used to define the section geometry. Steel02 material was selected for the fibers. The respective measured yield properties were specified for the web and flange fibers. The Young's modulus is equal to E = 200 GPa. The strain-hardening ratio b = 0.75% was assigned to define kinematic hardening of the steel material, and three parameters including R_0 = 24, cR_1 = 0.89, and cR_2 = 0.07 were used to simulate the transition from the elastic to inelastic phases. The isotropic hardening parameters were set equal to a_1 = 0.34, a_2 = 12.2, a_3 = 0.34, and a_4 = 12.2 to model the isotropic hardening of the steel material. An initial sinusoidal out-of-straightness corresponding to the column in-plane buckling mode was assigned to the column with maximum amplitude of 1/1000 of the height. The residual stress pattern proposed by Galambos and Ketter (1958) was specified for the columns.

Figure 3.3 shows the comparison between the test results and the numerical prediction for the first column specimen. For this specimen, a monotonic axial displacement was applied downward at the top of the column up to buckling of the column about its weak axis. A very good correlation was obtained between the test results and the numerical prediction by the *OpenSees* model of the column.

Figures 3.4a and 3.4b show the comparison of the weak-axis bending-storey drift response from the test and numerical prediction for two other W250x101 specimens. Both specimens were subjected to high axial loads and lateral displacement in the column weak-axis. Weak-axis flexural buckling was observed for both specimens under the applied loads. For the first specimen, axial compression load corresponding to 70% of the nominal compressive strength of the column P_n calculated with a yield strength of 385 MPa (from the test performed before coupon testing) was applied, and the loading was followed by six elastic cycles plus two large inelastic cycles corresponding to a storey

drift of 7.0%. In the test, buckling occurred during the second cycle of 7.0% drift. The second specimen was loaded axially first with an axial load equal to 0.9 P_n. Lateral displacement was then applied at the top of the column to induce weak-axis bending demand. The displacement history corresponds to the loading protocol specified for prequalification of beam-to-column connections in Appendix K of the AISC Seismic Provisions. As shown in Figure 3.4, a good match was found between the test results and numerical predictions for both specimens, indicating that the numerical model can properly reproduce the buckling response of the columns. Note that column buckling developed earlier in the numerical analysis compared to the test specimen.

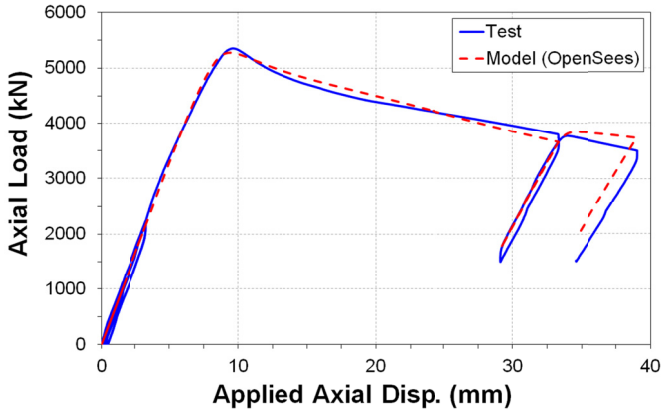

Figure 3.3: Calibration of column weak-axis flexural buckling against monotonic test results of W250x101 specimen under axial displacement (Auger 2015).

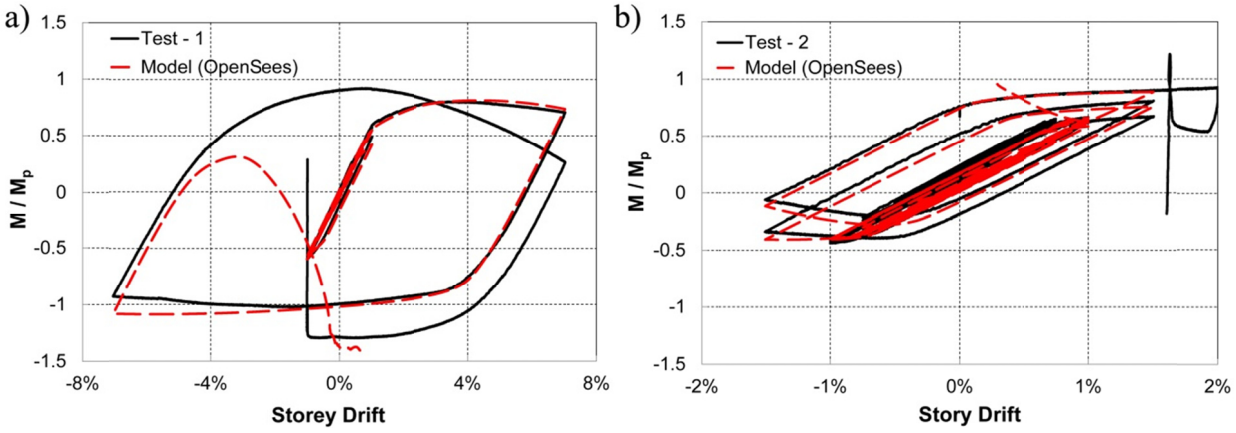

Figure 3.4: Calibration of column weak-axis flexural buckling against cyclic test results: a) W250x101 specimen under 0.7P_n plus 7.0% cyclic storey drift; and b) W250x101 specimen under 0.9 P_n plus storey drift corresponding to the AISC 341 loading protocol (Balazadeh-Minouei 2015).

3.2.3 Column buckling in MT-BFs

Once the numerical model is validated, column buckling response in a real MT-BF under a ground motion was studied. The history of Tier 1 drift, column axial force, and in-plane bending moment demands are illustrated in Figures 3.5b to 3.5d for the first tier column of a 4-tiered CBF with W610x195 columns designed in accordance with the 2010 AISC Seismic Provisions. This column buckled at 16.6 seconds due to the large axial compression and weak-axis in-plane bending demands after two plastic hinges formed at the top of and within Tier 1.

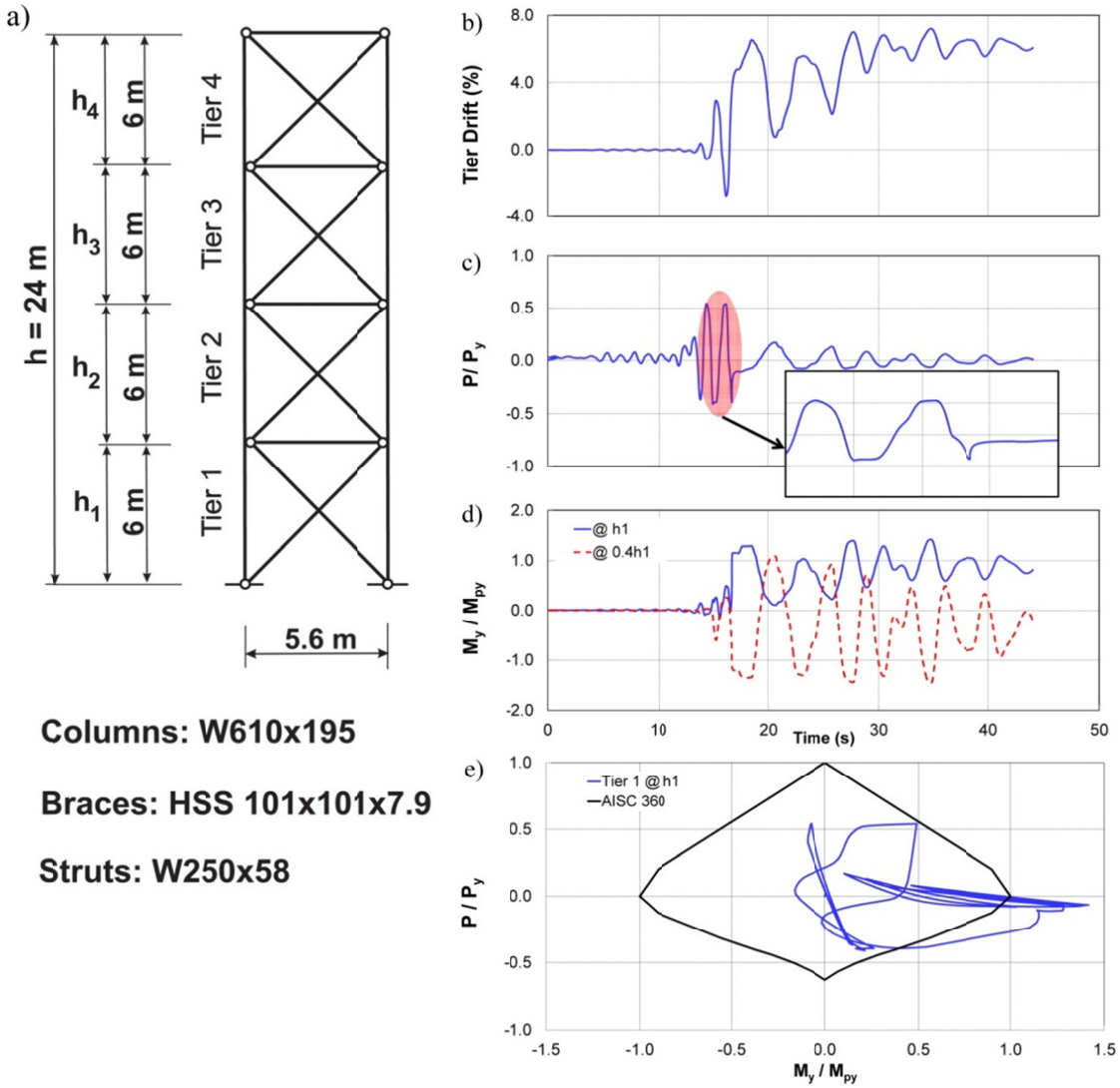

Figure 3.5: Demand history for a 4-tiered CBF under the 1992 Landers, Yermo Fire Station record: a) Frame configuration and member sizes; b) Drift in critical Tier 1; c) Column axial force demand; d) Column in-plane bending demand; e) Column P-M_y interaction demand vs capacity.

For the first tier column of the 4-tiered braced frame studied, the P-M_y interaction exceeds the AISC interaction curve as shown in Figure 3.5e, which indicates the larger capacity of the column compared to the predictions from the code interaction curves.

In Chapter 10, the buckling response of isolated and MT-BF columns will be studied in detail to understand the sequence of events leading to column buckling and examine the influence of the loading conditions on the buckling mode and column strength.

3.2.4 Parametric study

NLRH analysis was performed on a variety of MT-BFs (MT-SCBFs, MT-OCBFs, and MT-BRBBFs) to evaluate the influential parameters on the seismic response of the frames. The results of the NLRH analyses were processed using MATLAB software (MathWorks 2012). The frame global response including storey drift, tier drift, and storey shears, as well as local response including member forces and moments, section stresses, and member deflections were obtained and analyzed to estimate the effect of various parameters on the seismic response of MT-BFs.

For the frames designed in accordance with the U.S. design standards, the results of the NLRH analyses confirmed that the MT-BF columns are prone to buckling as a result of the large in-plane bending demands together with axial compression force, and drift concentration results in large tier drifts capable of causing brace failure. The results of the parametric study also showed that the tendency of drift concentration still exists when designing frames for higher seismic forces (MT-OCBFs); however, the severity of the drift concentration is diminished and the occurrence of column instability is reduced when the buckling-restrained braces are used. Thus, it was demonstrated that there is a need to propose a new design method for steel CBFs to prevent the observed unsatisfactory response.

For the Canadian applications, the results of the NLRH analysis were compared to the design demands anticipated when applying CSA S16 provisions to verify these requirements and/or examine the need to improve the design provisions. It was found that the CSA S16-14 provisions predict well the column demands for the frames within the limits specified in the standard. However, an improved design method needs to propose for the frame exceeding the CSA S16 limits on number of tiers as actual inelastic response of such frames is not properly predicted by the CSA S16 provisions.

3.2.5 Proposed seismic analysis and design methods

To achieve the second objective of this research, developing seismic analysis and design methods for MT-BFs, for the frames designed in accordance with the U.S. design standards, a literature review on brace inelastic response was performed and foundations were laid out to propose new seismic design procedures for MT-BFs based on the observed response. A few critical cases were selected in which column buckling and excessive tier drifts were observed. The inelastic response of the bracing members in these frames was then properly tracked through the nonlinear incremental static and dynamic analyses. Storey shear resistances provided by the braces, which induce unbalanced loads and eventually in-plane bending demands on the columns, were obtained and used to determine the column in-plane flexural bending moments. Meanwhile, the causes of column instability were identified by carefully looking at the column's overall strength, stability, and yielding of the column section where the combination of the axial force and bending demands are maximum. These observations and verifications led to the idea of increasing the column flexural strength and stiffness by introducing in-plane flexural demands in design of MT-BF columns. It was expected that this design would result in an acceptable seismic performance for the MT-BFs, such that brace tension yielding is distributed between the bracing panels and column instability is prevented. An example of such improved response for a 2-tiered CBF is shown in Figures 3.6a to 3.6d. As shown, the proposed method makes use of continuity of the columns to prevent drift concentration in the critical Tier 2.

As shown in Figure 3.6e, since the storey shear resistances are the same for the adjacent Tiers 1 and 2, column seismic induced in-plane flexural bending moment (M_{c1}) is related to the storey shear resistances provided by the braces in the inelastic range at brace yielding initiation in Tier 1. At this point, shear forces that develop in the columns add to the horizontal shear resisted by the bracing members in Tier 2 and brace tension yielding in Tier 1 is triggered when the total storey shear resisted in Tier 2 exceeds the storey shear causing brace tension yielding in Tier 1. Once brace tension yielding has been initiated in Tier 1, further storey drift tends to develop in both tiers, which leads to uniform inelastic demands between the tiers and relaxation of the flexural demand on the columns as they are straightened. Drifts eventually develop in both tiers until the anticipated storey drift is reached.

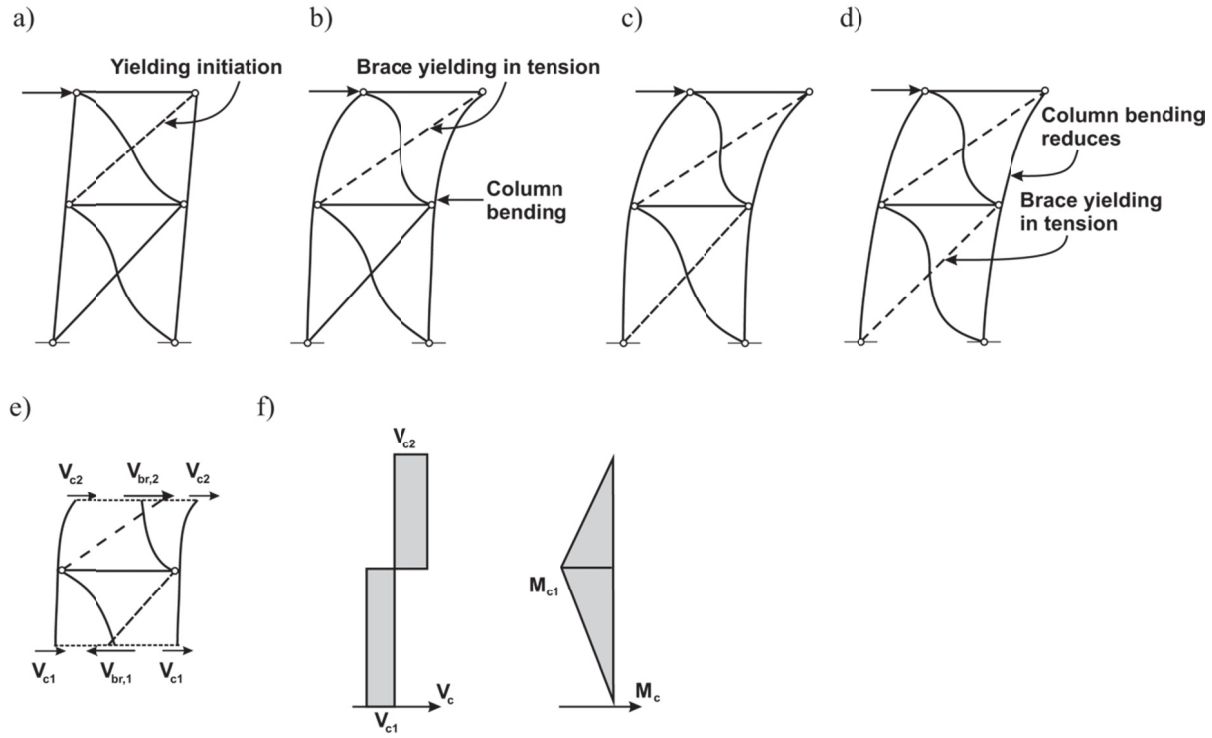

Figure 3.6: Inelastic response of a 2-tiered CBF: a) Initiation of brace tension yielding in critical Tier 2; b) Drift developing in critical Tier 2; c) Initiation of yielding in non-critical Tier 1; d) Drift developing in non-critical Tier 1; e) Horizontal storey shear resisted by braces and columns; and f) Shears and bending moments in columns.

In order to achieve the improved response shown in Figure 3.6, MT-BF columns are redesigned to resist the seismic induced bending moments and axial compression forces as obtained from this analysis. It was confirmed that redesigning columns always results in stronger columns compared to the initial braced frame columns designed in accordance with the 2010 AISC Seismic Provisions. Tier drift calculation was also performed for 2-tiered CBFs to limit the tier drift demand by increasing the column flexural stiffness. An equation was proposed to obtain the critical tier drift for 2-tiered CBFs.

In the proposed design method, the compression brace forces required to compute the storey shear resistances of the tiers depend on the brace axial deformations as confirmed by the brace hysteretic response (Figure 2.1). This dependency is shown for a 2-tiered CBF in Figure 3.7. As shown, when brace yielding is triggered in the first tier, brace compression resistances vary with the tier drift in both tiers. The compression-acting brace force in Tier 1 is less than its buckling resistance C_{exp}

and the compression brace in Tier 2 develops higher force than the minimum post-buckling resistance C'_{exp}. This indicates that the demand on MT-BF columns depends on the relative lateral deformations taking place in the two different tiers. This dependency is accounted for in the proposed design method by assuming brace buckling resistances for the compression braces of the tier that nearly remain in the elastic range, and brace post-buckling resistances for the compression braces of the tiers that experience severe inelastic demands. The reasons for this assumption are as follows:

- the evolution of the compression brace force in the post-buckling range is difficult to estimate in design stage as it varies with tier drift,
- it leads to a conservative design approach for columns, as it increases the unbalanced brace force resistances between adjacent tiers, and
- it is consistent with the brace loading scenarios implicit in the current seismic design provisions in the Canadian and the U.S. standards.

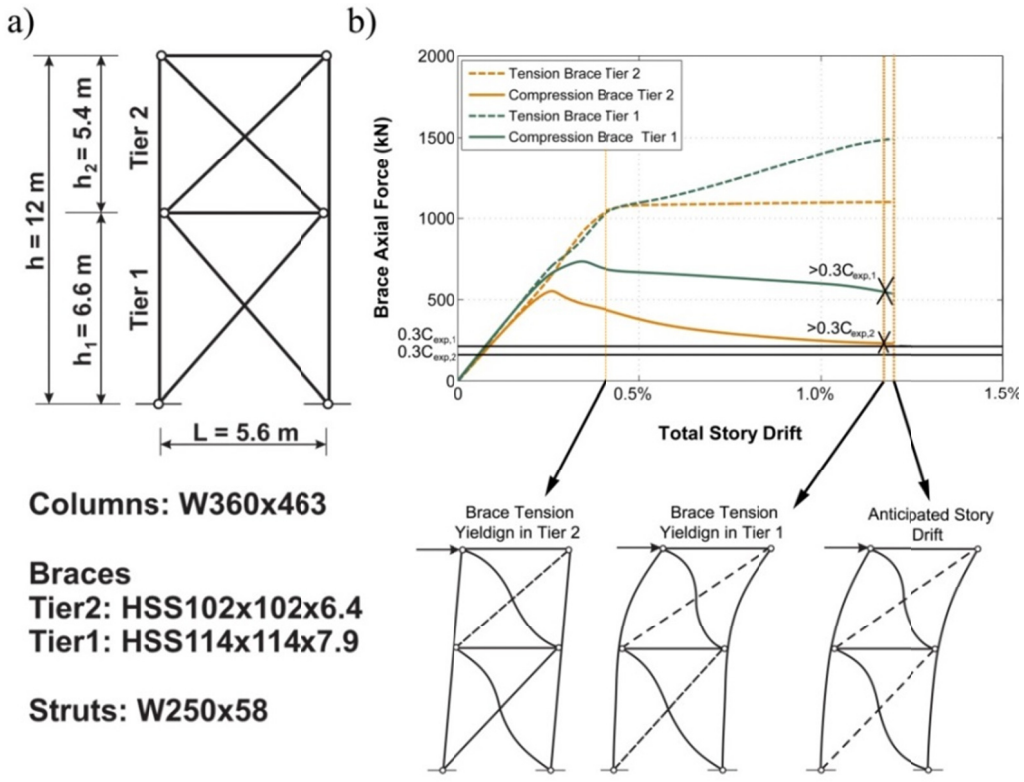

Figure 3.7: a) Frame configuration and member sizes b) Brace axial forces for the improved frame with W360x463 columns (both tension and compression forces shown positive).

The calculation of the required in-plane flexural strength and stiffness for 2-tiered CBF columns paved the way for an analysis method for taller MT-BFs with three or more tiers. Two analysis methods, the sub-structuring technique and the stiffness analysis based method, were proposed for these frames to determine the strength and stiffness of the column for in-plane seismic demand. The methods account for initiation of brace tension yielding in the critical tier and subsequent propagation of brace tension yielding in other tiers, as observed in the NLRH analysis of MT-BFs. In both methods, analysis steps are performed that correspond to occurrences of brace tension yielding as the storey drift increases. In each step, brace forces that represent brace buckling and yielding sequences are considered to determine the column force and tier demands. Bending moments obtained from the methods can be used to design the columns for strength and stability and therefore prevent the column from buckling. The methods also provide minimum column stiffness requirements to trigger propagation of brace tension yielding and minimize drift concentration. The sub-structuring method (Figure 3.8) is a simpler method introduced for well-proportioned braced frames with uniform tier properties over the frame height. It assumes a bottom up or top down brace yielding sequence. As shown in Figure 3.8, each analysis is performed on a simple sub-structure that includes the yielding tiers.

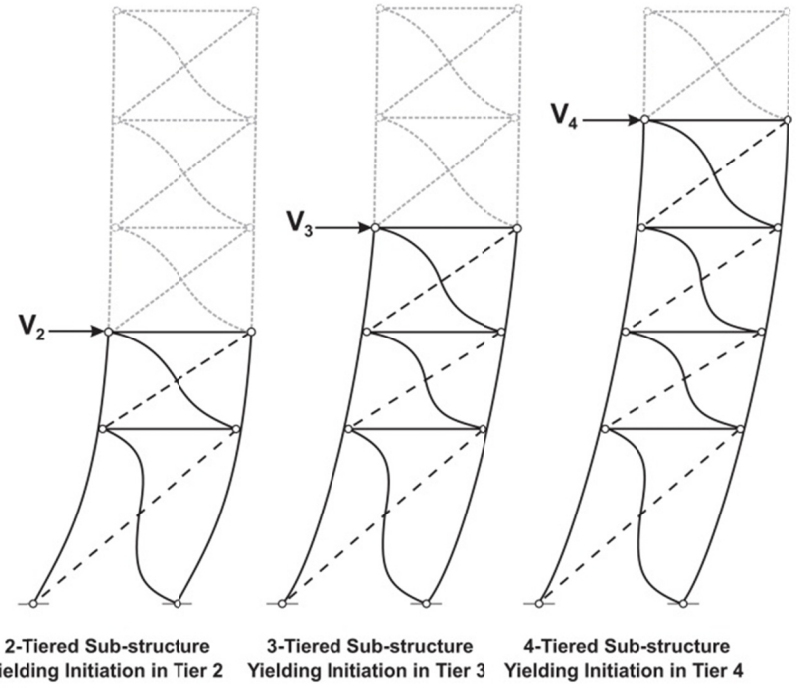

Figure 3.8: Sub-structures analyzed for the bottom up brace tension yielding sequence.

The stiffness analysis method (Figure 3.9) is a more rigorous procedure that predicts the progression of brace tension yielding with consideration of the actual nonlinear response of the frame. The stiffness analysis is performed on an isolated column by solving the stiffness equations for the column under horizontal unbalanced brace forces between two adjacent tiers as external loads. Therefore, the method can be used for any regular or irregular MT-BFs.

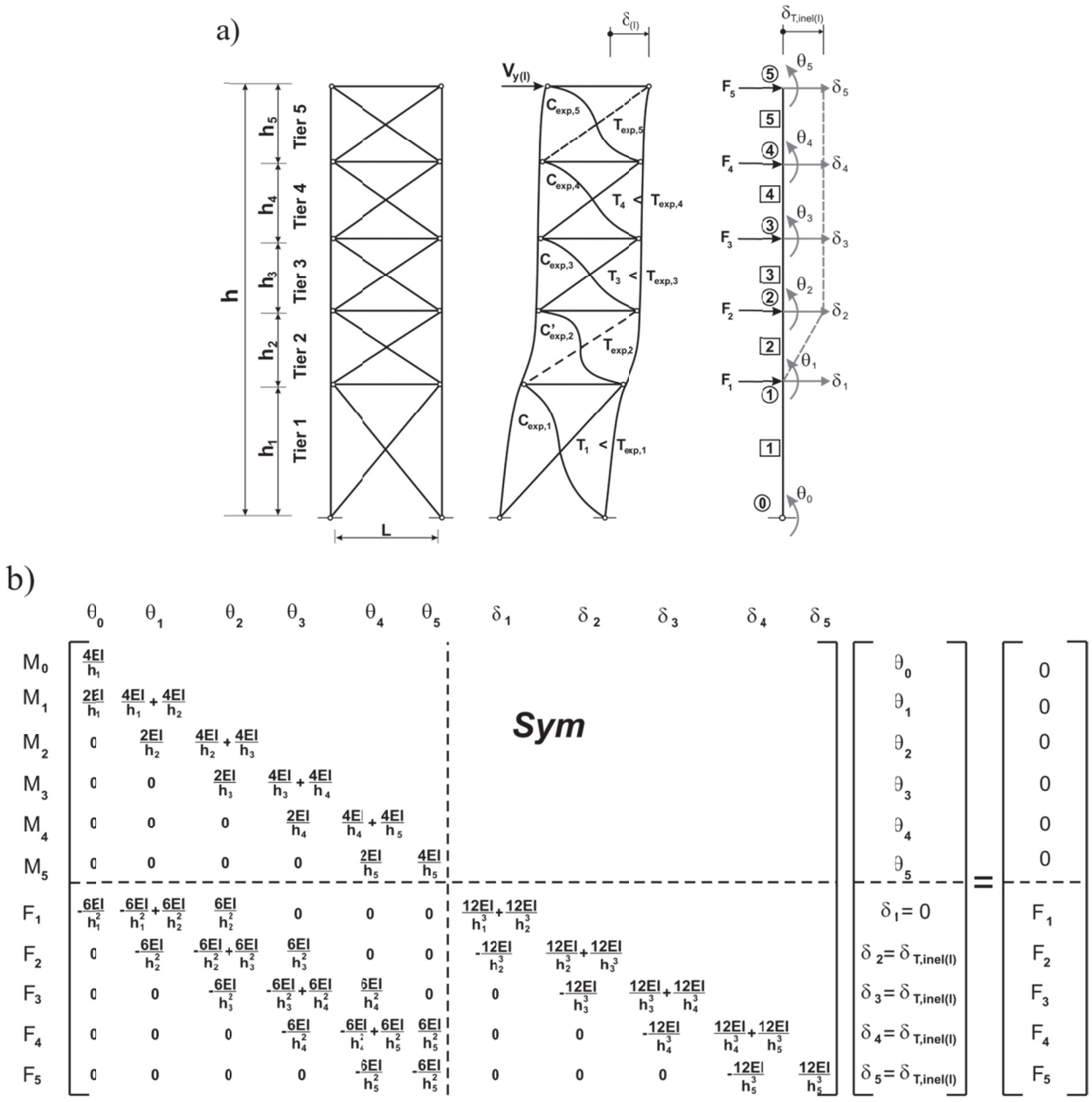

Figure 3.9: Stiffness analysis of a 5-tiered CBF at yielding initiation in Tier 5: a) Frame deformed shape and the isolated RHS column; and b) Corresponding stiffness matrix.

Several alternate strategies were also studied to achieve the second objective of the research. Among those alternatives, the possibility of mobilizing gravity columns in the resistance of in-plane bending moments imposed on the MT-BF columns was examined for applications in the U.S. Figure 3.10 shows the lateral response of a 4-tiered CBF with contribution from gravity columns to resist the seismic induced in-plane bending moments.

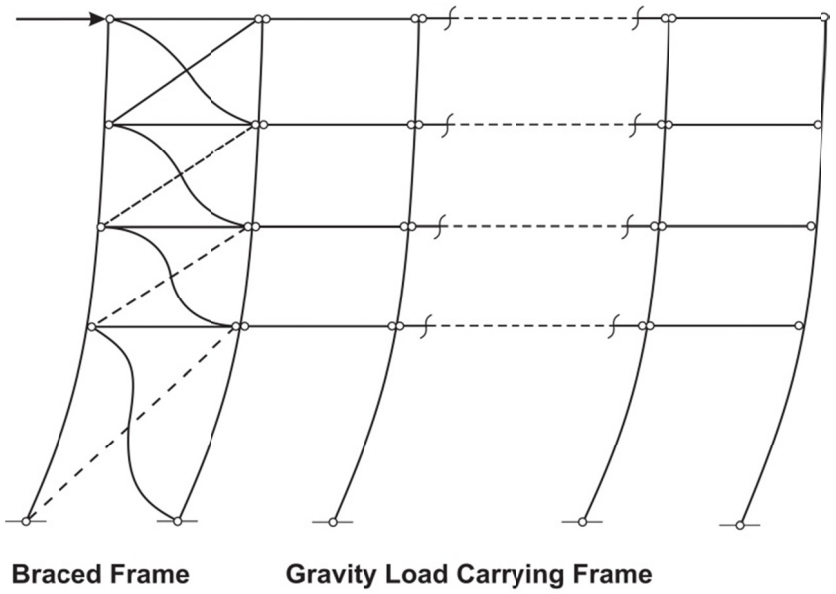

Figure 3.10: Lateral response of a 4-tiered CBF with contribution from gravity columns.

Three approaches were proposed to design the braced frame and gravity columns with the objective of achieving adequate seismic performance and cost-effective design:

1) The gravity columns are designed to carry their share of in-plane bending moments from MT-BF seismic behaviour, and the braced frame columns are only designed for axial compression load.
2) The braced frame columns are sized to resist their share of the MT-BF in-plane flexural demand and no seismic bending demand is considered for the design of the gravity columns.
3) The MT-BF in-plane flexural demand was shared between the braced frame and gravity columns based on their relative in-plane flexural stiffness.

An analysis method was proposed to obtain the column bending moments in these approaches assuming bottom up or top down brace tension yielding sequences. The relationship between the

column shear forces, V_c, in the critical and yielding tier is obtained from the horizontal equilibrium of the storey shears acting in these tiers (Figure 3.11a). Another relationship between the column shear forces in these tiers can be defined assuming that the columns act as continuous members spanning over the tiers studied with assumed brace yielding sequence as shown in Figure 3.11b for the isolated column of a 4-tiered CBF. The ratio between shears in the braced frame columns V_{bc} and gravity columns V_{gc} are based on the relative flexural stiffness of the columns. Once column shears are determined, the bending moments are obtained at tier levels. Figure 3.11b shows a shear force and bending moment diagram along the height of the 4-tiered CBF columns when brace tension yielding initiates in Tier 2.

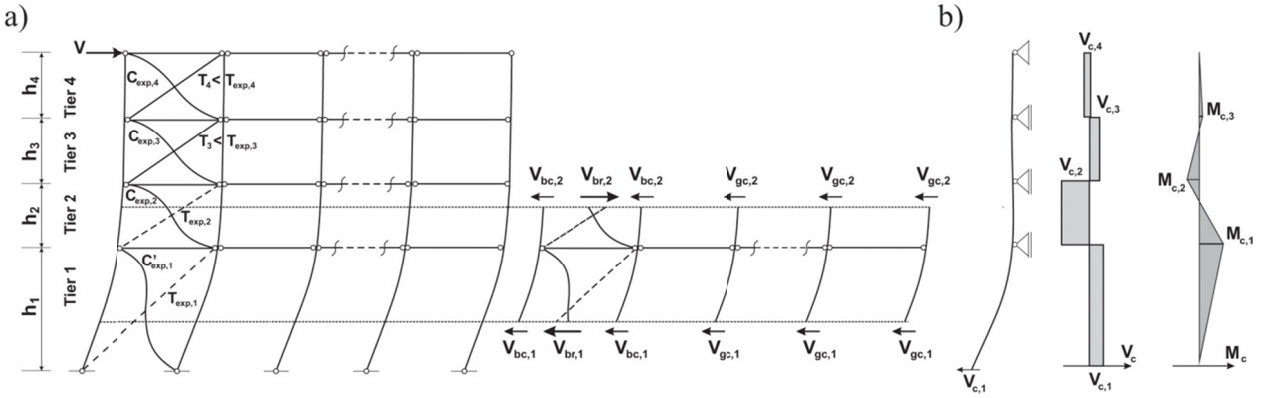

Figure 3.11: Analysis of a 4-tierd CBF with contribution from gravity columns at brace tension yielding in Tier 2: a) Storey shears resisted by the braces and columns; b) Analysis of the isolated column of the 4-tiered braced frame.

The effectiveness of incorporating the gravity load carrying system in preventing the column buckling is shown in Figure 3.12 for a 4-tiered CBF. This frame was designed first in accordance with the 2010 AISC Seismic Provisions (AISC Design) and then redesigned with gravity columns to resist the in-plane bending demands induced by the non-uniform seismic tier drifts. This design was performed based on the second approach proposed. As shown, the braced frame column (BFC) of AISC Design buckled under the ground motion, whereas for Design with gravity columns (GCs), P-M ratios remained below 1.0 for both braced frame columns and gravity columns and no column buckling was observed.

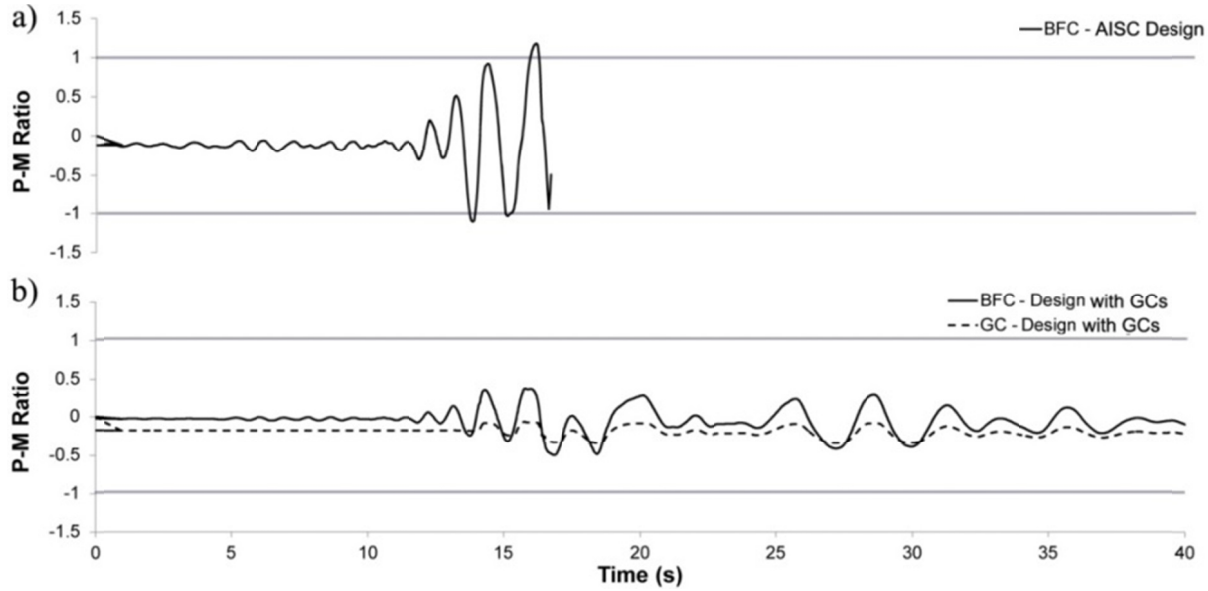

Figure 3.12: P-M ratios in the Gravity Columns (GCs) and Braced Frame Columns (BFCs) under the 1992 Landers, Yermo Fire Station record for a) AISC Design; and b) Design with contribution from gravity columns using the second approach.

In order to achieve the second objective of this thesis research, developing seismic analysis and design methods for MT-BFs, for the frames designed in accordance with CSA S16, the adequacy of the current (2014) design provisions was first verified for the frames complying with CSA S16 limitations. A computer-based analysis method was proposed to analyze and design MT-BFs with uniform or non-uniform properties and frames where brace inelastic deformations distribute in several tiers. An example of such an analysis is shown in Figure 3.13 for a 3-tiered CBF satisfying the CSA S16 limit. As shown, the braces in the critical Tier 1 that have reached their probable resistances are removed and replaced by axial forces corresponding to their probable resistances. Column force demands are then computed using an elastic analysis of the modified frame.

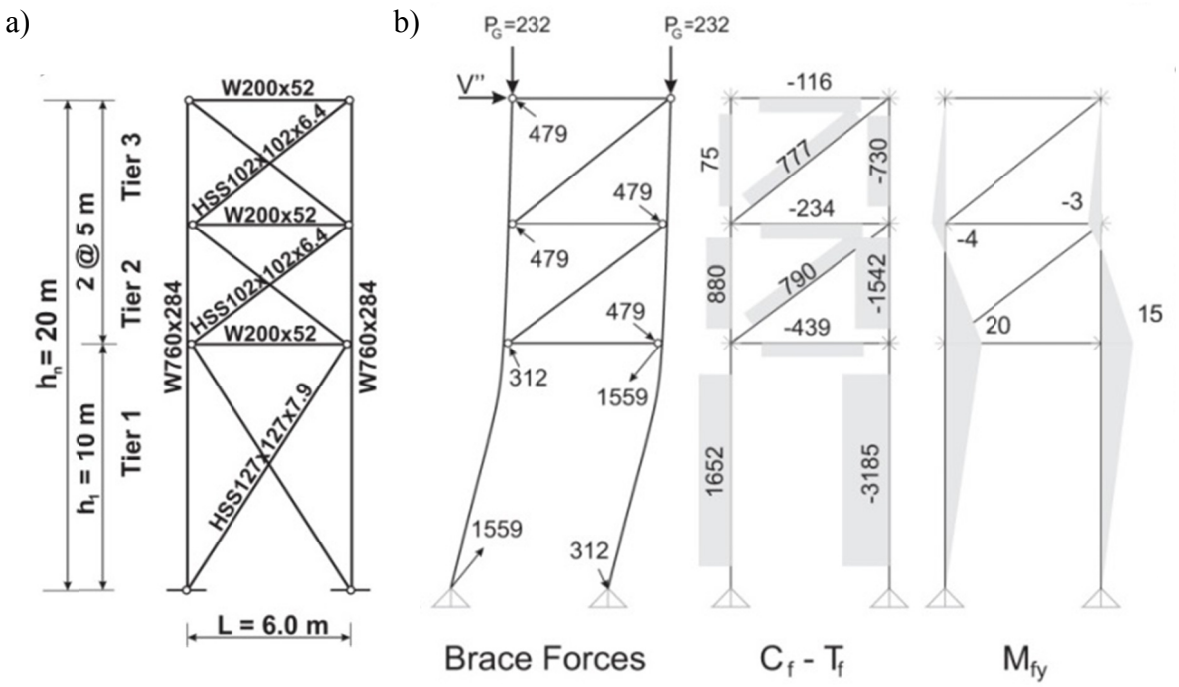

Figure 3.13: Seismic analysis of a non-uniform 3-tiered Type MD CBF: a) Frame configuration and member sizes; and b) Brace forces, axial loads and bending moments in the columns from nonlinear static analysis assuming inelastic demand is concentrated in Tier 1. (forces in kN, moments in kN-m)

A modified analysis procedure was proposed to account for the expected propagation of brace yielding along the height for tall Type MD CBFs with large number of tiers exceeding the CSA S16 limits on the number of tiers. Figure 3.14 shows the concept of progressive brace yielding for a 5-tiered braced frame. As shown, brace tension yielding initiates in Tier 2 and propagates to Tier 3 until the anticipated storey drift is attained. The response is not consistent with the assumption of brace yielding in only one tier implicit in the CSA S16 seismic provisions. However, the proposed analysis/design procedure allows the successive analysis steps to be performed corresponding to the initiation of brace yielding in the frame until the anticipated storey drift is attained (Figure 3.14). NLRH analysis was performed on the prototype braced frames and it was shown that column bending demands and tier drifts were well predicted by this proposed analysis method.

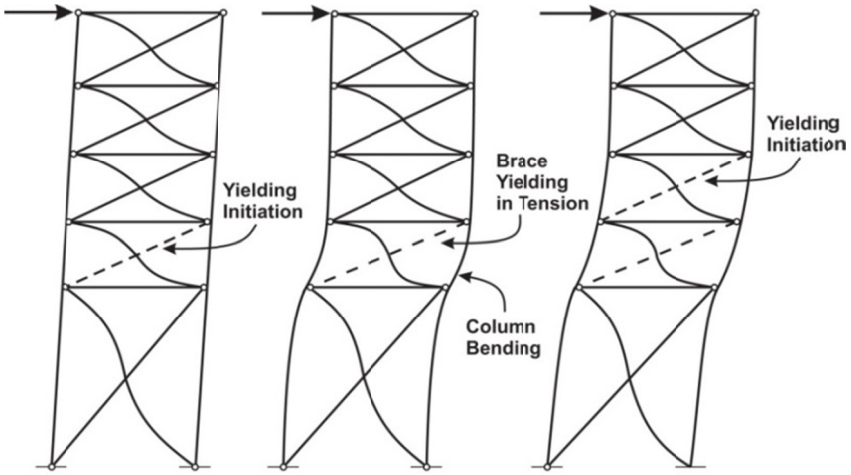

Figure 3.14: Progressive brace yielding scenario for a 5-tiered CBF.

The findings of this thesis research have been shared with the engineering community through several conference papers, reports to and continuous meetings with code committees in Canada and the U.S. Regular meetings were also held with the U.S. research collaborators. These conference papers, which include the findings of several phases of this research project, and journal articles are introduced in Section 3.3.

Extensive numerical validations were performed throughout the research to support the proposals delivered to the code committee. Additionally, several alternative design strategies were investigated for various braced frame systems and their applications were presented to the code committee in the U.S. These strategies include simplified amplification factor method for design of MT-OCBFs, simply-supported column technique for MT-BRBFs, and application of the pushover analysis for MT-BFs. Design recommendations were also delivered to the code developers in Canada based on the knowledge obtained in this study for the frames designed in accordance with the CSA S16 special requirements for MT-BFs.

3.2.6 Development of the MT-BF hybrid simulation

To complement the assessment of the column buckling response, a hybrid simulations test program was initiated to investigate the response of full-scale column specimens that are part of steel CBFs and MT-BFs using Multi-Directional Structural Testing System (MDHTS) at the Structural Engineering Laboratory at Polytechnique Montréal. The main components, features, and capacity of the testing system were reviewed. A 3D finite element model of the MDHTS was created using

the *Abaqus* program. The model included the upper and lower platens, concrete strong floor, connecting plates and bolts. The column specimen was also modeled and connected to the upper and lower platens. Various critical loading scenarios were examined using static displacement-controlled analyses to verify stress level in the components of the system and evaluate the impact of deformations of the connecting plates on the measured stiffness of the specimen.

In the first step of the experimental study, a group of MT-BFs were designed in accordance with the current Canadian and the U.S. design standards and the experimental specimens were selected such that they cover a wide range of the columns used in these frames. W250x101 (smaller square section) and W610x195 (larger deep section) were selected as the experimental specimens. The first group of the specimens including 14 identical W250x101 columns with 4 m height was fabricated. Eight of the specimens were tested under monotonic and cyclic loading to study the buckling response of the steel W-shape columns, evaluate the test setup and the controller system. An evaluation of the results for the preliminary tests confirmed the development of the frictional force in the testing machine, which differs from the measured forces and the expected forces in the specimen. In the next step of the experimental study, the computational model was created for the hybrid simulation using the *OpenSees* and *OpenFresco* (OpenFresco 2012) programs. Purely numerical hybrid simulations were performed using the model developed and MTS Simulation Interface (CSI) which represents the column specimen. The analysis results showed a good correlation between the nonlinear time history analysis and the purely numerical hybrid simulation. However, the main challenge expected in the real hybrid simulation was the consideration and treatment of the frictional forces. The frictional forces developing in the testing system were first measured and calibrated. Possible strategies were then investigated to compensate for the friction present in the system.

3.3 Research activities

This PhD thesis involves three main activities. In Phase 1, the seismic behaviour of MT-CBFs was studied, with focus on the stability of the columns. In Phase 2, seismic design guidelines were developed in the framework of the North American steel design standards to improve the current provisions for the design of multi-panel steel braced frames. In the last phase, a hybrid test program was developed for MT-BF columns. The following summarize the activities performed over the course of this PhD program:

- In the fall of 2010, three courses were taken at Polytechnique Montréal and McGill University in the fields of earthquake resistant design of structures, design of bridges, and research methods. Additionally, a literature review on seismic response of steel CBFs with a focus on nonlinear behaviour of braces was conducted. An initial MT-BF design was also performed in accordance with CSA S16-09.
- A preliminary finite element model was developed in the *OpenSees* program in the winter of 2011. This model was capable of performing static pushover and dynamic response history analyses on MT-BFs with different heights and numbers of tiers. The finite element model was validated against the results of the cyclic tests performed on steel CBFs. The preliminary study on seismic response of MT-BFs designed in accordance with CSA S16-09 provisions was conducted in the fall and summer of 2011. This study included a seismic response evaluation of 2-tiered CBFs using pushover analysis. The results were presented at the *STESSA 2012 conference* (Imanpour et al. 2012a). This study helped understand the seismic response of MT-BFs when the braces respond in inelastic range.
- From the fall of 2011 to summer 2012, a parametric study was performed to investigate the effect of the various parameters on column stability and evaluate the column seismic induced demands specified in CSA S16-09 for 2-, 3- and 4-tiered CBFs. The results of this study were presented at the *3rd International Structural Specialty Conference* (Imanpour and Tremblay 2012) and the *15th World Conference on Eartthquake Engineering* (Imanpour et al. 2012b). An elastic stability analysis was also performed to define the effective length factors for MT-BF columns considering column lateral bracings for in-plane response and variable axial load along the column height.
- A literature review was also engaged in the summer of 2012 on the column buckling response under seismic loading. In addition, a seismic design of prototype frames based on the U.S. design guidelines was performed.
- In the fall 2012 and winter 2013, the numerical analysis of the frames designed for U.S. applications were conducted in collaboration with researchers from the University of Illinois Urbana-Champaign and the University of Iowa. The study was performed in two phases: understanding the seismic response of these frames, and performing a parametric study on prototype frames. The results of this study were presented in a paper entitled “Seismic

Performance Assessment of Multi-Tiered Steel Concentrically Braced Frames Designed in Accordance with Current AISC Seismic Provisions" (Imanpour et al., 2015a) submitted to the *Journal of Structural Engineering, ASCE*. Also, the first part of this study, which involves the seismic performance evaluation of a 4-tiered CBF, was published in the proceedings of the *2013 ASCE Structures Congress* (Imanpour et al. 2013). In addition to a performance evaluation, the development of a new analysis and design method for 2-tiered CBFs was initiated in the spring of 2013.

- A report, which includes the seismic performance of the MT-BFs designed based on the 2010 AISC Seismic Provisions and the proposed seismic design method for 2-tiered CBFs, was prepared and submitted to the AISC Task Committee 9 – Seismic Design in summer 2013. Further refinement of the proposed analysis and design method led to a second journal article entitled: "Design and Analysis of Two-Tiered Steel Braced Frames for Enhanced In-plane Seismic Response" (Imanpour et al., 2015b) submitted to the *Journal of Structural Engineering, ASCE*. A 2-tiered CBF example designed in accordance with the 2010 AISC Seismic Provisions and the proposed method was presented at the *2014 ASCE Structures Congress* (Imanpour et al. 2014a).
- Starting in the fall of 2013, a theoretical study was performed on the steel W-shape columns using the numerical simulations to understand the buckling response of and inelasticity effects on an isolated column subjected to combined weak-axis flexural bending and axial compression force. Additionally, the numerical study on the seismic response of the MT-BFs designed in accordance with the Canadian design standards was expanded for 5-tier frames and the bases of requirements needed to improve the CSA S16 code provisions for the tall MT-BFs was developed. The results of this study were presented at the *10th National Earthquake Engineering Conference* (Imanpour and Tremblay 2014a).
- The application of the proposed analysis and design requirements to braced frames with three or more tiers was investigated in the winter of 2014 by examining the possibility of using pushover analysis to design a 4-tiered CBF. The results obtained from the analysis of the 4-tiered CBF with assumed brace tension yielding sequences were compared to the results of cyclic pushover analysis to verify the analysis method. The results including the application

of the pushover analysis for design of MT-BFs were presented in the conference paper published in the Proceedings of *Eurosteel 2014* (Imanpour and Tremblay 2014b).

- The preparation of the experimental program on columns started in spring 2014. In summer 2014, the experimental specimens including W250x101 and W610x195 columns were designed based on the parametric study performed on MT-BFs. The fabrication of the first group of the specimens (smaller specimens) started in summer 2014. In addition, the finite element model of the MDHTS was developed and influence of the various critical loading conditions on the testing system were analyzed to ensure that all components of the test setup would remain in the elastic range while loading the specimens.

- The contribution of adjacent gravity columns to the seismic performance of MT-BFs was studied in spring and summer 2014. The results were presented at the *12th International Conference on Computational Structures Technology* (Imanpour et al. 2014b). Further development of this concept by performing a parametric study on the frames designed based on the 2010 AISC Seismic Provisions and the proposed design procedure led to a third journal article entitled: "Seismic Design and Performance of Multi-Tiered Steel Braced Frames Including the Contribution from Gravity Columns under In-plane Seismic Demand" (Imanpour et al., 2015c) submitted to the *Journal of Advances in Engineering Software*.

- In summer and fall 2014, various analysis alternatives were investigated to design of MT-CBFs with three or more tiers. Two analysis procedures were eventually developed and proposed in the context of the AISC Seismic Provisions. These methods are presented in a fourth journal paper entitled: "Analysis Methods for the Design of Special Concentrically Braced Frames with Three and More Tiers for In-Plane Seismic Demand" (Imanpour and Tremblay, 2015a) submitted to the *Journal of Structural Engineering, ASCE*. Additionally, alternative design strategies, investigated in parallel, were proposed to the AISC Task Committee 9.

- The experimental program on CBF columns started at the Structural Engineering Laboratory of Polytechnique Montréal in the fall of 2014. This program involves cyclic and seismic quasi-static testing of the CBF and MT-BF columns, and is performed in collaboration with one Ph.D. and two M.Sc. students at Polytechnique Montréal. The author has been involved in this

program and the experience gained was useful in preparation of future hybrid simulations on MT-BF structures.

- Starting in the winter of 2015, a complementary study was performed on MT-BFs designed according to the last edition of the Canadian steel design standard (CSA S16-14), which involves the development of the analysis method consistent with the CSA S16 requirements for the CBFs designed within the limits of this standard. A modified analysis procedure was also developed for taller Type MD CBFs with a large number of tiers. A fifth journal paper entitled: "Seismic Design and Response of Steel Multi-Tiered Concentrically Braced Frames in Canada" (Imanpour and Tremblay, 2015b) was submitted to the *Canadian Journal of Civil Engineering* to present the results of this study.
- From the winter to summer of 2015, the author was involved in a test program including the cyclic testing and hybrid simulation of the steel W-shape columns using the new MDHTS. The computational model of MT-BFs was developed for the hybrid simulation. The numerical verification of the hybrid simulation was conducted using the *OpenSees* model of the frame (computational sub-structure), MTS 793 Software and MTS Simulation Interface (CSI) (MTS 2015). The main challenge in performing the hybrid simulation was the treatment and consideration of the frictional forces. Several tests were conducted to assess and calibrate the frictional forces present in the system. Four strategies were investigated to compensate for the friction forces in the hybrid simulation.

CHAPTER 4 ARTICLE 1 : SEISMIC PERFORMANCE ASSESSMENT OF MULTI-TIERED STEEL CONCENTRICALLY BRACED FRAMES DESIGNED IN ACCORDANCE WITH CURRENT AISC SEISMIC PROVISIONS

Ali Imanpour, A.M.ASCE [1], Robert Tremblay[2], Ali Davaran[3], Christopher Stoakes[4], and Larry A. Fahnestock P.E., M.ASCE [5]

[1]Ph.D. Candidate, A.M.ASCE, Dept. of Civil, Geological and Mining Engineering, Polytechnique Montreal, Montreal, QC, Canada H3C 3A7

[2]Professor, Dept. of Civil, Geological and Mining Engineering, Polytechnique Montreal, Montreal, QC, Canada H3C 3A7

[3]Visiting Researcher, Dept. of Civil, Geological and Mining Engineering, Polytechnique Montreal, Montreal, QC, Canada H3C 3A7

[4]Research Scientist, Dep. of Civil and Environmental Engineering, The University of Iowa, 4105 Seamans Center for the Engineering Arts and Sciences, 103 South Capitol St., Iowa City, IA 52242

[5]Associate Professor, Dept. of Civil and Environmental Engineering, University of Illinois at Urbana-Champaign, 205 North Mathews Ave., Urbana, IL 61801; (corresponding author). email: fhnstck@illinois.edu

The article was submitted to the *Journal of Structural Engineering, ASCE* on August 16, 2015.

Abstract

Multi-tiered steel concentrically braced frames (CBFs) are commonly used to provide lateral resistance for tall single-story commercial, performing arts, sports and industrial buildings. The seismic response of these frames is studied in this paper. A set of seven special concentrically-braced (SCBF) frames, ranging from 9 to 30 m tall with two to six tiers, located in a high seismic area was designed according to the current AISC Seismic Provisions. Fundamental behavior of the two- and four-tiered frames was investigated using 3D finite element models with shell

elements, with particular focus on the buckling response of the columns. The seismic response and stability of the columns were then studied more broadly for all frames using more computationally-efficient 3D finite element models with fiber-based beam-column elements, which were validated against the shell element models. SCBFs designed by current procedures are shown to develop drift concentration in a single tier and high in-plane column bending demand that in some cases leads to flexural yielding and column instability. As potential solutions to this problem, alternate design strategies were studied and their seismic performance is also presented. Designing for higher seismic forces did not appreciably improve column stability, but use of fixed column bases or buckling-restrained braces provided improved distribution of drift over multiple tiers and reduced the occurrence of column instability. Unlike multi-story braced frame seismic design, column flexural demands must be considered in multi-tiered braced frame seismic design.

Keywords: Multi-tiered braced frames, Seismic performance, Column buckling, Nonlinear analysis.

4.1 Introduction

Concentrically-braced frames (CBFs) are effective for providing lateral resistance to single-story steel structures used in a variety of commercial, performing arts, sports and industrial facilities. In building applications that require tall open spaces, it is common to use a multi-tiered bracing configuration when long single bracing members extending from the foundations to the roof level are no longer practical. Figure 4.1 shows two examples of multi-tiered braced frames (MT-BFs) with an X-bracing configuration in each tier. Brace sizes can be reduced significantly with the MT-BF arrangement. In addition, the columns of MT-BFs can be considered laterally braced in the plane of the frame at every tier level, which also reduces the steel tonnage. Adjacent gravity columns located along MT-BF lines can similarly be laterally braced by adding horizontal struts at tier levels, and this is typically done along exterior walls where the struts act as wall girts (Figure 4.1b). Multi-tiered bracing is also used when intermediate lateral bracing is needed along the column height, such as for crane runway girders in industrial buildings.

Multi-tiered bracing can be designed with X-, chevron, V- or single diagonal bracing configurations in the tiers. These tiers in MT-BFs are typically chosen to be uniform over the frame

height, but project-specific constraints may require different tier heights, for example in the first tier to accommodate door openings. Braces and struts can be made from a variety of shapes including angles, pipes, tubes or I-shapes. However, columns are typically I-shaped members oriented for out-of-plane strong axis bending so that the column can resist out-of-plane buckling over the full building height. This column orientation is also preferred when columns must resist out-of-plane moments, as is the case for columns located on exterior walls (wind loads), columns resisting crane loading, and/or that are part of moment frames spanning perpendicular to the braced frame plane.

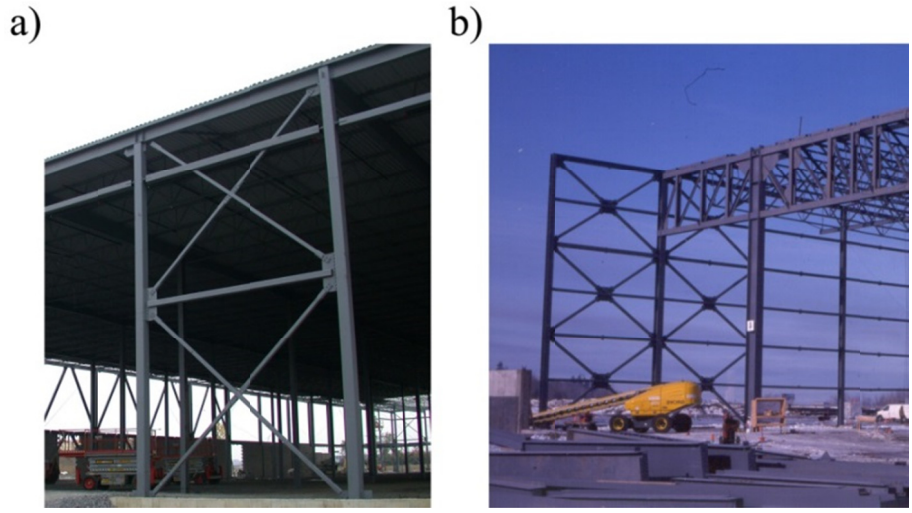

Figure 4.1: Tall single-story steel buildings: a) 2-tiered configuration and b) 3-tiered configuration.

For seismic applications, MT-BFs can be an attractive solution when the selection of the braces is governed by the stringent cross-section and overall slenderness limits specified in the AISC Seismic Provisions (AISC 2010a) for special concentrically-braced frames (SCBFs) to achieve ductile seismic response. In these frames, design forces for brace connections, columns and beams depend on the brace expected axial strengths. Since the stringent slenderness limits can be more easily satisfied with the shorter braces needed in MT-BFs, smaller sections are needed and reduction in design forces for adjoining components can be expected when using this braced frame configuration.

Currently, there is no specific design procedure for MT-BFs in the AISC Seismic Provisions (2010a), and they are in fact not permitted since they are classified as K-braced frames (K-BFs) due to the lack of lateral (out-of-plane) column support at intermediate brace-to-column connection points. Despite this similarity, the inelastic behavior and resulting seismic performance characteristics of K-BFs and MT-BFs are quite different. In the current AISC Seismic Provisions, K-BFs are prohibited for Ordinary Concentrically Braced Frames (OCBFs) and Special Concentrically Braced Frames (SCBFs) because large flexural demands are imposed on the columns due to the horizontal unbalanced brace forces that develop after brace buckling, a condition that may lead to column failures. MT-BFs are designed with horizontal struts at tier levels that can resist the unbalanced brace loads such that lateral loads are still entirely resisted by the braces through truss action after brace buckling, without imposing unbalanced lateral loads on the columns. It is therefore expected that well-proportioned MT-BFs can outperform K-BFs.

Numerical studies recently performed on 2- and 4-tiered X-braced frames designed as SCBFs in accordance with current AISC Seismic Provisions (Imanpour et al. 2013, 2014) showed that properly designed struts can adequately resist and transfer brace unbalanced seismic loads through the braced frame. However, it was also observed that inelastic brace response does not distribute evenly along the frame height, leading to variations in tier drifts and, thereby, bending of the columns (Figure 4.2). Tier drift typically concentrates in the tier where brace tension yielding occurs first, as softening of the buckled compression brace in the same tier limits the story shear in the frame, which prevents brace tension yielding from developing in other tiers. Even in the case of a ideally uniform MT-BF (i.e., uniform tier heights and brace strengths), brace buckling in compression will realistically occur first in only one of the tiers due to unavoidable inherent differences in brace boundary conditions, brace out-of-straightness and material properties. The resulting column flexural demand may compromise the stability of the columns. Furthermore, the larger drifts in the critical tier may impose excessive ductility demand on the braces, which may lead to premature brace low-cycle fatigue fracture. Columns must therefore be designed to resist the expected flexural demands. Consideration of these column flexural demands is a unique aspect of MT-BF seismic design that is not required for multi-story CBFs. As already noted, MT-BFs do not have out-of-plane support at the tier levels and coupled in-plane and out-of-plane column limit states are possible, whereas multi-story CBFs do have out-of-of plane support at the floor levels. In addition, MT-BFs do not develop inertial forces at

the tier levels, so all inelastic force redistribution must happen within the braced frame. In contrast, multi-story CBFs have significant inertial forces at the floor levels, which play a significant role in equilibrating unbalanced forces that develop after brace buckling and yielding.

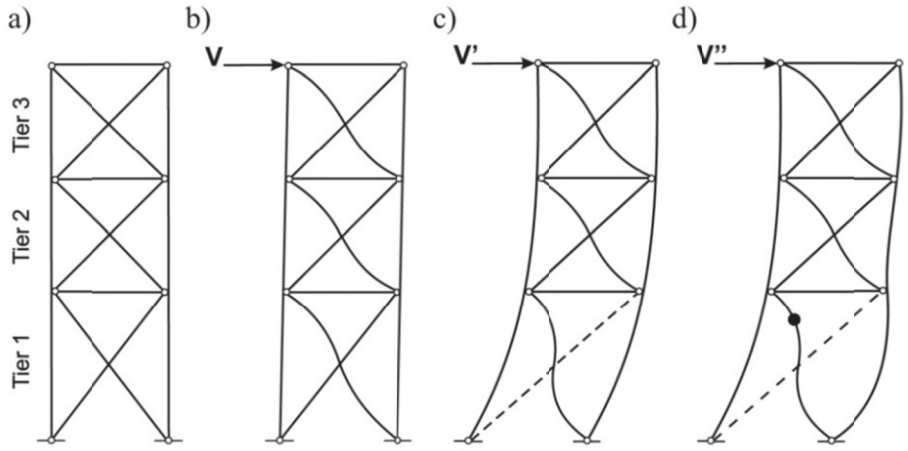

Figure 4.2: Concentration of inelastic demand in a 3-tiered CBF.

In past MT-BF studies, analysis was performed using the *OpenSees* analysis platform with fiber-based nonlinear beam-column elements for the braces and columns. although this modeling approach had been extensively validated for single-plane flexural buckling of braces (e.g., Aguerro et al. 2006, Uriz et al. 2008) and columns (e.g., Lamarche and Tremblay 2011), it has not been verified for cases such as in-plane buckling of MT-BF columns, which have no out-of-plane lateral support and may exhibit flexural-torsional response due to bi-axial moment demands. In addition, previous studies have been limited to two MT-BF configurations and a broader study considering the influence of the number of tiers and tier heights as well as possible methods for improving MT-BF response was needed. Furthermore, recent finite element simulation by Stoakes and Fahnestock (2012) showed that the strong-axis buckling strength of isolated MT-BF W-shape columns can be reduced under monotonic loading due to the presence of weak-axis flexure if the weak-axis rotation is large and torsional restraint is not provided at the tier levels. This study raised concerns regarding the possibility of coupled in-plane and out-of-plane buckling of W-shape columns that are part of MT-BFs under in-plane seismic demand induced by brace nonlinear response. Therefore, the interaction between columns and the other members of a MT-BF during a seismic is an important consideration.

This paper presents a parametric numerical study that was performed to examine the seismic response of seven MT-CBFs having different heights, number of tiers and tier height ratios. The study focuses on tier drift demands, column flexural demands, and column stability. Alternative designs are also presented, including the use of OCBFs, SCBFs designed for larger seismic forces or buckling restrained braces (BRBs). The influence of column base fixity is also examined. Nonlinear three-dimensional (3D) finite element analyses using shell elements were performed on four-tiered and two-tiered braced frame prototypes, which were designed according to current AISC Seismic Provisions, to study the fundamental inelastic seismic frame behavior with focus on column stability. The results of these *Abaqus* analyses were used to validate the more computationally-efficient *OpenSees* 3D finite element modeling approach using fiber-based beam-column elements, which was then used for the parametric study.

4.2 Seismic design of MT-BFs according to current AISC provisions

MT-BFs having different heights and number of tiers are examined in this study (Figure 4.3). All frames are used to laterally brace a tall single-story industrial steel building having 128.8 m x 50.4 m plan dimensions. In each of the two orthogonal directions, four multi-tiered CBFs are used to resist lateral loads. All braced frames have a width of 5.6 m. The columns support 50.4 m long roof trusses that span over the full width of the building. For simplicity, the braced frames do not provide lateral intermediate in-plane bracing to the other columns along the exterior walls. Horizontal struts are provided at all tier levels to maintain a lateral load path in the braced frame after brace buckling and to avoid the undesirable K-BF configuration. All frames were designed in accordance with ASCE 7-10 (ASCE 2010), and member design was performed in accordance with the AISC 360-10 Specification (AISC, 2010b) and the AISC 341-10 Seismic Provisions (AISC 2010a). In this section, the seismic design of the uniform 4-tiered X-braced-frame with total height of 24 m (Frame 4) is illustrated. Details of the frame are given in Figure 4.4.

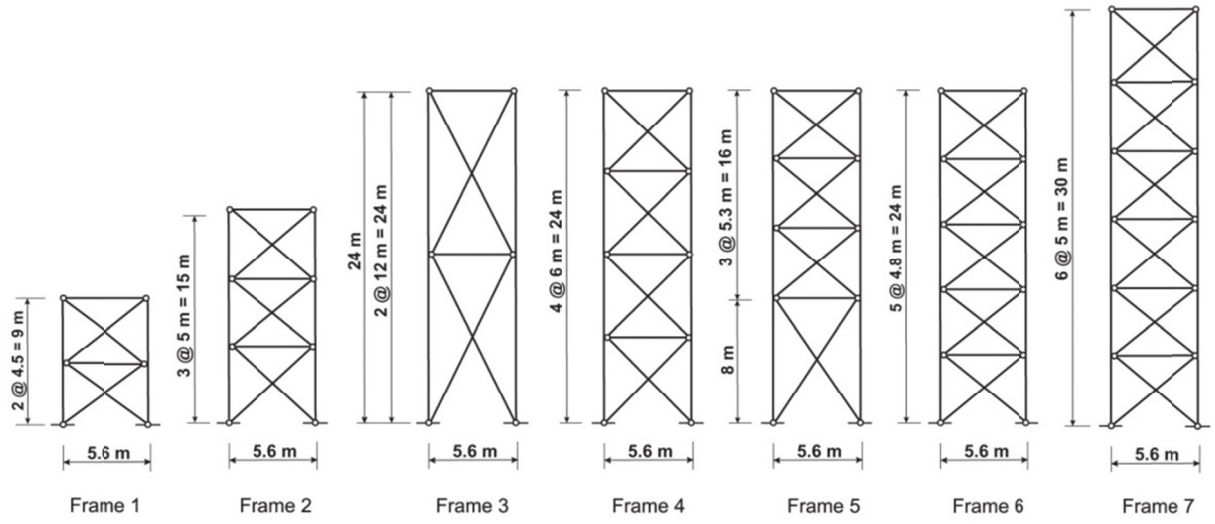

Figure 4.3: Geometry of MT-BFs studied.

Roof dead (D) and live (L) loads were taken equal to 1.2 kPa and 0.96 kPa, respectively and the exterior wall weight was 1.2 kPa. For simplicity, only the load combination involving the dead load (D) and the seismic loads (E) is considered herein. For seismic loading, the structure is assumed to be located on a site class D in coastal California and design spectral response acceleration parameters are S_{DS} = 1.0 and S_{D1} = 0.6. The structure is assigned to Seismic Design Category (SDC) D. The SCBF system, with response modification coefficient R = 6.0 and deflection amplification factor C_d = 5.0, was selected. The importance factor, I_e, is equal to 1.0. The equivalent lateral force procedure was used to calculate the seismic load. The fundamental period, T, the resulting seismic response coefficient, C_s, and the design story shear per braced frame, V, are equal to 0.74 s, 0.135, and 481 kN respectively.

The bracing members are designed with an effective length factor of 0.45, and the required brace compressive strength including seismic and gravity load effects is equal to 364 kN. HSS 102x102x7.9 members conforming to ASTM A500, Grade C (F_y = 345 MPa), were selected. According to AISC 341-10, beams and columns in SCBFs must be designed to resist tributary gravity loads plus the larger of the axial forces induced by the following brace force scenarios (Figures 4.4b and 4.4c): 1) braces reaching their expected strength in tension (T_{exp}) and in compression (C_{exp}); and 2) all tension braces reaching their expected strength (T_{exp}) while all compression braces reach their expected post-buckling strength ($C'_{exp} = 0.3\ C_{exp}$).

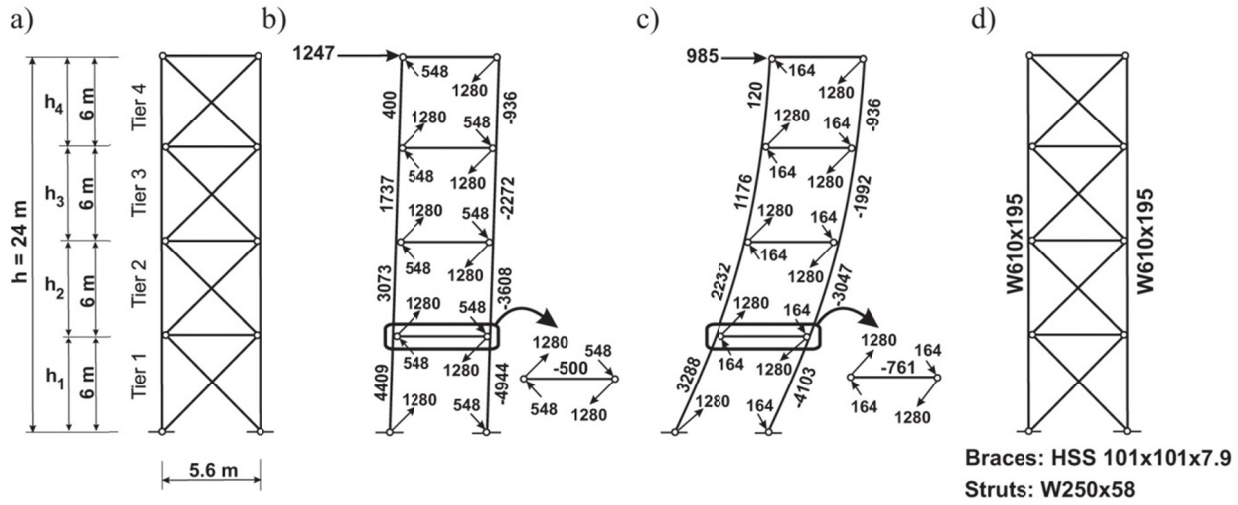

Figure 4.4: Four-tiered BF: a) Geometry; b) Axial forces in columns and struts due to brace forces $T_{exp} + C_{exp}$ (kN); c) Axial forces in columns and struts due to brace forces $T_{exp} + C'_{exp}$ (kN); and d) Selected members.

The continuous columns are made of W-sections conforming to ASTM A992 with F_y = 345 MPa. They are assumed to be pin-connected about both axes at the base and torsionally restrained at their top and bottom ends. Torsional restraint is also provided at every tier level by the struts. Column design was performed considering only axial load effects, as currently permitted in AISC 341-10. Reduced column buckling lengths were considered for in-plane (0.80 h_1) and out-of-plane (0.79 h) flexural buckling limit states due to the variation of the axial load over the column height (Simão et al. 2012; Dalal 1969; Timoshenko and Gere 1961), and a W610x195 section was selected.

A W250x58 ASTM A992 section was selected for the struts to resist the compressive axial forces corresponding to the horizontal projection of the unbalanced brace forces for the scenarios of Figures 4.4b and 4.4c. To prevent torsional buckling of the columns, the struts are oriented with their webs horizontal. They are also rigidly connected to the columns such that they can restrain the torsional rotation of the columns through bending about their strong axis in the horizontal plane. An example of a strut-to-column connection detail proposed to achieve this behavior is illustrated in Figure 4.5a, and the 3D shell element model of this connection is shown in Figure 4.5c.

Table 4.1: Design parameters and properties of the MT-BFs studied.

Parameter	Frame 1	Frame 2	Frame 3	Frame 4	Frame 5	Frame 6	Frame 7
Design fundamental period (T), s	0.36	0.52	0.74	0.74	0.74	0.74	0.88
Seismic response coefficient (C_s)	0.167	0.167	0.135	0.135	0.135	0.135	0.114
Design story shear per frame (V), kN	446	485	481	481	481	481	447
Design story drift (Δ), %	0.88	1.13	1.04	1.25	1.25	1.33	1.41
Computed fundamental period (T_1), s	0.58	0.88	1.16	1.28	1.28	1.32	1.65
Design story drift (Δ_{T1}), %	0.88	0.79	0.67	0.72	0.75	0.76	0.77
Braces (Square HSS, b x d)	102x 6.4	102x 6.4	152x 9.5	102x 7.9	89x9.5 &114x 7.9	102x 6.4	102x 6.4
Columns (W)	360x 79	410x 114	690x 419	610x 195	610x 195	610x 195	690x 240
Struts (W)	250x 58	250x 58	250x 58	250x 58	250x 58	250x 58	250x 58

The chosen member sizes are given in Figure 4.4d. Under the seismic load of 481 kN, the design story drift, $\Delta = C_d\delta_e/I_e$, is equal to 299 mm. This corresponds to 1.25% h, less than the allowable story drift of 0.02 h prescribed in ASCE 7-10. The fundamental period of the frame from modal analysis, T_1, is equal to 1.28 s, which is longer than the period T = 0.74 s corresponding to the upper limit C_uT_a that was used in design. As permitted in ASCE 7-10, drift can be calculated using seismic loads obtained with T_1, which gives a design story drift Δ_{T1}= 0.72% h. The same design procedure was used for the other frames of Figure 4.3 and key properties and member sizes are given in Table 4.1.

4.3 Seismic response using shell element models

4.3.1 Numerical model and ground motions

Nonlinear analysis of the 2-, 3- and 4-tiered SCBF structures of Figure 4.3 (Frames 1, 2 and 4) was performed using a 3D finite element model with shell elements in *Abaqus* (Simulia 2011). Nonlinear static and dynamic analyses were performed to study column in-plane bending demand and evaluate stability of the columns subjected to axial load and biaxial bending. An isometric view of the *Abaqus* model for Frame 2 is shown in Figure 4.5b.

As shown in Figure 4.5b, four-node shell elements with reduced integration, were used to model the columns, braces, gusset plates, and splice plates. Sensitivity analysis of an isolated column model was performed to determine an appropriate mesh discretization (Stoakes and Fahnestock 2012). A 500-mm long strut stub was also modeled with shell elements within the strut-column-brace connection region at each tier level. A finer mesh discretization was used in the connection regions to capture stress concentrations in these areas (Figure 4.5c). Outside the tier-level connection region, the struts were modeled with three-dimensional beam elements with cubic shape functions. A leaning column and an axially rigid link connecting the leaning column to the MT-BF were also modeled with three-dimensional beam elements to account for P-delta effects. Geometric nonlinearity was included through large-displacement element formulations. Material nonlinearity was incorporated through the Maxwell-Huber-Hencky-von Mises yield criterion with associated flow rule. Steel stress-strain behavior was adapted from prior experimental studies (Stoakes and Fahnestock 2012a, Peng 2001, Kauffman and Pense 1999). The nonlinear kinematic/isotropic cyclic hardening model in *Abaqus* (2011) was chosen, and the hardening parameters were determined based on cyclic stress-strain data from Kauffman and Pense (1999). Residual stresses were specified for the columns (Galambos and Ketter 1958) and initial out-of-straightness having a half-sine profile with maximum amplitude of 1/1000 of the member unsupported length was specified for the columns in both orthogonal directions and out-of-plane for the bracing members. At the bottom of the MT-BF and leaning columns, the three translational degrees of freedom and rotation about the y-axis (torsion) were restrained to simulate pinned column bases. At the top of all columns, only the out-of-plane (z-direction) translation was restrained. Gravity loads were applied as concentrated forces at the top of all three columns. To account for possible non-uniform material properties among the members, the yield stress in Tier 1 was assumed to be 5% lower than the yield stress in the remaining tiers. As the first tier column segment carries the maximum axial force demand, reducing the brace yield strength in Tier 1 may lead to the most critical condition.

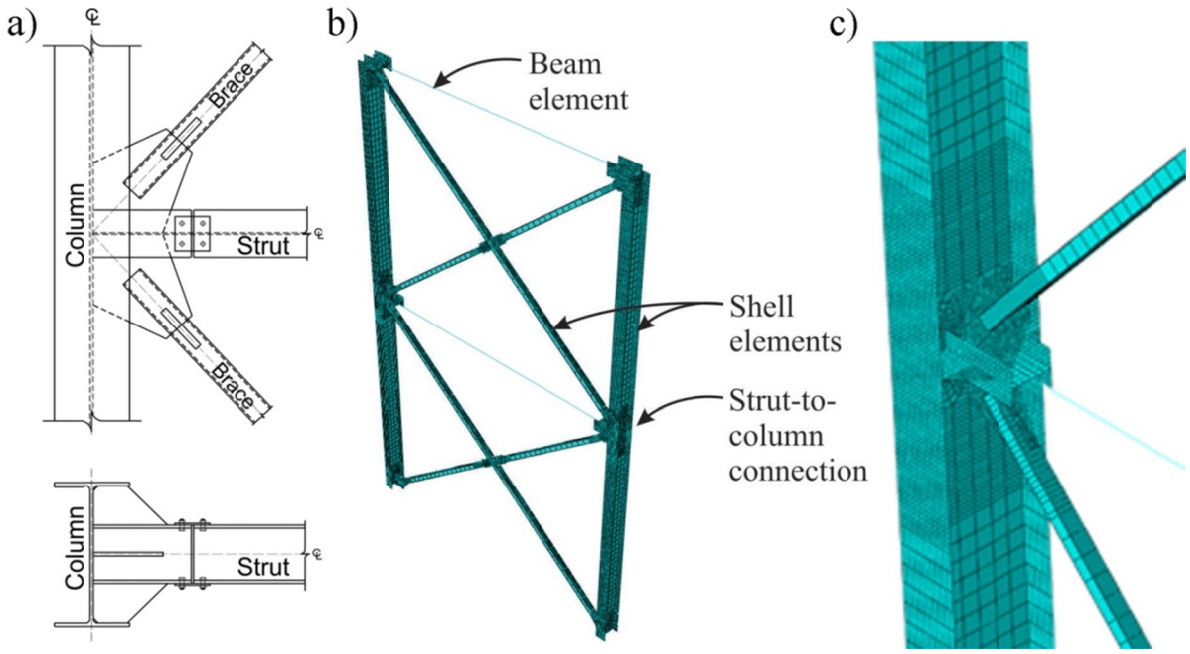

Figure 4.5: a) Torsional bracing of columns using the flexural stiffness of the struts and a torsionally stiff strut-to-column connection; b) Finite element model of 2-tiered SCBF (Frame 1) and; c) Detail of strut-to-column connection from finite element model.

For Nonlinear Response History (NLRH) analyses, ground acceleration records were prescribed for the in-plane direction (x-direction) at the base of the frame. The first component of the 22 motion, far-field ground acceleration record set proposed in FEMA P695 (FEMA 2009), was used as the basis for the NLRH analyses. The ground acceleration records were normalized by peak ground velocity, and then scaled so the median spectral acceleration of the ground acceleration suite matched the code-prescribed maximum considered earthquake (MCE) response spectra at the fundamental period of each braced frame (FEMA 2009). Point masses accounting for the seismic weight of the roof and exterior wall cladding were applied at the top of the MT-BF columns. Mass and stiffness proportional damping corresponding to 2% of critical were considered in the finite element model.

4.3.2 Single-record case study of 4-tiered MT-BF seismic response

In this section, the results for the 4-tiered braced frame (Frame 4) are first illustrated for one of the 22 ground motions, and subsequently the response for the full suite is summarized. As shown in Figure 4.6a, the peak story drift reached nearly 4% at t = 56 s, which is approximately 3.2

times the story drift anticipated in design. The tier drift histories shown in Figure 4.6b illustrate that drift is concentrated in Tier 1, reaching approximately 9.0% h_1 at t = 56 s, or nearly double the peak story drift. Drifts in all other tiers remained below 1.5% until 56 seconds indicating that nearly all nonlinear deformations of the frame develop in Tier 1. Tier 1 and 2 brace hysteretic responses are shown in Figures 4.6c and 4.6d respectively. In Tier 1, the two braces experienced large inelastic excursions in tension and compression whereas the braces in Tier 2 only buckled without yielding in tension. At around t = 56, plastic hinges formed in the right hand side (RHS) column at the Tier 1 strut level and at mid-height of Tier 1 because the non-uniform distribution of tier drift induced large in-plane flexural bending in the column. In the presence of large compressive axial force, these two hinges led to in-plane column buckling in Tier 1 that caused the frame to collapse. The frame deformed shape at incipient collapse is shown in Figure 4.6e. Although column buckling was initiated by in-plane demands, out-of-plane column deformation subsequently developed within the full story height, and the final buckling mode involved flexural-torsional response. This response is expected as in-plane and out-of-plane demands can localize compression yielding unsymmetrically at the tips of the column flanges and trigger a flexural-torsional buckling mode. In Figure 4.6b, it should be noted that the rapid growth in Tier 2 drift when approaching collapse is not due to deformation within the tier, but rather due to rigid body motion of Tier 2 as the column in Tier 1 is buckling.

For this frame, Tier 1 is called the critical tier as inelastic brace response concentrated in that tier, causing in-plane bending and eventually buckling of the columns in that tier. A second important consequence of drift concentration in the critical tier is the inelastic deformation (ductility) demand being imposed on the bracing members. Past inelastic cyclic tests on steel bracing members have shown that they generally fail due to low-cycle fatigue at the location of the plastic hinge forming upon brace buckling. For HSS members, failure typically takes place at drifts varying between 1.5 to 2.5% (Tremblay 2002; Tremblay et al. 2003, 2008; Fell et al. 2009; Hsiao et al. 2013). Low-cycle fatigue failure of the braces was not modelled in this study. However, in view of the large tier drift demand, it is very likely that the brace in Tier 1 would have failed under this ground motion, even if the story drift did not exceed 1% h (Figure 4.6b).

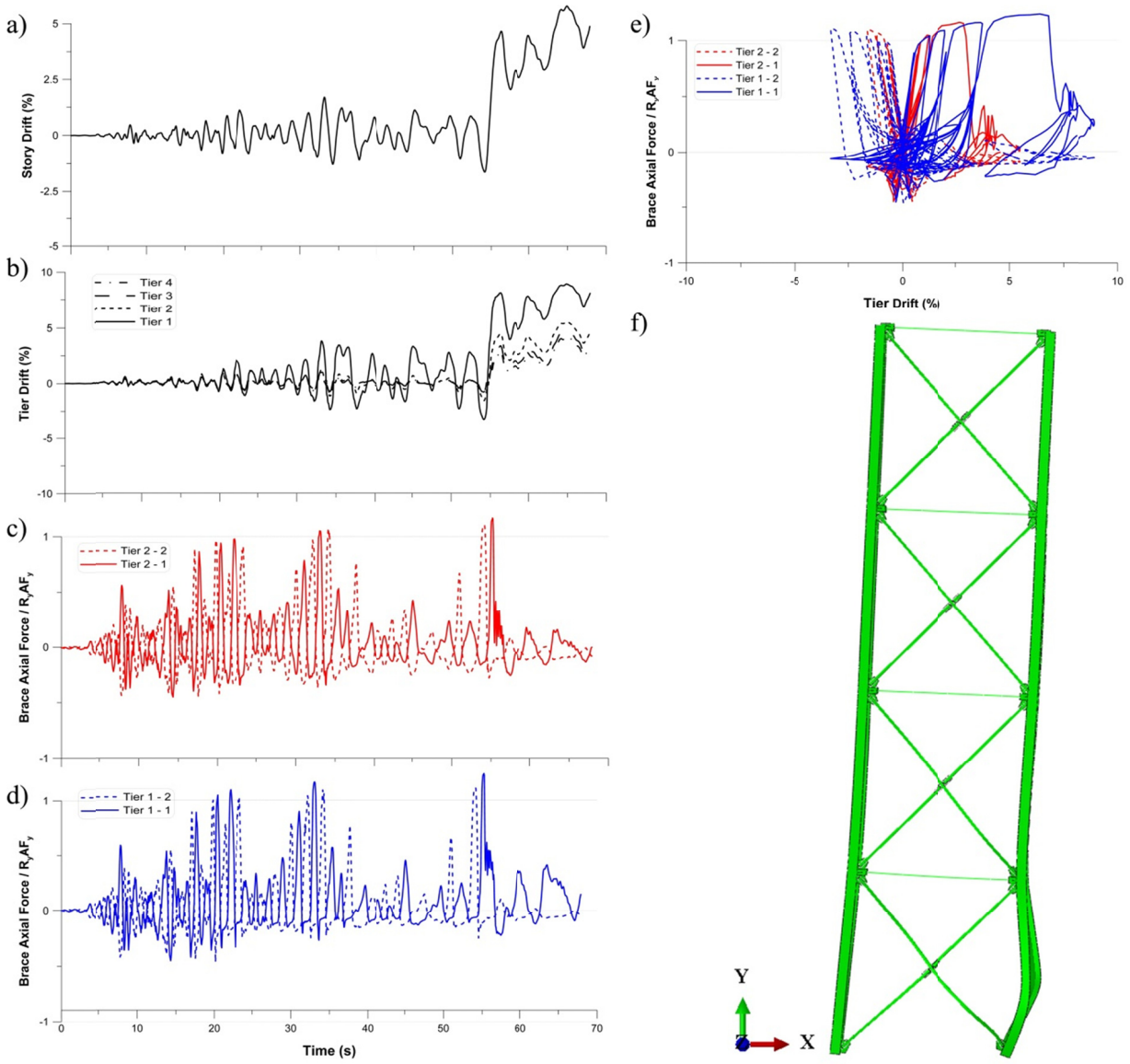

Figure 4.6: Response of 4-tiered BF under the 1979 Imperial Valley, Delta record: a) Story drift; b) Tier drifts; c) Brace axial forces in Tier 1; d) Brace axial forces in Tier 2; e) Hysteretic response of the braces at Tiers 1 and 2; and f) Frame deformed shape at column buckling (t = 56 s).

The statistics of the NLRH analysis results for the suite of 22 ground motions applied to Frames 1, 2, and 4 are given in Table 4.2. For Frame 4, one collapse case was observed as discussed above, whereas for shorter frames with 2 and 3 tiers (Frames 1 and 2) eight and six collapse cases were reported, respectively. For the collapse cases, column buckling developed within the first tier similar to the mechanism described above. The concentration of drift in Tier 1 is evident for all cases studied. However, more non-uniform tier drift distribution was observed for the shorter

frames (Frames 1 and 2). In addition, the roof displacement significantly exceeds the design estimate, particularly for the shorter frames.

Table 4.2: Median values of peak seismic response parameters for Frames 1, 2, and 4 from NLRH analysis in *Abaqus*.

Parameter	Frame 1	Frame 2	Frame 4
Story drift (%)	2.22	2.08	1.43
Story drift / Δ	2.52	1.84	1.44
Critical tier drift (%)	3.87	4.52	2.97
Number of column failure cases	8	6	1

4.4 Validation of fiber-based numerical models

4.4.1 Numerical model

In this section the fiber-based model of the 2-tiered braced frame (Frame 1 shown in Figure 4.3) created using *Opensees* (McKenna and Fenves 2004) was validated against the corresponding *Abaqus* shell-element described above. The 3D model in Figure 4.7 captures out-of-plane buckling of the braces as well as in-plane and out-of-plane flexural buckling of the columns. These members were modeled using force-based beam-column elements with fiber discretization of the cross-section to include distributed plasticity. The uniaxial Giuffré-Menegotto-Pinto (Steel02) material model was selected to simulate the Bauschinger effect as well as kinematic and isotropic strain hardening behavior. The nominal yield strength F_y = 345 MPa was assigned to the material used for the columns whereas the expected steel yield stress, R_yF_y, was used for the bracing members. To account for possible non-uniform material properties among the members, a reduced yield strength equal to 0.95 R_yF_y = 459 MPa was assigned to the braces in Tier 1 as in the *Abaqus* model. The residual stress pattern and out-of-straightness were assumed as defined in the *Abaqus* model. A co-rotational formulation was chosen to consider geometric nonlinearities for the braces and columns. The roof beam and strut members were modelled as elastic beam elements. Since MT-BFs have only one dynamic degree of freedom that corresponds to roof

horizontal displacement, for dynamic analysis, mass proportional damping corresponding to 2% of critical was assumed in that vibration mode.

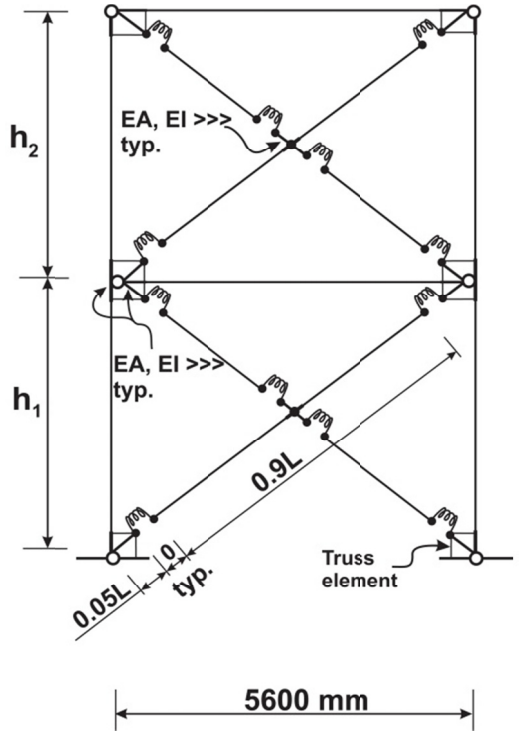

Figure 4.7: *OpenSees* numerical model of a 2-tiered CBF.

The model Figure 4.7 is referred to as the pinned base model because the columns are pin connected at their bases, consistent with the conditions assumed in design. The struts and the roof beam are also pin-connected to the columns for in-plane flexure. Nonlinear rotational springs are used to connect the bracing members to rigid elements extending from the roof beam, struts, and column bases. The springs reproduce the flexural hysteretic response exhibited by the gusset plates upon brace buckling out-of-plane. The same springs were considered in the middle gusset plate to connect discontinuous brace segments to rigid elastic beam-column elements assigned to the middle gusset plate. In each tier, the continuous brace is rigidly connected at the intersection point. Rigid elements were considered at both ends of struts and column segments to simulate connection size effects. Truss members were also used at the brace ends to simulate in-plane stiffness of the gusset plates. A leaning column was included in the model to account for P-delta effects (not shown in Figure 4.7). In the analyses, the roof dead load was applied at the top of the braced frame and the leaning

column. As was the case for frame analysis using *Abaqus*, response history analysis was performed using the far-field record set of 22 ground motion records proposed in FEMA P695.

4.4.2 Validation of fiber-based model with shell element model

To validate the fiber-based (*OpenSees*) model, results of nonlinear incremental static (pushover) analysis of Frame 1 obtained from the corresponding shell element (*Abaqus*) model were compared. Since inertial seismic forces only develop at the roof level for MT-BFs, the frame response under the first significant inelastic displacement cycle of a ground motion record during which column flexure develops can be reproduced by gradually incremented lateral roof displacement using pushover analysis. Pushover analysis is therefore appropriate to investigate the development of brace inelastic response leading to concentration of inelastic demand in tiers and column bending moments, and possible subsequent column buckling failure.

Key results from the nonlinear static analyses performed in *Abaqus* and *OpenSees* are presented in Figure 4.8. As shown in Figure 4.8a, frame base shear vs. story drift response is correlated well between *OpenSees* and *Abaqus*. The frame exhibited linear elastic response up to a story drift of 0.40% *h* when buckling of the compression brace in the first tier occurred. Figure 4.8b shows good agreement for the tier drifts, and both analyses predict drift concentration in the Tier 1. The Tier 1 compression brace buckled first, then brace buckling developed in both tiers and the frame lateral stiffness slightly reduced as it became governed by the tension braces (Figure 4.8c). The frame lateral strength reached its maximum value when yielding initiated in the tension brace in Tier 1, at a story drift of 0.50% *h*. That brace maintained its yield strength with strain hardening effects when being stretched in the inelastic range, but the strength of the compression brace in the same tier gradually reduced in the post-buckling range, which resulted in a diminution of the frame lateral resistance. The steadily increasing difference between Tier 1 and 2 drifts induced in-plane bending of the columns in Tier 1, which increased up to approximately 2.0% story drift (Figure 4.8d). At a story drift of 2.0% *h,* the column axial strength suddenly dropped due to in-plane flexural buckling of the compression (RHS) column in Tier 1. Figure 4.8e shows the in-plane and out-of the plane displacement of the RHS column and illustrates that column in-plane buckling developed first as the column in-plane lateral displacement increased rapidly. This instability mode occurred as a result of plastic hinges forming in the column at the top of and within Tier 1. At the Tier 1 level, complete curvature reversal occurred compared to the flexural deformations that had gradually

developed prior to initiation of buckling. In Figure 4.8e, complete plastic hinge formation at $0.4h_1$ associated with in-plane buckling triggered out-of-plane buckling response of the RHS column over the full height due to the lack of lateral support at the tier level. This biaxial buckling mode is shown in the frame deformed shapes from *Abaqus* and *OpenSees* (Figures 4.8f and 4.8g). As observed in the NLRH finite element analysis of Frame 4 (Figure 4.6), torsional deformation of the buckled column is also predicted for this 2-tiered frame in Figure 4.8f. The details of this mode were not explicitly observed in the *OpenSees* analysis since torsion is not captured in the fiber-based element formulation, however, the inclusion of coupled column in-plane and out-of-plane flexural buckling in the *OpenSees* fiber model is shown to adequately capture the critical stability behavior since the failure is driven by in-plane flexural buckling.

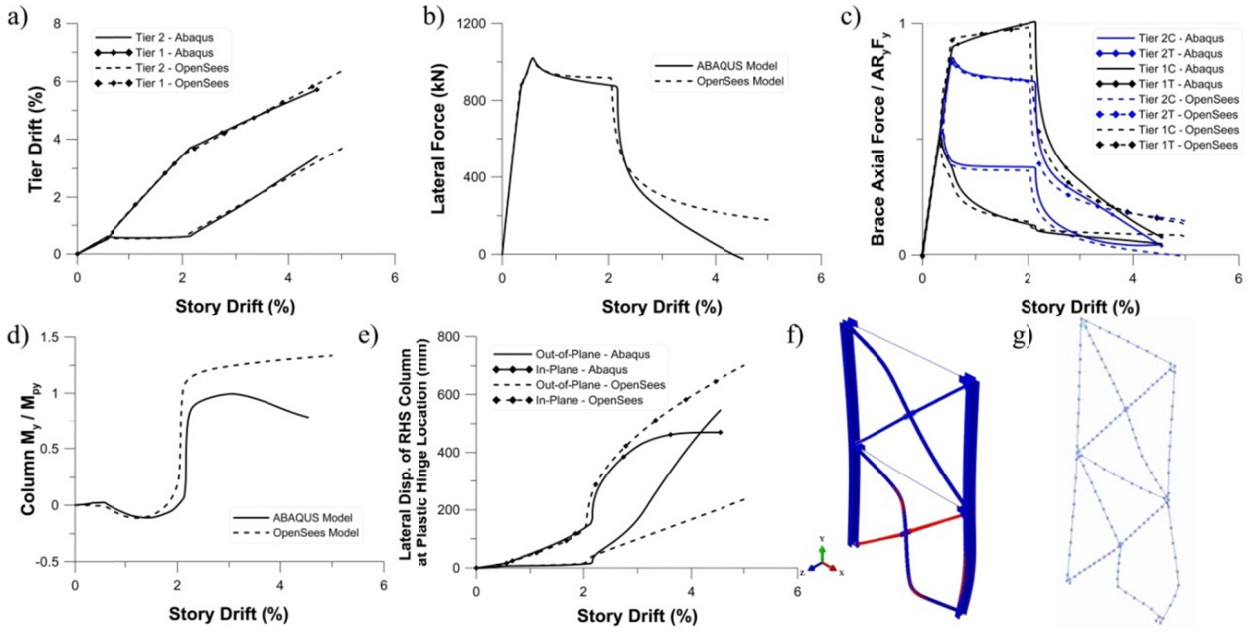

Figure 4.8: Response of the 2-tiered CBF from nonlinear static analysis: a) Tier drift; b) Lateral load; c) Brace axial forces (tension and compression forces shown positive to ease comparison); d) In-plane bending moment in the compression (RHS) column; e) RHS Column lateral displacement at 0.4h1; f) frame deformed shape in *Abaqus*; and g) frame deformed shape in *OpenSees*.

To further compare analyses, the results of the NLRH analysis for Frames 1, 2, and 4 were also used to compare the *Abaqus* and *OpenSees* modeling approaches. Figure 4.9 compares tier drift time history responses for Frames 1 and 4 from both approaches. For Frame 1, tier drift response

histories from two ground motions are shown in Figures 4.9a and 4.9b. Tier drifts plotted in Figure 4.9a illustrate a case where both the *OpenSees* and *Abaqus* models remained stable. In both models, the frame experienced a significant concentration of inelastic drift in Tier 1 in the positive direction around 15 seconds. In Figure 4.9b, both the *OpenSees* and *Abaqus* models indicated structural collapse due to column in-plane flexural buckling. The *Abaqus* model sustained larger tier drifts between 6 and 8 seconds but both models collapsed in the negative direction between 8 and 10 seconds. In this case, the global frame response was similar for the *OpenSees* and *Abaqus* models even though the details of column buckling behavior were slightly different.

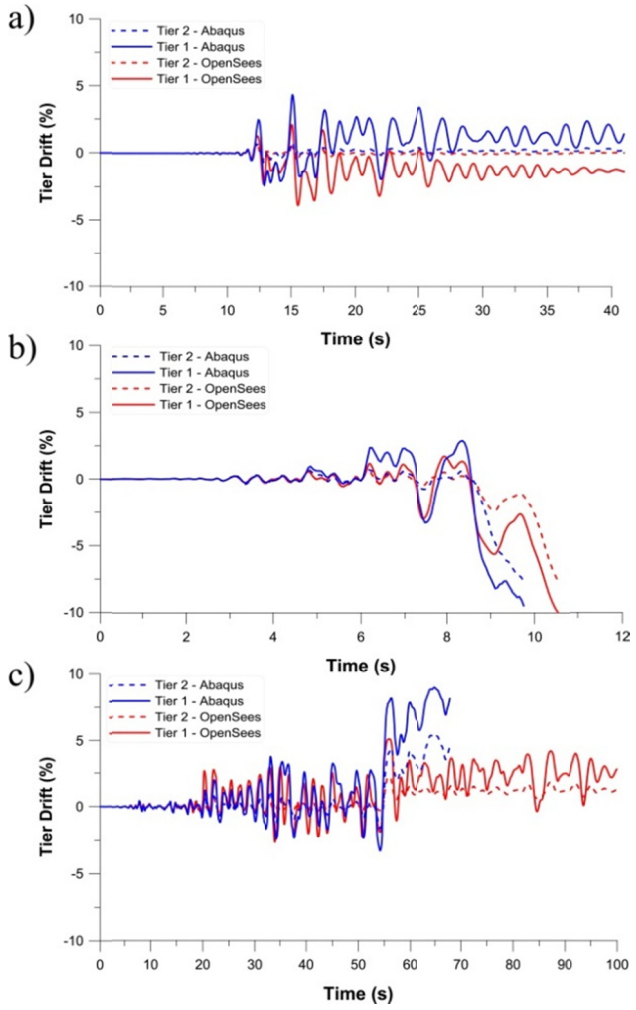

Figure 4.9: Comparison of *OpenSees* and *Abaqus* models for seismic response of: a) Frame 1 tier drift history under the 1995 Kobe, Shin-Osaka record; b) Frame 1 tier drift history under the 1989 Loma Prieta, Capitola record; and c) Frame 4 tier drift history for Tiers 1 and 2 under the 1979 Imperial Valley, Delta record.

In Figure 4.9c, a similar comparison was performed for Frame 4 under the same ground motion record whose results were presented in Figure 4.6. For this case, the history of tier drifts for Tiers 1 and 2 from *Abaqus* and *OpenSees* are in good agreement. Tier drift prediction using *OpenSees* compares well with the *Abaqus* results. Tier drift concentration was more pronounced in Tier 1 until 56 s where the column in-plane flexural buckling occurred in the *Abaqus* model in the Tier 1 column. Column in-plane buckling initiated in the *OpenSees* model but the column remained stable due to reversal of the direction of the ground shaking.

Statistics of the *OpenSees* NLRH analyses are given in Table 4.3. For Frame 4, one column buckling occurred under the 1992 Landers, Yermo Fire Station record. In the *Abaqus* model, no column failure was observed for that record, but large tier drift and partial column yielding were observed in Tier 1. A close match was also obtained for critical tier drift from both models (3.10 vs 2.76%). Similar agreement on critical tier drift and column failures can be found for Frames 1 and 2 in Tables 2 and 3.

Table 4.3: Median values of peak seismic response parameters for the MT-BFs studied.

Parameter	**Frame 1**	**Frame 2**	**Frame 3**	**Frame 4**	**Frame 5**	**Frame 6**	**Frame 7**
Story drift (%)	1.53	1.33	1.22	1.26	1.42	1.19	1.08
Story drift / Δ	1.82	1.20	1.47	1.05	1.17	0.93	0.78
Critical tier drift (%)	2.52	2.71	1.70	2.76	2.17	2.89	2.09
Drift ratio (critical tier / story)	1.66	2.05	1.40	2.14	1.47	2.09	1.97
Tier drift ratio (max / min)	4.36	4.20	2.26	3.62	1.93	3.92	2.67
$M_{cy,max}/M_{py}$ at Tier 1	0.36	0.39	0.14	0.40	0.40	0.47	0.28
$M_{cy,max}/M_{py}$ at Tier 2		0.18		0.17	0.20	0.15	0.12
$M_{cy,max}/M_{py}$ at Tier 3				0.12	0.11	0.10	0.09
$M_{cy,max}/M_{py}$ at Tier 4						0.09	0.08
$M_{cy,max}/M_{py}$ at Tier 5							0.06
$P_{c,max}/P_n$ in Tier 1	0.79	0.75	0.69	0.74	0.83	0.63	0.62
Number of column failure cases	5	5	5	1	2	0	0

These comparisons of *OpenSees* and *Abaqus* models with different element formulations illustrate several key points. Most importantly, the models are generally in good agreement, predict column buckling and demonstrate the need for improved design provisions for MT-BFs. Although the more computationally efficient *OpenSees* models do not capture the column

torsional response, they still capture in-plane column flexural buckling, which is the dominant failure mode for columns in MT-BFs, and subsequent out-of-plane movement of the buckled column. The *OpenSees* modeling approach may in isolated cases provide a slightly more optimistic outlook on collapse potential than *Abaqus*, but this approach is deemed adequate for extensive parametric exploration in support of developing an improved design approach.

4.5 Parametric study using fiber-based models

In this section the seismic performance of a wide range of MT-BFs was evaluated through NLRH analysis using the *Opensees* modeling approach validated against the *Abaqus* models. As shown in Figure 4.3, four building heights are considered: h = 9, 15, 24, and 30 m. For the 24 m tall building, four braced frame geometries are studied to examine the effects of the number of tiers, the Tier 1 height, h_1, relative to that of the other tiers, and frame uniformity. Four braced frame types are also considered to study the influence of fixed column bases, reduced base shear and application of other systems including OCBF and Buckling Restrained Braced Frame (BRBF).

4.5.1 Baseline MT-BF response

Out of the 22 ground motions, column in-plane flexural buckling was observed in four cases. Buckling failure under one of those four motions is presented later when discussing the alternate fixed base condition. The statistics of key response parameters for the 22 analyses are given in Table 4.4. For this frame, the median story drift demand corresponds well to the design story drift, Δ. As shown in Figure 4.6b, lateral deformations under all ground motions concentrated in Tier 1, resulting in large tier drifts capable of causing brace failure. The drift ratio in the table represents the ratio of the peak critical tier drift to the peak story drift. Drift concentration can also be assessed through the tier drift ratios, i.e. the ratio between the maximum and minimum peak tier drifts. Statistics of the peak weak-axis column moment, M_{cy}, as normalized with respect to the column plastic moment, M_{py}, are given in the table at every tier level. The results indicate large in-plane bending moment demand being induced in the columns at Tier 1 compared to the other tiers due to the larger drifts that develop in that tier creating a kink at the top of Tier 1. However, in-plane bending demand in the column top tiers indicates initiation of tension yielding in Tiers 2 and 3 under some of the ground motions, although these tiers have lesser contribution to overall inelastic deformation of the frame. These flexural demands, together with the column

buckling case, indicate that column in-plane bending moments must be taken into consideration in the design of MT-BF columns.

Table 4.4: Statistics of peak seismic response parameters for the 4-tiered CBF example.

Parameter	**Statistics of converged analyses**[1]			
	50th percentile	**84th percentile**	**Min**	**Max**
Story drift (%)	1.26	1.80	0.57	2.97
Story drift / Δ	1.05	1.50	0.47	2.47
Critical tier drift (%)	2.76	4.19	0.42	5.06
Drift ratio (critical tier / story)	2.14	2.40	0.75	2.45
Tier drift ratio (max / min)	3.62	4.74	0.77	4.96
$M_{cy,max}/M_{py}$ at Tier 1	0.40	0.70	0.17	1.21
$M_{cy,max}/M_{py}$ at Tier 2	0.17	0.17	0.10	0.19
$M_{cy,max}/M_{py}$ at Tier 3	0.12	0.14	0.09	0.16
$P_{c,max}/P_n$ in Tier 1	0.74	0.75	0.63	0.77

[1]Column failure was observed in 1 analysis

Nonlinear response history analysis was also performed on the six remaining MT-BFs of Figure 4.3. Table 4.3 presents the median values of key response parameters under the 22 ground motions for these frames. The number of cases where column instability failure occurred in Tier 1 is given at the bottom of Table 4.3. The results show that the median story drift demand generally reduces when increasing the structure total height. For the 24 m tall frame with uniform tier heights (Frames 3, 4, and 6), it also reduces slightly when the number of tiers is increased. When comparing the story drift demand from analysis to the design story drift, Δ, the design prediction is too low for the shortest frame, reasonably good for the 24 m frames and conservative for the tallest frame. In all frames except Frames 6 and 7, lateral displacements concentrated in Tier 1 and brace tension yielding was triggered only in that tier. For the 24 m tall frame with uniform tier heights (Frames 3, 4, and 6), peak drifts in the critical tier increase when the number of tiers is increased. This is due to the fact that smaller, more flexible columns are used when the height of bottom tier is smaller and the column effective length is reduced. In addition, because significant inelastic brace response occurred in only one tier, tier drifts resulting from a given story drift are higher when the critical tier height is smaller. For the same two reasons, tier drifts are more pronounced in Frame 4 compared to Frame 5 because the critical tier

in Frame 5 was taller. Generally, tier drifts, drift ratios and tier drift ratios are larger for a smaller h_1/h ratio. For all frames studied, the largest bending moment demands developed in the first tier. Peak moments are expected to vary with the frame geometry, the tier drift and the column stiffness; for the cases studied, moments in the two-tiered frame with taller tiers are smaller than those in the frames with more tiers.

Occurrences of column buckling failure do not correlate well with the bending moment demand as failure cases were observed in Frames 1 and 3 for which peak M_y/M_{py} values are respectively 0.36 and 0.14 whereas column buckling did not occur for Frames 5 and 6 where the columns sustained much higher flexural demands. Table 4.3 also presents the peak axial load demand in the columns relative to the required axial strength used in design. As shown, the peak demand is approximately the same for all frames, even if the number of braces inducing the axial load increases with the number of tiers. Hence, this parameter cannot explain this apparent better performance and this aspect will require further attention in future studies.

4.5.2 Alternative MT-BF designs and MT-BFs with fixed column bases

In view of the unsatisfactory seismic performance observed for MT-BFs designed as SCBFs, Frame 4 was redesigned to explore the benefits of reducing the inelastic brace response and, thereby, reducing drift concentration and column flexural demand. These redesigns were: an SCBF using a reduced R factor equal to 4.0, and an OCBF with R = 3.25. The design procedure for the SCBF system with R = 4.0 is the same described in the previous section with R = 6.0. The OCBF system with R = 3.25 was designed in accordance with AISC 341-10. The selected shapes for the two systems are given in Figure 4.10a, and the frame properties are summarized in Table 4.5.

Table 4.5: Design parameters and properties of the alternative 4-tiered CBF designs.

Parameter	**SCBF** R **= 4.0**	**OCBF** R **= 3.25**	**BRBF** R **= 8.0**
Design fundamental period (T), s	0.74	0.74	0.74
Seismic response coefficient (C_s)	0.202	0.249	0.101
Design story shear per frame (V), kN	721	888	361
Design story drift (Δ), %	1.58	1.17	1.25
Computed fundamental period (T_1), s	1.17	1.12	1.51
Design story drift (Δ_{T1}), %	0.99	0.79	0.61

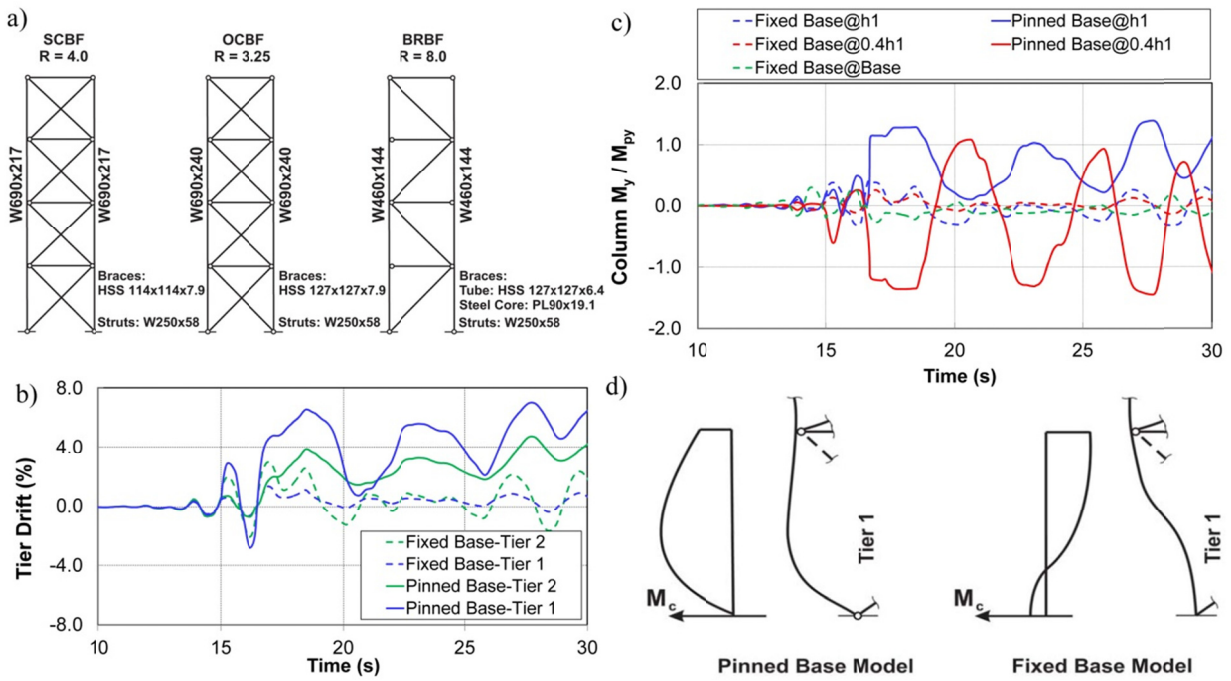

Figure 4.10: Selected member shapes for the alternative 4-tiered CBF designs; b) Histories of Tier drift for 4-tiered SCBF with pinned and fixed bases; c) Histories of the bending moment demands in the LHS column in Tier 1 for 4-tiered SCBF with pinned and fixed bases; and d) Schematic of column deflected shape and bending moment in Tier 1 for pinned and fixed bases.

Key response parameters from nonlinear dynamic analysis are given in Table 4.6. The results obtained for the SCBF frame designed with R = 6.0 are repeated in the table to ease comparison. As shown, reducing the R factor for the SCBF system or using the OCBF system had negligible impact on the peak story drifts, which is in agreement with the equal displacement principle (Newmark and Hall 1982). In both frames, brace tension yielding was also constrained to the bottom tier, which led to similar, although slightly lower peak tier drifts, drift ratios and tier drift ratios compared to the R = 6.0 SCBF. The resulting column bending moment demand and number of column buckling cases are also comparable. Hence, the increase in member sizes due to the higher design seismic loads did not have much effect and, more importantly, did not raise the seismic performance to an acceptable level. The reduction in localized demand can be attributed to the larger column sections exhibiting higher in-plane stiffness. However, the similarities in overall performance are attributed to the fact that, in spite of the stronger braces used in the alternative frame designs, the peak drifts in the critical tiers (2.61-2.17 % h_1)

remained sufficient to induce significant brace inelastic response and the column properties scaled up by a margin comparable to story shear strengths and axial load demands, meaning that the potential for unsatisfactory column performance remained nearly unchanged even if R was reduced significantly from 6.0 to 3.25.

Table 4.6: Median values of peak seismic response parameters for alternate 4-tiered CBF designs.

Parameter	***R* = 6.0**	***R* = 4.0**	***R* = 3.25**	***R* = 8.0 β = 1.1[1]**	***R* = 8.0 β = 1.2[1]**	***R* = 6.0 Fixed Base Columns[2]**
Story drift (%)	1.26	1.23	1.11	1.43	1.40	1.25
Story drift / Δ	1.05	0.77	0.97	1.15	1.12	1.05
Critical tier drift (%)	2.76	2.61	2.17	1.58	1.65	2.05
Drift ratio (critical tier / story)	2.14	2.13	1.96	1.29	1.26	1.51
Tier drift ratio (max / min)	3.62	3.59	2.94	1.25	1.41	2.75
$M_{cy,max}/M_{py}$ at Tier 1	0.40	0.38	0.28	0.16	0.16	0.41
$M_{cy,max}/M_{py}$ at Tier 2	0.17	0.17	0.18	0.10	0.13	0.22
$M_{cy,max}/M_{py}$ at Tier 3	0.12	0.12	0.10	0.11	0.13	0.15
$P_{c,max}/P_r$ in Tier 1	0.74	0.77	0.77	0.51	0.55	0.75
Number of column failure cases	1	2	2	0	0	0

[1]Tier 1 is critical
[2]Tier 2 is critical

Frame 4 was also redesigned with buckling-restrained braces (BRBs) to examine if this option could improve the frame seismic response. BRBs yield both in tension and compression, without buckling, and BRBFs are designed with R = 8. BRBFs exhibit stable inelastic response with greater strain hardening behavior, which should lead to more uniform inelastic demand over the frame height. Well-proportioned MT-BFs with pairs of nearly identical tension- and compression-acting BRBs in every tier are not prone to drift concentrations as every tier is expected to develop and maintain comparable story shear resistances in the inelastic range. An alternating single diagonal configuration MT-BF with BRBs was selected and the frame was designed assuming brace core plates made from ASTM A572, Gr. 50 (F_y = 345) steel and using strain hardening factor, ω = 1.3 and compression strength adjustment factor, β = 1.1. The

columns were designed for axial load only. Design parameters are given in Table 4.5 and the selected shapes and frame properties are shown in Figure 4.10a.

Truss elements were used to model the diagonal BRB members (one diagonal per tier) with the Steel02 and Hysteretic materials acting in combination to reproduce BRB response. As shown in Table 4.6, the median peak story drifts for the BRBF solution are much larger than for the standard CBF designs. The higher displacement demand can be attributed to the greater frame flexibility, but its extent could not be entirely estimated at the design stage. However, the peak tier drifts are comparable and the drift ratios and tier drift ratios are much lower than in the CBF. The resulting bending moment demands in the columns are also reduced and do not localize in Tier 1 when using a BRBF. No buckling case was observed for the BRBFs.

All results presented above were obtained assuming pinned column bases. Since column bases could be detailed to provide a fixed boundary, an *OpenSees* model with fixed column bases was developed to explore the effect of this option. In Figures 4.10b and 4.10c, the partial (10-30 s) histories of Frame 4 with pinned and fixed bases are compared for the 1992 Landers, Yermo Fire Station record. Drift in Tiers 1 and 2 and bending demand in the LHS column in Tier 1 are presented. For the pinned base columns, predicted buckling of the LHS column occurred in Tier 1 at time t = 16.6 s. Schematics of the LHS column deformed shape and bending moment in Tier 1 at the critical time are given in Figure 4.10d. For the pinned base frame, the evolution of the bending moment when approaching buckling failure is the same as described in Figure 4.6b: the moment in the lower third increased rapidly due to member P-delta effects and a plastic hinge formed at that location, which precipitated column in-plane buckling. At the top of the tier, the curvature of the column reversed when a plastic hinge formed in the column span. Column buckling was not observed for the fixed base frame. In the response cycles prior to the large demand from the ground motion at t = 16.6 s, the bending moments at the base, at 0.4 h_1, and at h_1 are of the same sign indicating single curvature column response. The moment at the top of Tier 1 was consistently largest. At the time of maximum ground motion demand, the column was in double curvature, a condition significantly less critical for buckling since formation of an additional plastic hinge at the base is required for buckling. The column in double curvature also exhibited greater effective flexural stiffness at the first tier that redistributed inelastic deformation to Tier 2 as shown in Figure 4.10b.

As shown in Table 4.6, column buckling was not observed under any of the 22 ground motions for the fixed base frame, compared to 4 occurrences of buckling for the corresponding pinned base frame. Table 4.6 shows that column in-plane bending moment demands in Tier 1 are comparable but the moments in Tier 2 and 3 are higher with fixed column bases. Thus, the fixed column bases provide additional stiffness to distribute yielding into the bracing members of Tiers 2 and 3. The median peak drift in the critical tier reached 2.05%, which is lower than the corresponding value for the pinned bases (2.68%). Hence, the potential for severe drift concentration and column buckling in the first tier of MT-BFs is expected to reduce when column base connections are detailed as fixed.

4.6 Summary and conclusions

This article presented numerical simulations performed to evaluate the seismic performance of steel multi-tiered braced frames (MT-BFs) designed in accordance with the AISC Seismic Provisions. The seismic response of two, three and four-tiered CBFs was first evaluated using an *Abaqus* 3D shell-element finite element model through nonlinear response history analysis. The seismic response of seven SCBFs having different heights, number of tiers and tier relative heights was then studied through dynamic response history analyses using *OpenSees* 3D fiber-based finite element model validated against the *Abaqus* analysis results. Alternative MT-BF designs were also examined for the 4-tiered, 24 m tall frame with uniform tier heights. The study focused on the in-plane tier drift demand as well as stability response of the columns. The primary findings of this study are:

- Column flexural buckling is the dominant failure mode for MT-BFs and occurs due to combined axial force and bi-axial flexure.
- In a 2-tiered frame studied with a shell-element *Abaqus* model, column torsional movement was observed after column buckling as the location of maximum out-of-plane imperfection is adjacent to the critical tier for in-plane column hinging.
- A validation study showed that fiber-based *OpenSees* models can appropriately capture tier drift concentration, column buckling and collapse in MT-BFs.
- Story (roof) drift demand in MT-BFs subjected to MCE level earthquake cannot be reliably estimated by the design story drift determined in accordance with the ASCE 7-10 provisions.

Story drifts were generally underestimated for the shorter frames and overestimated for taller ones when story drifts were determined considering code period upper limit. Story drifts obtained using the computed period T_1 were underestimated for all frames studied.

- Inelastic brace deformations in MT-BFs tend to concentrate in the critical tier, which is the tier exhibiting relatively lower story shear resistance. Drift concentration is more important when the height of the critical tier is small relative to the story height.
- Tier drift concentration induces in-plane flexural demand on the columns, which can lead to column flexural buckling. The anticipated flexural demand must therefore be assessed and considered in the design of the columns.
- Column buckling is more likely to occur when the critical tier is located at the bottom of the frame, where axial load demand on the column is maximum.
- Column buckling essentially developed in flexure about the weak axis in the plane of the frame. For the frames studied, buckling occurred over the first tier height, indicating that positive lateral bracing can be provided to the columns by the brace-strut assemblies even if the braces respond in the nonlinear range to seismic effects.
- Tier drift concentrations in MT-BFs may lead to excessive inelastic demand on the members and connections of the structure. In particular, tier drift values sufficient to cause low-cycle fatigue failure of HSS braces were observed in this study. Tier drift should therefore be explicitly considered as a limit state in the design of MT-BFs.
- The use of higher design seismic loads by specifying a lower R factor did not have significant beneficial effect on the flexural demand imposed on the columns and the occurrence of column buckling failure. More uniform drift demand and smaller column bending moments were however observed when using buckling-restrained bracing members instead of conventional braces.
- Columns with fixed base conditions exhibited higher in-plane flexural stiffness than pinned base columns, which reduced drifts in the bottom tier and can triggered brace inelastic response in adjacent tiers, resulting in less critical conditions for the stability of the columns.

This study covered a limited number of braced frames and the conclusions should be validated for other MT-BF configurations. Additional three-dimensional finite element analysis should be

performed to further investigate flexural-torsional buckling if out-of-plane flexural demand exists (e.g. crane loading). The buckling failure of the columns as obtained in the numerical simulations should be examined through experimental programs. The observations made in this study showed that the distribution of the brace inelastic response and drift concentration over the frame height can be influenced by the flexural stiffness of the columns. In design, one could take advantage of this behavior by selecting column sections that would improve the drift response and minimize the potential for column buckling failure.

Acknowledgments

Partial funding for this research was provided by the Natural Sciences and Engineering Research Council (NSERC) of Canada and the American Institute of Steel Construction.

References

Aguero, A., Izvernari, C., and Tremblay, R. (2006). "Modelling of the Seismic Response of Concentrically Braced Steel Frames using the OpenSees Analysis Environment." *Int. J. of Advanced Steel Construction*, 2(3), 242-274.

AISC. (2010a). *ANSI/AISC 341-10, Seismic Provisions for Structural Steel Buildings.* American Institute of Steel Construction, Chicago, IL.

AISC. (2010b). *ANSI/AISC 360-10, Specifications for Structural Steel Buildings.* American Institute of Steel Construction, Chicago, IL.

ASCE. (2010). *SEI/ASCE 7-10, Minimum Design Loads for Buildings and Other Structures.* American Society of Civil Engineers.

Dalal, S.T. (1969). "Some non-conventional cases of column design." *Eng. J.*, AISC, 6(1): 28-39.

Fell, B. V., Kanvinde, A. M., Deierlein, G.G., and Myers, A.T. (2009). "Experimental Investigation of Inelastic Cyclic Buckling and Fracture of Steel Braces." *J. Struct. Eng., ASCE*, 135(1), 19-32.

FEMA. (2009). *ATC 63, FEMA P695: Quantification of Building Seismic Performance Factors*." Applied Technology Council, , Redwood City, CA.

Galambos, T.V. and Ketter, R.L. (1958). *Columns Under Combined Bending and Thrust,* Fritz Engineering Laboratory Report 205A.21, Bethlehem, Pennsylvania.

Imanpour, A., Stoakes, C., Tremblay, R., Fahnestock, L., and Davaran, A. (2013). "Seismic Stability Response of Columns in Multi-Tiered Braced Steel Frames for Industrial Applications." *ASCE Structures Congress*, Pittsburgh, PA, 2650-2661.

Imanpour A., Tremblay R., Davaran A. (2014). "A New Seismic Design Method for Steel Multi-Tiered Braced Frames." *ASCE Structures Congress*, Boston, MA, 2707-2720.

Imanpour, A., Tremblay, R., Fahnestock, L., and Stoakes, C. (2015). "Analysis and Design of Two-Tiered Steel Braced Frames under In-plane Seismic Demand." Submitted to *J. Struct. Eng., ASCE*.

Lamarche C. P., Tremblay R., (2011) "Seismically induced cyclic buckling of steel columns including residual-stress and strain-rate effects." *J. of Constr. Steel Res.*, 67, 1401–1410.

Hsiao, P-C., Lehman, D.E., and Roeder, C.W. (2013). "A model to simulate special concentrically braced frames beyond brace fracture." *Earthquake Engineering and Structural Dynamics*, 42, 183-200.

Kauffman, E. J. and Pense, A. W. (1999). *Characterization of Cyclic Inelastic Strain Behavior on Properties of A572 Gr. 50 and A913 Rolled Sections*, AISC-PITA Project Progress Report, ATLSS Research Center, Lehigh University, Bethlehem, Pennsylvania.

McKenna, F. and Fenves, G.L. (2004). "*Open System for Earthquake Engineering Simulation (OpenSees).*" Pacific Earthquake Engineering Research Center (PEER), University of California, Berkeley, CA. http://opensees.berkeley.edu/.

Peng, S. W. (2001). *Seismic Resistant Connections for Concrete Filled Tube Columns-to-WF Beam Moment Resisting Frames*, Doctoral Dissertation, Department of Civil and Environmental Engineering, Lehigh University, Bethlehem, Pennsylvania.

Simão, P.D., Girão Coelho, A.M., and Bijlaard, F.S.K. (2012) "Stability design of crane columns in mill buildings." Engineering Structures 42: 51–82.

Simulia (2011). *Abaqus FEA*, www.simulia.com.

Stoakes, C.D. and Fahnestock, L.A. (2012a). "Cyclic flexural analysis and behavior of beam-column connections with gusset plates." *J. Const. St. Res.*, 72(2012), 227-239.

Stoakes, C.D. and Fahnestock, L.A. (2012b). "Influence of weak-axis flexural yielding on strong-axis buckling strength of wide flange columns." *Proceedings, Annual Stability Conference, SSRC,* Grapevine, Texas, April 17-20.

Timoshenko, S.P. and Gere, J.M. (1961). *Theory of Elastic Stability*, 2nd ed., McGraw-Hill Book Company, Inc., Engineering Societies Monographs, New York, N.Y., 541 p.

Tremblay, R. (2002). "Inelastic seismic response of steel bracing Members." *J. Constr. Steel Res.*, (58), 665-701.

Tremblay, R., Archambault, M.H., and Filiatrault, A. (2003). "Seismic Performance of Concentrically Braced Steel Frames made with Rectangular Hollow Bracing Members." *J. of Struct. Eng.*, ASCE, 129, 12, 1626-1636.

Tremblay, R., Haddad, M., Martinez, G., Richard, J., and Moffatt, K. (2008). "Inelastic Cyclic Testing of Large Size Steel Bracing Members." *Proc. 14th World Conf. on Earthquake Eng.*, Beijing, China, Paper No. 05-05-0071.

Uriz, P., Filippou, F.C., and Mahin, S.A. (2008). "Model for Cyclic Inelastic Buckling of Steel Braces." *J. Struct. Eng., ASCE*, 134(4), 619-628.

Symbols

C_d	Deflection amplification factor
C_{exp}	Brace expected strength in compression
C'_{exp}	Brace expected post-buckling strength
C_s	Seismic response coefficient
C_u	Coefficient for upper limit on calculated period
D	Dead load
E	Seismic load
F_y	Yielding strength
h	Total frame height
h_i	Tier height (i = 1 to 4)

I_e	Importance factor
L	Live load
M_{cy}	Column weak-axis flexural moment
M_{py}	Column plastic moment
P_c	Column axial load
P_n	Column nominal compressive strength
R	Response modification coefficient
R_yF_y	Expected steel yield stress
S_{D1}	Design spectral response acceleration parameter at a period of 1.0 s
S_{DS}	Design spectral response acceleration parameter in the short period range
T	Fundamental period of the building
T_1	Fundamental period of the building from modal analysis
T_a	Approximate fundamental period of the building
T_{exp}	Brace expected strength in tension
V	Design story shear
β	Compression strength adjustment factor
δ_e	Story drift under V
ω	Strain hardening factor
Δ	Design story drift
Δ_{T1}	Design story drift with fundamental period of the frame from modal analysis

CHAPTER 5 ARTICLE 2 : ANALYSIS AND DESIGN OF TWO-TIERED STEEL BRACED FRAMES UNDER IN-PLANE SEISMIC DEMAND

Ali Imanpour, A.M.ASCE[1], Robert Tremblay[2], Larry A. Fahnestock, P.E., M.ASCE[3], and Christopher Stoakes[4]

[1]Ph.D. Candidate, Dept. of Civil, Geological and Mining Engineering, Polytechnique Montreal, Montreal, QC, Canada H3C 3A7.

[2]Professor, Dept. of Civil, Geological and Mining Engineering, Polytechnique Montreal, Montreal, QC, Canada H3C 3A7 (corresponding author). E-mail: robert.tremblay@polymtl.ca.

[3]Associate Professor, Dept. of Civil and Environmental Engineering, University of Illinois at Urbana-Champaign, 205 North Mathews Ave., Urbana, IL 61801.

[4]Research Scientist, Dep. of Civil and Environmental Engineering, The University of Iowa, 4105 Seamans Center for the Engineering Arts and Sciences, 103 South Capitol St., Iowa City, IA 52242.

The article was submitted to the *Journal of Structural Engineering, ASCE* on May 13, 2015.

Abstract

A seismic design strategy, which is intended to be implemented within the framework of the AISC Seismic Provisions, is presented for single-story steel concentrically-braced frames that are divided into two tiers. In this method, the columns are designed to resist the axial loads acting in combination with the in-plane flexural demand resulting from uneven distribution of brace inelastic deformations over the frame height. This design procedure, which establishes enhanced requirements beyond the current AISC Seismic Provisions, prevents concentration of deformation in one tier and causes frame nonlinear deformation to be distributed between the tiers. The column bending moments depend on the story shear resistance that develops in each tier when the bracing members are at buckling and in the post-buckling range. The method also aims to control tier drifts to protect the bracing members from excessive inelastic demand, which could cause brace fracture. Nonlinear static and dynamic analyses are performed to validate the proposed design procedure.

Keywords: Multi-tiered braced frames, Seismic design, Inelastic deformations, Nonlinear analysis.

5.1 Introduction

Steel multi-tiered braced frames (MT-BFs) consist of two or more bracing panels that are stacked vertically in a building that has a single story. This framing configuration is generally used when the story height is too large and conventional braces extending the full story height no longer represent an economical or practical solution. MT-BFs are extensively employed in tall commercial, recreational and industrial buildings (Figure 5.1a), and they represent an effective solution in seismic applications as the more stringent brace slenderness and cross-section width-to-thickness limits associated with ductile braced frame requirements can be more easily satisfied with shorter braces. MT-BFs are also common for non-building structures such as legs of conveyors in industrial plants. Various bracing configurations can be used for MT-BFs. For high seismic applications, X-, chevron- or V-bracing configurations are commonly used such that story shear is shared between compression- and tension-acting braces (Figure 5.1b). Struts are needed at every tier level to resist unbalanced brace axial loads that develop after the compression braces have buckled and, thereby, avoid undesirable K-braced frame behavior. The columns are typically I-shaped members oriented such that strong axis bending is used to resist out-of-plane buckling over the full frame height, and wind loading effects when columns are on the building exterior.

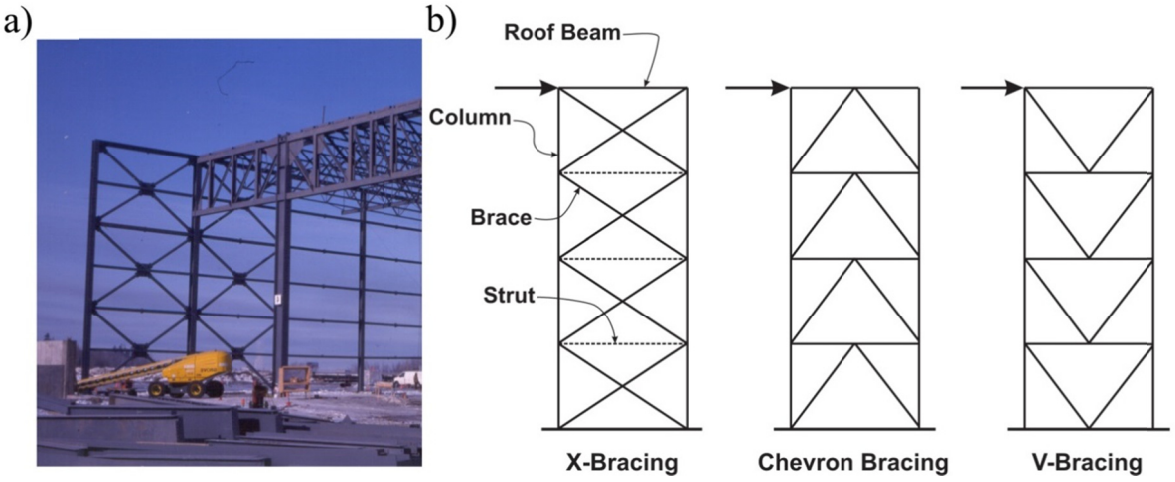

Figure 5.1: a) Typical MT-BF structure; b) MT-BF bracing configurations.

Nonlinear seismic analysis of MT-BFs using fiber based frame models has shown that brace inelastic response under strong seismic ground motions will likely distribute non-uniformly along the structure height, even if the braces are well proportioned to provide uniform story shear resistance (Imanpour et al. 2013; Imanpour and Tremblay 2014). Typically, inelastic deformations tend to initiate and concentrate in one tier where brace tension yielding is triggered first. This tier is referred to as the critical tier, as shown in Figure 5.2a and 5.2b for a 2-tiered frame. This behavior may result in excessive inelastic demand in the critical tier, which in turn, may precipitate failure of the bracing members due to low-cycle fatigue (Figure 5.2c). Non-uniform drift also induces in-plane bending moment demands on the columns that may lead to column plastic hinging and, in some cases, to flexural buckling (Figure 5.2d). The results of recent studies using three-dimensional fiber based and finite element analyses showed that column buckling may also include out-of-plane deformations as yielding progresses in the column. Localized torsional effects were also observed in the finite element analysis (Imanpour et al., 2015). However, controlling in-plane behavior of MT-BF columns is the primary strategy for ensuring stable seismic response, and it is the focus of this paper.

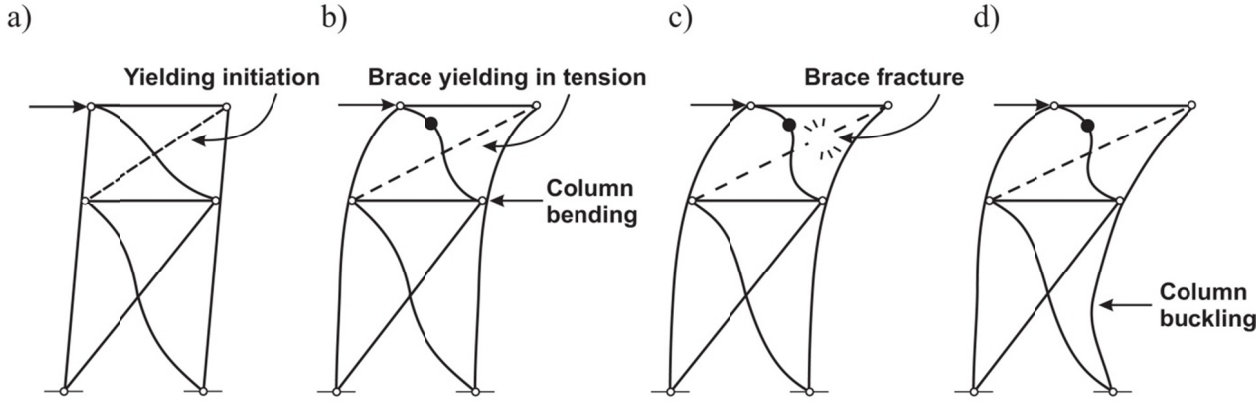

Figure 5.2: Concentration of inelastic demand in Tier 2 (Tier 2 is critical).

This paper presents a design procedure to address this unsatisfactory behavior with the specific objectives of: (1) preventing column instability and (2) limiting tier drift demands to protect the braces from fracture. The method is developed for two-tiered braced frames subjected to in-plane seismic demand and is illustrated for a prototype special concentrically braced frame (SCBF) located in a high seismic region. Current seismic design provisions for SCBFs are first reviewed

and applied to the prototype frame. The seismic performance of that initial frame design is examined using nonlinear static and dynamic analyses, with focus on the vertical distribution of the brace inelastic deformations and its effects on the column response. Additional seismic analyses are then performed to assess the anticipated flexural demand on the columns and design provisions are proposed to ensure that the columns can resist the combined axial and flexural demands. The design method also aims at controlling tier drifts to prevent excessive inelastic demand on the bracing members. The frame is redesigned based on the proposed provisions and nonlinear analyses are performed to verify column stability conditions and assess brace ductility demand.

5.2 Frame design in accordance with current provisions

5.2.1 Frame configuration and design loads

The 2-tiered braced frame studied is shown in Figure 5.3a. The braced frame has a width of 5.6 m and tension-compression X-bracing is used in each tier. As shown, the frame has unequal tiers with h_1 = 8.0 m in Tier 1 and h_2 = 4.0 m in Tier 2. An unequal tier height configuration was chosen as this geometry leads to more pronounced MT-BF response (Figure 5.2). Additionally, the height of the bottom tier is often governed by the size of wall openings. The braced frame is part of a lateral load resisting system of a tall single-story industrial building located on a site class D in coastal California. The building has 128.8 m x 50.4 m plan dimensions and the structure has two braced frames along each of the four perimeter walls.

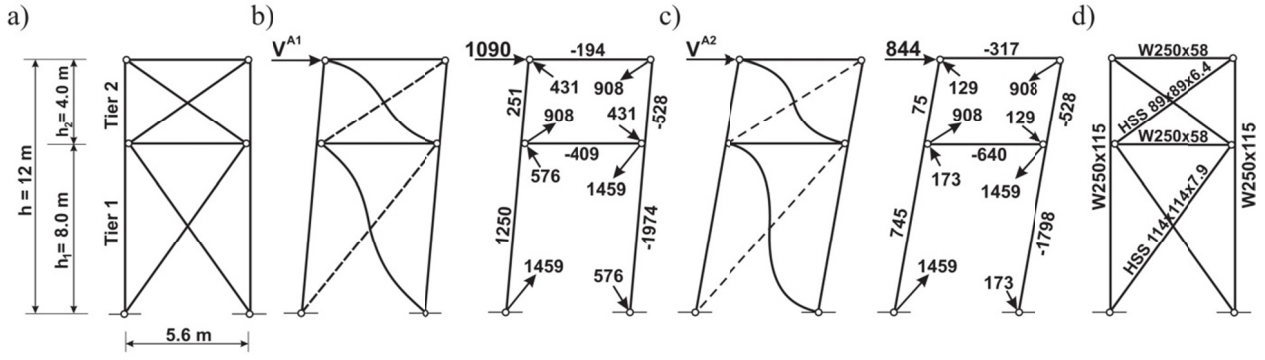

Figure 5.3: a) Frame geometry; b) Member axial loads from Analysis A1; c) Member axial loads from Analysis A2; and d) Member sizes. (Forces in kN)

The design is performed in accordance with ASCE 7-10 (ASCE, 2010). The roof dead load and the weight of the exterior cladding are equal to 1.2 kPa. For seismic loading, the mapped MCE_R spectral response acceleration parameters are $S_s = 1.5g$ at short period, and $S_1 = 0.6g$ at 1.0 s period. The structure is assigned to the Seismic Design Category (SDC) D and the SCBF system with an R factor of 6.0 is selected for the braced frames. For this building, the importance factor is $I_e = 1.0$, the design period is equal to 0.44 s, and the total building seismic weight is 10370 kN, which gives a design seismic load per braced frame of 475 kN, including 10% amplification for accidental torsion.

5.2.2 Seismic design

The steel frame members are designed with the AISC 360-10 Specification and the AISC 341-10 Seismic Provisions (AISC 2010a, b), hereafter called the Specification and Seismic Provisions, respectively. Only the relevant key design steps are summarized herein; additional information on the Seismic Provisions can be found elsewhere (e.g., AISC 2012; Bruneau et al. 2011; and Filiatrault et al. 2013). For SCBFs, the story shears must be resisted by compression- and tension-acting braces. Square HSS bracing members conforming to ASTM A500, Grade C, with $F_y = 345$ MPa are selected for this frame. Detail of the selected brace members is given in Table 5.1, including axial compression strength calculations. A brace effective length corresponding to 0.45 times the overall brace workpoint dimensions, l, was used assuming that the tension brace provides a support at the mid-length of the compression brace. In both tiers, the demand-to-capacity ratios for the braces ($P_u / \phi_c P_n$) are nearly identical and equal to 1.0.

Table 5.1: Properties of the bracing members.

Tier	HSS	A mm^2	r_x (mm)	t_{des} (mm)	l (mm)	Kl/r	b/t_{des}	P_u (kN)	$\phi_c P_n$ (kN)	$P_u / \phi_c P_n$
2	89x89x6.4	1880	33.5	5.92	6883	92	12.0	300	312	0.96
1	114x114x7.9	3020	43.2	7.39	9764	102	12.5	440	440	1.00

According to the Seismic Provisions, the columns must resist the tributary gravity loads plus the forces induced by the braces upon yielding and buckling. In this calculation, the larger brace-induced column forces from the following two analyses must be used: (1) Analysis A1 in which

all braces are assumed to reach their expected strength in tension (T_{exp}) or in compression (C_{exp}), as shown in Figure 5.3b; and (2) Analysis A2 in which all tension braces are assumed to reach their expected strength (T_{exp}) and the compression braces reach their expected post-buckling strength ($C'_{exp} = 0.3\ C_{exp}$), as shown in Figure 5.3c. The brace expected strengths, shown in Table 5.2, are determined with the steel expected yield strength for HSS members, $R_y F_y = 483$ MPa.

Table 5.2: Expected brace strengths and associated story shear strengths from braces.

Tier	**HSS**	T_{exp} **(kN)**	C_{exp} **(kN)**	C'_{exp} **(kN)**	$V_{br,exp}$ **(kN)**	$V'_{br,exp}$ **(kN)**
2	89x89x6.4	908	431	129	1090	844
1	114x114x7.9	1459	576	173	1167	936

In Figure 5.3, the maximum seismic-induced column axial compression load from the braces (1974 kN) occurs in Tier 1 from Analysis A1 (Figure 5.3b). The columns must also support a factored axial load of 237 kN due to gravity ($1.2D$) plus vertical acceleration effects ($= 0.2\ S_{DS}D$), which gives a total required column compression strength of 2211 kN. The columns are wide-flange shapes made from ASTM A992 steel ($F_y = 345$ MPa). They are continuous over the whole building height and are oriented such that in-plane bending occurs about their weak axis. They are assumed to be pin-connected at their top and bottom ends for flexure about both axes. Torsional restraint is provided at both column ends and at the tier level. The column effective length factors for in-plane and out-of-plane flexural buckling modes can be taken less than 1.0 recognizing that the axial load varies along the height of the columns and the columns are continuous over the two tiers (Simão et al. 2012; Dalal 1969). From elastic buckling analysis, the column effective lengths are $0.80\ h_1$ and $0.85\ h$, for the in-plane and out-of-plane buckling modes, respectively. A W250x115 section was selected, which has design axial strengths ($\phi_c P_n$) equal to 2524 kN and 2279 kN for strong and weak axis buckling modes, respectively. The member torsional buckling strength is 3755 kN for a distance of 8000 mm between braces, which is also satisfactory. The column shape also complies with the highly ductile member cross-section limits, as required for SCBFs in the Seismic Provisions. For this frame, out-of-plane (strong axis) bending moment was zero. Lateral-torsional buckling would need to be checked if out-of-plane flexural demand existed (e.g. crane loading).

A horizontal strut is provided at the tier level to resist the axial compression load of 640 kN resulting from the unbalanced horizontal brace load components in the post-buckling range (Analysis A2 in Figure 5.3c). The struts also provide in-plane lateral support as well as torsional restraint to the column at the tier level. Torsional restraint is achieved by using an I-shaped strut member placed with the web in the horizontal plane and rigidly connected to the columns to resist column torsion (Figure 5.4). Column torsional bracing at tier levels has been shown to be beneficial for MT-BF columns (Stoackes and Fahnestock 2012). A W250x58 section made of ASTM A992 steel is selected to resist the axial compression force demand.

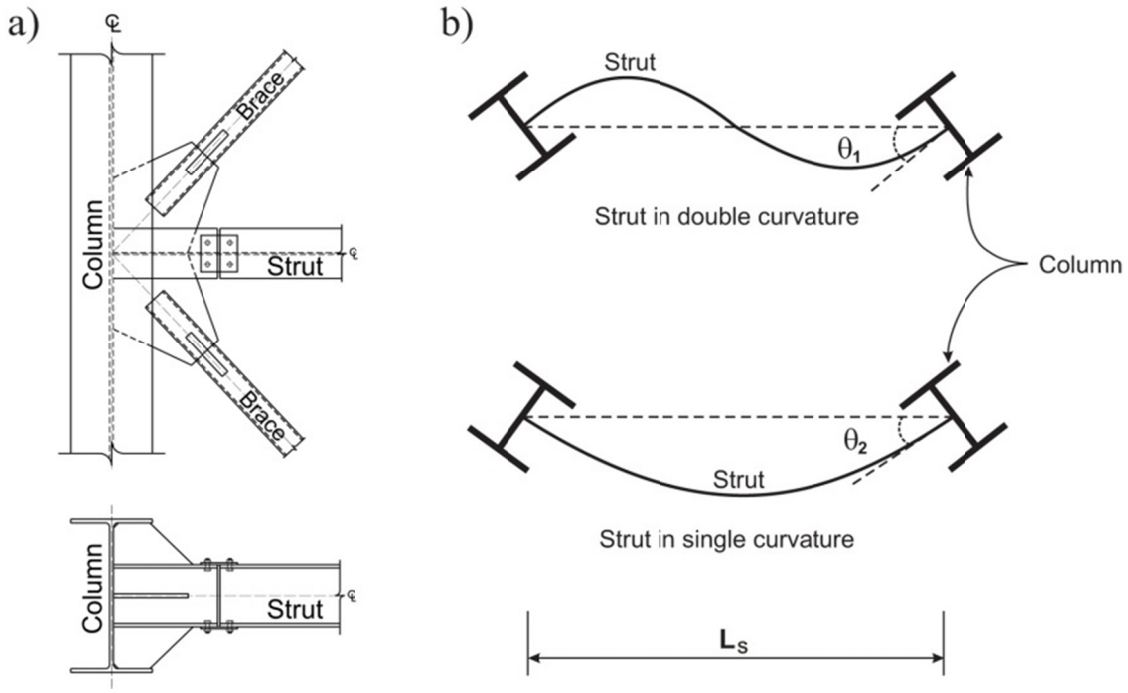

Figure 5.4: Torsional bracing of columns using the flexural stiffness of the struts: a) Torsionally rigid strut-to-column connection; b) Column torsional buckling modes inducing bending of the struts in double and single curvatures.

Member sizes are presented in Figure 5.3d. According to ASCE 7-10, the anticipated roof deflection for the structure, $C_d\delta_e/I_e$, is equal to 119 mm with $C_d = 5.0$. This corresponds to a roof (or story) drift of 0.99% h, which is adequate for this structure. The computed fundamental period of the structure is 0.72 s, longer than the period assumed for the design seismic load calculations (0.44 s). This frame design is therefore satisfactory according to current design provisions.

5.3 Seismic performance of current frame design

5.3.1 Numerical model

The *OpenSees* 2.2 analysis program (McKenna and Fenves, 2004) was used to perform nonlinear static and dynamic analyses. The braces and columns are modelled using nonlinear force-based beam-column elements with fiber discretization of the cross-section. The Giuffré-Menegotto-Pinto (Steel02) material model was selected to account for the Bauschinger effect and to simulate both kinematic and isotropic strain hardening responses. The nominal yield strength F_y = 345 MPa was assigned to the steel material for the columns and struts. The expected steel yield stress, R_yF_y = 483 MPa was utilized for the bracing members. Initial sinusoidal out-of-straightness with maximum amplitude of 1/1000 of the unsupported member length corresponding to the brace out-of-plane buckling mode was specified for the braces. Bi-directional initial sinusoidal out-of-straightness corresponding to the column in-plane and out-of-plane buckling modes was applied to the columns with maximum amplitude of 1/1000 of the length between nodal points. A co-rotational formulation was chosen to consider geometric nonlinearities for braces and columns. The residual stress pattern by Galambos and Ketter (1958) was specified for the columns. Past studies have shown that this model can reproduce adequately inelastic flexural buckling response under cyclic loading for HSS bracing members (Aguerro et al. 2006; Uriz et al. 2008) and I-shaped columns (Lamarche and Tremblay 2011). For dynamic analysis, mass proportional damping corresponding to 2% of critical in the structure lateral vibration mode was specified (MT-BFs have only one degree of freedom which corresponds to roof lateral displacement).

5.3.2 Nonlinear static (pushover) analysis

The lateral response of the frame is first evaluated using static incremental (pushover) analysis. It is noted that the seismic response of MT-BFs to ground motions is entirely defined by the roof displacement as they behave as single-degree-of-freedom systems. Hence, statically incrementing lateral roof displacement in pushover analysis imposes a lateral loading condition similar to the one that exists during the first significant inelastic displacement cycle under a ground motion. This analysis can then be used to study the development of brace inelastic response leading to concentration of inelastic demand in tiers and subsequent column bending moments. The analysis was performed by gradually increasing the top lateral displacement up to 2% h, i.e. approximately

two times the anticipated story drift including inelastic response. It was also performed for two column sizes: W250x115, as obtained in design in the previous section, and a W360x196 column with higher in-plane flexural stiffness. The second column size was arbitrarily chosen to illustrate the influence of the column stiffness on the frame response. The frame response with the smaller columns is presented first and the frame with the stronger columns is discussed later. In Figure 5.5a, tier drifts obtained by dividing the relative tier lateral displacements by the respective tier heights are plotted against the story drift. Brace axial forces in Tiers 1 and 2 are presented in Figures 5.5b and 5.5c, respectively. For simplicity, brace compression forces are plotted positive. Brace buckling occurred in both tiers at approximately 0.3% h. In Figure 5.5a, tier drifts continued to increase nearly linearly in both tiers until brace tension yielding initiated in Tier 2 at approximately 0.5% story drift. Beyond that point, further lateral deflection developed almost exclusively in Tier 2 as the tension brace in that tier was being stretched in the inelastic range. Conversely, drift in Tier 1 did not increase anymore because the tension brace in that tier remained elastic until the end of the analysis. The difference between the brace tension forces relative to their expected yield tensile strengths in the two tiers can be seen in Figures 5.5b and 5.5c.

Initiation of brace tension yielding in Tier 2 could be predicted by comparing the story shear resistances provided by the braces in both tiers. The story shear $V_{br,exp}$ corresponds to the sum of the horizontal components of the brace strengths, T_{exp} and C_{exp}, as given in Table 5.2. Although this parameter does not reflect the exact brace resistances at initiation of brace tension yielding, because the strength of the compression braces have already started to reduce at that point, the values indicate that the braces in Tier 2 develop lower expected lateral strength than those in Tier 1, suggesting that the tension brace in Tier 2 would likely reach its yield tensile strength first. For this frame, Tier 2 is therefore referred to as the critical tier as it is the weakest tier where brace tension yielding is likely to initiate first.

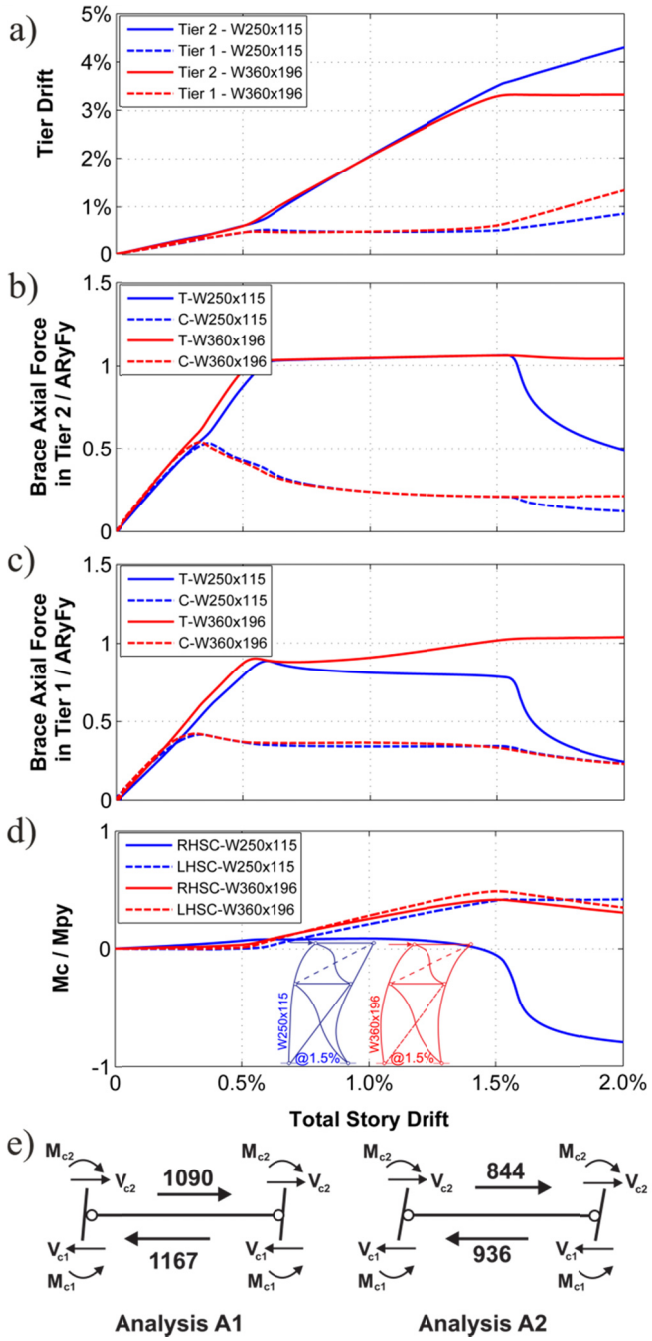

Figure 5.5: Tier drift and brace axial loads from pushover analysis results: a) Tier drifts; b) Brace axial forces in Tier 2; c) Brace axial forces in Tier 1; d) Column in-plane bending moment at the top of Tier 1; and e) Horizontal equilibrium at tier level for brace loads specified for Analyses A1 and A2 (axial loads in braces and columns not shown for simplicity).

In Table 5.2, examination of the story shears $V_{br,exp}$ and $V'_{br,exp}$ calculated in each tier with the brace forces specified in Analysis A1 and A2 in the current AISC Seismic Provisions also reveals that

horizontal equilibrium is violated between Tiers 1 and 2 with these shears. As illustrated in Figure 5.5e, the specified brace forces cannot co-exist in both tiers and tension yielding in Tier 1 cannot be initiated unless shear forces (V_c) develop in the columns to resist the unbalanced story shear from the unbalanced brace forces. Note that the direction of V_{c1} and V_{c2} in Figure 5.5e corresponds to positive values according to commonly used beam theory. In fact, the unbalanced shear V_{c1} would act in the opposite direction, resisting a portion of the unbalanced story shear from the braces. This behavior is responsible for the bending moments that gradually develop in the columns at top of Tier 1 after initiation of brace tension yielding in Tier 2, as shown in Figure 5.5d.

That flexural demand is induced by the difference in tier drifts that steadily increased after 0.5% story drift (Figure 5.5a). The left-hand-side (LHS) column is subjected to tension when applying lateral roof displacement in the analysis. Bending moments in that column increase linearly with the story drift. The moment also increases in the right-hand-side (RHS) column under compression, but the rate eventually reduces because the column flexural stiffness gradually reduces due to member stability effects. At a story drift of 1.2%, a plastic hinge started to form in the column near the mid-height of Tier 1 due to the moment amplified by the large axial load from the braces and gravity loads acting on the deformed column. In Figure 5.5d, the bending moment at top of Tier 1 then gradually reduced as the curvature of the column was affected by the formation of the plastic hinge and the reduction in the column effective flexural stiffness. In-plane flexural buckling of the RHS column eventually occurred in that tier at a roof displacement of 1.5% h. The buckling mode then progressively changed to bi-axial buckling as out-of-plane deformations also developed as a result of column plastic hinging at mid-height of the first tier, as was observed for 2-tiered frames in the study by Imanpour et al. (2015). Although this response is observed at a story drift exceeding the design story drift of 0.99%, this behavior is not deemed satisfactory in the context of ductile seismic design.

The observed behavior suggests that the frame response could be improved by increasing the column flexural stiffness, as stiffer columns could contribute to triggering earlier brace tension yielding in the non-critical tiers, leading to more uniform tier drift and brace inelastic deformations along the frame height. To examine the effect of a stiffer column, a pushover analysis was conducted with W360x196 columns, which have a moment of inertia about their weak axis 3.56 times higher than that of the W250x115 columns. The larger contribution of the stiffer columns to lateral resistance through bending is evident in Figure 5.5d. The column shears

were sufficient to initiate yielding of the tension brace in Tier 1 at a story drift of 1.5%. After this point, the difference between the tier drifts started to reduce, as well as the bending moments and shears in the columns, as the columns gradually straightened. Member stability effects were also smaller for these stiffer columns: both columns offered comparable contributions to story shears and column buckling did not occur. The higher strength of the stiffer columns also contributed to prevent column plastic hinging and buckling. It is therefore clear that the variations in tier drifts and the brace inelastic demand over the frame height can be controlled and that better column behavior can be achieved by selecting larger columns with sufficient in-plane flexural stiffness and strength. This observation inspired the design method that is proposed later in the article. In Figure 5.5d, it is noted, however, that stiffer columns can attract greater forces, which must also be considered in design. Fortunately, peak flexural demand on the columns occurs when brace tension yielding is triggered in the non-critical tier, a condition that can be accurately predicted and defined at the design stage. The demand is therefore bounded and independent of the structure lateral displacement, a situation much preferable to the case where forces keep increasing as the structure laterally displaces. These aspects are also considered in the design method proposed later.

5.3.3 Nonlinear response history analysis

Nonlinear response history (NLRH) analysis was also performed on the frame designed in accordance with the current AISC Seismic Provisions. The FEMA P695 (FEMA 2009) far-field set of 22 ground motion records for Seismic Design Category D was used for this study. These motions are compatible with the seismic hazard level used for the frame design. The first component of each ground motion record was considered for the analyses (total of 22 analyses). The amplitudes of the records were first adjusted to exhibit the same peak ground velocity. The entire ensemble was then scaled such that the median acceleration spectrum for the suite matches the maximum considered earthquake (MCE_R) spectrum at the structure design period.

Under three ground motions, column flexural buckling occurred in Tier 1 when the compression axial force demand from gravity plus seismic loads exceeded the column capacity. In all three cases, the load-carrying capacity of the column reduced in the post-buckling range and the analyses halted when the column could not carry axial force due to gravity load. Figure 5.6 shows the result for one case where large demands developed in the columns without causing column

buckling such that the response under the entire ground motion can be examined. The peak story drift reached nearly 2.5%, which is approximately 2.5 times the design story drift, Δ (Figure 5.6a). As shown in Figure 5.6b, large drifts developed in Tier 2 (up to approximately 5%) while the drift in Tier 1 remained small. The history of the normalized column bending demand at the top of Tier 1 in the RHS column is plotted in Figure 5.6c. That column undergoes axial compression when the peak story drift and Tier 2 drift are reached. As shown, the column flexural demand increases as drift increases in Tier 2, reaching nearly the column plastic moment capacity at peak lateral displacement. Similar behavior was observed under the 21 other ground motions considered. In three ground motions, the flexural demand was large enough to form plastic hinges causing column buckling. This frame global behavior and column demand agree well with the prediction from pushover analysis, the reason being that large column demands develop shortly after initiation of brace tension yielding, which occurs in the first large inelastic displacement cycles during ground motions. For the 22 records, the median values of the total story drift, the drift in Tier 1, the drift in Tier 2, and column flexural demand ($M_{cy,max}/M_{py}$ at top of Tier 1) are 1.27%, 0.53%, 2.82%, and 0.32 respectively.

Although brace fracture was not modelled in the numerical simulations, the large tier drifts observed in the NLRH analyses are sufficient to cause failure of HSS bracing members due to low-cycle fatigue, as was observed in several past test programs (Tremblay et al. 2003; Yang and Mahin 2005; Uriz and Mahin 2008; Fell et al. 2009; Roeder et al. 2011; Palmer et al. 2012; Hsiao et al., 2013). Tremblay et al. (2003) proposed an empirical expression to predict the brace end rotation at failure of HSS braces in single diagonal and X-bracing configurations. That rotation at failure is a function of the brace slenderness and width-to-thickness ratio of its cross-section. For the HSS 89x89x6.4 braces in Tier 2, this model predicts failure at a rotation of 0.215 rad., which translates into a tier drift of approximately 2.1% for the frame geometry. This value is similar to test data reported by Roeder et al. (2011) and Palmer et al. (2012), indicating that brace failure could have occurred in a large portion of the ground motions considered. Column buckling and brace failure represent unsatisfactory performance, meaning that current design methods cannot provide adequate safety for MT-BFs in the event of an earthquake.

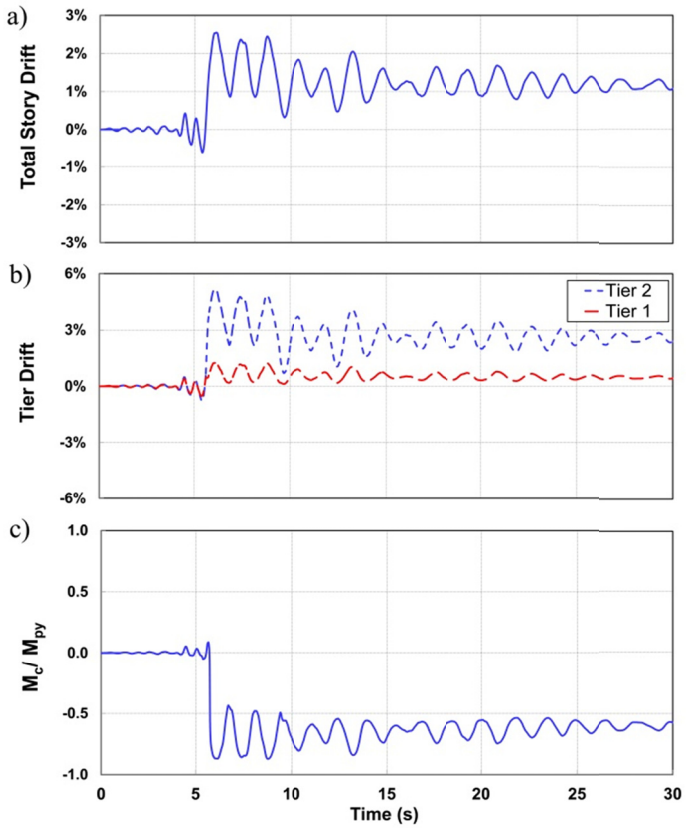

Figure 5.6: Nonlinear response history analysis results under 1992 Cape Mendocino (Rio Dell Overpass record): a) Total story drift; b) Tier drifts; and c) In-plane bending moment at the top of Tier 1 in the RHS column.

5.4 Proposed analysis and design requirements for MT-BF columns

As observed in the MT-BF example presented above, brace tension yielding tends to initiate and develop more in the tier where braces offer the lowest story shear resistance (critical tier). This is expected because seismic story shear demand is the same over the frame height and a full plastic mechanism including the brace yielding will develop first in the tier having the lowest story shear resistance. This behavior induces flexural demand on the columns that must be accounted for in their design. Drift concentration in the critical tier may also lead to excessive inelastic demand and premature failure of the braces and frame connections. That inelastic demand can be controlled by using columns with sufficient in-plane flexural stiffness. Special analysis and design requirements are therefore required to identify the critical tier and ensure that the columns have sufficient strength and stiffness to achieve satisfactory performance. These aspects are therefore addressed in

this section. Although the bracing members have significant impact on the frame design and response, their design need only comply with the current AISC Seismic Provisions and is therefore not covered here. As will become evident, however, engineers must carefully select the bracing members such that differences in story shear resistances between the two tiers are minimized.

5.4.1 Determination of the critical tier

The critical tier can be identified by comparing the story shear resistances provided by bracing members in each tier, i.e. when the tension braces reach their expected yield tensile strength, T_{exp}. At that time, the braces in compression have already buckled and started to lose some of their compressive strength. For this calculation, however, it can be assumed for simplicity that the braces still exhibit their expected compressive strength C_{exp}. This story shear resistance corresponds to $V_{br,exp,}$ as defined previously, and detail of the calculation of $V_{br,exp}$ for the frame example is given in Table 5.2. As discussed, the shear resistances in Tiers 1 and 2 are respectively equal to 1167 kN and 1090 kN, which led to the response obtained from the nonlinear analyses.

For MT-BFs with uniform tier properties or approximately equal story shear resistance over the frame height, the critical tier may not be distinguishable in view of the uncertainties associated with the prediction of brace resistances. This uncertainty originates from several different sources such as the unavoidable variations in material strength (Dexter et al. 2000; Schmidt and Bartlett 2002) and brace cross-section properties (Schmidt and Bartlett 2002), increase in material strength due to strain rate effects (Rao et al. 1966; Anderson 1995; Tremblay and Filiatrault 1996; Bruneau et al. 2011; Lamarche and Tremblay 2011, Moreau et al. 2014), and the influence of complex inelastic cyclic loading on brace resistances (Tremblay 2002). The connection details that will be used by the steel fabricator, which are usually not known at the time of design, is another factor that can affect the brace boundary conditions and, thereby, their buckling strength (Davaran 2001; Davaran and Hoveidae 2009; Davaran et al. 2014). To account for these uncertainties in design, potential critical tier scenarios can be identified by varying the brace resistances by a given margin, say +/– 5%. As shown in Table 5.3, for the present frame example, Tier 1 becomes critical if brace resistances are multiplied by 0.95 and 1.05 in Tiers 1 and 2, respectively. In the subsequent sections, the column design is performed assuming that Tier 2 is critical but the columns will also be verified at the end of the process for the scenario where Tier 1 is critical.

Table 5.3: Modified expected brace strengths and story shear strengths from braces.

Tier	HSS	T_{exp} (kN)	C_{exp} (kN)	C'_{exp} (kN)	$V_{br,exp}$ (kN)	$V'_{br,exp}$ (kN)
2	89x89x6.4	953	453	136	1144	886
1	114x114x7.9	1386	547	164	1108	889

5.4.2 Minimum column strength requirements

The column axial load and in-plane bending moments are determined in two analysis steps that correspond to the condition when brace tension yielding initiates in each of the two tiers.

5.4.2.1 Analysis Step 1

Analysis step 1 is shown in Figure 5.7 for the frame example. This step represents the condition when brace tension yielding is reached in the critical tier (Tier 2) and the axial force in the tension brace at that tier is therefore set equal to $T_{exp,2}$. At this point, all compression braces have just buckled but the drifts are still small and degradation of the brace compressive strengths is limited. Therefore, all compression braces can be assigned their expected compression strength, C_{exp}. Because the braces in Tier 1 can develop a larger shear force, $V_{br,exp}$, than in Tier 2, the brace tension force in Tier 1 takes a value smaller than T_{exp} such that the story shear contributed by the braces in that tier is equal to $V_{br,exp}$ in the critical tier. In Analysis Step 1, the frame response is essentially elastic and relative lateral displacement between the two adjacent tiers is negligible, so in-plane bending demand is small and can be neglected.

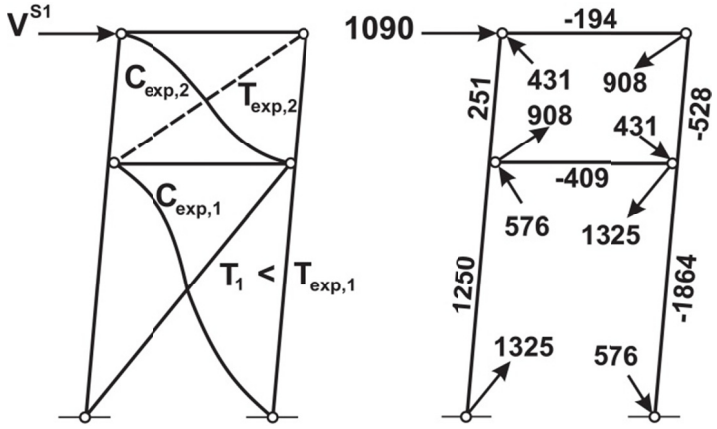

Figure 5.7: Analysis Step 1.

5.4.2.2 Analysis Step 2

Upon increasing the roof displacement further, Analysis Step 2 is reached when the frame attains the condition shown in Figure 5.8 where brace tension yielding is triggered in the tier adjacent to the critical tier. At this stage, the compression brace in Tier 2 has deformed significantly in the inelastic range due to the large tier drift that had developed in that tier as the tension brace deformed through yielding. The brace compressive resistance in Tier 2 is therefore set equal to the post-buckling compression resistance C'_{exp}. In Tier 1, the compression brace has also buckled; however, because the associated tension brace has not yet been stretched plastically, its compressive resistance is taken as C_{exp}. Brace tension forces are equal to T_{exp} in both tiers.

In Figure 5.8b, the shear force in each tier includes the column shear forces, V_c, and the story shear resisted by the braces, V_{br}. From horizontal equilibrium at the tier level:

(1) $$2V_{c2} + V_{br,2} = 2V_{c1} + V_{br,1}$$

In each tier, column bending moments are directly related to shears by the distance from the column free ends. Hence, the column bending moment at the top of Tier 1, M_{c1}, and at the bottom of Tier 2, M_{c2}, are equal to:

(2) $$M_{c1} = V_{c1} h_1$$

(3) $$M_{c2} = V_{c2} h_2$$

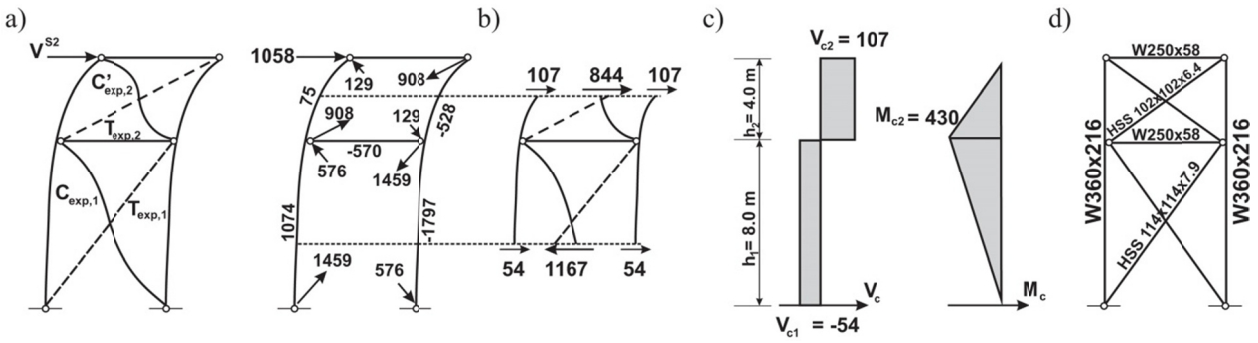

Figure 5.8: Analysis Step 2: a) Member axial loads; b) Horizontal shear forces in Tiers 1 and 2; c) Column in-plane shears and bending moments; and d) Member sizes. (Forces in kN, moments in kN-m)

From moment equilibrium at the tier level, the following relationship between column shears is obtained: $V_{c2}\ h_2 = -V_{c1}\ h_1$. Introducing this relation in Eq. 1, together with the unbalanced story shear resisted by the braces in both tiers, $\Delta V_{br} = V_{br,1} - V_{br,2}$ gives:

$$V_{c2} = \frac{1}{2}\left(\frac{1}{1+h_2/h_1}\right)\Delta V_{br} \tag{4}$$

Analysis Step 2 is performed for the condition where the difference between the story shears resisted by the braces in the two tiers is maximum (ΔV_{br} = 1167 – 844 = 323 kN), which produces the largest column shears and moments. Beyond that point, the strength of the compression brace in Tier 1 is expected to decrease and ΔV_{br} will also diminish, reducing the flexural demand on the columns. For the frame studied, the maximum shears and bending moments are given in Figure 5.8c.

The columns are redesigned to resist the combination of axial load and flexural demand obtained from the two analysis steps. Only the column segment in Tier 1 is examined because the axial loads are maximum in the first tier, the bending moments in both tiers have the same maximum values and distribution, and Tier 1 has a longer unsupported (buckling) length. From Analysis Step 1, the required column axial strength when including gravity load effects (237 kN) is P_u = 2101 kN. In-plane bending moments are small and can be neglected. From Analysis Step 2, the required axial strength is P_u = 2034 kN and the required in-plane flexural strength is $\phi_b M_{ny}$ = 430 kN-m. The second case is more critical and is used to select the new columns. In the AISC Specification, the column segment in Tier 1 is checked for combined axial force, in-plane flexural buckling and out-of-plane flexural buckling. As done earlier, reduced effective lengths equal to 0.80 h_1 and 0.86 h are found for buckling about weak and strong axes, respectively, with a ratio of 0.376 between axial loads in Tiers 2 and 1. A W360x216 section is selected for the columns. This section has design axial strengths ($\phi_c P_n$) equal to 6322 kN, 6365 kN, and 7050 kN for strong axis, weak axis, and torsional buckling, respectively. The design flexural strength of the section, $\phi_b M_{ny}$, about the weak axis is 677 kN-m and the interaction equation for in-plane stability (weak axis) gives:

$$\frac{P_u}{\phi_c P_n} + \frac{8}{9}\frac{M_{uy}}{\phi_b M_{ny}} = \frac{2034}{6322} + \frac{8}{9}\left(\frac{430}{677}\right) = 0.32 + 0.57 = 0.89 \tag{5}$$

5.4.3 Drift and period checks

With the W360x216 columns, the anticipated story (roof) deflection is equal to 106 mm, which gives a design story drift, $\Delta = 0.88\%$, less than the limit of 2% prescribed in ASCE 7-10. The computed fundamental period of the frame is equal to 0.68 s, longer than the period assumed in design.

5.4.4 Minimum column stiffness requirement

Tier drifts must be verified to ensure that the frame components will not be subjected to excessive inelastic deformation demand that may cause premature failure under the MCE hazard level. For this frame, a limit of 2% was adopted for tier drifts, which corresponds to the drift limit imposed for building structures in ASCE 7. As previously discussed, this value also appears reasonable for preventing occurrence of low-cycle fatigue failure of brace members and connections.

Nonlinear response history analysis of steel braced frame structures performed in recent studies (e.g., Hsiao et al., 2013; Chen and Mahin 2010) showed that low-rise buildings such as the one studied herein typically experience story drifts that exceed the design story drift predicted in accordance with the ASCE 7 provisions. For instance, for the initial frame design studied in this article, peak story drifts in the nonlinear dynamic analysis reached, on average, 1.4 times Δ, with a maximum value of 2.6 Δ. On this basis, it is appropriate to evaluate maximum anticipated tier drifts for story drift values that reflect this observed trend. For the frame example, the expected story drift Δ_{exp} is conservatively taken equal to 2.0 $\Delta = 1.76\%$.

Past seismic analyses have also shown that the largest tier drifts in MT-BFs generally develop in the critical tier (Imanpour and Tremblay 2012; Imanpour et al. 2013); essentially because brace tension yielding initiates first in that tier and additional drifts continue to develop in that tier before yielding of tension brace has started in other tiers. For a 2-tiered CBF with Tier 2 being the critical tier, the expected drift in Tier 2, $\Delta_{exp,2}$, when the story drift reaches Δ_{exp} can be estimated from:

$$\Delta_{exp,2} = \Delta_{exp} + \frac{1}{h_2}\left(\frac{\Delta V_{br}}{2}\right)\left(\frac{h_1^2\, h_2^2}{3EI_c\, h}\right) \tag{6}$$

where EI_c is the column flexural stiffness. The first term on the RHS of the equation corresponds to the story drift assuming linear variation over the entire frame height whereas the second term represents the additional tier drift due to bending of the column under the unbalanced story shear resisted by the braces, ΔV_{br}. For this calculation, the force in the compression braces in both tiers can be set equal to C'_{exp} as the two braces in a well-proportioned MT-BF are expected to have sustained substantial inelastic response when Δ_{exp} is attained. The value of ΔV_{br} then corresponds to the difference between the $V'_{br,exp}$ values in Table 5.2: 936 – 844 = 92 kN. Using this value in Eq. 6, it is found that $\Delta_{exp,2}$ = 2.34% with the W360x216 section for which $I_{cy} = 2.82 \times 10^8$ mm^4. This value exceeds the limit of 2.0% and stiffer columns are required. When selecting a column section, one may take advantage that the design story drift Δ diminishes when using larger columns, which gives a smaller value of Δ_{exp} in Eq. 6. After a few trials, it is found that a W360x347 section ($I_{cy} = 4.79 \times 10^8$ mm^4) would be sufficient. With this section, Δ = 0.84% and Δ_{exp} = 2 x 0.84% = 1.68%. With these values, Eq. 6 gives a drift of 2.02% in Tier 2, which is deemed acceptable.

For this example, the steel tonnage for the column must be increased by 60% (347/216) to satisfy the adopted tier drift limit. For a specific project, the column size requirement could be reduced by refining the estimate of Δ_{exp} through nonlinear response history analyses, as will be presented in the next section. Peak tier drifts can also be obtained directly from this type of analysis. Alternatively, the engineer may examine the possibility of using more effective column cross sections such as tubular sections or built-up cruciform sections made of welded W shapes (Figure 5.9). Other options to develop large in-plane stiffness with less material include latticed columns or forming a vertical truss with the columns (Tremblay 2003; Mac Rae et al. 2004; Qu et al 2015).

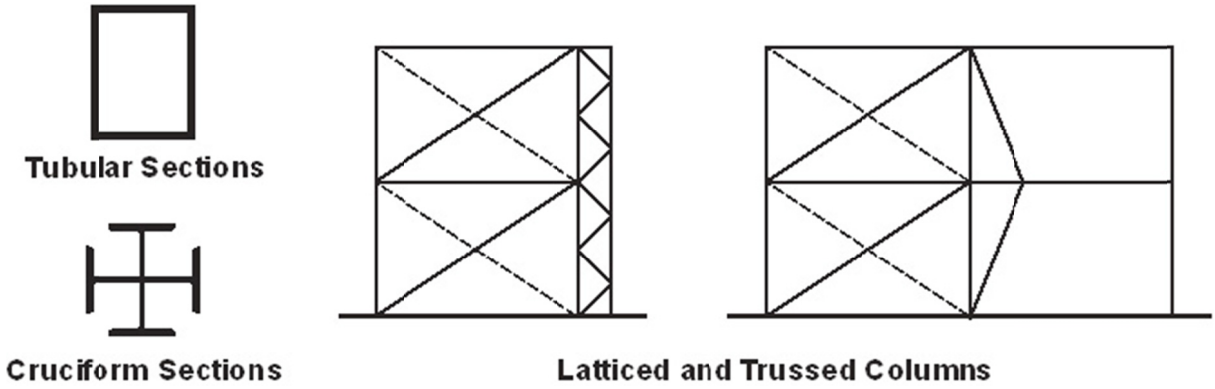

Figure 5.9: Alternative MT-BF column solutions.

5.4.5 Strut design

As discussed in the initial design, horizontal struts are employed between tiers to create a load path for the unbalanced horizontal components of the brace loads that develop at the brace-to-column connections. As shown in Figures 5.7 and 5.8a, the strut is subjected to axial compression forces of 409 and 570 kN in Analysis Steps 1 and 2, respectively. In the second case, shears in the columns must be included in the horizontal equilibrium at the strut-to-column nodes. The struts are also part of the lateral bracing system that constrains in-plane buckling of the columns within tiers, which results in additional axial load demand on the strut. If the braces are ignored, as they offer no or limited axial stiffness in the inelastic range, that bracing system includes the strut and the flexural and geometric stiffness of the column in tension. When examining the frame inelastic response, it can be expected that maximum additional compression in the strut, as induced by the column subjected to compression, is likely to occur for the conditions used in Analysis Step 2, when the Tier 2 column segment is markedly inclined and the Tier 1 segment is nearly vertical. For design purposes, the additional strut load due to stability effects can be conservatively taken equal to the axial load in the compression column in Tier 2 multiplied by the maximum expected drift in that tier (2%), thus neglecting the beneficial effect of the inclination of the column in Tier 1. The column axial compression is 528 + 237 = 765 kN, which gives 15 kN additional compression in the strut. Hence, for Analysis Step 2, the total required axial strength P_{rs} increases to 585 kN. The selected W250x58 section is found adequate for this loading condition. As discussed, the strut must also be designed to torsionally restraint the column at the tier level. This calculation is not illustrated here.

5.4.6 Critical Tier 1 scenario

For this frame, the story shear resistances from the braces in both tiers are close to each other and it is prudent to verify the design for the scenario where Tier 1 becomes critical after slightly modifying the brace expected strengths as was done in Table 5.3. Analysis Step 2 is examined here, i.e. when yielding is triggered in the tension brace in Tier 2, and the conditions are shown in Figure 5.10. In Tier 1, the brace forces are set equal to C'_{exp} and T_{exp}, respectively, for the compression and tension acting braces. In the non-critical tier (Tier 2), the corresponding forces are T_{exp} and C_{exp}. Compared to the critical Tier 2 scenario in Figure 5.8, the seismic induced axial compression load in the column increases from 1797 kN to 1952 kN for this scenario, which gives P_u = 237 + 1952 =

2189 kN, whereas the required flexural strength reduces from 430 to 340 kN-m. The W360x347 columns designed for the first critical tier scenario satisfy this strength requirement.

When Tier 1 is critical, Eq. 6 for the expected drift in the critical tier must be modified to read:

$$\Delta_{exp,1} = \Delta_{exp} + \frac{1}{h_1}\left(\frac{\Delta V_{br}}{2}\right)\left(\frac{h_1^2\, h_2^2}{3EI_c\, h}\right) \tag{7}$$

For this verification, ΔV_{br} is the difference between $V'_{br,exp}$ values in Table 5.3. For this frame, the two story shear resistances are nearly identical and it is therefore anticipated that the drift in Tier 1 will eventually become the same as the expected story drift (1.68%) after the compression and tension braces have experienced significant inelastic deformations. This behavior is adequate.

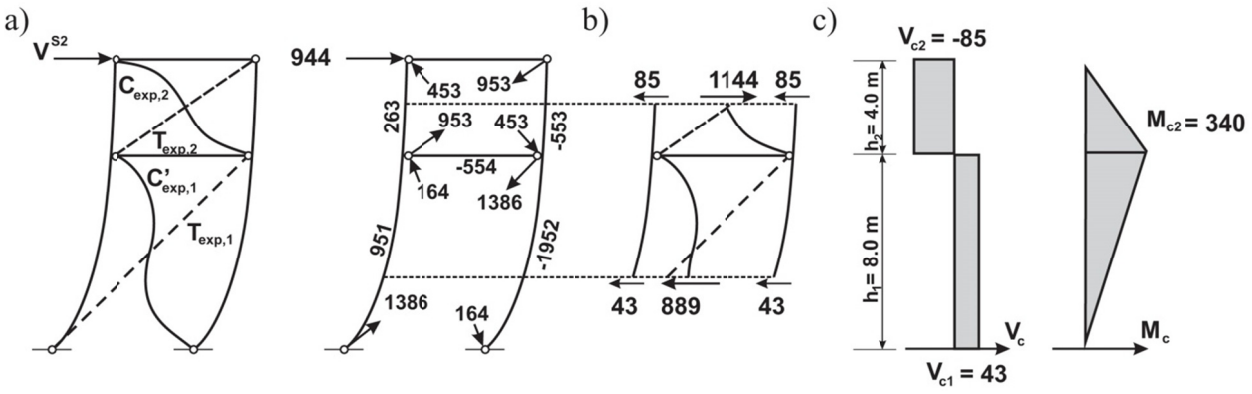

Figure 5.10: Analysis Step 2 for second scenario: a) Members axial loads; b) Horizontal shear forces in Tiers 1 and 2; and c) Column in-plane shears and bending moments. (Forces in kN, moments in kN-m)

5.5 Seismic performance of the proposed MT-BF design

5.5.1 Nonlinear static analysis

Nonlinear static analysis of the enhanced frame design is performed to validate the proposed analysis and design requirements. The analysis is carried out using the *OpenSees* program and the modeling assumptions described earlier. The brace properties that lead to the critical Tier 2 scenario are considered in the analyses.

The tier drifts are plotted against the imposed story drift in Figure 5.11a. As expected, brace tension yielding developed first in Tier 2, at a story drift of 0.5%, after brace buckling had occurred in both tiers at a drift of 0.3% (Figure 5.11b). Upon increasing further the roof lateral displacement, the tension brace in Tier 1 also yielded at a story drift of 0.9%, meaning that the columns are stiff enough to mobilize inelastic response in the non-critical tier and possess sufficient strength to resist without buckling the combined axial and flexural force demands associated with this behavior. In Figure 5.11c, the bending moment in the column at top of Tier 1 initiated when brace tension yielding started in Tier 2, reached a peak value when brace tension yielding initiated in Tier 1 and then gradually decreased, as anticipated in design. After yielding initiated in both tension braces, drifts increased at a similar rate in both tiers (Figure 5.11a). At the expected story drift of 1.68%, the drift in Tier 2 is equal to 2.15% which is close to the expected value of 2.0%. This good agreement was expected as the brace force conditions from the analysis in Figure 5.11c correspond well with the brace force scenario considered in the calculations. While the lateral deformations tended to concentrate in the critical tier when the frame was designed in accordance with the current AISC Seismic Provisions (Figure 5.5), the proposed design method produced more uniform tier drift and inelastic responses and prevented undesirable column in-plane flexural buckling and subsequent bi-axial buckling.

In design, a bending moment of 430 kN-m was predicted in Analysis Step 2, a value that corresponds to 0.34 M_{py} of the selected W360x347 columns. In Figure 5.11c, the peak bending moment reached in the analysis is approximately 0.19 M_{py}, suggesting that the analysis method contains conservative assumptions. This discrepancy can be explained by examining the evolution of the brace forces in Figure 5.11b. As considered in design, brace buckling occurred nearly simultaneously in both tiers. However, contrary to what was assumed, the resistance of the compression brace in Tier 1 did not remain equal to C_{exp} as the tension brace in that tier deformed in the elastic range prior to yielding, i.e. between 0.3 to 0.9% story drift. When that tension brace eventually reached yielding, the strength of the compressive brace in Tier 1 had reduced to 0.82 C_{exp}. Meanwhile, the compressive resistance of the brace in Tier 2 had degraded to 0.48 C_{exp}, a value higher than the AISC value for $C'_{exp} = 0.3C_{exp}$ assumed in design, which suggests that brace strength degradation in the analysis is less pronounced than that considered in design. Part of this discrepancy can be attributed to the fact that brace post-buckling compressive strength from pushover analysis is overestimated as degradation due to cyclic seismic demand is not

accounted for in the analysis (Imanpour and Tremblay 2014). This aspect is discussed below when examining dynamic seismic response of the frame. These differences between the brace compressive resistances obtained in both tiers from nonlinear analysis and those assumed in Analysis Step 2 resulted in a smaller unbalanced story shear ΔV_{br} and, thereby, a smaller flexural demand on the column.

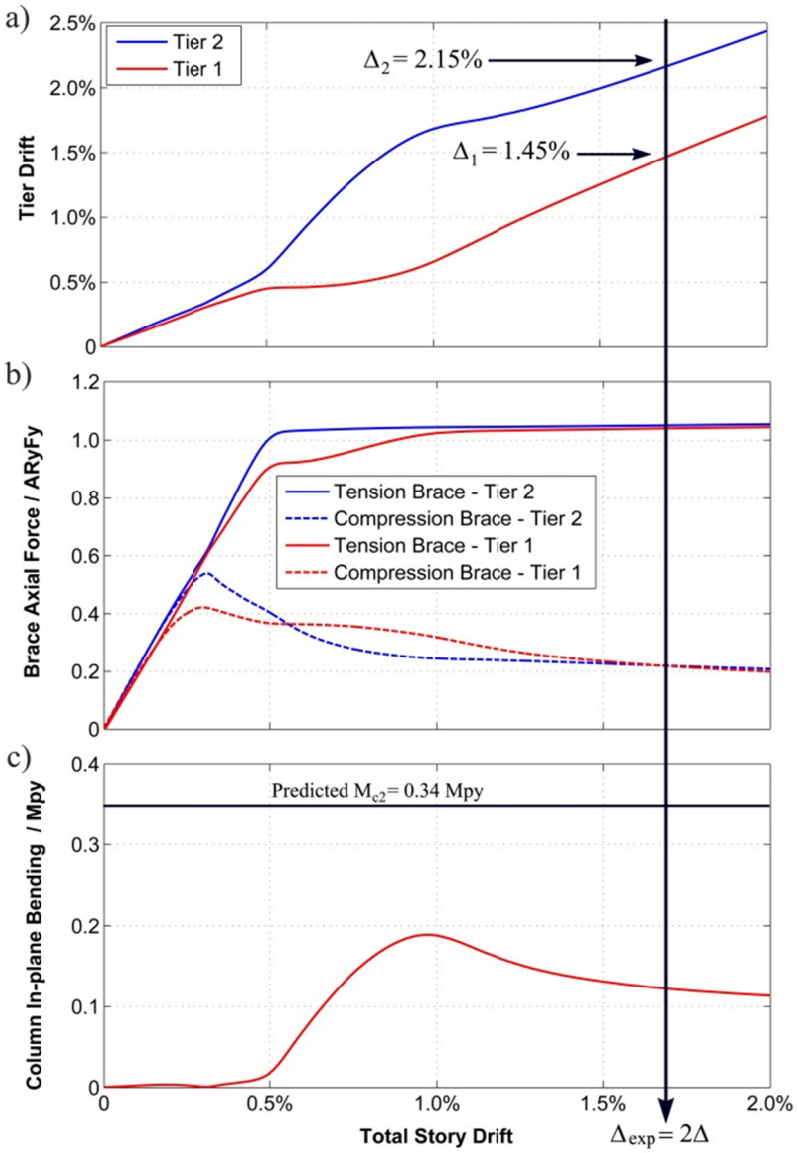

Figure 5.11: Pushover analysis of improved 2-tiered frame: a) Tier drift; b) Brace axial forces; and c) Column in-plane bending moment at the top of Tier 1.

5.5.2 Nonlinear response history analysis

Nonlinear response history NLRH analysis was performed under the far-field record set of 22 ground motion records described earlier. No column buckling was observed in the analyses and the response under the motion used to illustrate the performance of the frame designed with the current AISC Seismic Provisions in Figure 5.6 is presented in Figure 5.12. The peak story drift reached nearly 1.9%, which is approximately 2.3 times the design story drift (Figure 5.12a). In Figure 5.12b, both tier drifts are very similar and the peak tier drift in the critical tier reached 2.3%, which is close to, although larger than the 2% limit considered in design for this particular ground motion.

Brace axial force time history responses in Tiers 1 and 2 are illustrated in Figure 5.12c. As expected, the braces in both tiers buckled in compression and, more importantly, yielded in tension, which resulted in the uniform tier drift response. The history of ΔV_{br} and the column bending moment at the tier level are presented in Figures 5.12d and 5.12e, respectively. Both parameters exhibit nearly identical traces, confirming that the moment demand on the columns is directly related to the unbalanced horizontal components of the brace forces, as considered in design. Also, maximum values for both parameters are reached when brace tension yielding occurs first in the non-critical tier, at t =5.67 s, as assumed in Analysis Step 2. However, as was observed in the pushover analysis, both values are lower than those predicted in design. At t = 5.67 s in Figure 5.12c, it can be seen that the brace compressive resistance in Tier 1 has reduced to approximately 0.81 C_{exp} whereas the compression brace in Tier 2 (critical) has reduced to 1.37 C'_{exp} , i.e. close to the value assumed in design.

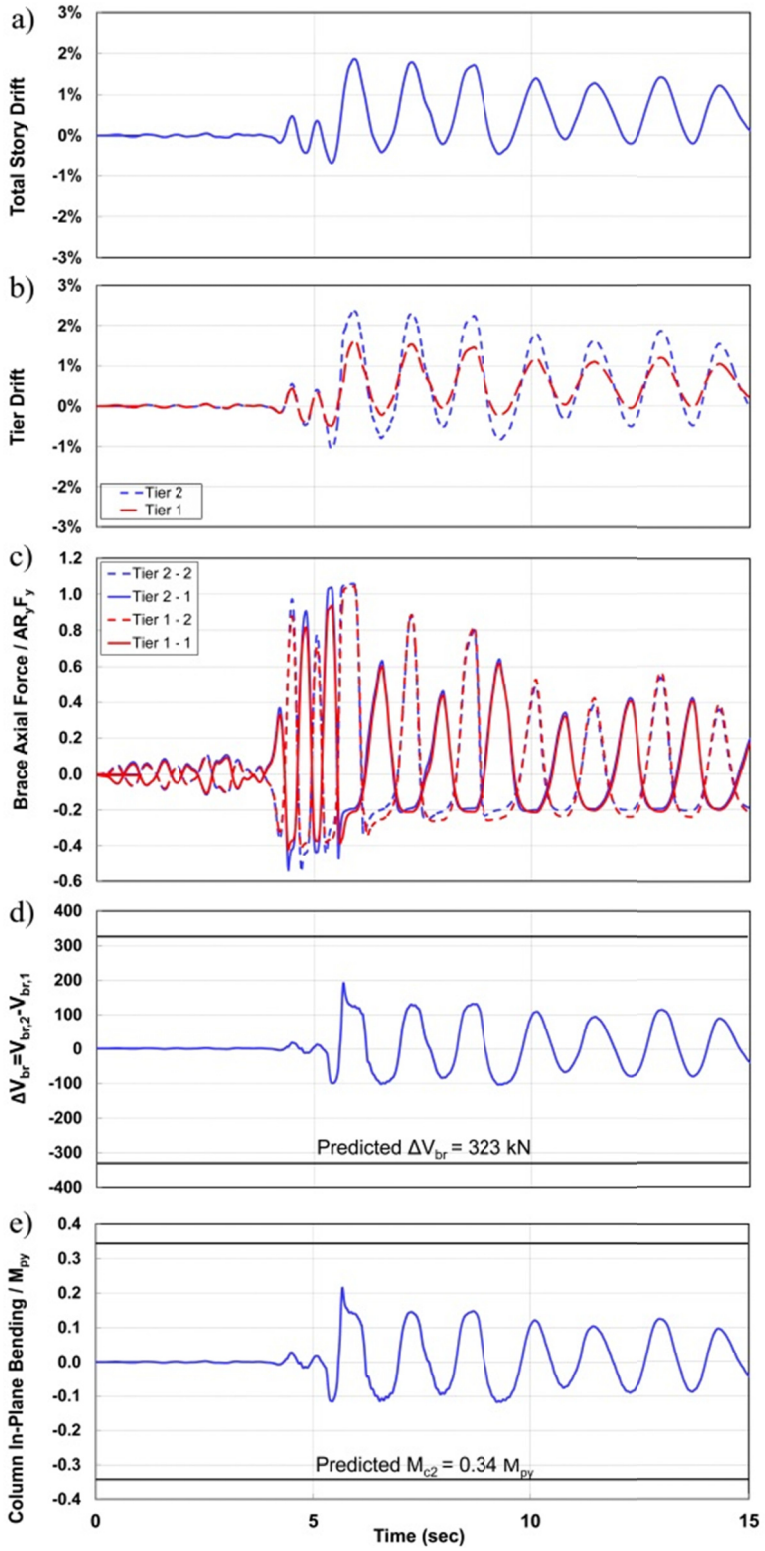

Figure 5.12: Time history analysis of enhanced 2-tiered frame under 1992 Cape Mendocino (Rio Dell Overpass record): a) Story drift; b) Tier drift; c) Brace axial forces; d) Story shear differences between Tier 1 and 2; and e) Column in-plane bending moment at the top of Tier 1.

Statistics of key response parameters under the 22 seismic records are given in Table 5.4. Results are shown for the W360x216 and W360x347 column sections, respectively the section satisfying the proposed minimum strength requirement and the section satisfying both the proposed strength and stiffness requirements. For both column sizes, the median and 84th percentile story drift values are larger than the design story drift Δ, which confirms that tier drifts in design should be predicted using expected story drift values larger than design story drifts. For this frame, the expected story drift adopted in design ($2.0\,\Delta$) appears appropriate, yet probably conservative. Peak story drifts are not sensitive to the column size; however the ratio between story drifts from analysis and design story drifts is higher with the larger columns. This suggests that the design story drift based on elastic stiffness is a weak indicator of peak seismic displacements including inelastic effects. Examination of the tier drift values shows that selecting a W360x347 section was necessary to maintain peak tier drifts within the 2% limit adopted in design. The tier drifts anticipated with W360x216 columns would likely lead to excessive inelastic demand on the braced frame components, confirming the need for minimum stiffness requirements for the columns. In the table, the marked reductions in tier drift ratios (ratio between peak tier drifts in the tiers) when using the W360x347 columns clearly show the benefit of using a sufficiently stiff columns to enforce a more uniform distribution of brace inelastic demand over the frame height.

Table 5.4: Statistics of peak frame response from NLRH analysis.

Parameter	**Frame with W360x216 columns**				**Frame with W360x347 columns**			
	50th perc.	**84th perc.**	**Max**	**Min**	**50th perc.**	**84th perc.**	**Max**	**Min**
Total story drift (%)	1.25	1.99	3.29	0.49	1.25	1.91	3.28	0.42
Roof displacement / Δ	1.42	2.25	3.73	0.56	1.49	2.27	3.90	0.50
Critical tier drift (%)	2.62	3.11	3.91	0.59	2.02	2.41	3.67	0.46
Tier drift ratio (Max / Min)	3.86	4.42	4.79	1.28	2.11	2.62	2.92	1.14
Critical tier drift (design / analysis)	0.89	0.75	3.98	0.60	0.99	0.83	4.31	0.54
Drift ratio (critical tier / roof)	1.98	2.08	2.23	1.19	1.54	1.70	1.84	1.09
$M_{cy,max}/M_{py}$ at top of Tier 1	0.36	0.43	0.48	0.04	0.22	0.24	0.27	0.02
$M_{c2}/ M_{cy,max}$ at top of Tier 1	1.58	1.34	15.7	1.20	1.59	1.42	16.9	1.28

In Table 5.4, the prediction of the peak tier drifts with the stiffer columns is acceptable. However, this good match is partly attributed to the conservatism in the selection of Δ_{exp}, since the median story drift only reached 1.5 Δ. In the table, the drift ratio represents the ratio between the peak tier drift and the peak story drift. With the W360x347 columns, the 50th and 84th percentile values of the tier drift ratio (1.54 and 1.70) are comparable, although larger than the ratio obtained in design (2.0%/1.68% = 1.2). This observation is different from the findings from pushover analysis, indicating that the brace force conditions at peak story drift during an earthquake are more critical than those assumed in design or obtained from static nonlinear analysis. Hence, tier drift predictions would have likely been too low had a lower Δ_{exp} been considered in design. Statistics of the column bending moments are given in Table 5.4. The parameter $M_{c2}/M_{cy,max}$ is the ratio of the design value to the peak value from the analysis. The values obtained for this ratio confirms that the compression brace force scenario assumed in design is conservative. It is worth noting that comparable ratios were obtained for both column sizes, which is consistent with the assumption that column maximum moments depend on brace forces and are not affected by the column stiffness.

5.6 Discussion on brace force estimates

For MT-BFs, the evolution of brace post-buckling strength in adjacent tiers is a key parameter in determining column bending moments and tier drifts. For simplicity in the proposed design procedure, maximum and minimum expected brace compressive strengths, C_{exp} and 0.3 C_{exp}, were used, as is currently done for SCBFs in the AISC Seismic Provisions. Actual brace force values under seismic ground motions can be different from these assumptions. For instance, for the brace in the non-critical tier (Tier 1), the brace compressive strength of interest is the value at a brace ductility of 1.0, i.e. when the companion tension brace in the same tier reaches yielding. Past experimental cyclic tests on bracing members show that this resistance varies between 0.4 and 1.0 C_{exp} (Figure 5.13), depending on factors such as brace slenderness, initial out-of-straightness, and imposed displacement signal. The average values are 0.78 and 0.89 C_{exp} for braces that were first loaded in compression and tension, respectively, in the tests. This shows that C_{exp} assumed for the compression brace for this tier is higher than the actual value. For the critical tier, the assumption that the force in the buckled brace has reduced to 0.3 C_{exp} is also conservative compared to actual

behavior. The impact of design brace compression strengths on column moments and tier drifts for MT-BFs is discussed herein based on the NLRH analysis of the frame example.

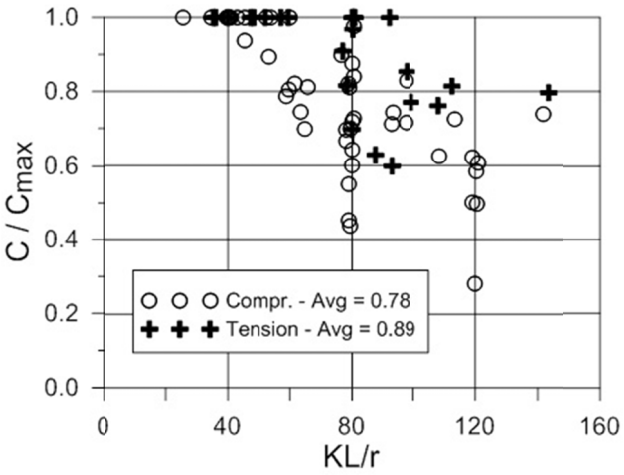

Figure 5.13: Strength degradation of the brace compressive strength at a ductility of 1.0 (adapted from Tremblay 2002).

Statistics of the brace compressive forces obtained from NLRH analysis of the frame example are given in Table 5.5. The values correspond to the forces at the time when yielding was triggered in non-critical Tier 1. Note that brace tension yielding did not occur in Tier 1 under four records, and the statistics are only presented for 18 analyses. The brace forces observed in NLRH analyses in non-critical Tier 1 are lower than the value assumed in design (C_{exp}), whereas the brace forces in critical Tier 2 are higher than the design value, C'_{exp} (= 0.3 C_{exp}). Column bending demand can be obtained from the median values of compressive brace forces presented in Table 5.5. Assuming brace compression forces equal to 0.8 C_{exp} and 0.5 C_{exp} in the non-critical and critical tiers would give ΔV_{br} = 186 kN, and M_{c2} = 248 kN-m = 0.20 M_{py} of the W360x347 column, a value that corresponds well to the seismic demand in Table 5.4. Comparing column bending demand obtained from NLRH analysis to the design value (248/430 = 0.58) shows that the brace forces assumed in design of the column represent conservative estimates of the brace forces when the column bending demand reaches its maximum value. Since these values only reflect the response of a single prototype structure, and brace force differences between adjacent tiers would vary with MT-BF geometry and brace sizes, it is recommended that a conservative approach be used to determine minimum in-plane flexural strength requirements of the columns as proposed in this paper.

Table 5.5: Statistics of compression brace forces from NLRH analysis (W360x347 columns).

Parameter	50th percentile	84th percentile	Max	Min
At peak story drift				
$(C/C_{exp})_1$	0.70	0.85	0.98	0.41
$(C/C_{exp})_2$	0.41	0.52	0.95	0.32
At brace tension yielding in Tier [1]				
$(C/C_{exp})_1$	0.79	0.83	0.86	0.54
$(C/C_{exp})_2$	0.49	0.52	0.53	0.39

[1]Statistics for 18 analyses

Statistics of the brace compression forces in both tiers at peak story drifts are also given in Table 5.5. The compression brace force in the non-critical tier (Tier 1) is higher than C'_{exp} assumed in the calculation of ΔV_{br} used in Eq. 6 to predict the maximum tier drift. The expected drift in Tier 2 (Eq. 6) can be recalculated using the median brace compression forces from Table 5.5, 0.7 C_{exp} and 0.4 C_{exp} in the non-critical and critical tiers, respectively, which gives ΔV_{br} = 188 kN. Using the median value of the roof drift from NLRH analysis for Δ_{exp} (= 1.26%) in Eq. 6 gives $\Delta_{exp,2}$ = 1.96%, close to the median value obtained from time history analysis. This calculation shows that Eq. 6 predicts tier drifts well provided that ΔV_{br} and Δ_{exp} are known. Realistically, conservatism must be maintained in critical tier drift predictions because the parameters Δ_{exp} and ΔV_{br} in Eq. 6 are difficult to estimate at the design stage.

5.7 Summary and conclusions

A two-tiered steel braced frame was designed in accordance with the current AISC 341-10 Seismic Provisions for special concentrically braced frames. Nonlinear static and response history analyses of the frame were performed to assess and investigate its response under seismic loading. New seismic analysis and design requirements have been proposed for two-tiered braced frames. The example frame was redesigned using the proposed method, and nonlinear static and response history analyses were performed to verify column stability conditions and assess brace ductility demand. The main conclusions of this study can be summarized as follows:

– The frame designed in accordance with the current AISC Seismic Provisions experienced concentration of inelastic demand in one (critical) tier, which induced in-plane flexural

demand on the columns that may lead to column buckling failure. In addition, concentration of drift in the critical tier produces large inelastic deformation on the bracing members and connections, which may lead to premature failure.

- The flexural demand on the column is due to the differences in story shear resisted by the bracing members in their inelastic range. The columns can be designed to compensate for this unbalance in story shears resistances and achieve more uniform tier drift demand.
- Minimum in-plane flexural strength requirements have been proposed to prevent buckling failure of the columns.
- Minimum in-plane flexural stiffness requirements have been proposed to control the peak tier drifts and prevent excessive inelastic demand. However, tier drift calculation depends on peak roof drift and brace forces at peak roof drift, and those parameters are difficult to estimate at the design stage.
- The analyses showed that the proposed design requirements produce MT-BFs that achieve the target behavior and avoid undesirable limit states.
- For the frame example studied, the analyses also showed that the brace force scenarios assumed in design resulted in conservative column bending moment demands.
- The proposed method indicates that both column moment and tier drift demand are proportional to the unbalanced story shear ΔV_{br}, and this parameter should therefore be minimized to achieve cost-effective designs. Frame geometries with equal tier heights should therefore be favored. Tightly sizing the bracing members should also contribute to reducing ΔV_{br}.

The proposed analysis and design requirements were developed and validated for one 2-tiered brace frame example. This method should be validated for a wider range of 2-tiered braced frames. Results of future studies should be also used to refine column bending moment and tier drift predictions. Similar design requirements should be developed for frames with three and more tiers. This study only examined MT-BF columns subjected to in-plane seismic demands. The stability of columns subjected to concomitant out-of-plane flexural demand (e.g., crane loading), including torsional response, should be investigated in future studies.

Acknowledgments

Funding from the Natural Sciences and Engineering Research Council (NSERC) of Canada is acknowledged. The authors would like to express their thanks to Professor Ali Davaran for his most valuable assistance in the development of the numerical models used in this study.

References

Aguero, A., Izvernari, C., and Tremblay, R. (2006). "Modelling of the Seismic Response of Concentrically Braced Steel Frames using the OpenSees Analysis Environment." *Int. J. of Advanced Steel Construction*, 2(3), 242-274.

Anderson, T. L. (1995). Fracture mechanics, 2nd Ed., CRC Press, Boca Raton, Fla.

ASCE. (2010). *SEI/ASCE 7-10, Minimum Design Loads for Buildings and Other Structures.* American Society of Civil Engineers.

AISC. (2010a). *ANSI/AISC 341-10, Seismic Provisions for Structural Steel Buildings.* American Institute of Steel Construction, Chicago, IL.

AISC. (2010b). *ANSI/AISC 360-10, Specifications for Structural Steel Buildings.* American Institute of Steel Construction, Chicago, IL.

AISC. (2012). *Seismic design Manual, 2nd ed.,* American Institute of Steel Construction, Chicago, IL.

Bruneau, M., Uang, C.-M., and Sabelli, R. (2011). *Ductile Design of Steel Structures, 2nd ed.,* McGraw-Hill Professional, New York, NY, 928 p.

Chen, C.-H., and Mahin, S. (2010). "Seismic Collapse Performance of Concentrically Steel Braced Frames." *Proc. ASCE Structures Congress 2010*, Orlando, FL, Paper No. 1265-1274.

Dalal, S.T. (1969). "Some non-conventional cases of column design." *Eng. J.*, AISC, 6(1): 28-39.

Davaran, A. (2001). "Effective length factor for discontinuous X-bracing systems." *J. Eng. Mech., ASCE*, 127(2): 106-112.

Davaran, A., and Hoveidae, N. (2009). "Effect of mid-connection detail on the behavior of X-bracing systems." *J. Constr. Steel Res.,* 65(4), 985–990.

Davaran, A., Gélinas, A., and Tremblay R. (2014). "Inelastic Buckling Analysis of Steel X-Bracing with Bolted Single Shear Lap Connections." *J. Struct. Eng., ASCE*, DOI: 10.1061/(ASCE)ST.1943-541X.0001141.

Dexter, R.J., Graeser, M., Saari, W.K., Pascoe, C., Gardner, C.A., and Galambos, T.V. (2000). Structural shape material property survey. Technical Report for Structural Shape Producers Council, University of Minnesota, Minneapolis, Minn.

Fell, B. V., Kanvinde, A. M., Deierlein, G.G., and Myers, A.T. (2009). "Experimental Investigation of Inelastic Cyclic Buckling and Fracture of Steel Braces." *J. Struct. Eng., ASCE*, 135(1), 19-32.

FEMA. (2009). *ATC 63, FEMA P695: Quantification of Building Seismic Performance Factors*." Applied Technology Council, Redwood City, CA.

Filiatrault, A., Tremblay, R., Christopoulos, C., Folz, B., and Pettinga, D. (2013). *Elements of Earthquake Engineering and Structural Dynamics, 3rd ed.*, Presses Internationales Polytechnique, Montreal, QC, 874 p.

Galambos, T.V. and Ketter, R.L. (1958). "*Columns Under Combined Bending and Thrust."* Fritz Engineering Laboratory Report 205A.21, Bethlehem, Pennsylvania.

Hsiao, P-C., Lehman, D.E., and Roeder, C.W. (2013). "A model to simulate special concentrically braced frames beyond brace fracture," *Earthquake Engineering and Structural Dynamics*, 42, 183-200.

Imanpour, A., Stoakes, C., Tremblay, R., Fahnestock, L., and Davaran, A. (2013). "Seismic Stability Response of Columns in Multi-Tiered Braced Steel Frames for Industrial Applications." ASCE Structures Congress, Pittsburgh, PA, 2650-2661.

Imanpour, A., and Tremblay, R. (2014). "Seismic design of steel multi-tiered braced frames: Application of incremental static analysis for design of steel multi-tiered braced frames." *Proc. Eurosteel 2014*, Naples, Italy, Paper no. 688.

Imanpour, A., Tremblay, R., Davaran A., Stoakes, C., and Fahnestock, L. (2015). "Seismic Performance Assessment of Multi-Tiered Steel Concentrically Braced Frames Designed in Accordance with Current AISC Seismic Provisions." Submitted to *J. Struct. Eng., ASCE*.

Lamarche C. P., Tremblay R., (2011) "Seismically induced cyclic buckling of steel columns including residual-stress and strain-rate effects." *J. of Constr. Steel Res.*, 67, 1401–1410.

MacRae, G. A., Kimura, Y., and Roeder C. (2004). "Effect of Column Stiffness on Braced Frame Seismic Behavior." *J. Struct. Eng., ASCE*, 130:3(381), 381-391.

McKenna, F. and Fenves, G.L. (2004). "*Open System for Earthquake Engineering Simulation (OpenSees).*" Pacific Earthquake Engineering Research Center (PEER), University of California, Berkeley, CA. http://opensees.berkeley.edu/.

Moreau, R., Rogers, C.A., and Tremblay, R. (2014). "Inelastic performance of the "Modified-hidden-gap" connection for square HSS brace members", *Proc. 10th National Earthquake Eng. Conf.*, Anchorage, AK, Paper No. 1010.

Palmer, K.D., Roeder, C.W., Lehman, D.E., Okazaki, T., Shield, C.K., and Powell, J. (2012). "Concentric X-Braced Frames with HSS Bracing," *Int. J. of Steel Struct.*, 12(3), 443-459.

Qu, B., Sanchez-Zamora, F., and Pollino, M. (2015). "Transforming Seismic Performance of Deficient Steel Concentrically Braced Frames through Implementation of Rocking Cores." *J. Struct. Eng., ASCE*, DOI: 10.1061/(ASCE)ST.1943-541X.0001085.

Rao, N.R.M., Lohrmann, M., and Tall, L. 1966. Effects of strain rate on the yield stress of structural steels. ASCE Journal of Materials,1: 242–262.

Roeder, C.W., Lehman, D.E., Clark, K, Powell, J., Yoo, J-H, Tsai, K-C, Lin, C-H, and Wei, C-Y (2011). "Influence of Gusset Plate Connection and Braces on the Seismic Performance of X-Braced Frames." *Earthquake Engineering and Structural Dynamics*, 40(4), 355-374.

Schmidt, B.J., and Bartlett, F.M. (2002). "Review of resistance factor for steel: data collection." Can. J. Civ. Eng. 29: 109–118.

Simão, P.D., Girão Coelho, A.M., and Bijlaard, F.S.K. (2012). "Stability design of crane columns in mill buildings." Engineering Structures 42: 51–82.

Stoakes, C., and Fahnestock, L. (2012). "Influence of weak-axis flexural yielding on strong-axis buckling strength of wide flange columns." Proc. of the Annual Stability Conference, Structural Stability Research Council, Grapevine, Texas.

Tremblay, R., and Filiatrault, A. (1996). "Seismic Impact Loading in Inelastic Tension-Only Concentrically Braced Frames: Myth or Reality?." *Earthquake Engineering and Structural Dynamics*, 25, 1373-1389.

Tremblay, R. (2002). "Inelastic seismic response of steel bracing Members." *J. Constr. Steel Res.*, (58), 665-701.

Tremblay, R., Archambault, M.H., and Filiatrault, A. (2003). "Seismic Performance of Concentrically Braced Steel Frames made with Rectangular Hollow Bracing Members." *J. of Struct. Eng., ASCE*, 129(12), 1626-1636.

Tremblay, R. (2003). "Achieving a Stable Inelastic Seismic Response for Concentrically Braced Steel Frames." *Eng. J., AISC*, 40(2), 111-129.

Uriz, P., Filippou, F.C., and Mahin, S.A. (2008). "Model for Cyclic Inelastic Buckling of Steel Braces." *J. Struct. Eng., ASCE*, 134(4), 619-628.

Uriz, P., and Mahin, S. (2008). *Toward Earthquake-Resistant Design of Concentrically Braced Steel-Frame Structures*. Report No. PEER 2008/08, Pacific Earthquake Engineering Research Center, University of California, Berkeley.

Yang, F., and Mahin, S. (2005). *Limiting net section fracture in slotted tube braces*. SteelTIPS, technical information and product service, Structural Steel Educational Council, Moraga, Calif.

Symbols

b	Brace width
C_d	Deflection amplification factor
C_{exp}	Brace expected strength in compression
C'_{exp}	Brace expected post-buckling strength
D	Dead load
EI_c	Column flexural stiffness
F_y	Yielding strength
g	Acceleration due to gravity
h	Total frame height

h_i	Tier height (i = 1 and 2)
I_{cy}	Column moment of inertia about weak-axis
I_e	Importance factor
K	Brace effective length factor
l	Brace workpoint dimension
M_{cy}	Column weak-axis flexural moment
M_{c1}	Column bending moment at the top of Tier 1
M_{c2}	Column bending moment at the bottom of Tier 2
M_{ny}	Column weak-axis nominal flexural strength
M_{py}	Column weak-axis plastic moment
M_{uy}	Column weak-axis required flexural strength
P_n	Nominal compressive strength
P_u	Required axial strength
P_{us}	Required strut axial strength
R	Response modification coefficient
r_x	Brace radius of gyration
R_yF_y	Expected steel yield stress
S_{DS}	Design spectral response acceleration parameter
S_s	Spectral response acceleration parameters at short period
S_1	Spectral response acceleration parameters at 1.0 s
t_{des}	Design wall thickness
T_{exp}	Brace expected strength in tension
V	Design story shear
V_{br}	Story shear resisted by the braces

$V_{br,exp}$	Story shear corresponds to the sum of the horizontal components of the brace strengths, T_{exp} and C_{exp}
$V'_{br,exp}$	Story shear corresponds to the sum of the horizontal components of the brace strengths, T_{exp} and C'_{exp}
V_c	Column shear force
δ_e	Story drift under V
ϕ_c	Resistance factor for compression
$\phi_c P_n$	Design axial strength
ϕ_b	Resistance factor for flexure
$\phi_b M_{ny}$	Column weak-axis design flexural strength
Δ	Design story drift
Δ_{exp}	Expected story drift
ΔV_{br}	Unbalanced story shear resisted by the braces in Tiers 1 and 2

CHAPTER 6 ARTICLE 3 : SEISMIC DESIGN AND PERFORMANCE OF MULTI-TIERED STEEL BRACED FRAMES INCLUDING THE CONTRIBUTION FROM GRAVITY COLUMNS UNDER IN-PLANE SEISMIC DEMAND

Ali Imanpour, Karl Auger, and Robert Tremblay

Polytechnique Montréal, Québec, Canada

The article was submitted to the *Journal of Advances in Engineering Software* on July 10, 2015.

Abstract

This paper examines the possibility of mobilizing gravity columns in the resistance of in-plane bending moments imposed on the columns of multi-tiered steel braced frames subjected to seismic loading. This would be the case when horizontal struts are used to connect gravity columns to braced frames at every tier level, as is often seen along exterior walls. A seismic design strategy based on the AISC Seismic Provisions is presented for 4-tiered prototype steel concentrically braced frames. Three different approaches are proposed for the design of the braced frame and gravity columns. A set of 12 four-tiered X-braced frames, ranging from 15 to 30 m in height and located in a high seismic area were designed based on the proposed design approaches. The seismic behaviour of the frames is evaluated using nonlinear response history analysis. The results show that the seismic performance of the braced frames is improved as nonlinear seismic demand on the bracing members is reduced when mobilizing the gravity columns for lateral resistance. Furthermore, gravity columns bending moment demands are distributed between braced frame and gravity columns in proportion of their relative flexural stiffness. Adequate seismic performance and cost-effective design can be achieved when columns of both types are designed to resist their respective share of the flexural demand. It is also found that the flexural demand can be omitted in the design of the gravity columns provided that the selected columns have sufficient nominal strength to carry that demand.

Keywords: multi-tiered braced frame, seismic performance, gravity column, nonlinear analysis.

6.1 Introduction

Tall single-storey steel buildings are commonly used for various applications such as industrial buildings, convention centres or airplane hangars. Steel braced frames are typically employed as lateral load resisting systems for these buildings. Two examples of this application are illustrated in Figure 6.1. The braced frames include multiple bracing panels over their height to form multi-tiered braced frames (MT-BFs). Different bracing configurations including X, V, Inverted V, and diagonal bracing can be utilized in multi-tiered braced frames. Various bracing systems such as tension-compression, tension only or buckling restrained braces (BRBs) can also be chosen for MT-BFs. Multi-tiered braced frames represent a practical and economical option for tall single-storey buildings or tall storeys in multi-storey buildings since brace lengths in MT-BFs are reduced compared to tall frames with only one single bracing panel, allowing smaller braces to be chosen. The use of shorter braces is also beneficial in seismic applications as it is easier to meet the stringent brace slenderness limits that are prescribed for ductile seismic behaviour. More importantly, reduced brace sizes result in lower seismic forces being transferred to brace connections, as well as beams, columns and diaphragms along the lateral load path.

a) b)

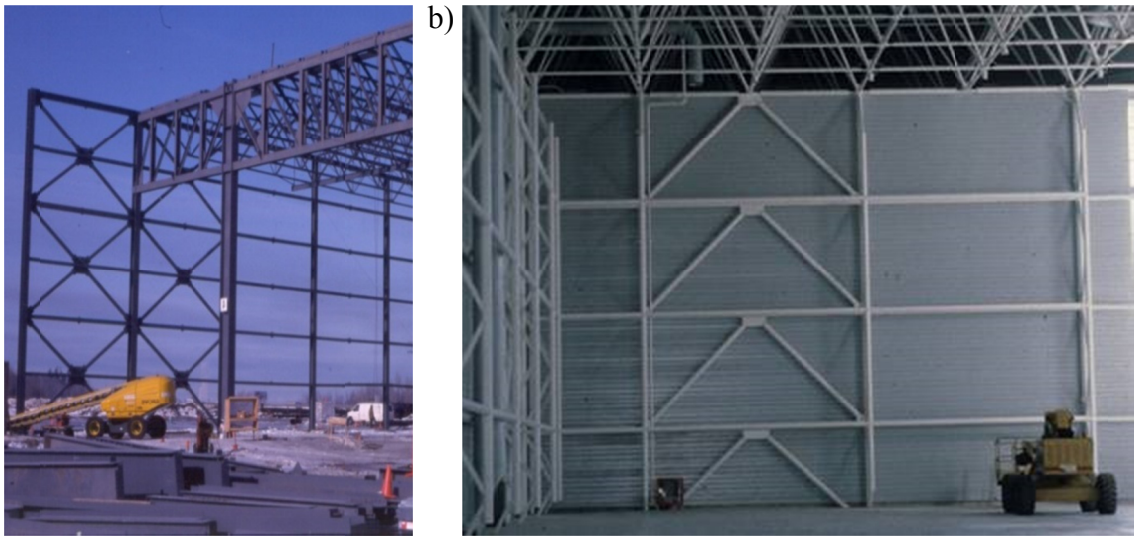

Figure 6.1: Multi-tiered steel braced frames: a) 3-tiered braced frame with X-bracing; and b) 4-tiered braced frame with Inverted V-bracing (Courtesy of the Canadian Institute of Steel Construction).

Nonlinear static and seismic dynamic response history analyses of multi-tiered steel braced frames have revealed that nonlinear response tends to concentrate in the tier where brace tension yielding occurs first (critical tier) because the storey shear resistance provided by the braces in that tier reduces as the strength of the compression brace degrades upon buckling, preventing inelastic response to develop further in the other tiers. This behaviour is illustrated for a 4-tiered braced frame in Figure 6.2 for the case where brace tension yielding starts in Tier 1. This behaviour may lead to excessive ductility demands on the braces in the critical (weakest) tier, which may cause premature failure of the bracing members due to low-cycle fatigue. Furthermore, the columns are subjected to in-plane bending moments due to the differences in drifts between adjacent panels; this demand may lead to plastic hinging forming in the columns and, possibly, column buckling and global frame instability. As the MT-BF columns lack the lateral out-of-plane support at intermediate brace-to-column connection points, column in-plane flexural buckling could initiate out-of-plane buckling response. This behaviour is anticipated in all MT-BFs, even if the braces are well proportioned to provide uniform storey shear resistance over the frame height because of unavoidable variations in geometric imperfections, material properties (brace yield strengths) or boundary conditions that will make one tier actually weaker than the other ones [1].

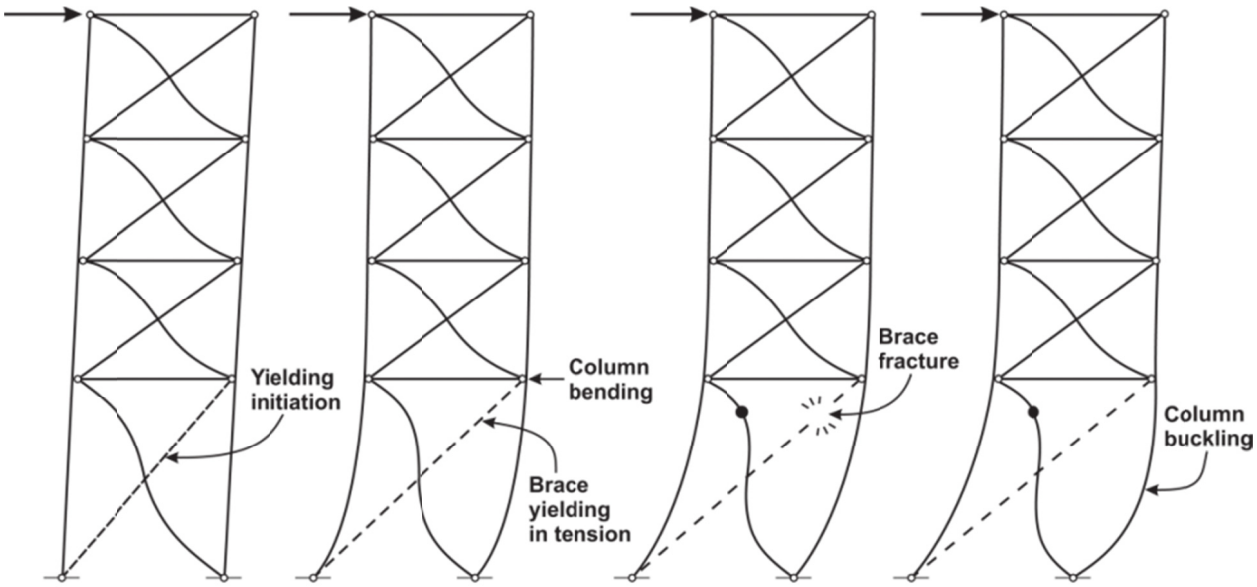

Figure 6.2: Concentration of inelastic demand in Tier 1 of a 4T-BF (Tier 1 is critical).

This non-uniform brace inelastic response must be accounted for and controlled to prevent brace fracture and column buckling. This can be achieved by providing the columns with sufficient in-plane flexural stiffness to distribute the brace inelastic response along the frame height such that the drift in the critical tier remains within acceptable limits. The columns must also be designed to resist the axial compression load in combination with the in-plane flexural moment demands resulting from the non-uniform brace inelastic response along the frame height. Horizontal struts must also be provided at every tier level to provide in-plane lateral bracing to the columns and avoid individual columns to resist the horizontal unbalanced forces after brace buckling has occurred [1-4].

In multi-tiered braced frames used along exterior walls of buildings, all columns including the braced frame columns (BFCs) and the adjacent gravity columns (GCs) are typically I-shaped members oriented such that wind loads induce bending moment about strong axis. This column orientation is also preferred when columns should resist crane loading or are part of moment frames spanning perpendicular to the braced frame plane. Horizontal struts are typically placed between all columns to provide in-plane lateral bracing for the gravity columns at the tier levels. During a strong earthquake, the GCs being laterally tied to the BFCs will be forced to also bend in-plane and, thereby resist a portion of the in-plane moment demand imposed to the braced frame columns due to sequential yielding of the braces. This behaviour reduces the moment demands on the BFCs, but the GCs must be able to carry the in-plane bending without buckling. A preliminary study was performed by the authors on a 4-tiered concentrically braced frame where the BFCs and GCs tied together at tier levels were designed taking into account the in-plane flexural bending demand imposed on each column [5]. The study showed that the seismic demand on the bracing members and braced frame columns can be effectively reduced by involving the gravity columns in the resistance of the in-plane flexural demand. Additionally, more economical and effective design can be achieved when BFCs are designed to resist the in-plane bending demand and GCs are only sized to carry gravity loads plus wind loads.

This paper presents a complementary study on the seismic design and performance of multi-tiered steel braced frames with struts connecting to adjacent gravity columns. Two criteria are used to evaluate the seismic performance of the frames: 1) column instability; and 2) tier drift demands. The design and seismic response of a prototype 4-tiered braced frame with X-bracing panels are examined in detail. Five design strategies are examined. The frame was first designed

in accordance with current AISC Seismic Provisions [6] for Special Concentrically Braced Frame (SCBF) systems, neglecting the contribution of the gravity columns. In the second design, the BFCs were redesigned using the additional analysis and design requirements for MT-BF columns, still neglecting the GCs. In the three subsequent designs, different approaches were investigated when considering the contribution of the gravity columns, which resulted in three different column sizes. The inelastic behaviour of the frame is examined using nonlinear incremental static analysis. The frame response is then investigated under a suite of ground motions through Nonlinear Response History (NLRH) analysis to verify column stability conditions and assess tier drift demand. The study is then extended to of 12 different 4-tiered braced frames having different heights and tier height ratios. The frames were located in zones of high, moderate and low seismicity in the United States and were also designed as Ordinary Concentrically Braced Frame (OCBF) systems. Values assumed in design are compared with the results obtained from the NLRH analyses. The cost-effectiveness of the different design strategies is also compared.

6.2 Flexural demand on MT-BF columns

Special seismic analysis and design requirements have recently been proposed for MT-BFs [2, 7]. These requirements aim at limiting the ductility demand on bracing members and avoiding column instability under strong seismic events by distributing the nonlinear deformation demand between bracing panels. Such desired response is shown in Figure 6.3 for the 4-tiered frame of Figure 6.2. After brace tension yielding has been initiated in the critical tier, the MT-BF columns acting in flexure are used to progressively trigger yielding of the tension braces in the adjacent tiers as the storey drift is increased, with the objective of limiting the brace inelastic deformations in the critical tier within an acceptable value when the roof displacement reaches the anticipated seismic lateral displacement.

In order to achieve this behaviour, the columns must possess sufficient in-plane flexural strength and stiffness. More specifically, the columns of a weaker tier where brace tension yielding and buckling has developed must be capable of carrying a portion of the storey shear such that the total storey shear resisted by the braces and columns in that tier is sufficient to initiate brace tension yielding in adjacent tiers of the frame. Shear strength does not generally control the column design; however, the associated bending moments which may require stronger columns. Additionally, the

flexural stiffness of the columns must be large enough to limit the drift in the critical tier and prevent brace or brace connection fracture in that tier. The number of tiers that must contribute to inelastic frame deformations therefore depends on the maximum allowable tier drift.

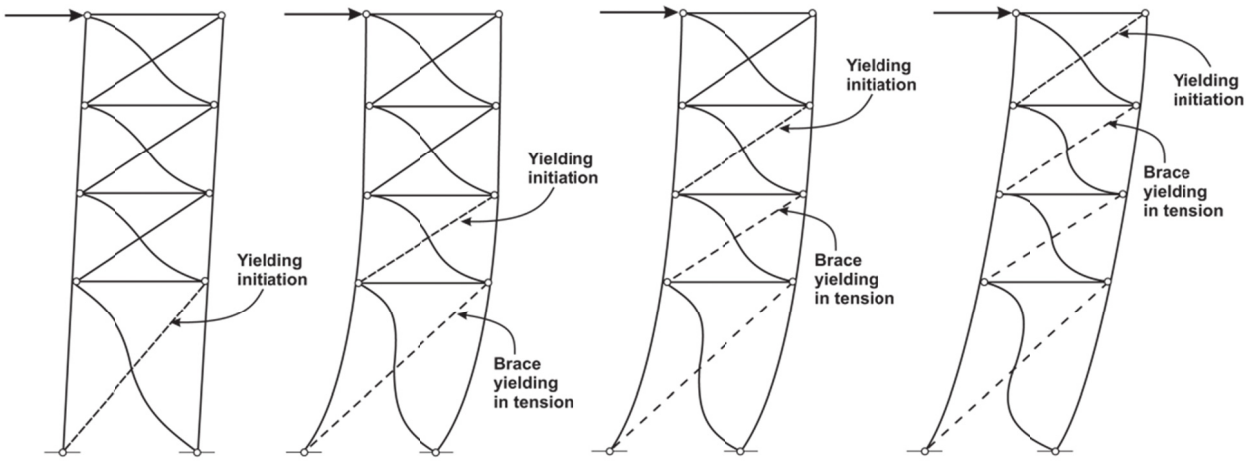

Figure 6.3: Desired lateral response of 4-tiered braced frame.

As shown in Figure 6.4, gravity columns become involved in the braced frame response when horizontal struts are present between the braced frame and the gravity load carrying frame as both the BFCs and GCs are subjected to the same in-plane bending deformations imposed at every tier. In that situation, the gravity columns can contribute to achieve the aforementioned desired MT-BF seismic response, provided that they are designed to resist the induced in-plane bending moments. The horizontal struts connecting BFCs and GCs also need to resist axial compression and tension forces resulting from this interaction.

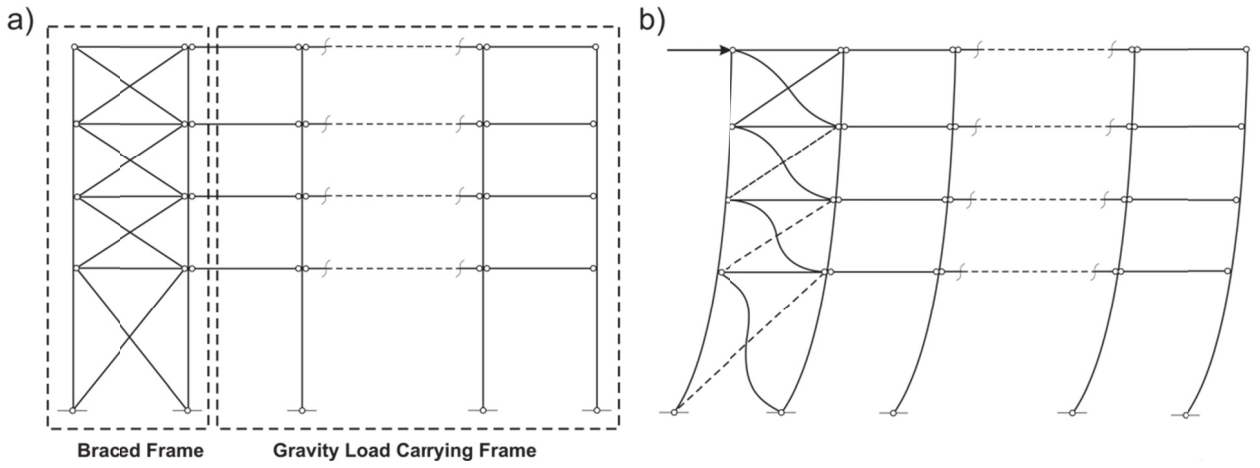

Figure 6.4: a) 4-tiered braced frame with gravity columns; and b) Lateral response of the 4-tiered frame with gravity columns involvement.

Figure 6.5 shows the free body diagram of the columns of the 4-tiered frame when brace tension yielding is initiated in Tier 2. In this case, it is assumed that the braces in Tier 2 can resist a higher storey shear compared to those in Tier 1 but smaller than those in Tiers 3 and 4. Hence, the braces acting in tension in Tiers 1 and 2 reach their expected strength in tension (T_{exp}) before brace tension yielding initiates in the other tiers. It is also assumed that the tension brace in Tier 1 was stretched significantly in the inelastic range before yielding is triggered in the tension brace in Tier 2, which caused severe buckling of the compression brace in Tier 1. Hence, when brace tension yielding eventually occurs in Tier 2, the compression brace in Tier 1 has reduced to its post-buckling strength (C'_{exp}), while all other compression braces have just reached their expected buckling strengths (C_{exp}). In Figure 6.5, the storey shears resisted by the braces in Tiers 1 and 2 are referred to as V_{br1} and V_{br2}, respectively. These shear forces can be determined by projecting the brace axial forces on the horizontal plane. As shown, columns are bent due to the relatively larger drift in Tier 1, inducing shear forces in the columns in Tiers 1 and 2: V_{bc1} and V_{bc2} in the BFCs, and V_{gc1} and V_{gc2} in the GCs. Column shears in Tier 1 increase the total storey shear resistance at this tier while column shears in Tiers 2 reduce the total storey shear resistance in Tier 2, which permits to trigger brace yielding in the stronger Tier 2.

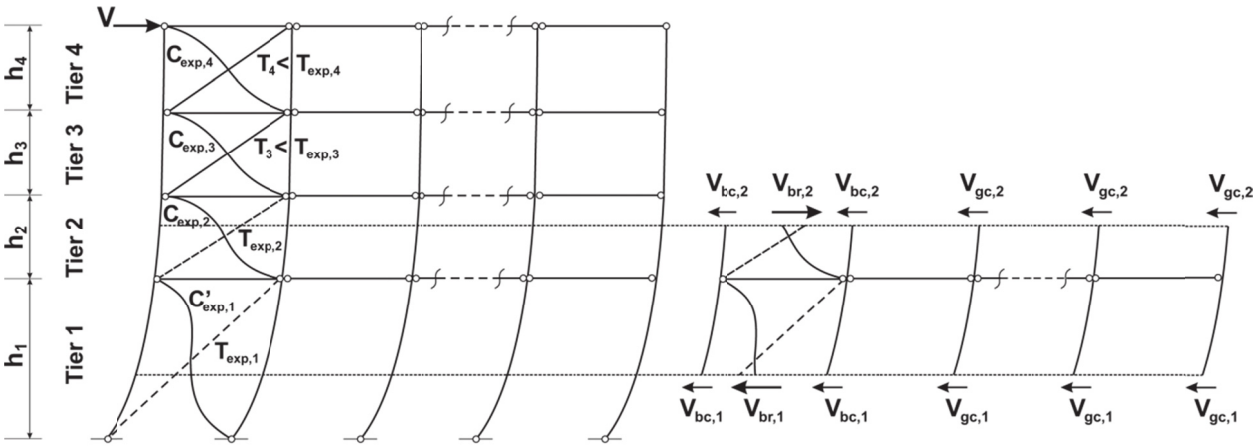

Figure 6.5: Storey shears resisted by the braces and columns when brace tension yielding is initiated in Tier 2 of the 4-tiered frame example.

The column shears V_{bc1} and V_{gc1} can be determined from the horizontal equilibrium of the storey shears acting in Tiers 1 and 2:

(1) $$2V_{bc2} - 2V_{br,2} + n_{gc}V_{gc2} = -2V_{bc1} - 2V_{br,1} - n_{gc}V_{gc1}$$

where n_{gc} is the number of gravity columns interacting with the braced frame columns. When solving Eq. 1, the ratio between column shears in Tiers 1 and 2 are estimated assuming that the columns act as continuous members spanning over the two tiers and the ratio between shears in the BFCs and GCs are based on the relative flexural stiffness of the columns. Once columns shears are determined, the bending moments can be obtained. For the conditions shown in Figure 6.5, bending moments in the columns are maximum at Tier 1 strut level:

(2) $$M_{bc1} = V_{bc1}h_1$$

(3) $$M_{gc1} = V_{gc1}h_1$$

The process is repeated until the minimum required number of tiers where brace tension yielding must be initiated is attained when the roof displacement reaches the anticipated seismic lateral displacement. In-plane bending demands on the BFCs and GCs are then obtained at every step.

6.3 Frame studied and design loads

A 20 m high, single-storey industrial building located on a site class D in coastal California was selected to study the contribution of the gravity columns to the seismic response of MT-BFs. The building has 120 m x 54 m plan dimensions and two concentrically braced frames are placed along each of the four exterior walls. One of the braced frames located along one of the 120 m long walls was chosen for the study. Along those walls, there is a total of 20 column bays, 6 m wide, resulting in 4 BFCs and 17 GCs including the corner columns. The studied frame is shown in Figure 6.6a. This is a 4-tiered X-braced frame with a width L = 6 m. The tier heights are 8 m for Tier 1 and 4 m for Tiers 2 to 4. The corner columns of the building are relatively small because they carry limited gravity loads and are laterally braced in both orthogonal directions. They were therefore ignored in the design and analysis of the braced frame. The studied braced frame was then assumed to laterally brace a total of 7.5 gravity columns (n_{gc} = 7.5).

The structure design was performed in accordance with the ASCE 7-10 provisions [8], the AISC 360-10 Specification [9] and the AISC 341-10 Seismic Provisions [6]. The building was assigned to Risk Category II, which gives importance factors of 1.0 for seismic and wind loads. The equivalent lateral force procedure was used to calculate the design seismic loads. The design spectral accelerations for the site are 1.0 and 0.6 at periods of 0.2 and 1.0 s. The design roof and wall dead loads are equal to 1.2 kPa, which gives a seismic weight of 11952 kN. The braced frames are special concentrically braced frames (SCBFs) with R = 6.0 and C_d = 5.0. The design period for the structure was 0.65 s, which resulted in a base shear of 15.5% of the seismic weight. Design seismic load per braced frame was 509 kN considering accidental torsion. For the load combination including seismic loads, each column carries a factored axial dead load of 272 kN, including vertical ground motion effects.

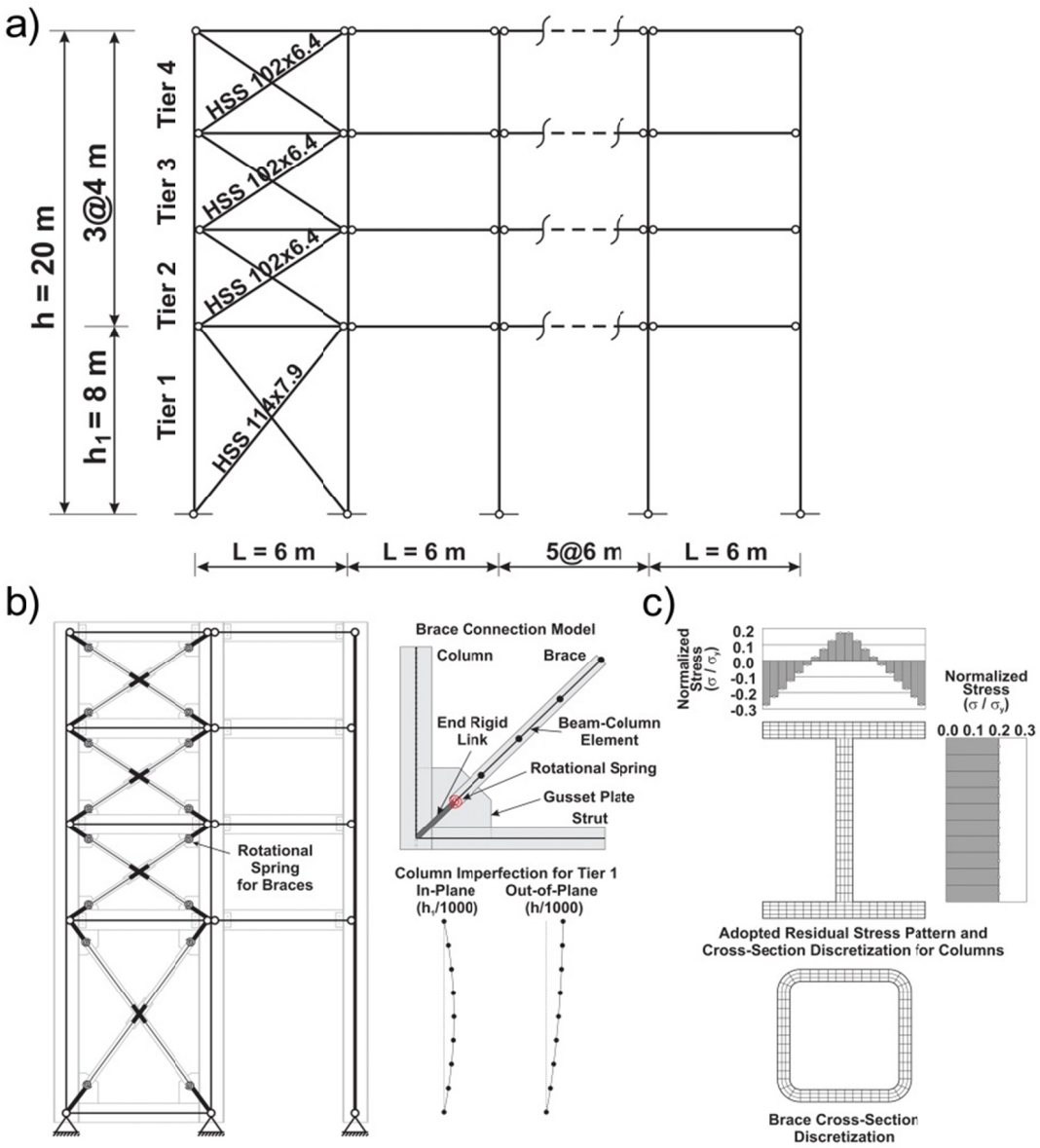

Figure 6.6: Studied 4T-BF with tributary gravity columns: a) Frame configuration and selected bracing members; b) Numerical model with gravity columns and brace connection model; and c) brace and column cross-section discretization and adopted residual stress pattern for columns.

Wind loading influenced the design of the columns located along the exterior walls. A design wind pressure of 0.89 kPa was determined assuming a basic wind speed of 49 m/s, an Exposure Category C and enclosed building conditions. That pressure induces a maximum factored out-of-plane moment of 257 kN-m for each column, assuming that the columns are simply supported at ground and roof levels. This moment is combined with a concomitant factored axial dead load of 233 kN.

6.4 Braced frame design

6.4.1 Design of the bracing members

The bracing members in each tier were designed to resist in tension and compression the 509 kN seismic storey shear. The required compression strengths (P_u) and design axial strength ($\phi_c P_n$) are given in Table 6.1. The brace members were selected from cold-formed square tubing (HSS members) conforming to ASTM A500, grade C, with F_y = 345 MPa and $R_y F_y$ = 483 MPa. Two different HSS sizes were selected due to the different brace lengths. Their properties are given in the table. The brace effective length for out-of-plane buckling was taken as the net length between end and mid-length connections. As prescribed in AISC 341, the brace slenderness ratio, KL/r, was limited to 200 and the cross-sections had to meet the limits specified for highly ductile members. Cross-sectional areas (A) of the selected braces are given in Table 6.1.

Table 6.1: Brace design for the 4-tiered braced frame example.

Tier	**Shape HSS**	***A*** **mm_2**	***KL*** **mm**	P_u **kN**	$\phi_c P_n$ **kN**	T_{exp} **kN**	C_{exp} **kN**	C'_{exp} **kN**	V_{exp} **kN**
2 to 4	102x102x6.4	2170	3245	311	401	1048	579	173	1354
1	114x114x7.9	3020	4350	425	446	1459	588	176	1105

6.4.2 Design of the columns

The columns are continuous over the whole building height and are oriented such that out-of-plane bending occurs about their strong axis. For design, they were assumed to be pin-connected for flexure about both axes at their top and bottom ends. The columns were verified for in-plane flexural buckling and out-of-plane flexural-torsional buckling according to the AISC 360 Specification. Torsional restraint was considered at both ends and at every tier level. For the braced frame columns, axial and flexural demands were maximum in the first tier and column effective lengths of 16.3 m and 6.4 m were considered for out-of-plane and in-plane buckling, respectively, based on the results from elastic buckling analysis of the columns for the axial loads acting in every tier level. These reduced effective length values account for non-uniform axial loading [10, 11]. As prescribed for SCBFs in the AISC Seismic Provisions, the columns also had

to meet the cross-section limits for highly ductile members. Effective lengths of 20 and 8 m were assumed for the gravity columns as the axial loads in these columns are same over their full height. In this study, GCs were selected from shapes satisfying the limits specified in the AISC Specification for non-slender members. Additional information on member design is given in Imanpour et al. [1].

Five different approaches were used for the design of the braced frame and gravity columns. In Design Approach 1, the in-plane flexural demand from MT-BF response was neglected, as currently assumed in the AISC Seismic Provisions. In the second approach, the MT-BF column flexural demand was assumed to be entirely resisted by the braced frame columns only, neglecting the interaction with the gravity columns. In the first two designs, the gravity columns were therefore designed for gravity and wind load effects only. In the third approach, the gravity columns were designed to carry their share of in-plane bending moments from MT-BF seismic behaviour, and the braced frame columns were only designed for axial compression load. Conversely, in the fourth approach, the braced frame columns were sized to resist their share of the MT-BF in-plane flexural demand and no seismic bending demand was considered for the design of the gravity columns. In Design Approach 5, the MT-BF in-plane flexural demand was shared between the braced frame and gravity columns based on their relative in-plane flexural stiffness. For each design approach, the strength of the columns was verified for the combination of axial loads with in-plane and/or out-of-plane bending moments, as applicable. In Design Approaches 2 to 5, the columns designed for in-plane bending moments were verified to possess sufficient flexural stiffness to limit the drift in the critical tier to 2% of the tier height when the frame roof drift reaches $1.5C_d\Delta_e / h$, where Δ_e is the roof displacement under the design seismic load and h is the total frame height. The multiplier 1.5 accounts for the possibility of peak storey drift exceeding design storey drift for MT-BFs under maximum considered earthquake (MCE) hazard level [1]. It should be noted that flexural stiffness of the BFCs in Design Approach 3, and the GCs in Design Approach 4 were included in drift calculation. Results for each design approach are summarized in Table 6.2 and detail is given below.

Table 6.2: Shapes selected for the braced frame and gravity load carrying columns.

Design Approach	In-plane MT-BF bending demand	Braced Frame Columns		Gravity Columns		Column steel tonnage (t)
		Section	In-plane moment	Section	In-plane moment	
1	Not Shared	W610x174	No	W310x86	No	19.9
2	Not Shared	W360x421	Yes	W310x86	No	29.7
3	Shared	W610x174	No	W360x162	Yes	31.3
4	Shared	W360x347	Yes	W310x86	No	26.8
5	Shared	W360x262	Yes	W310x107	Yes	26.5

6.4.2.1 Design Approach 1 (AISC design procedure)

In Design Approach 1, the braced frame columns were designed in accordance with the requirements of the current AISC Seismic Provisions. Two analyses cases must be considered to obtain the column axial force demand due to the seismic effects: Analysis case 1 where all the braces reach their expected strength in tension (T_{exp}) and compression (C_{exp}); and Analysis case 2 where all the tension braces reach their expected yield tensile strength (T_{exp}) whereas the compression braces reach their expected post-buckling strength (C'_{exp}). The flexural demand from these two analysis cases need not be considered for column design. The expected brace strengths were determined with the expected brace yield strength R_yF_y = 483 MPa; the values are given in Table 6.1. For this frame, Analysis case 1 was more critical and the required axial strength, P_u, when combining gravity load effects was equal to 4154 kN. A W610x174 shape was selected to carry this axial load.

The gravity columns were designed to resist the axial gravity loads (P_u = 233 kN) plus the out-of-plane bending moment due to wind loading, M_{ux} = 257 kN-m. The columns were verified for in-plane stability under gravity plus seismic loading using Eq. 4 and out-of-plane stability under gravity plus wind loading using Eq. 5 (AISC 360-10, Section H1):

$$\frac{P_u}{\phi_c P_n} + \frac{8}{9}\left(\frac{M_{ux}}{\phi_b M_{nx}} + \frac{M_{uy}}{\phi_b M_{ny}}\right) \le 1.0 \qquad \text{where } \frac{P_u}{\phi_c P_n} \ge 0.2 \tag{4}$$

$$\frac{P_u}{2\phi_c P_n} + \frac{M_{ux}}{\phi_b M_{nx}} + \frac{M_{uy}}{\phi_b M_{ny}} \le 1.0 \qquad \text{where } \frac{P_u}{\phi_c P_n} \le 0.2$$

(5) $$\frac{P_u}{\phi P_{ny}} + \left(1.5 - 0.5\frac{P_u}{\phi P_{ny}}\right) + \left(\frac{M_{ux}}{C_b \phi_b M_{ux}}\right)^2 \leq 1.0$$

where P_u and M_u are respectively the column required axial and flexural strengths, $\phi_c P_n$ is the column design axial strength, set equal to the minimum of column axial strength due to in-plane buckling, $\phi_c P_{ny}$, out-of-plane buckling, $\phi_c P_{nx}$, and torsional buckling, $\phi_c P_{nz}$, $\phi_b M_n$ is the design flexural strength, and C_b is the lateral-torsional buckling modification factor. W310x86 columns were found to be adequate for the gravity columns. The BFCs were also verified using Eqs. 4 and 5 for gravity and wind loading.

6.4.2.2 Design Approach 2

In Design Approach 2, the braced frame columns were designed to resist the entire in-plane bending demand induced by progressive brace yielding along the frame height, not counting on the contribution of the gravity columns. The maximum design in-plane moment in the BFCs was at Tier 1 level and was equal to M_{bc} = 423 kN-m. As shown in Table 6.2, much heavier sections, W360x421 *vs* W610x174, with greater in-plane flexural strength and stiffness, were needed to achieve the desired MT-BF response shown in Figure 6.3 [2]. The gravity columns remained same as per Design Approach 1.

6.4.2.3 Design Approach 3

In Design Approach 3, the in-plane flexural demand generated by sequential yielding of the bracing members was shared between the braced frame and gravity columns as a function of their relative flexural stiffness. The approach was therefore iterative since the column sections must be known to determine the flexural demand. However, only the gravity columns were designed to resist their share of the in-plane bending flexural demand, the objective being to verify if the BFCs could perform adequately, without explicit consideration of MT-BF in-plane bending in their design, because that demand would have been reduced by the presence of the GCs. For each GC, the maximum in-plane bending moment was M_{gc} = 96 kN-m (= 0.18 $M_{py\text{-}gc}$) and occurred at Tier 1 level. The column sections were increased from W310x86 to W360x162. The maximum in-plane moment demand on each BFC was 58 kN-m at Tier 1 level. When considering this demand, the required strength from Eq. (4) exceeds by 32% the column available strength and limited seismic inelastic response was therefore anticipated for these columns. In this and

subsequent design approaches, the BFCs and GCs as designed were verified to possess a total flexural stiffness sufficient to limit the drift in the critical tier to 2% of the tier height.

6.4.2.4 Design Approach 4

Design Approach 4 is similar to Design Approach 3 except that only the BFCs were designed for their share of the in-plane flexural demand induced by MT-BF seismic response. This is to verify if gravity columns designed for gravity and wind loads only can sustain the part of the in-plane flexural demand they would attract because they are tied to the BFCs by means of the struts. In that design, the moment in each BFC in Tier 1 was equal to M_{bc} = 315 kN-m and a W360x347 section was selected for these columns. W310x86 sections were kept for the GCs. From analysis, these columns were found to develop in-plane seismic bending moment of 28 kN-m at Tier 1 level, resulting in combined axial plus flexural demands equal to 45% of the columns capacities when applying the AISC Specification interaction equations.

6.4.2.5 Design Approach 5

In Design Approach 5, both the BFCs and GCs were designed to resist their respective share of the in-plane bending moments induced by inelastic MT-BF seismic response. That demand was maximum at Tier 1 level: M_{bc} = 228 kN-m (= 0.25 $M_{py\text{-}bc}$) and M_{gc} = 53 kN-m (= 0.19 $M_{py\text{-}gc}$) for braced frame and gravity columns, respectively. The two selected column sizes were W360x262 and W310x107, respectively, as shown in Table 6.2. It is noted that smaller GCs are needed in this design compared to those from Design Approach 3, the reason being that the BFCs from Design Approach 5 are larger and attract a larger portion of the bending moments. Similarly, BFCs from Design Approach 5 are smaller than those required in design Approach 4 because the GCs in Design Approach 5 carry a larger faction of the total in-plane flexural demand than in Design Approach 3.

6.4.3 Design of the struts

The struts are made from ASTM A992 W shapes with F_y = 345 MPa. They were oriented such that their webs were in the horizontal plane. The struts were assumed to be pin-connected to the columns for rotation in the plane of the frames. The struts in the braced frames were designed to resist the axial compression load due to brace horizontal unbalanced loads of Analysis Case 2 of

AISC 341. The design axial compression load was 769 kN and W250x58 shapes were selected. The struts also satisfied the AISC 341 width-to-thickness ratio limits for moderately ductile members.

Struts connecting the gravity columns to the braced frames were designed to resist the axial loads induced when the GCs are mobilized to resist the MT-BF in-plane flexural demand. Only one design was performed for the most critical condition among all struts and column design approaches. The critical case was Design Approach 3 in which the design axial compression load was 120 kN. AW250x49 section was chosen for these members. All struts were also checked for out-of-plane bending induced by wind pressure acting on the exterior walls. Key design values and results are summarized in Table 6.3. In this table, P_u and M_u are the strut required axial and moment strengths, respectively, and $\phi_c P_n$ and $\phi_b M_n$ are the design axial strength and weak axis moment strength.

Table 6.3: Design of the struts for axial compression and out-of-plane bending.

Frame	**Shape**	A **mm^2**	KL **mm**	$P_{u\text{-strut}}$ **kN**	$\phi_c P_n$ **kN**	$P_{u\text{-strut}}/\phi_c P_n$	M_u **kN-m**	M_n **kN-m**	$M_u/\phi_b M_n$
Braced	W250X58	7420	6000	769*	903	0.95	26**	265	0.11
Gravity	W250X49	6260	6000	120*	731	0.18	26**	219	0.13

*Load combination 1.2D + 1.0E

**Load combination 1.2D + 1.0W

The struts are also used to laterally and torsionally brace the BFCs and GCs at tier levels. For torsional bracing, the struts were moment-connected to the columns for bending in the horizontal plane such that they could provide torsional restraint to the columns at braced points through horizontal bending about their strong axis. An example of such strut-to-column connection to achieve this behavior can be found in [1].

6.5 Static incremental analysis

6.5.1 Numerical model

A numerical model was created using the *OpenSees* platform [13] to assess the nonlinear seismic response of the 4T-BFs. Details of the numerical model are shown in Figures 6.6b and 6.6c. The columns and braces were modelled with fiber discretization of the cross-section using the force-based beam-column element to reproduce the inelastic flexural buckling response of these members subjected to cyclic loading. Force-based beam-column elements account for distributed inelasticity through integration of material response over the cross section and integration of the section response along the length of the element [14, 15, 16, 17]. Force-based formulation was used to model the braces and columns as it offers higher accuracy compared to the displacement-based formulation. Additionally, post-bucking axial compressive strength degradation, which is the case for brace and column buckling, can be properly predicted from the equilibrium of force field at any level of the inelastic deformation [16]. Past studies have shown that this model can reproduce adequately inelastic flexural buckling response under cyclic loading for HSS bracing members [18, 19] and I-shaped columns [20]. The selected force-based beam-column element uses the Gauss-Lobatto quadrature rule for the numerical integration within each segment. Five integration points were considered for this element to obtain a smooth spreading of the inelastic deformation along the members. A number of integration points larger than four is recommended [16, 21], although it has limited impact on the response of CBFs [14]. Since the force-based beam-column is using local coordinates with small deformation assumptions, a co-rotational formulation was chosen for the braces and columns to account for large displacements [22]. Five and eight elements were specified respectively in each of the half-brace segments and column segments. For the braces, respectively, eight and five fibers were employed along the width and through the thickness. For the columns, 20 fibers were used for each flange and 10 fibers were considered in the web respectively [16, 23]. Figure 6.6c shows the cross-section discretization for the braces and columns. In this figure, fibers through the thickness were reduced for illustration purpose.

A uniaxial stress-strain relationship is assigned to each fiber in order to obtain the cross-section behaviour of the element. The Giuffré-Menegotto-Pinto (Steel02) material model was selected to account for the Bauschinger effect and simulate both kinematic and isotropic strain hardening responses [24]. This material is defined by specifying the yield stress, F_y, the Young's modulus E

(= 200 GPa), the strain-hardening ratio, b (= 0.4%) to define kinematic hardening of the steel material, and three parameters including R_0 (= 30), cR_1 (= 0.925), and cR_2 (= 0.15) to simulate the transition from the elastic to inelastic phases. Four isotropic hardening parameters, a_1 (= 0.4), a_2 (= 15), a_3 (= 0.4), and a_4 (= 15) are used to model the isotropic hardening of the steel material. The minimum specified steel yield strength F_y = 345 MPa was assigned to the columns whereas the expected steel yield stress (R_yF_y = 483 MPa) was utilized for the bracing members. A reduced yield strength equal to 0.95 R_yF_y = 459 MPa was assigned to the braces in Tier 1 in the numerical model for the frames with identical tier heights or frames for which Tier 1 was not the critical tier. This reduction in Tier 1 brace yield strengths was specified intentionally to simulate unavoidable material variability and initiate yielding of the bracing member in Tier 1, where column axial loads are maximum. Fiber-based elements cannot simulate the local buckling of the members. It was shown by Uriz et al. [19] that the effect of the local buckling on the overall hysteretic force-displacement response of braces made of compact sections is small. However, using a smooth transition from the elastic to inelastic region of material stress-strain response (strain hardening ratio in Steel02 material) allows to indirectly compensate the effect of local buckling [16]. As shown in Figure 6.6b, bi-directional initial sinusoidal out-of-straightness corresponding to the column in-plane and out-of-plane buckling modes was applied to the columns with maximum amplitude of 1/1000 of the length between nodal points. The residual stress pattern proposed by Galambos and Ketter [25] was specified for the columns (Figure 6.6b). As shown in Figure 6.6b, the 7.5 gravity columns were modelled as one single W-shape member placed next to the braced frame. For this member, the thickness of the flanges and depth of the web were those of gravity column sections multiplied by 7.5. The bracing members were assigned initial sinusoidal out-of-plane imperfection with maximum amplitude of 1/1000 of the unsupported member length. Rigid elements were assigned at both ends of each mid-length segment to simulate the end and mid-length gusset plates [26]. As shown in Figure 6.6b, nonlinear rotational springs were used between the rigid and brace elements to simulate the hysteretic flexural response of the gusset plates. These springs were modeled by zero-length element available in the *OpenSees* program. The struts were modelled using elastic beam column elements. Concomitant gravity loads were applied on the columns and P-Δ effects were included in the analyses.

6.5.2 Analysis results

For MT-BFs, since inertia seismic forces only develop at the roof level, the frame response under the first significant inelastic displacement cycle of a ground motion record during which column flexure develops can be realistically reproduced by gradually incrementing lateral roof displacement using nonlinear static (pushover) analysis. This analysis is therefore an appropriate tool to investigate the development of brace inelastic response leading to concentration of inelastic demand in tiers and column bending moments, and possible subsequent column buckling failure. Pushover analysis of the studied 4-tiered brace frame was then performed to determine member forces and tier drifts as the frame laterally deforms up to the storey deflection anticipated under MCE hazard level. That deflection was taken equal to $1.5C_d\,\Delta_e = 1.73\%\ h$, where h is the total storey (frame) height (20 m). Figure 6.7 presents the results of the pushover analysis for the frame designed using Design Approaches 1 and 2. For consistency with the design assumptions, the GCs were not included in the numerical model for these two cases; the GCs were replaced by a single leaning column carrying the total gravity load supported by the GCs to include P-Δ effects. In Figure 6.7a, the tier drifts and in-plane bending moment in the compression column at Tier 1 (right-hand side column) are plotted against the imposed storey drift for Design Approach 1. Brace buckling occurred in all tiers at a storey drift of approximately 0.5% h. Drifts linearly increased in all tiers until brace tension yielding initiated in Tier 1 at a storey drift of approximately 0.6% h. Beyond that point, further lateral deflections concentrated in Tier 1 as the tension brace in that tier was stretched in the inelastic range. Drifts in the other tiers remained nearly constant as the tension braces in these tiers remained elastic. The column moment increased steadily up to a value of 10% $M_{py\text{-}bc}$ at initiation of brace tension yielding in Tier 1. Then, bending increased more rapidly to reach to approximately $M_{py\text{-}bc}$ at a storey drift of 1.15% h. At that displacement level, in-plane flexural buckling of the column occurred after two flexural plastic hinges had formed in the column due to the increasing in-plane bending demand combined with the large axial compression load imposed by the braces and the gravity loading. The first plastic hinge formed at mid-height of Tier 1 at a storey drift of 0.8% h. Upon increasing further the roof lateral displacement, the second plastic hinge formed at the top of Tier 1, which led to column buckling before the structure could reach the expected seismic lateral displacement [1]. In pushover analysis, the analysis could be continued up to the target displacement even if column buckling occurred.

Figure 6.7b shows the results of the pushover analysis for the frame designed according to Design Approach 2. For this design, the structure could reach the anticipated storey drift without buckling of the compression BFC. As shown, the BFCs were strong and stiff enough to trigger yielding of the tension brace in Tier 2 at a roof drift of approximately 0.7% *h*. Upon increasing further the roof drift, tensile yielding eventually took place in Tier 3 at 1.15% *h* after which the column bending moment started to stabilize. At the end of the analysis, the maximum tier drift in Tier 1 (critical tier) remained close to the design target value of 2% of the tier height.

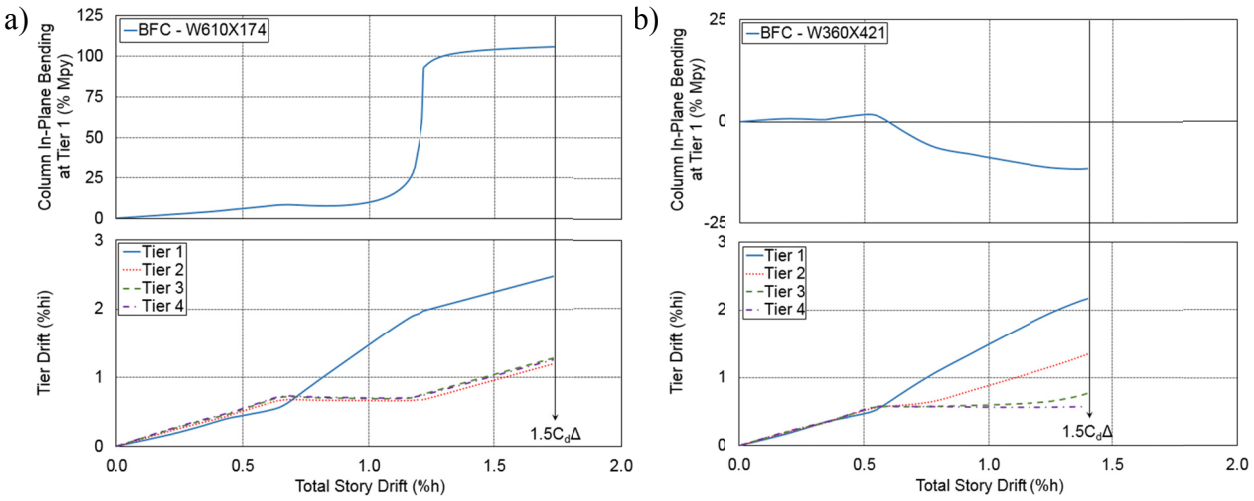

Figure 6.7: Pushover analysis of frames designed based on: a) Design Approach 1; and b) Design Approach 2.

Figure 6.8a shows the results of the pushover analysis for the frame designed according to Design Approach 3. For this frame, W610x174 shapes were assigned to the BFCs, same as in Design Approach 1. However, the GCs were included in the numerical model and contributed to resist the flexural demand imposed to the BFCs when inelastic brace response gradually developed. In this analysis, flexural buckling of the BFC acting in compression (right-hand-side column) was observed as plastic hinging formed at two points along the column span. Yielding was observed in this BFC, initiating at approximately 0.7% *h*. That yielding took place in a limited portion of the column cross-section and the column could continue carrying the axial load from gravity and brace loads. At roof drift equal to 1.4%, in-plane flexural buckling of the column occurred after two flexural plastic hinges had formed in the column due to the increasing in-plane bending

demand combined with the large axial compression load imposed by the braces and the gravity loading as this column has not been designed to carry the seismic bending demand imposed by non-uniform distribution of the lateral displacement in MT-BFs. The column buckling mode observed was similar to that of frame with Design 1. The results of the pushover analysis showed that the stability of the BFCs is not guaranteed, although the gravity columns are designed to resist their share of the in-plane flexural demand. At the end of the analysis, when the storey drift reached the anticipated maximum value, the column bending moments were maximum at Tier 1 level and were equal to 0.12 $M_{py\text{-}bc}$ for the BFCs and 0.13 $M_{py\text{-}gc}$ for the GCs. The drift in Tier 1 reached approximately 2.6% of the tier height, in excess of the target value. This behaviour was expected as the braced frame column buckled before anticipated storey drift is reached.

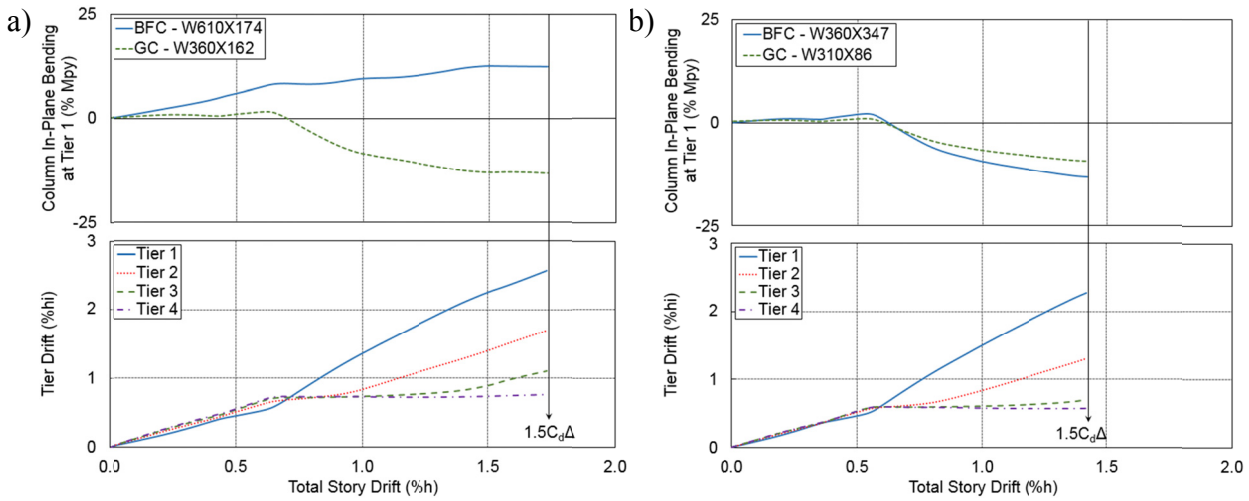

Figure 6.8: Pushover analysis of frames designed based on: a) Design Approach 3; and b) Design Approach 4.

In Design Approach 4, column bending moments remained below 0.15 $M_{py\text{-}bc}$ for the BFCs and 0.12 $M_{py\text{-}gc}$ for the GCs (Figure 6.8b). That in-plane flexural bending demand distribution between the BFCs and GCs was consistent with the predictions made at the design stage. Column buckling did not occur with this frame design, indicating that gravity columns designed solely for gravity and wind loading conditions can possess sufficient reserve capacity to sustain the seismic induced in-plane flexural demand without buckling, provided that the BFCs are designed to resist their share of that flexural demand. For this particular frame, the GCs remained elastic up to the end of

the analysis when the roof displacement reached the target values of 1.42% h ($1.5C_d\Delta_e$). At this displacement level, it was found that the columns could satisfy Eq. 4 under the axial compression acting in combination with the bending moments due to the non-uniform tier drift pattern. The maximum tier drift in Tier 1 (critical tier) reached 2.2% of the tier height, slightly in excess of the 2% drift limit adopted in design. This behaviour is due to the fact that the columns were provided with sufficient stiffness to control drift in the critical tier.

Figure 6.9 shows the results of the pushover analysis for the frame designed using Design Approach 5. The bending demand was distributed proportionally between BFCs and GCs with respect to their flexural stiffness and that demand was considered in the design of all columns. Bending demands reached $0.13M_{py\text{-}bc}$ for the BFCs and $0.13M_{py\text{-}gc}$ for the GCs. The maximum drift in Tier 1 was similar to the values obtained with Design Approaches 2 and 4, i.e. close to the design target value.

In the pushover analyses, the columns experienced lesser bending demands compared to the values assumed in design. The difference is attributed to the rate of degradation of the compressive strength of the compression braces that was considered in the numerical model. In design, the reduced compressive strength (C'_{exp}) was used in the calculations; in the analyses, the brace compressive strength diminished progressively as the storey drift was imposed, which resulted in a reduced flexural demand imposed on the columns [2].

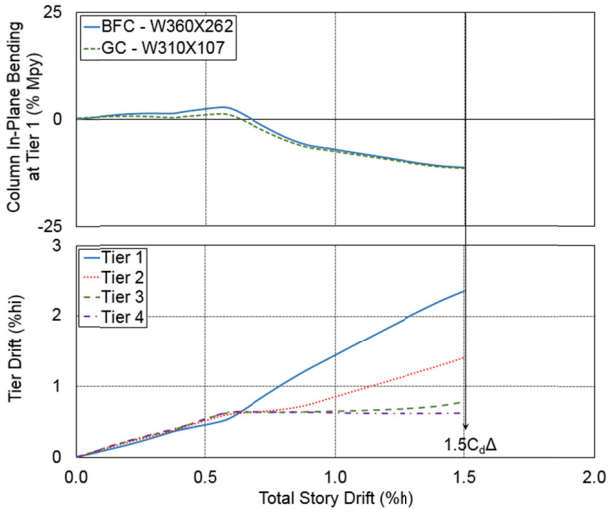

Figure 6.9: Pushover analysis of the frame designed based on Design Approach 5.

The total steel tonnage for the two braced frame columns and the 7.5 gravity columns are given in Table 6.2. As shown, Design Approach 1 requires the least amount of steel but the analysis clearly showed that this approach is not adequate. Satisfactory inelastic response was achieved for Design Approaches 2, 3, and 5, with progressive brace tension yielding and stable column response. Design Approach 3 required the largest amount of steel. In that design, the BFCs were not designed to carry the bending demand and yielding developed in these columns. In view of its low cost-efficiency and observed response, this approach is not recommended. More effective and robust designs were obtained when following Design Approaches 4 and 5. Both methods led to comparable behaviour. Design Approach 4 is simpler because the GCs remains unchanged, which reduces the amount of calculations required to complete the column design. However, adequate performance for this design relies on the drift ductility and reserve strength of the GCs resulting from gravity and wind load design. In Design Approach 5, all columns are designed to resist their respective shares of the seismic induced in-plane bending moments, which should lead to stable and satisfactory seismic performance where the column buckling is prevented and tier drifts are limited to protect the braces and their adjacent connections from fracture.

6.6 Nonlinear response history analysis

Nonlinear Response history (NLRH) analysis was performed to examine the influence of the design approach on the frame seismic performance. For this analysis, mass proportional damping corresponding to 2% of critical in the structure lateral vibration mode was specified because MT-BFs have only one dynamic degree of freedom which corresponds to roof lateral displacement. The numerical response is calculated using the Newmark numerical integration scheme. The acceleration input is applied in the plane of the frame. The far-field record set of 22 ground motion records proposed in FEMA P695 for Seismic Design Category D was used to perform the analyses [27]. Only the first component of each pair of ground motions was used in this study and the records were scaled according to the procedure described in FEMA P695 such that the median spectral acceleration of the set matched the MCE spectrum at the structure design period.

The result from the nonlinear response history analysis of the frame example under one of the 22 records (1994 Northridge, Beverly Hills – Mulhol, 0˚ component) is presented herein. Figure 6.10 shows time histories of the in-plane bending moments in the BFCs and GCs at Tier 1 level and the tier drifts for all five design approaches. For Design Approaches 1 and 2, bending

moments are only given for the BFCs. The frame from Design Approach 1 experienced BFC flexural buckling at a time t = 9 s, after brace tension yielding has developed in Tier 1 but before it occurred in Tier 2, which is consistent with the results from pushover analysis. Figure 6.10b shows that Design Approach 2 resulted in a satisfactory seismic response with in-plane bending demand not exceeding $0.15M_{\text{py-bc}}$ and the total storey drift being appropriately distributed between the tiers. Under this ground motion, the roof displacement reached 1.7% h, a larger value than the one considered in design (= 1.21 %). Similar acceptable response was obtained for frames obtained from the remaining three design approaches. In all cases, column in-plane bending moment demands remained below the values considered in design and no column buckling was observed. Brace tensile yielding developed in Tiers 1 to 3 and all these tiers contributed to the nonlinear deformation of the frame. Drifts in Tier 1 reached between 2.3 and 2.6% of the tier height, which is in excess of the target value, partly due to the large displacement demand imposed under this particular motion. The drifts in the other tiers remained under 2%. Design Approach 3 (Figure 6.10c) resulted in partial yielding of the BFCs during the ground motion. These results presented here confirm the findings from pushover analysis and verify column bending demand calculation performed for each approach.

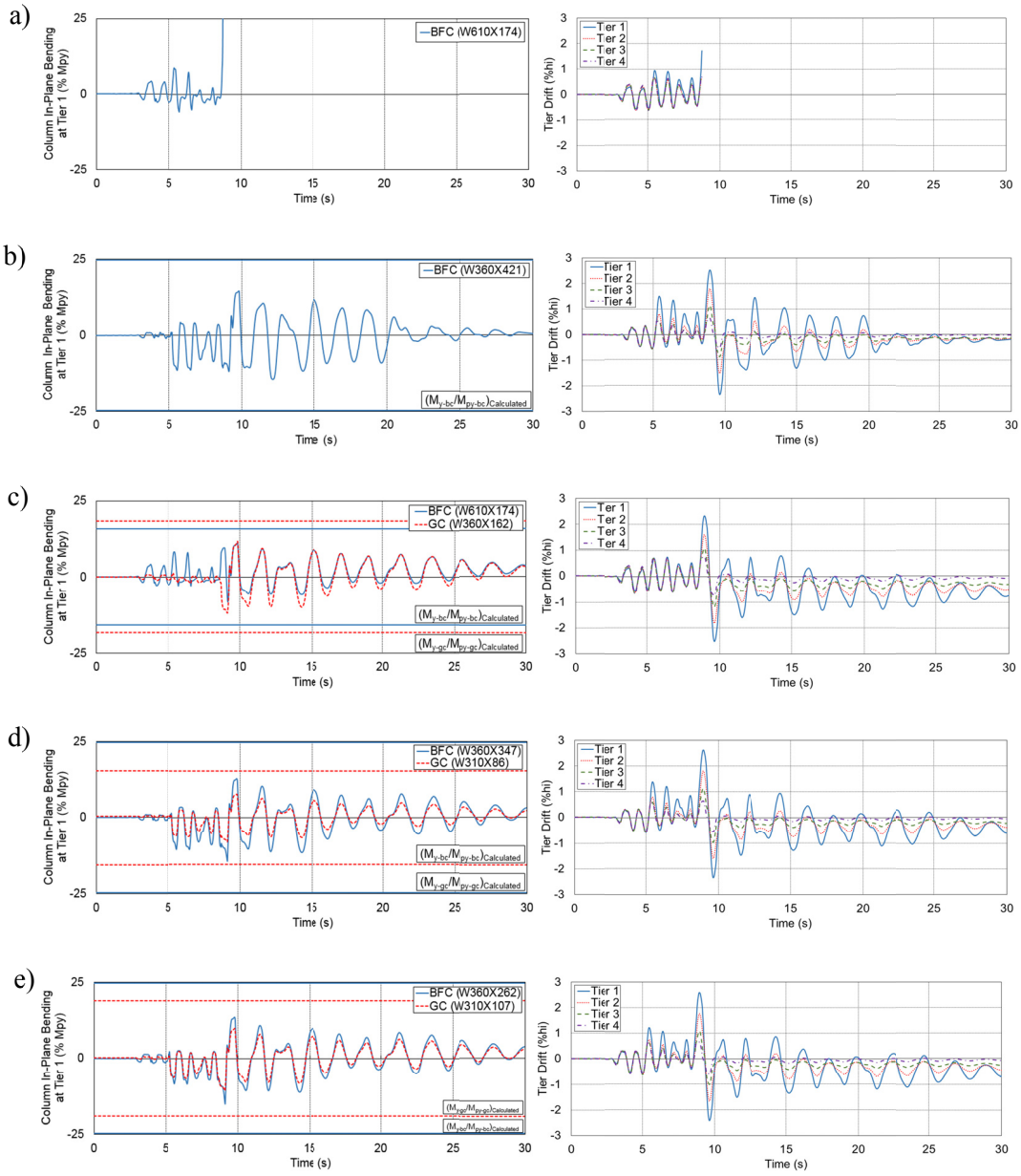

Figure 6.10: Time history analysis of frames designed based on Design Approaches 1 (a) to 5 (e).

The statistics of key response parameters under the 22 seismic records are given in Table 6.4 for the five design approaches. For the frames studied, the median storey drift demand is always higher than the design storey drift, $C_d\Delta_e$. The ratios obtained from NLRH analysis is consistent with the 1.5 amplification factor assumed in design to estimate storey drifts at the MCE level. As was shown for one of the ground motion in Figure 6.10a, lateral deformations under all ground motions concentrated in Tier 1 for Design Approach 1, resulting in higher bending demand in the

columns and large tier drifts capable of causing buckling of the columns. Buckling of the column occurs when plastic hinges form at mid-height and at the top of Tier 1, meaning that complete curvature reversal occurred at the upper end of Tier 1. Large flexural deformations develop prior to initiation of buckling, as a result of the large ductility demand imposed in the critical tier [1].

Table 6.4: Median values of peak seismic response parameters for the 4T-BFs studied.

Parameter	**Design 1**	**Design 2**	**Design 3**	**Design 4**	**Design 5**
Storey drift (%)	1.47	1.39	1.42	1.36	1.33
Storey drift / $C_d\Delta_e$	1.29	1.53	1.24	1.43	1.32
Critical tier drift (%)	2.82	2.40	2.30	2.36	2.30
Drift ratio (critical tier / storey)	1.73	1.70	1.59	1.71	1.66
$M_{bc,max}$ / $M_{py\text{-}bc}$ at Tier 1	0.44	0.24	0.20	0.25	0.24
$M_{bc,max}$ / $M_{py\text{-}bc}$ at Tier 2	0.10	0.12	0.08	0.10	0.08
$M_{bc,max}$ / $M_{py\text{-}bc}$ at Tier 3	0.02	0.01	0.01	0.01	0.01
$M_{gc,max}$ / $M_{py\text{-}gc}$ at Tier 1			0.18	0.14	0.17
$M_{gc,max}$ / $M_{py\text{-}gc}$ at Tier 2			0.09	0.07	0.06
$M_{gc,max}$ / $M_{py\text{-}gc}$ at Tier 3			0.01	0.01	0.01
PM Ratio – BFCs	0.91	0.40	0.69	0.42	0.58
PM Ratio – GCs			0.20	0.31	0.24
Number of column near-buckling cases	4	0	3	0	0
Number of column buckling cases	3	0	0	0	0

Failure of the BFCs by flexural buckling occurred under three ground motions for Design Approach 1. In four other ground motions, BFCs experienced large deformations and/or flexural yielding. To reflect this behaviour, the columns were considered as being near buckling when either one of the three following criteria was met: 1) in-plane relative lateral displacements of the column within tier heights greater than corresponding displacement at tier level; 2) full plastic hinging of the column cross-section near the mid-height and at tier level; and 3) result of the AISC 360 interaction equation for compression and flexure (PM) greater than 1.0:

$$PM = \frac{P_u}{P_{ny}} + \frac{M_{ux}}{M_{nx}} + \frac{M_{uy}}{M_{ny}} \tag{6}$$

In this equation, the column axial strength due to in-plane buckling, P_{ny}, was used as column instability occurred first in-plane and member capacities were determined using nominal yield

strength and resistance factors equal to 1.0. The number of column buckling and near-buckling cases are reported in Table 6.4. Median values of the PM parameter are also given in the table. It is noted that the buckling and near-buckling cases were not included in the calculations of the median values presented in Table 6.4.

For Design Approach 1, column instability occurred or close to occur under seven ground motions out of the 22 motions of the ensemble. The median peak tier drifts for the remaining ground motions is 2.82%, which may lead to low-cycle fatigue fracture for HSS braces [28-30]. Statistics of the peak column weak axis moments M_y / M_{py} are given at every tier level for the BFCs and GCs. For Design Approach 1, large in-plane bending moment demand was induced in the BFCs at Tier 1 compared to the other tiers. This is attributed to relatively larger drifts that developed in that tier, which created a noticeable kink in the column at the level of Tier 1.

For Designs 2 to 5, lesser drift concentration was observed in the critical tier (Tier 1) as the column flexural stiffness was adjusted to limit the tier drift in design stage. For the frame designed based on Design Approach 2, the columns were sized to resist anticipated seismic flexural demand and satisfactory performance was observed under all ground motions. No column buckling or near-buckling case was observed, and the PM ratio for the BFCs remained under 1.0 in all the cases with the median value equal to 0.40.

In Design Approach 3, the BFCs are the same as in Design Approach 1 but the gravity columns interacted with the braced frame, which reduced the in-plane bending demand on the BFCs. In Table 6.4, this behaviour is reflected by no occurrence of column buckling and smaller PM values obtained for Design Approach 3 (0.69 *vs* 0.91). However, for Design Approach 3, three near-buckling cases occurred for the BFCs because these columns had to carry a bending moment demand that had not been considered in design in addition to the large axial force resulting from the brace forces. This confirms the finding from pushover analysis that this design approach cannot be identified as a reliable design method. Conversely, in Design Approaches 4 and 5, no indication of column plastic hinging or column failure was observed under the 22 ground motion records. Lower PM ratios ranging between 0.40 and 0.58 were observed for BFCs in these two designs respectively. This is due to the larger BFC sizes used in these two designs (Table 6.2) that are less prone to plastic hinging and instability compared to Design Approach 3. For Design Approaches 2, 4, and 5, the BFCs were deigned to resist their share of seismic induced bending

demand. In Table 6.4, the statistics of the peak column weak axis moments M_y / M_{py} for BFCs are nearly identical for the three frames indicating that the moments from the ground motions are consistent with the level of bending moment anticipated in design for all three approaches.

A Comparison between the flexural bending demand for BFCs and GCs shows similar variation along the height as drift demands are the same for braced frame and gravity load carrying systems. Additionally, comparing the PM ratios for the GCs of Design Approaches 4 and 5 (0.31 *vs* 0.24) indicates that larger seismic demand was imposed on the GCs of Design Approach 4 as these columns were only sized to carry gravity plus wind loads. However, for this particular structure, the ratio is much lower than 1.0, which explains the adequate performance of the structure.

In order to study the cases where column flexural buckling occurred, the history of the PM parameter is plotted in Figure 6.11 for the BFCs of Design 1 approach and the BFCs and GCs of Design Approaches 3 and 4 under the 1992 Landers record (Yermo Fire Station, 270˚ component). The PM values are computed at Tier 1 level and the BFCs located on the right-hand-side of the frame studied. The BFC of Design Approach 1 buckled under that ground motion. The axial-bending interaction equation exceeds 1.0 for the BFC of Design Approach 3. For this frame, near buckling condition was observed in the left hand side column in Tier 1 at a time of 15.2 seconds when PM reached a value of 1.0; however, column buckling did not lead to the failure of the frame. For this design approach, gravity columns did not buckle as the PM parameter remained below 1.0. For Design Approach 4, PM always remained below 1.0 for both BFCs and GCs and no column buckling was observed for this frame. Comparison between PM histories for Design Approaches 3 and 4 showed that additional in-plane bending induced in the BFCs designed based on Design Approach 3 can lead to column flexural buckling whereas no such response was observed for the BFCs resulting from Design Approach 4 as these columns were designed to carry combined axial force and in-plane bending demands. Gravity columns in Design Approach 4 also remained stable under the ground motion record used in Figure 6.11, because the reserve strength of these columns resulting from gravity and wind load design was sufficient to accommodate the demands induced by the MT-BF inelastic seismic response.

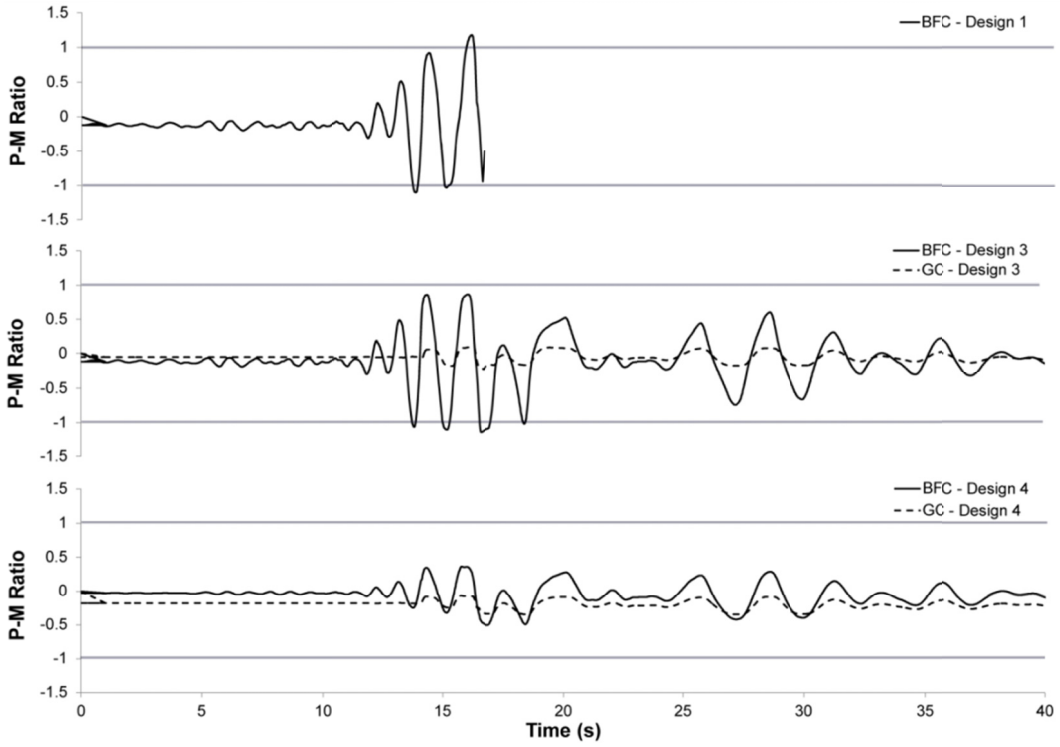

Figure 6.11: PM ratios in the GCs and BFCs for Design Approaches 1, 3 and 4.

6.7 Parametric study on column bending demands

This section presents a parametric study performed to verify if the conclusions drawn from the sample frame studied in the previous section can be generalized for a variety of frames having typical geometrical properties and loading conditions. A total of 12 different frames were designed by varying the following parameters: the frame height (h = 15, 20 and 30 m), the Tier 1 to frame height ratio (h_1/h = 0.25 and 0.40), and the braced frame system (Ordinary Concentrically Braced Frames (OCBFs) with R = 3.25 and C_d = 3.25, and SCBFs as defined earlier). In OCBFs, the BFCs need not be designed for brace induced forces corresponding to Analysis cases 1 and 2 prescribed in the AISC Seismic Provisions for SCBFs. Instead, seismic axial loads amplified by a factor of 2.0 were considered. Design Approaches 2 to 5 as described for SCBFs were then applied to account for MT-BF response and the interaction with the GCs.

Each frame and gravity columns were designed using the five different approaches discussed earlier and NLRH analysis was performed using the same numerical model and 22 seismic

records. As mentioned in the numerical model section, in order to ease the comparison of the results, the critical tier was kept the same (Tier 1) for all the studied cases.

In total, six and three column buckling failures were respectively observed for SCBFs and OCBFs designed using Design Approach 3. These occurrences suggest that Design Approach 3 does not represent a suitable methodology to design MT-BF columns interacting with gravity columns since the braced frame columns may not be capable of resisting the in-plane bending demand that may develop when they are subjected to high axial compression load resulting from the braces reaching their expected strengths in tension and compression. The results of the NLRH analyses for the frames designed with Design Approach 4 show no column buckling or near-buckling cases for the studied cases, even if the gravity columns of these frames were sized only based on the gravity and wind load effects. For frames designed with Design Approach 5, no column or frame failure was observed in the NLRH analysis. All columns possessed sufficient strength to resist induced in-plane bending moments.

Median values of storey drifts and Tier 1 (critical tier) drifts are presented in Table 6.5 for the frames designed using Design Approaches 3 to 5. Only the non-buckling cases were included for Design Approach 3. As shown, the design method has limited impact on the peak drift demand in the critical tier. In all SCBF cases, the demand is close to the low-cycle fatigue capacity of HSS bracing members. For frames designed as OCBFs, the tier drift demand is reduced due to the lower R factor used in design (3.25). These results suggest that, in general, the columns as designed have sufficient stiffness to distribute well the brace inelastic deformation demand over the frame height.

Table 6.5: Median values of frame storey drifts and Tier 1 (critical tier) drifts.

System	Parameter	Design 3	Design 4	Design 5
SCBFs:	Storey drift (%)	1.33	1.27	1.22
	Roof Displacement / $C_d\Delta_e$	1.19	1.38	1.27
	Tier 1 drift (%)	2.13	2.27	2.22
OCBFs:	Storey drift (%)	1.10	0.99	1.00
	Roof Displacement / $C_d\Delta_e$	1.09	1.30	1.25
	Tier 1 drift (%)	1.47	1.57	1.57

Figures 6.12 and 6.13 show a comparison between the in-plane bending moment anticipated at the design stage and the median bending moments obtained from NLRH analysis for the GCs and BFCs when applying Design Approaches 3 to 5. These moments are expressed in percent of the total flexural demand on the BFCs and GCs. The comparison of the bending demand anticipated at the design stage for the studied frames (Figures 6.12 and 6.13) shows that larger bending moments are induced in the gravity columns of the Design Approach 3, i.e. when the BFCs are small because they are not designed to resist their share of the anticipated flexural demand, resulting in higher moments being transferred to the gravity columns. Conversely, the BFCs play the main role in the resistance of the in-plane seismic bending demand when using Design Approach 4. In Design Approach 5, both the BFCs and GCs are explicitly designed to resist the anticipated bending moment demand. When adopting this approach, the percentage of in-plane bending demand resisted by the GCs is generally smaller than in the corresponding frames designed in accordance with Design Approach 3 and larger than in the corresponding frames designed in accordance with Design Approach 4.

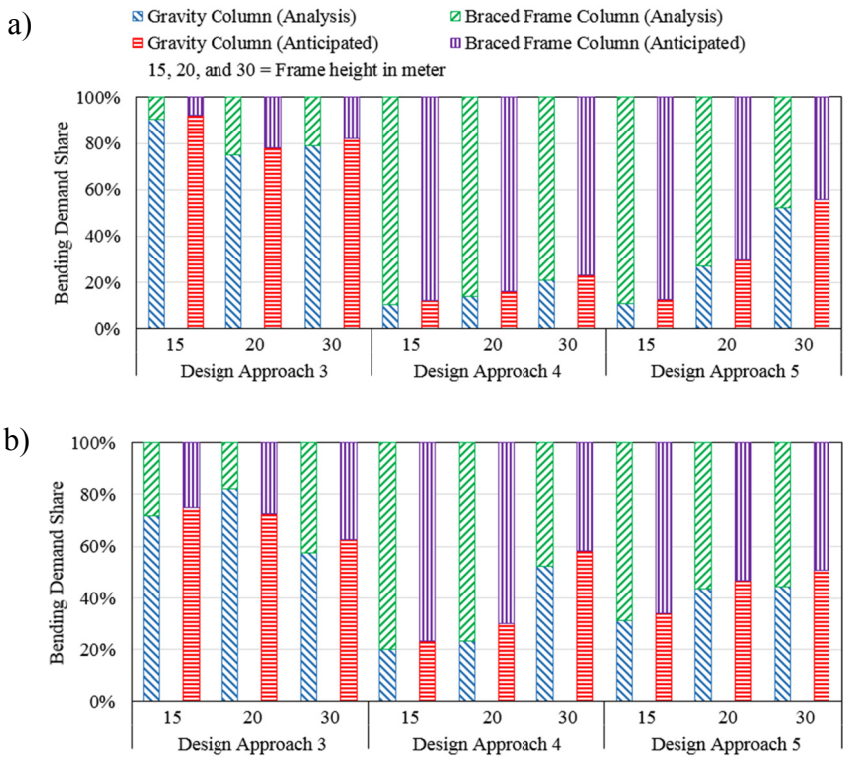

Figure 6.12: Anticipated vs Analysis in-plane bending moments in the GCs for SCBFs with: a) $h_1/h = 0.25$; and b) $h_1/h = 0.40$.

As shown in Figures 6.12 and 6.13, the anticipated in-plane bending moments from design calculations and NLRH analyses agree well with each other for the frames studied. The results obtained from the NLRH analyses revealed that bending demands are shared between braced frame and gravity columns with respect to their flexural stiffness as was assumed in design. The comparison between the results for frames with different height ratios shows relatively higher contribution from gravity columns for frames having a higher height ratio. Additionally, the results reveal that the bending demand sharing between GCs and BFCs are independent of the braced frame system chosen to design the frame (OCBFs *vs* SCBFs).

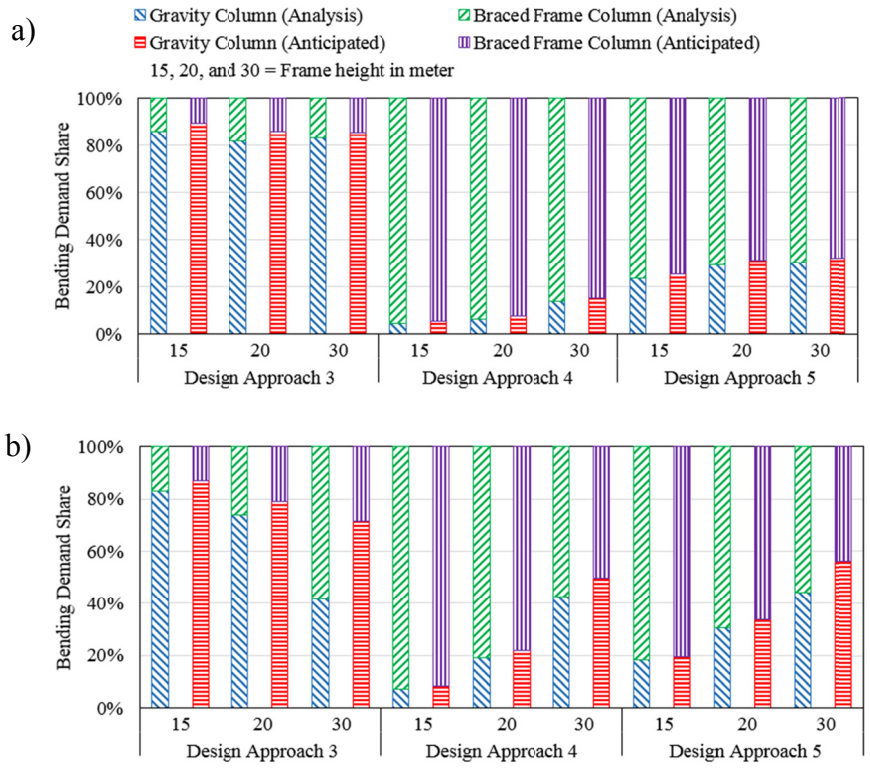

Figure 6.13: Anticipated vs Analysis in-plane bending moments in the GCs for OCBFs with: a) $h_1/h = 0.25$; and b) $h_1/h = 0.40$.

The 50th (median) and 84th percentile values of the in-plane bending moments from NLRH analyses are compared to the values anticipated in design in Figure 6.14. Actual moment values are presented in this table, not fractions of the total demands. In all cases, the values predicted in design are always higher than the values from analysis. The differences are due to the fact that extreme brace compressive force scenarios are considered when predicting column bending moments for

design (C_{exp} in one tier *vs* C'_{exp} in the adjacent tier). Under actual ground motions, the difference in compressive brace forces between adjacent tiers is in fact smaller, resulting in lower flexural demand. In several cases, the 84th value from analysis comes close to the design estimate, meaning that the assumption made in design, although conservative, is still realistic. Larger differences are observed for OCBFs, especially for the frames with uniform tier heights (h_1/h = 0.25). Lower ductility demand is expected in OCBF frames, which reduces the necessity that brace tension yielding be triggered in more than one tier before the maximum roof displacement is reached, which reduces the flexural demand on the columns. Furthermore, as shown in Table 6.5, the ratios between peak frame storey drifts from analysis to design storey drifts ($C_d\Delta_e$) are smaller than the 1.5 value assumed in design when determining the required column stiffness. This likely resulted in lower flexural deformations of the columns at peak displacement compared to what was considered in design. The frame height or column design approach did not have much influence for SCBFs. The influence of these factors is more pronounced for OCBFs.

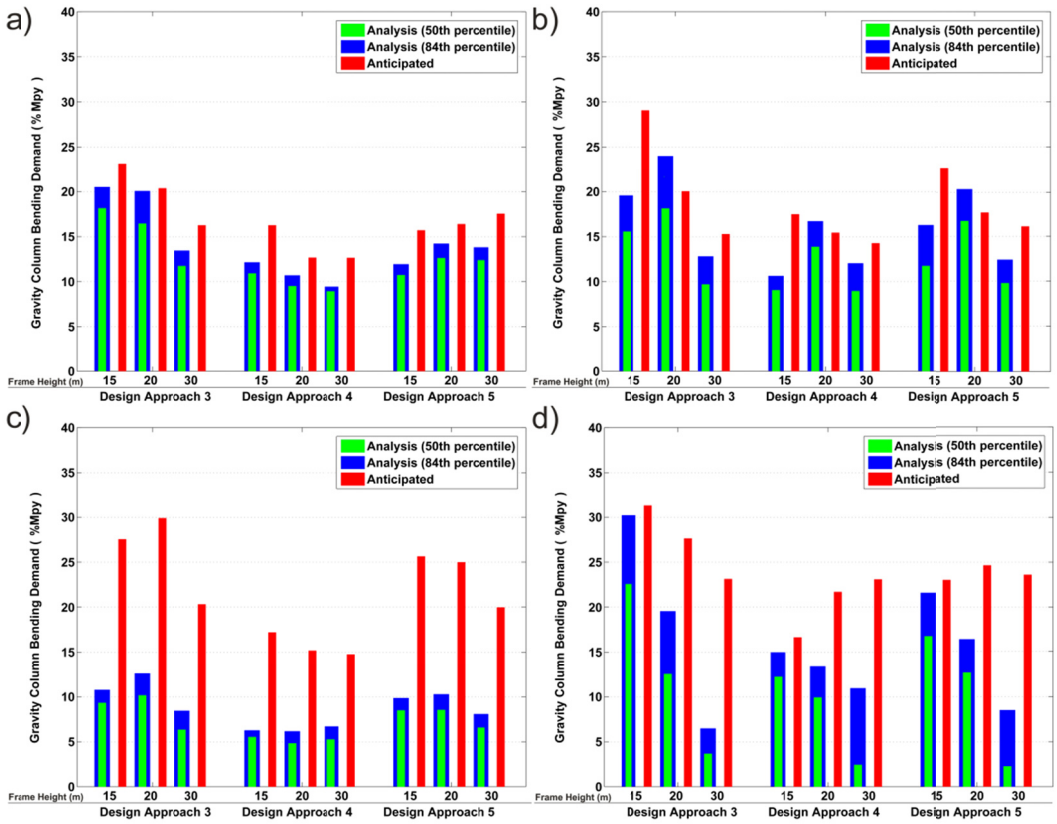

Figure 6.14: Anticipated vs Analysis in-plane bending moments in the GCs for: a) SCBFs with h_1/h = 0.25; b) SCBFs with h_1/h = 0.40; c) OCBFs with h_1/h = 0.25; and d) OCBFs with h_1/h = 0.40.

In Figure 6.14, the median in-plane bending moments induced in the GCs in Design Approach 4 vary between 5 and 15% of the column weak axis flexural capacities. This demand is very low, mainly because the stiffer BFCs attracted most of the seismic bending moment demand, which explains why GCs designed solely for gravity and wind loading could sustain without buckling the seismic in-plane deformations imposed by the MT-BFs.

6.8 Column cost comparison

In this section, cost effectiveness of the different design approaches is evaluated by comparing the total steel tonnage required for all BFCs and GCs of all frames studied. For this study, the number of frames was increased to 36 to also include the effect of the seismicity level on the column design. Three seismicity levels were considered by examining three different sites in the U.S.: high seismicity (Coastal California, CA), moderate seismicity (Seattle, WA), and low seismicity (Boston, MA). The results are presented in Figure 6.15 for Design Approaches 2 to 5. As expected, the required steel tonnage increases with the frame height. Also, column design in regions with lower seismicity is less affected by earthquake effects and variations in column weight due to the design approach or braced frame system are therefore more pronounced in higher seismic hazard areas.

Among the methods used to design the columns, Design Approaches 2 and 3 generally require the larger amount of structural steel whereas the required steel tonnage is typically reduced when Design Approaches 4 and 5 are adopted. Between these two approaches, Design Approach 5 requires the same or slightly lower amount of steel. On average for the structures studied herein, the steel tonnage resulting from Design Approach 5 was 5% less than from Design Approach 4. The difference is attributed to the fact that Design Approach 4 generally requires larger BFCs because only BFCs are designed to resist moments in the early stage of the design process.

Figure 6.15 shows that heavier columns are generally needed for OCBFs compared to SCBFs due to the higher design seismic forces. This increase mainly occurs in the braced frame columns as smaller in-plane bending demand is induced in the gravity load carrying columns as OCBFs require larger and stiffer BFCs attracting a larger portion of the moment demands.

In most cases, higher column flexural demand developed in frames with non-uniform tier heights because a different brace size is needed in the taller tiers, which generally results in larger shear

forces and bending moments in the columns compared to frames with equal tier heights. In frames with unequal tiers, both BFCs and GCs in the first tier have longer effective lengths, which represents a more critical condition. For BFCs, the situation is even worse as maximum axial loads also occur in the first tier. Hence, frames with non-uniform tier heights typically require stronger columns compared to their uniform counterpart.

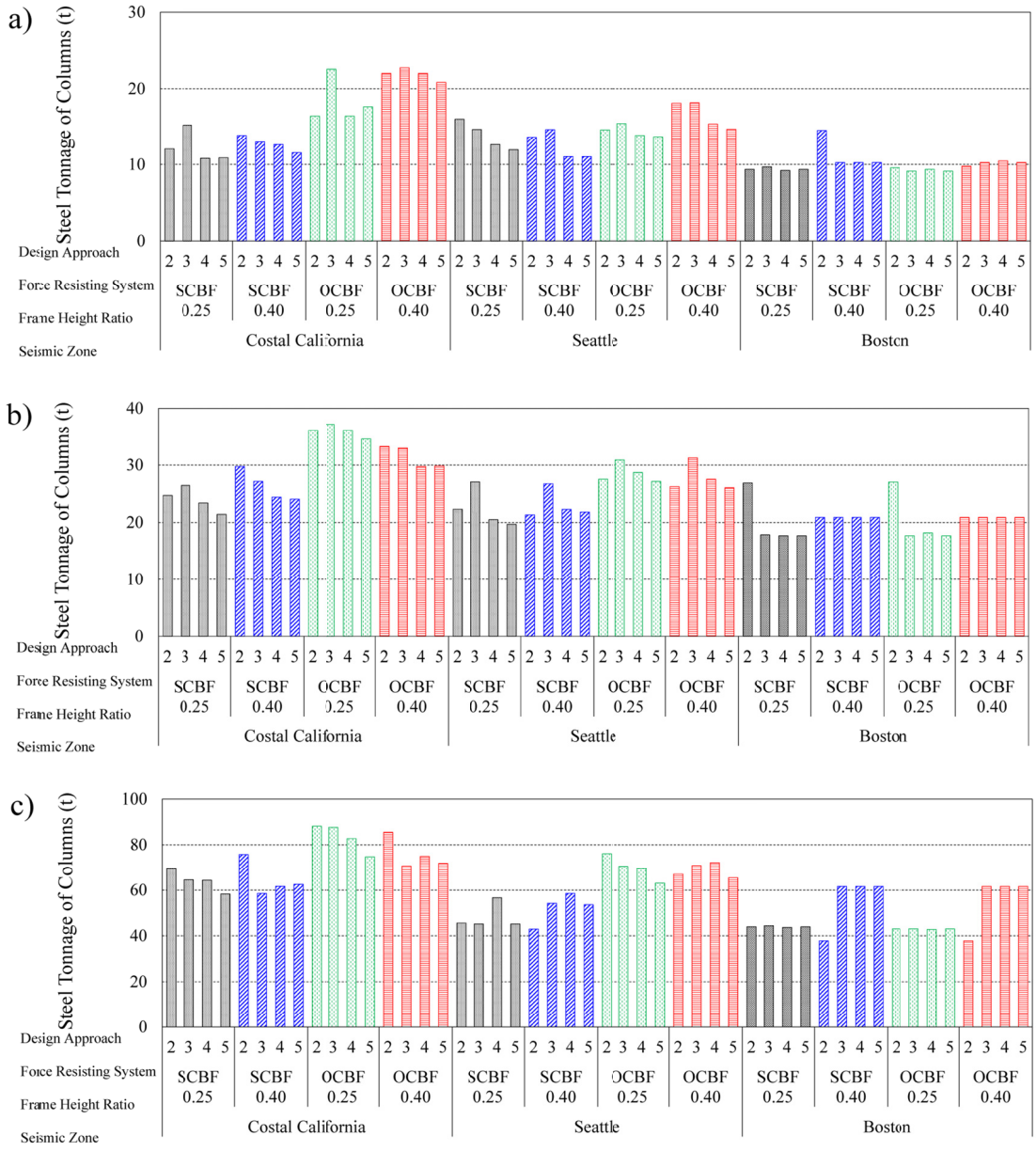

Figure 6.15: Steel tonnage required for the BCFs and GCs of the frames with: a) h = 15 m; b) h = 20 m; and c) h = 30 m.

6.9 Discussion

In Design Approaches 3 to 5, the gravity columns are considered to interact with the braced frame and contribute to reducing the flexural demand on the braced frame columns. In the parametric study, flexural buckling of the BFCs occurred in several cases in the frame designed in accordance with Design Approach 3 (Figure 6.11 presented one of these cases). However, satisfactory seismic performance was observed when using Design Approaches 4 and 5.

In Design Approach 4, the BFCs are designed to resist their share of the seismic induced bending moments whereas GCs are only sized for gravity plus wind load effects. GCs in these frames are however subjected to in-plane bending moment resulting from MT-BF seismic response. Whether or not they can resist to the combined axial load and bending moments due to gravity and seismic effects depends on their reserve capacity, which depends on several factors such as the ratio between wind and seismic loads, the relative importance of gravity loads, the shape of the column cross-sections, etc. As applied in this study, Design Approach 4 cannot consistently guarantee that the GCs will have sufficient resistance to perform well under future MCE level events.

Design Approach 4 could be improved by designing the gravity columns for amplified axial loads, as an attempt to indirectly provide sufficient flexural strength to achieve adequate performance. Alternatively, the design approach could be improved by explicitly verifying at the design phase that the parameter PM from Eq. 6 does not exceed 1.0 when the columns carry their share of the anticipated seismic bending moments plus concomitant gravity axial loads. Since this represents an extreme loading condition, the verification could be performed using the nominal or probable resistances of the GCs. Table 6.6 gives the PM values for the GCs of all structures examined in the parametric study, as determined using anticipated seismic bending moments. The calculations were performed using the nominal and probable material properties. In all cases, the GCs are found to have sufficient resistance to accommodate the expected flexural demand, which explains the observed satisfactory performance. In case PM is more than 1.0 in design, stronger GCs will need to be selected until the parameter PM is equal to or less than 1.0. In the process, the bending moments to be resisted by the GCs will need to also be increased in proportion of their flexural stiffness properties.

Table 6.6: Median values of PM values for the gravity columns in Design Approach 4.

System	Column Resistances	h = 15 m		h = 20 m		h = 30 m	
	h_1/h =	0.25	0.40	0.25	0.40	0.25	0.40
SCBFs:	Nominal	0.32	0.32	0.23	0.31	0.17	0.17
	Probable	0.29	0.29	0.21	0.28	0.15	0.15
OCBFs:	Nominal	0.27	0.33	0.20	0.26	0.14	0.12
	Probable	0.25	0.30	0.18	0.24	0.13	0.11

Design Approach 5 represents a comprehensive design approach where all BFCs and GCs of MT-BFs are designed to resist their respective shares of the anticipated in-plane seismic bending moments. As a result, satisfactory seismic performance can be reliably predicted, as demonstrated in this study. The design process is longer than in Design Approach 4 as the portions of the bending moments resisted by BFCs and GCs must be recalculated at every step in the design. In Design Approach 4, GCs are only verified for seismic loading conditions at the end of the design process; and their sizes are modified only when required. The cost comparison showed, however, that Design Approach 5 generally represents a more effective approach to resisting seismic bending moments imposed to columns when multi-tiered braced frames are used.

6.10 Conclusions

The seismic response of an ensemble of 4-tiered X-braced frames was examined though nonlinear static and dynamic analyses. The braced frames studied were located along the exterior wall of a building and were tied to adjacent gravity columns by horizontal strut members placed at every tier level. Frames having different heights and with uniform and non-uniform tier heights were considered. Two different systems (SCBFs and OCBFs) were also examined. The braced frames were designed according to current AISC Seismic Provisions and their columns were strengthened and stiffened to resist the seismic induced flexural demand imposed on columns by the sequential yielding of the braces in MT-BFs. Three different approaches were then examined to design the gravity columns interacting with the braced frames. The required steel tonnage for the braced frame columns (BFCs) and gravity columns (GCs) were evaluated for each approach. The influence of the seismicity level on column steel tonnage was also studied. The main conclusions are as follows:

- The seismic response of multi-tiered braced frames (MT-BFs) is characterized by non-uniform distribution of the inelastic brace deformations over the frame height, which induces in-plane bending moments in the columns and may lead to excessive tier drifts. Bending moments may cause buckling of the columns if not accounted for in design.
- Satisfactory seismic performance can be achieved when MT-BF columns are properly designed to resist in-plane bending moments and have sufficient flexural stiffness to trigger brace tension yielding in a sufficient number of tiers along the height of the frame and prevent excessive tier drifts. In particular, the design procedure used in this study was found to give conservative yet realistic estimates of the bending moment demands on the columns, allowing safe design against column instability. Tier drifts were well controlled but were slightly underestimated by the design procedure used. This aspect should be examined further in future studies.
- The in-plane bending moments are distributed between the gravity and braced frame columns with respect to their flexural stiffness, as predicted by analysis at the design stage. The in-plane flexural strength and stiffness of gravity columns interacting with MT-BFs can then be mobilized to reduce the demands on the braced frame columns.
- Among the design approaches examined, Design Approach 5 where BFCs and GCs are designed to resist their respective share of the bending moments was found to require the minimum amount of steel and lead to satisfactory seismic performance.
- A simpler approach where only the BFCs are designed to resist the anticipated bending moments (Design Approach 4) can also result in adequate seismic behaviour provided that the selected GCs have sufficient strength to resist the bending moments that they will attract under a seismic event. The method requires similar or slightly higher steel tonnage than Design Approach 5.

A limited number of multi-tiered braced frames was covered in this study. Further investigation is needed to verify the appropriateness of Design Approaches 4 and 5 for other MT-BF configurations (number of tiers, relative tier heights, etc.) and seismic zones where gravity column design is not governed by the seismic load effects. Three-dimensional finite element analysis should be also performed to include the local buckling effect and lateral-torsional

buckling response in the analysis of the stability of the gravity columns under axial gravity and in-plane seismic induced flexural demands.

Acknowledgements

Funding from Natural Sciences and Engineering Research Council (NSERC) of Canada and the Fonds de recherche du Québec en nature et technologies (FRQNT) are gratefully acknowledged.

References

[1] Imanpour, R. Tremblay, A. Daravan, C. Stoakes, and L.A. Fahnestock, “Seismic Performance Assessment of Multi-Tiered Steel Concentrically Braced Frames Designed with Current AISC Seismic Provisions”, Submitted to J. Struct. Eng., ASCE, 2015.

[2] Imanpour and R. Tremblay, “Seismic design of steel multi-tiered braced frames”, EUROSTEEL 2014, Naples, Italy, 2014.

[3] Imanpour, R. Tremblay, and A. Daravan, “A New Seismic Design Method for Steel Multi-Tiered Braced Frames”, ASCE Structures Congress, ASCE: 2707-2720, 2014.

[4] Imanpour, C. Stoakes, R. Tremblay, L. Fahnestock, and A. Davaran, “Seismic Stability Response of Columns in Multi-Tiered Braced Steel Frames for Industrial Applications” ASCE Structures Congress, Pittsburgh, PA, 2650-2661.

[5] Imanpour, K. Auger, R. Tremblay, "Seismic Design of Multi-Tiered Steel Braced Frames including the Contribution from Gravity Columns", in B.H.V. Topping, P. Iványi, (Editors), "Proceedings of the Twelfth International Conference on Computational Structures Technology", Civil-Comp Press, Stirlingshire, UK, Paper 53, 2014. doi:10.4203/ccp.106.53

[6] AISC, AISC-ANSI 341-10, “Seismic provisions for structural steel buildings”, Chicago (IL): American Institute of Steel Construction, Inc., 2010.

[7] Imanpour, R. Tremblay, L. A. Fahnestock, and C. Stoakes, “Analysis and Design of Two-Tiered Steel Braced Frames under In-plane Seismic Demand” Submitted to J. Struct. Eng., ASCE, 2015.

[8] ASCE. ASCE-SEI 7-10, “Minimum Design Loads for Buildings and Other Structures”, Reston (VA): American Society of Civil Engineers, 2010.

[9] AISC. AISC-ANSI 360-10, "Specification for Structural Steel", Chicago (IL): American Institute of Steel Construction, Inc., 2010.

[10] Simão, P.D., Girão Coelho, A.M., and Bijlaard, F.S.K., "Stability design of crane columns in mill buildings" Engineering Structures 42: 51–82, 2012.

[11] Dalal, S.T., "Some non-conventional cases of column design" Eng. J., AISC, 6(1): 28-39, 1969.

[12] T.A. Helwig, and J.A. Yura. "Torsional Bracing of Columns", J. of Struct. Eng., ASCE, 125(5), 547-555, 1999.

[13] F. McKenna, G.L. Fenves, "Open System for Earthquake Engineering Simulation (OpenSees)", Pacific Earthquake Engineering Research Center (PEER), University of California, Berkeley, CA, 2014. (http://opensees.berkeley.edu/)

[14] Aguero, A., Izvernari, C., and Tremblay, R, "Modelling of the Seismic Response of Concentrically Braced Steel Frames using the OpenSees Analysis Environment", Int. J. of Advanced Steel Construction, 2(3), 242-274, 2006.

[15] Neuenhofer, F.C. Filippou, "Evaluation of nonlinear frame finite-element models", ASCE, J. Struc. Eng. 123(7): 958–966, 1997.

[16] M. D'Aniello, G. La Manna Ambrosino, F. Portioli and R. Landolfo "Modelling aspects of the seismic response of steel concentric braced frames", Steel and Composite Structures, 15 (5): 539-566, 2013.

[17] K.K.Wijesundara, R. Nascimbene, G.A. Rassati, "Modeling of different bracing configurations in multi-storey concentrically braced frames using a fiber-beam based approach", Journal of Constructional Steel Research, 101: 426–436, 2014.

[18] E. Spacone, F. C. Filippou, and F. F. Taucer, "Fiber beam-column model for nonlinear analysis of R/C frames, part I: Formulation", Earthquake Eng. Struct. Dynam., 25(7): 711–725, 1996.

[19] Uriz, P., Filippou, F.C., and Mahin, S.A., "Model for Cyclic Inelastic Buckling of Steel Braces", J. Struct. Eng., ASCE, 134(4): 619-628, 2008.

[20] Lamarche C. P., Tremblay R., “Seismically induced cyclic buckling of steel columns including residual-stress and strain-rate effects”, J. of Constr. Steel Res., 67: 1401–1410, 2011.

[21] M. H. Scot and G. L. Fenves, “Plastic Hinge Integration methods for Force-Based Beam-Column Elements”, Journal of Structural Engineering, 132(2): 244-252, 2006.

[22] R. M. De Souza, “Force-based finite element for large displacement inelastic analysis of frames”, Ph.D. dissertation, University of California at Berkeley, Berkeley, CA, 2000.

[23] E. Karamanci, and D. G. Lignos, “Computational Approach for Collapse Assessment of Concentrically Braced Frames in Seismic Regions”, ASCE, Journal of Structural Engineering, A4014019, doi: 10.1061/(ASCE)ST.1943-541X.0001011, 2014.

[24] M. Menegotto, and P. E. Pinto, “Method of analysis for cyclically loaded reinforced concrete plane frames including changes in geometry and non-elastic behavior of elements under combined normal force and bending”, Proceeding of IABSE Symposium on Resistance and Ultimate Deformability of Structures Acted on by Well Defined Repeated Loads, 15–22, 1973.

[25] Galambos, T.V. and Ketter, R.L., “Columns Under Combined Bending and Thrust”, Fritz Engineering Laboratory Report 205A.21, Bethlehem, Pennsylvania, 1958.

[26] P. Uriz, “Towards earthquake resistant design of concentrically braced steel structures”, Ph.D. dissertation, Dept. of Civil and Environmental Engineering, University of California, Berkeley, CA, 2005.

[27] FEMA P695, “Quantification of building Seismic Performance Factors”, FEMA, Redwood City, CA, 2009.

[28] Hsiao, P-C., Lehman, D.E., and Roeder, C.W., “A model to simulate special concentrically braced frames beyond brace fracture”, Earthquake Engineering and Structural Dynamics, 42, 183-200, 2013.

[29] Fell, B. V., Kanvinde, A. M., Deierlein, G.G., and Myers, A.T., “Experimental Investigation of Inelastic Cyclic Buckling and Fracture of Steel Braces”, J. Struct. Eng., ASCE, 135(1), 19-32, 2009.

[30] Tremblay, R., Haddad, M., Martinez, G., Richard, J., and Moffatt, K., "Inelastic Cyclic Testing of Large Size Steel Bracing Members", Proc. 14th World Conf. on Earthquake Eng., Beijing, China, Paper No. 05-05-0071, 2008.

Symbols

A	Brace cross-sectional area
a_i	Isotropic hardening parameters (i = 1 to 4)
b	Kinematic hardening of the steel material
C_b	Lateral-torsional buckling modification factor
C_d	Deflection amplification factor
$C_d\Delta_e$	Design storey drift
C_{exp}	Brace expected strength in compression
C'_{exp}	Brace expected post-buckling strength
cR_i	Steel02 material parameters (i = 1 to 2) to simulate transition from the elastic to inelastic phases
D	Dead load
E	Seismic load
E	Young's modulus
F_y	Yielding strength
h	Total frame height
h_i	Tier height (i = 1 to 4)
K	Brace effective length factor
KL/r	Brace slenderness ratio
L	Braced frame width
M_{bc}	Braced frame column weak-axis bending moment
M_{gc}	Gravity column weak-axis bending moment

M_{ny}	Column weak-axis nominal flexural strength
M_{py}	Column weak-axis plastic moment
M_{ux}	Column strong-axis required flexural strength
M_{uy}	Column weak-axis required flexural strength
M_y	Column weak axis moment
n_{gc}	Number of gravity columns interacting with the braced frame columns
P_n	Nominal compressive strength (minimum of P_{nx}, P_{ny} and P_{nz})
P_{nx}	Nominal compressive strength due to in-plane buckling
P_{ny}	Nominal compressive strength due to out-of-plane buckling
P_{nz}	Nominal compressive strength due to torsional buckling
P_u	Required axial strength
$P_{u\text{-strut}}$	Required strut axial strength
R	Response modification coefficient
R_yF_y	Expected steel yield stress
R_0	Steel02 material parameter to simulate transition from the elastic to inelastic phases
T_{exp}	Brace expected strength in tension
V_{bc}	Braced frame column shear force
V_{br}	Story shear resisted by the braces
$V_{br,exp}$	Story shear corresponds to the sum of the horizontal components of the brace strengths, T_{exp} and C_{exp}
V_{gc}	Gravity column shear force
W	Wind load
$\phi_c P_n$	Design axial strength equal to minimum of ($\phi_c P_{nx}$, $\phi_c P_{ny}$, and $\phi_c P_{nz}$)
$\phi_c P_{nx}$	Design axial strength due to in-plane buckling

$\phi_c P_{ny}$	Design axial strength due to out-of-plane buckling
$\phi_c P_{nz}$	Design axial strength due to torsional buckling
ϕ_c	Resistance factor for compression
ϕ_b	Resistance factor for flexure
$\phi_b M_{nx}$	Column strong-axis design flexural strength
$\phi_b M_{ny}$	Column weak-axis design flexural strength
Δ_e	Roof displacement under the design seismic load

CHAPTER 7 ARTICLE 4 : ANALYSIS METHODS FOR THE DESIGN OF SPECIAL CONCENTRICALLY BRACED FRAMES WITH THREE AND MORE TIERS FOR IN-PLANE SEISMIC DEMAND

Ali Imanpour, A.M.ASCE[1] and Robert Tremblay[2]

[1]Ph.D. Candidate, Dept. of Civil, Geological and Mining Engineering, Polytechnique Montreal, Montreal, QC, Canada H3C 3A7 (corresponding author) E-mail: aimanpour@gmail.com.

[2]Professor, Dept. of Civil, Geological and Mining Engineering, Polytechnique Montreal, Montreal, QC, Canada H3C 3A7.

The article was submitted to the *Journal of Structural Engineering, ASCE* on September 11, 2015.

Abstract

This paper presents two analysis methods for the in-plane seismic response of steel multi-tiered concentrically braced frames with three or more tiers: 1) a sub-structuring technique; and 2) a stiffness analysis method. Both methods are consistent with the current AISC Seismic Provisions and have been developed to estimate column flexural demands and tier drifts in order to prevent column instability and mitigate concentration of tier drifts and premature brace failure under seismic loading. Both methods account for the progression of brace tension yielding along the frame height as observed in MT-BFs. The sub-structuring technique is simpler and is limited to regular frames as it assumes a predefined yielding sequence. The stiffness analysis based method is more rigorous and can predict the actual frame nonlinear response. It can be applied to both regular and irregular MT-BF configurations. Application of the methods is illustrated for two 5-tiered SCBF examples. Nonlinear response history analysis is performed to validate the proposed methods for the frames studied.

Keywords: Multi-tiered braced frames, seismic demand, column instability, tier drift, brace failure, sub-structure, stiffness analysis.

7.1 Introduction

Multi-tiered steel braced frames (MT-BFs) are used to resist lateral loads in tall single-story steel structures such as industrial and sports facilities, airplane hangars or warehouse buildings. They consist of two or more bracing panels that are stacked between ground and roof levels, as illustrated in Figures 7.1a and 7.1b for two tall industrial buildings. This configuration generally represents a more practical and cost-effective solution when excessively long bracing members are needed to construct a regular braced frame over the full building height. MT-BFs are also used for lateral bracing in tall stories of multi-story buildings (Figure 7.1c). The system is also effective in high seismic applications as brace slenderness limits can be more easily satisfied with shorter braces and the reduced brace sizes result in a lower seismic force demands on brace connections, struts and columns.

a) b) c)

Figure 7.1: a) 3-tiered X-bracing; b) 4-tiered chevron bracing (Courtesy of the CISC); and c) 2-tiered X-braced frame in the upper level of a 2-story structure.

For seismic resistance, struts are needed at every tier level to transfer the horizontal unbalanced brace forces that develop at brace-to-column intersecting points after buckling of the compression acting braces. MT-BF columns are typically I-shaped members oriented such that strong axis bending takes place out-of-plane. For stability design, the columns are unbraced over the full story height for buckling out of the plane of the braced frame. For in-plane buckling, the bracing panels provide in-plane lateral bracing at tier levels. Torsional bracing of the columns can also be

achieved at tier levels by mobilizing the flexural stiffness of the struts in their horizontal plane (Imanpour et al. 2015a).

Imanpour and Tremblay (2014) and Imanpour et al. (2015a) studied the nonlinear seismic response of MT-BFs having 2 and more tiers designed in accordance with the 2010 AISC Seismic Provisions for Structural Steel Buildings (AISC 2010a). They noted that brace inelastic response tends to concentrate in one tier over the frame height, causing non-uniform tier drifts and in-plane flexural demands on the columns. Column buckling was observed in several of the cases studied due to this flexural demand combined with the absence of out-of-plane support at tier levels. For some frames, the brace ductility demand resulting from drift concentrations was sufficient to cause premature failure of braces or their connections. Stoakes and Fahnestock (2012, 2013) studied the buckling response of individual MT-BF columns subjected to seismic induced in-plane bending demands. Imanpour et al. (2015b) proposed a seismic design procedure to predict in-plane shears and bending moments that must be resisted by columns in two-tiered braced steel frames. In their method, the critical tier where brace inelastic demand is expected to initiate and concentrate is first identified. Column forces and tier drifts induced by the corresponding uneven brace inelastic response can then be determined.

The response of MT-BFs with three and more tiers is more complex as the sequence of brace tension yielding along the frame height is influenced by the frame properties. More severe concentration of brace inelastic demand is expected when the number of tiers is increased or when tier heights and/or brace sizes vary in the frame. Canadian seismic provisions include special requirements for steel MT-BFs (CSA 2014). In this code, columns must be designed assuming that brace inelastic deformations concentrate in only one tier. Although simple and adequate for frames having a few tiers or designed for moderate or limited ductility, the approach generally gives conservative column designs for tall MT-BFs with large number of tiers (Imanpour and Tremblay 2015), and may lead to excessive tier drift demands in frames designed for higher ductile seismic response, as is the case for Special Concentrically Braced Frames (SCBFs) in the United States. In this paper, two alternative approaches are proposed to estimate maximum anticipated column in-plane flexural bending moments and tier drifts for the seismic design of such tall MT-BFs: 1) a sub-structuring technique; and 2) a stiffness analysis method. Both methods account for the progression of brace tension yielding along the frame height, which is representative of the expected response for these structures. The first approach is simpler and is

limited to regular frames. The second method is more rigorous and can be applied to all frames including irregular MT-BFs. The first part of the paper describes the seismic response of a prototype 5-tiered SCBF designed using the current AISC Seismic Provisions. The focus is put on the distribution of brace tension yielding, the resulting column flexural demand and how this response is affected by the frame geometry and relative brace resistances. The two proposed methods are then described and their application is illustrated for two 5-tiered SCBFs. For the second method, irregularity is introduced in the frame studied. Finally, the proposed methods are validated for the prototype frames by comparing the seismic demand considered in design to that obtained from nonlinear seismic response history analysis.

7.2 Seismic response of 5-tiered SCBF

The seismic response of the 5-tiered braced frame shown in Figure 7.2a is studied using Nonlinear Response History (NLRH) analysis under the FEMA P695 (FEMA 2009) far-field set of 22 ground motion records. The *OpenSees* 2.2 analysis program (McKenna and Fenves, 2004) was used to perform the analysis. The numerical model including the element types, material properties, connection model detail, and analysis procedure are as described in Imanpour et al. (2015a). The frame was designed in accordance with the 2010 ASCE 7 standard (ASCE 2010) and 2010 AISC Seismic Provisions (AISC 2010). The structure was assumed to be located on a class D site in coastal California, where the mapped MCE_R spectral response acceleration parameters are $S_s = 1.5g$ at short period and $S_1 = 0.6g$ at 1.0 s period. It was assigned to the Seismic Design Category (SDC) D and an SCBF system with an R factor of 6.0 was selected for the braced frame. The design period is equal to 0.74 s, which gave a seismic coefficient $C_s = 0.135$ and a base shear V of 490 kN per frame. The demand-to-capacity ratios for the braces ($P_u / \phi_c P_n$) are equal to 1.0 in the first tier and 0.88 in the other tiers, indicating a well-proportioned frame in spite of the larger tier height in Tier 1. The columns were designed for the first analysis case specified in AISC 341-10, i.e. assuming that all braces reach their expected tensile yield strengths and compressive strengths simultaneously. This led to a column axial compression load of 4615 kN in the first tier. Elastic buckling analysis of the columns was performed and effective lengths of 5.4 and 19.3 m were respectively obtained for in-plane and out-of-plane flexural buckling modes accounting for the variation of the axial load along the height of the columns and continuity of the columns.

In the NLRH analysis, column buckling and frame collapse occurred in Tier 1 under 11 of the 22 ground motions. Time history results are plotted in Figure 7.2b for one ground motion producing collapse at approximately 16.7 s. As shown, brace buckling and tension yielding concentrated in Tier 1 while braces buckled but did not yield in tension in the upper tiers. The resulting uneven tier drifts induced weak-axis bending moments (M_c) in the first tier column segment. In the figure, the moment M_c reached the column plastic moment capacity at 16.7 s and the combined axial and flexural demands eventually caused buckling of the column in that tier (Figure 7.2c). Brace fracture was not modelled in the numerical simulations. Using the fracture model by Tremblay et al. (2003) for rectangular HSS braces, failure of the HSS 114x114x7.9 braces in Tier 1 is expected to occur at a tier drift of approximately 1.9%. In the analysis, this drift was reached at 15.16 s, indicating that column buckling and brace failure are two limit states that can be reached for this frame under MCE_R seismic events.

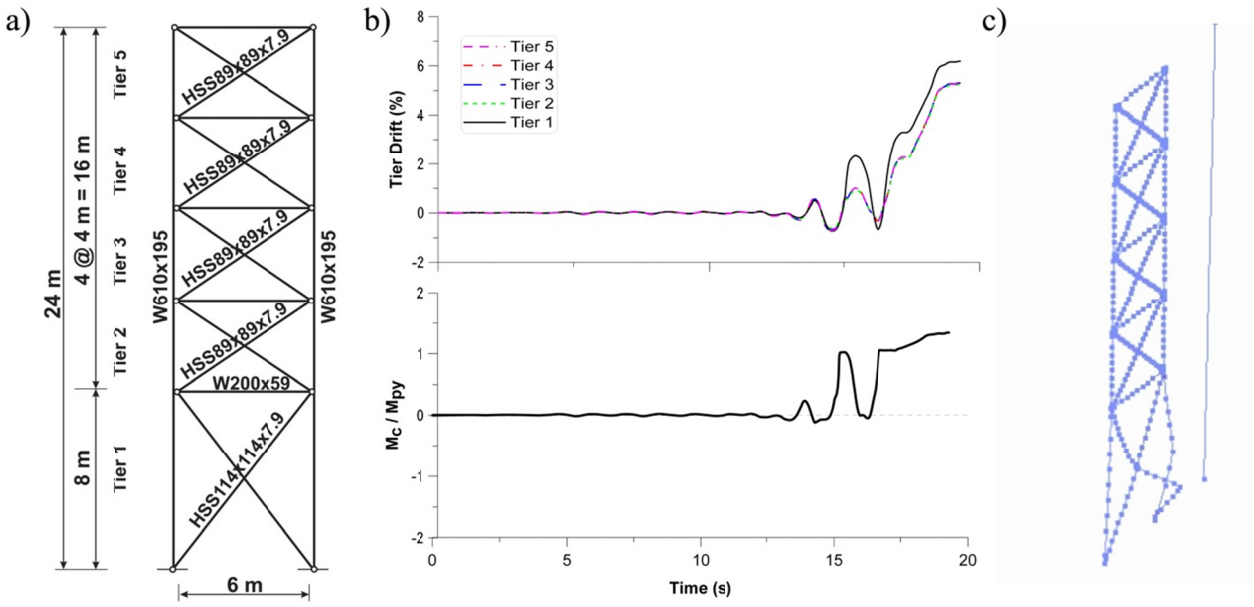

Figure 7.2: Prototype 5-tiered frame studied: a) Geometry; b) Time history analysis results under 1992 Landers (Yermo Fire Station record): c) Column buckling mode.

The column design was redone with an effective length factor of 1.0 along both axes, i.e. KL = 24 and 8 m for strong and weak axis buckling, respectively, thus neglecting the beneficial effects on column stability of column continuity and variation of axial loads along the column height. A

stronger W690x240 column was required in that case. NLRH analysis of the modified frame showed that inelastic deformations still concentrated in Tier 1 and column flexural buckling was observed under 3 ground motions, which still represents non acceptable response.

To investigate the sensitivity of the frame response to variations in brace resistances along the height, the braces in Tier 1 were replaced by a larger HSS114.3x114.3x9.5 section, a scenario that can be encountered in practice when stronger shapes are used due to material availability. This change resulted in an increased design axial load for the columns (5058 kN) that could be resisted by the initially selected W610x195 columns. NLRH analysis was redone for this modified frame and it was found that inelastic deformations concentrated in Tiers 2 to 5, inducing moments in the first tier column segment that resulted in column buckling in that Tier 1 under 11 ground motions.

Improved design provisions are needed to achieve satisfactory seismic response for this type of braced frame. For two-tiered braced frames, Imanpour et al. (2015b) proposed to increase the flexural strength and stiffness of the columns so that inelastic brace tension yielding propagates to adjacent tiers and more uniform tier drift demand is achieved. The columns must then have sufficient strength to resist the anticipated combined axial and bending demands. This enhanced response is schematically illustrated in Figure 7.3 for a taller frame with 5 tiers. Methods to achieve this behavior are proposed in the next section.

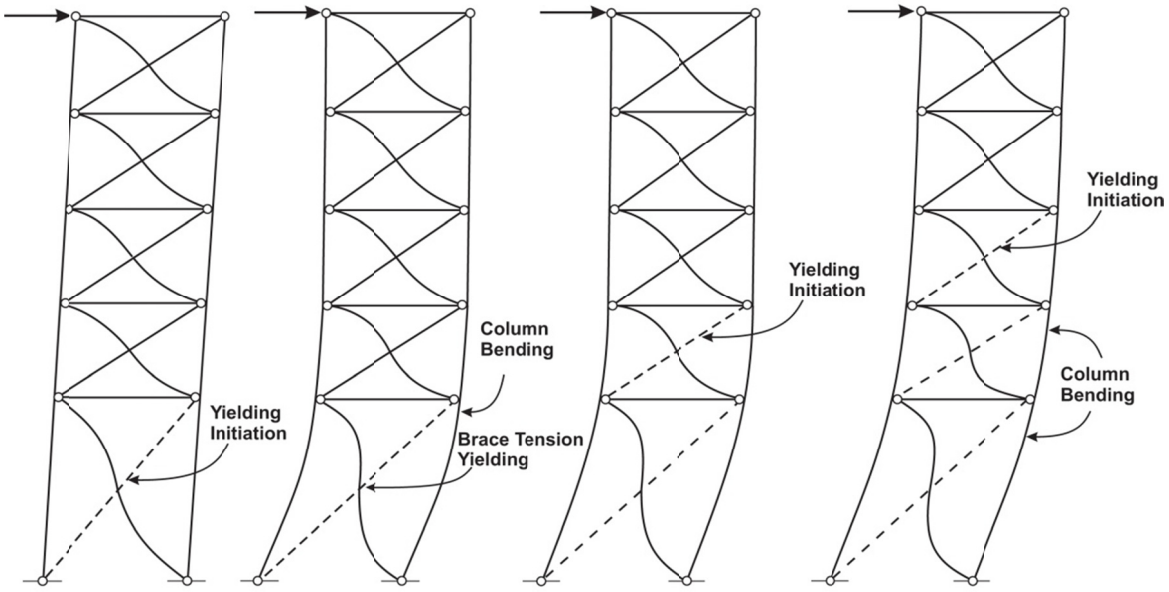

Figure 7.3: Improved MT-BF seismic response.

7.3 Proposed analysis procedures for MT-BFs

Two methods are introduced in this section to predict column bending moments and tier drifts in tall MT-BFs with the objectives of avoiding column instability and excessive drift demands in tiers. The two methods account for the possible propagation of brace tension yielding in other tiers after brace yielding has initiated in the critical (weakest) tier. The methods can therefore be used to select columns having sufficient in-plane flexural strength and stiffness properties to distribute brace inelastic deformation demands along the frame height to achieve acceptable, more uniform tier drifts, while preventing column buckling.

Both methods are similar to incremental nonlinear static (pushover) analysis where the story drift is gradually incremented until the anticipated story drift including inelastic deformations is reached. In the proposed methods, however, the analysis is performed in a limited number of steps that correspond to occurrences of brace tension yielding in individual tiers as the frame laterally deforms. At every step, brace forces corresponding to the current brace buckling and yielding states are used to determine column forces and deformations. If needed, the analysis can be pursued until a complete brace tension yielding mechanism is reached. The first method, the sub-structuring approach, assumes a pre-determined sequence of brace tension yielding along the frame height. In the second method, the stiffness analysis method, propagation of brace tension yielding depends on the frame properties. Both methods can be easily implemented in automated design worksheets so that they can be applied in day-to-day practice.

Before initiating the analysis procedure, the design of braces, columns and struts is first performed following the current AISC Seismic Provisions for SCBFs. The critical tier where brace tension yielding is expected to initiate is then determined and the analysis methods can then be started. Column forces and tier drifts from the analysis are used to verify and adjust as necessary the column sizes.

7.3.1 Initial member design

Braced frame members are sized following the current AISC Seismic Provisions. For column design, a preliminary design is obtained by considering the first analysis case in which all braces are assumed to reach their expected strength in tension (T_{exp}) and in compression (C_{exp}). For most bracing configurations, this analysis case represents an upper bound brace force scenario for the

axial compression demand in MT-BF columns. For chevron bracing, the second analysis case where all compression braces have buckled and reached their post-buckling compressive strength C'_{exp} while all tension braces still resist T_{exp} should also be considered as it may result in higher column axial compression. This second loading scenario is the one used for the design of the struts.

7.3.2 Identification of the critical tier

Once the members are sized, one must identify the tier where brace tension yielding is expected to take place first in the frame. This tier is referred to as the critical tier. It is the tier that has the minimum story shear resistance, $V_{br,exp}$, as provided by the braces when the tension brace reaches its expected yield tensile strength, T_{exp}, and the compression brace reaches its expected compressive strength, C_{exp}:

(1) $$V_{br,exp} = (T_{exp} + C_{exp})\cos\theta$$

where θ is the angle between the braces and horizontal plane. As the equation implies, it is assumed, for simplicity, that the compression brace in the tier still carries an axial compression load equal to C_{exp} when the tension brace attains yielding, in spite of the fact that the brace has already buckled and lost part of its compressive resistance at this point. This simplification does not have significant impact on critical tier determination as the same assumption is made for every tier. It is also assumed that the columns do not contribute to the story shear resistance of the tiers as flexural deformations of the columns are small at the first occurrence of brace tension yielding over the frame height (Figure 7.3).

When identifying the critical tier, the engineer should consider that code expected brace strengths represent upper bound resistance estimates and that actual brace strengths may actually differ from these values due to unavoidable variations in material properties (yield strength), cross-sectional areas, member imperfections and boundary conditions. Since column forces and tier drifts depend on the position of the critical tier and subsequent propagation of brace yielding, all plausible critical tier scenarios should be examined by reducing brace resistances in selected tiers by a given margin representative of the expected variability in brace strength. For HSS bracing, that margin could be as much as 10 to 15%. Hence, more than one critical tier scenarios may need to be considered for a given frame. This is especially the case for uniform frames where all tiers have the same height

and brace sizes, as brace tension yielding in these frames is expected to initiate and concentrate in one of the panels.

When selecting critical tiers, one may take into consideration that maximum column moments typically develop in the critical tier. Therefore, critical tiers located in the lower tiers can lead to more severe design conditions as large bending moments would develop in the column segments where axial compression is maximum. In addition, a shorter critical tier generally impacts more the design as this results in larger tier drifts (displacement is divided by a shorter tier height) and larger bending moments in the columns (shorter columns are stiffer). In addition, braces in shorter tiers can accommodate less inelastic deformations and are more prone to failure. Finally, for uniform frames, nonlinear analysis showed that inelastic brace deformations are more likely to develop in top and bottom tiers as the columns in these tiers are relatively more flexible due to the pinned condition at their top and bottom ends, which favors concentration of brace inelastic deformations in these levels (Imanpour et al. 2015a).

7.3.3 Sub-structuring technique (assumed brace yielding sequence)

As shown in Figure 7.4, the method assumes that brace tension yielding will propagate progressively starting from the bottom tier (bottom up scenario) or from the top tier (top down scenario). Hence, the method is limited to well-proportioned braced frames with uniform tier properties for which the critical tier is more likely the bottom or top tier. The method would also apply to MT-BFs that have a bottom or top tier that is different from the other tiers.

The approach is referred to as a sub-structuring technique because the analysis is performed into a number of consecutive steps in which only part of the structure is examined. For instance, the three sub-structures that must be considered for the bottom up scenario of Figure 7.4a for a 5-tiered frame are schematically illustrated in Figure 7.5. As shown, each substructure includes the critical tier, the adjacent tier(s) where brace tension yielding has been subsequently triggered and, lastly, the tier where brace tension yielding is being triggered. In other words, at a given analysis step, the tiers where brace tension yielding has not been reached are removed from the original frame. For each substructure, a pin is assumed at the upper ends of the columns so that the individual columns can be analyzed for in-plane flexural response under the known brace forces using simple statics. Neglecting the continuity of the columns at the upper ends of the sub-

structures results in slightly larger column moments and flexural deformations compared to the actual situation, which introduces some conservatism in the design.

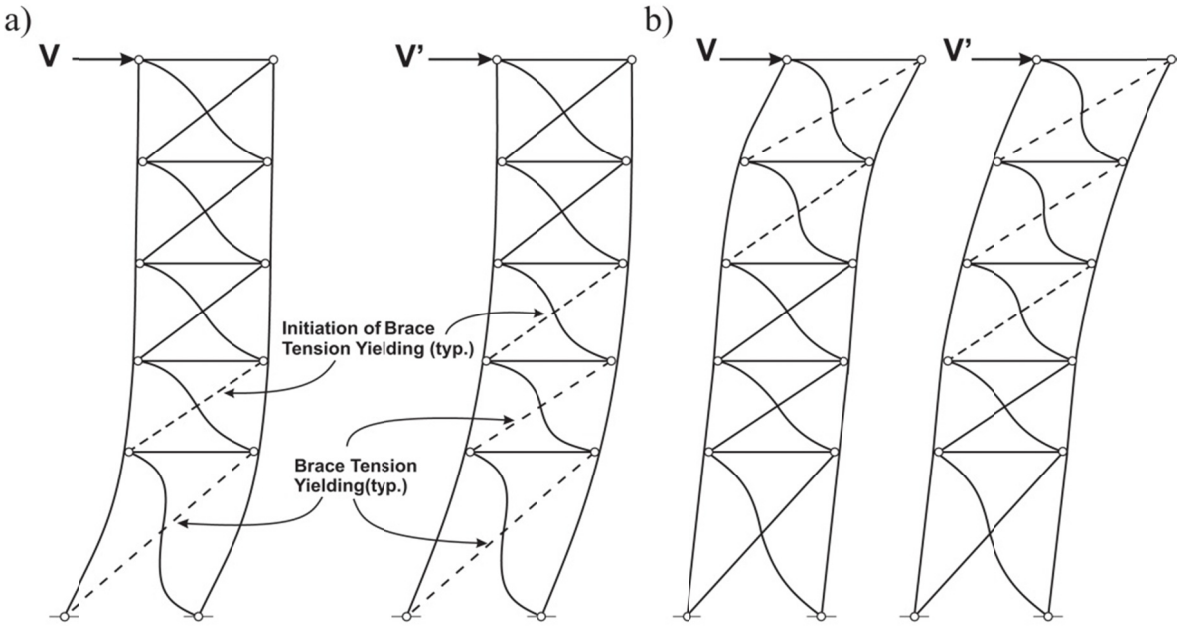

Figure 7.4: Assumed brace tension yielding sequence: a) Bottom up scenario; and b) Top down scenario.

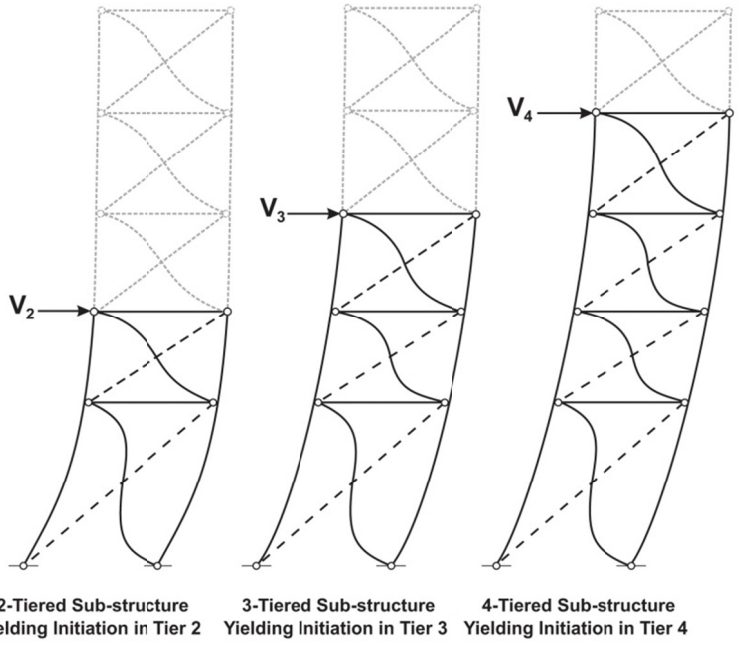

Figure 7.5: Sub-structures analyzed for the bottom up brace tension yielding sequence with assumed inelastic deformation.

In the sub-structuring technique, the minimum number of yielding tiers, n_y, must be determined before initiating the analysis process as it dictates the number of analysis steps to be performed. Under a ground motion, maximum tier drift is generally observed in the critical tier and n_y is determined so that the drift in the critical tier, Δ_{cr}, does not exceed the maximum allowable drift in the tier, $\Delta_{max,cr}$, when the maximum anticipated story drift, Δ, is reached. The value of $\Delta_{max,cr}$ can be limited by brace fracture or other limit states. The drift Δ_{cr} can be estimated from:

$$(2) \qquad \Delta_{cr} \approx \Delta_{y,cr} + \Delta_{inel}\left(\frac{h}{h_{cr}}\right)\left[1 - \frac{h_y\left(h-h_y\right)\left(h_y-h_{cr}\right)+1.5\,h_{cr}\left(h_y-h_{cr}\right)^2+\left(h_y-h_{cr}\right)^3}{hh_y^2}\right] \le \Delta_{max,cr}$$

where: $$\Delta_{y,cr} = \frac{R_y F_y}{E\sin\theta\cos\theta};\ \Delta_{inel} = \Delta - \Delta_e\left(\frac{V_{br,exp,cr}}{V}\right)$$

where R_yF_y and E are the expected brace yielding strength and Young's modulus of elasticity, respectively, h_{cr} is the height of the critical tier, $\Delta_{y,cr}$ is the drift in the critical tier when brace tension yielding initiates in that tier, and Δ_{inel} is the portion of the anticipated story drift that develops after brace tension yielding has initiated in the critical tier. The latter can be obtained by removing from Δ the elastic story drift Δ_e under the load V as amplified by the ratio $V_{br,exp,cr}/V$ calculated in the critical tier. Equation 2 is used to determine the height h_y over which brace tension yielding must propagate to limit Δ_{cr} to $\Delta_{max,cr}$ (Figure 7.6a). As will be discussed later, this is an approximation as the deformed shape is also influenced by unbalanced brace forces at tier levels (Figure 7.6b); however, the differences are small and the approximation is generally acceptable for determining h_y. The number of tiers required to cover the height h_y, n_y, is then determined. If the term $\Delta_{inel}(h/h_{cr})$ in Eq. 2 is smaller than $\Delta_{max,cr} - \Delta_{y,cr}$, propagation of brace tension yielding to other tiers is not necessary to prevent excessive critical tier drifts and brace tension yielding can be constrained to the critical tier. In that case, column forces should be determined from the stiffness analysis method instead of the sub-structuring technique.

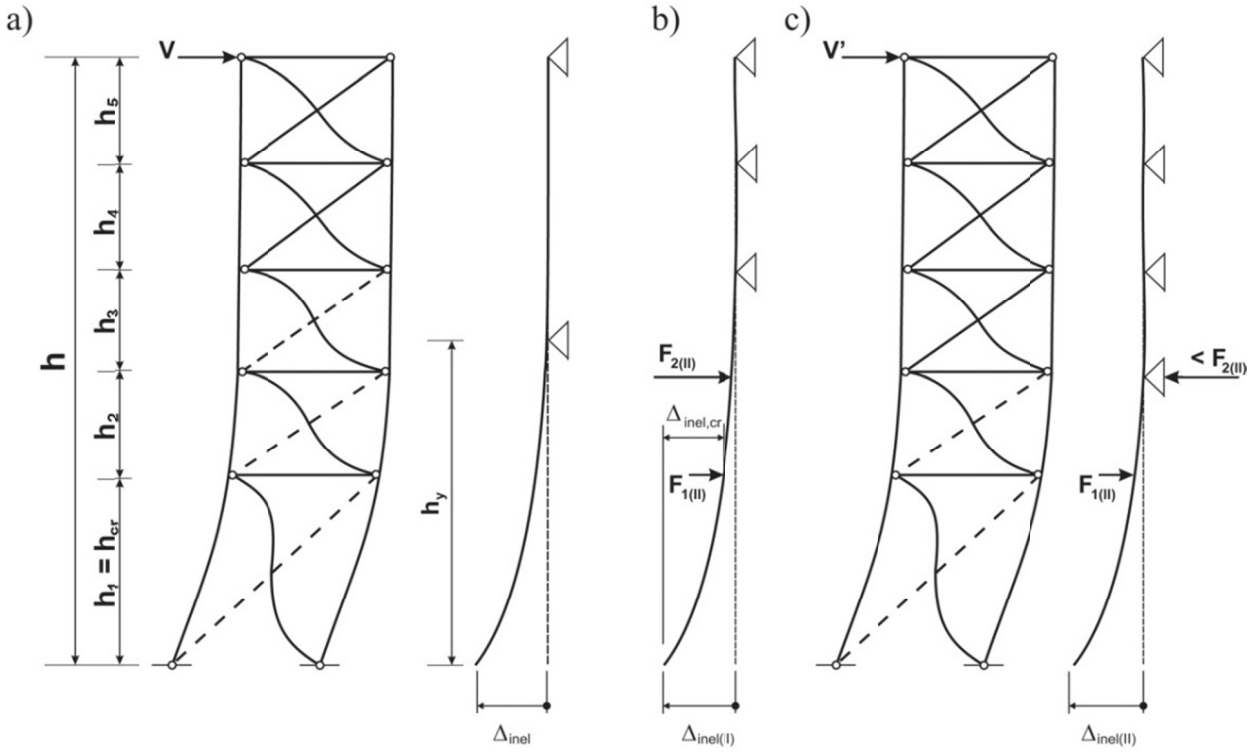

Figure 7.6: Frame deformed shape in the sub-structuring technique for bottom up brace yielding sequence: a) Deformed shape assumed in Eq. 2; b) After brace tension yielding in Tier 3 at story drift Δ; c) At brace tension yielding in Tier 3 in Analysis Step II.

Analysis Step I for a 5-tiered SCBF is illustrated in Figure 7.7 for the bottom up brace yielding sequence. The sub-structure includes Tiers 1 and 2. In both tiers, the tension brace forces are T_{exp}. However, at this step, significant brace inelastic deformations and large tier drift has only taken place in Tier 1 whereas brace tension yielding is just reached in Tier 2. The compression braces therefore resist their post-buckling strength C'_{exp} in Tier 1 and buckling strength C_{exp} in Tier 2. Column bending at this stage is maximum at Tier 1 level and can be determined from the column shear in Tier 1, V_{c1} (Figure 7.7):

(3) $$M_{c1(I)} = V_{c1(I)} h_1$$

In this equation, (I) stands for Analysis Step I. The column shear V_{c1} is obtained from the horizontal equilibrium of the story shears acting in both tiers of the sub-structure: $-2V_{c2} + V_{br,2} = 2V_{c1} + V_{br,1}$, where V_{c2} is the column shear in Tier 2 and $V_{br,1}$ and $V_{br,2}$ are respectively the horizontal story shears contributed by the braces in Tiers 1 and 2, and the relationships that exists

between column shears V_{c1} and V_{c2} that are proportional to tier heights h_1 and h_2: $V_{c1}\,h_1 = V_{c2}\,h_2$. Noting $F_{1(I)} = (V_{br,2} - V_{br,1}) / 2$ and making use of the relationship between V_{c1} and V_{c2}, the moment M_{c1} is obtained by studying the isolated two-tiered column supporting F_1:

$$(4) \qquad M_{c1(I)} = \frac{h_2}{h_{ss(I)}} F_{1(I)}\, h_1$$

where, $h_{SS(I)}$ is the total height of the substructure at step I. It is noted that the above equations apply to braced frames with identical columns; if the columns were different, column shears and moments would distribute in proportion to the columns' flexural stiffness.

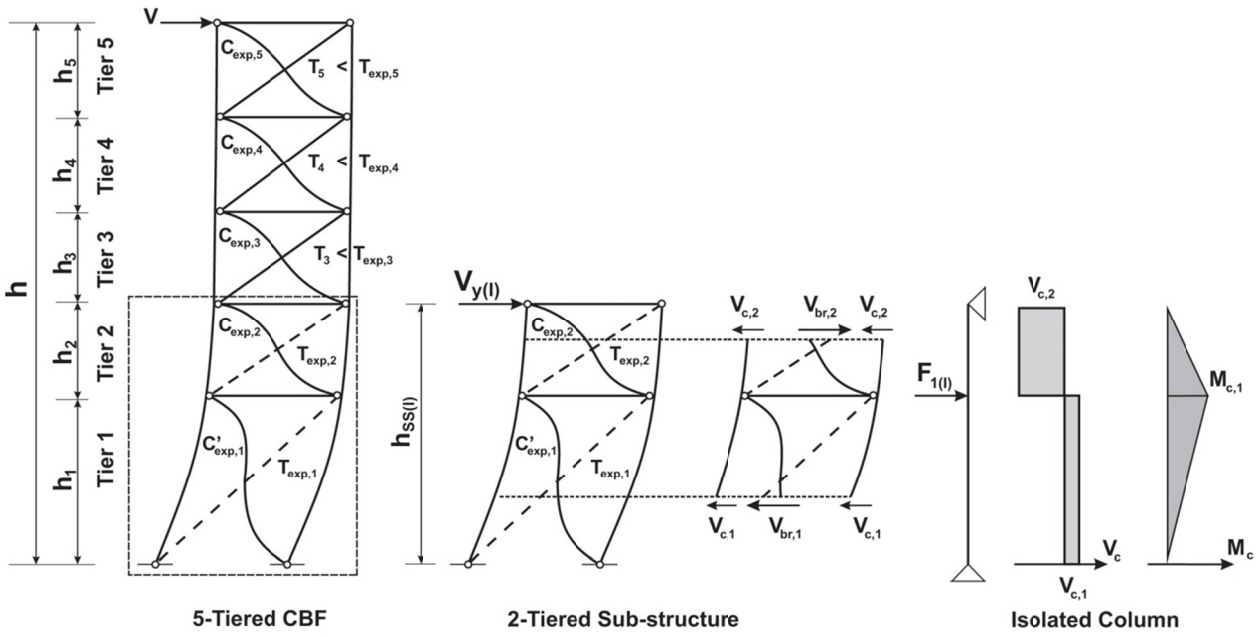

Figure 7.7: Analysis Step I for assumed bottom up brace yielding sequence: Brace yielding initiation in Tier 2.

The columns are verified for strength and stability under the combined axial load and bending moments obtained from Analysis Step I. For simplicity, the axial load in all steps can be taken equal to the axial load due to gravity loads plus the brace induced loads from the first analysis case specified in the AISC Seismic Provisions where brace forces are equal to T_{exp} and C_{exp} in all tiers. However, a more realistic axial force demand can be obtained from the brace forces in the sub-

structure and the brace forces corresponding to C_{exp} and T for the remaining upper tiers, where T is the brace tension force required to resist the story shear V_y for the analysis step. As illustrated in Figure 7.7, the shear V_y corresponds to the total story shears including column shears. If the column size is changed to meet strength requirements, the story drift Δ must be recalculated to verify the required number of yielding tiers n_y and adjust the analysis procedure accordingly.

Analysis Step II is illustrated in Figure 7.8. At this stage, plastic extension of the tension brace in Tier 2 has started and brace tension yielding initiates in Tier 3. The substructure includes the first three tiers and column moments $M_{c,1}$ and $M_{c,2}$ are obtained by examining the isolated 3-tiered column resisting unbalanced shears $F_{1(II)}$ and $F_{2(II)}$ reflecting post-buckling compression brace conditions in Tiers 1 and 2 and buckling compression brace condition in Tier 3. The column bending moments at the top of Tiers 2 and 1 are:

$$M_{c2(II)} = \frac{h_1}{h_{SS(II)}}\left[F_{1(II)}\left(h_2+h_3\right)+F_{2(II)}h_3\right] \tag{5}$$

$$M_{c1(II)} = \frac{h_1+h_2}{h_{SS(II)}}\left[F_{1(II)}\left(h_2+h_3-\frac{h_2 h_{SS(II)}}{h_1+h_2}\right)+F_{2(II)}h_3\right] \tag{6}$$

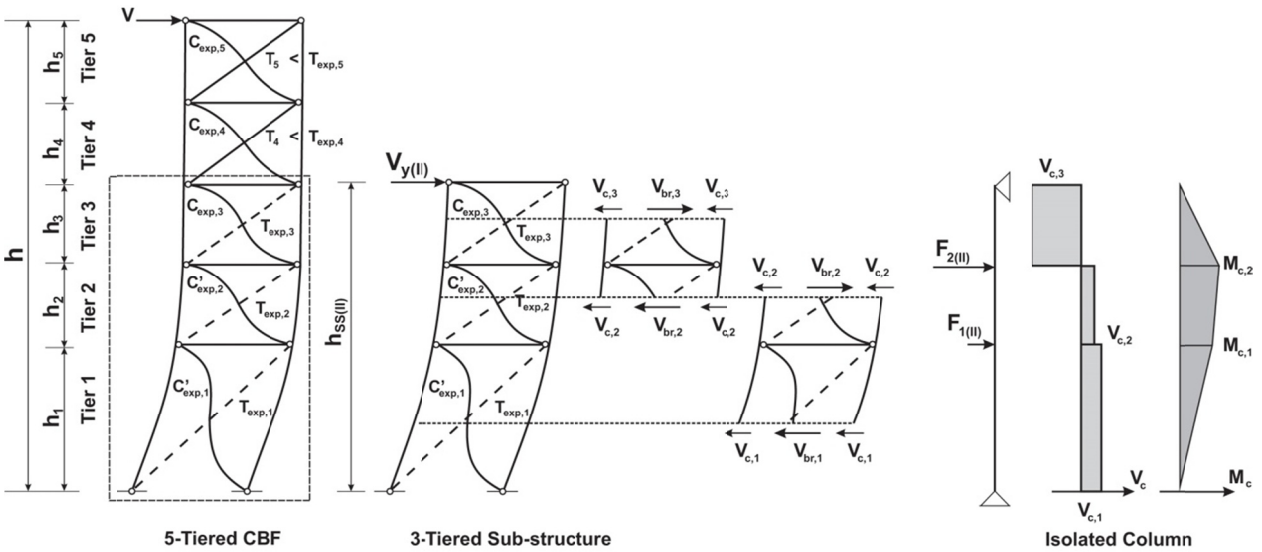

Figure 7.8: Analysis Step II for assumed bottom up brace yielding sequence: Brace yielding initiation in Tier 3.

The process is continued up to completion of analysis step $n_y - 1$, i.e. after brace yielding has been reached in Tier n_y. As said before, the column should be modified as necessary for strength and stability at each analysis step. If the columns are changed, the story drift Δ and the number of yielding tiers n_y should then be adjusted to verify if the analysis of the frame needs to be continued in the next step.

In that last analysis step, column flexural stiffness must be verified to ensure that it is sufficient to: 1) mobilize brace tension yielding in n_y tiers, as assumed in the procedure; and 2) limit the drift in the critical tier to $\Delta_{max,cr}$. For the first check, an analysis of the isolated column model shown in Figure 7.6c is performed at the point where brace tension yielding is just triggered in Tier n_y. The figure represents the situation of a 5-tiered frame when $n_y = 3$. Horizontal restraints are prescribed at Tier n_y and upper tiers. In the remaining tiers, forces F_i are applied that correspond to the horizontal resultant of the unbalanced brace loads in the yielded tiers. For frames with two identical columns:

$$(7) \qquad F_i = \frac{V_{br,i+1} - V_{br,i}}{2} \quad \text{, where: } V_{br} = (T + C)\cos\theta$$

where T and C are respectively taken equal to T_{exp} and C'_{exp}. The analysis is performed by applying a horizontal displacement at the column base equal to $\Delta_{inel(II)} = \Delta - \Delta_e (V_{y(II)} / V)$. The horizontal reaction at Tier n_y is compared to a force F_i determined with compression brace forces equal to C_{exp} and C'_{exp} in Tier n_y and Tier $n_y - 1$ respectively. If the reaction is larger than F_i, the columns designed for strength are sufficiently stiff to trigger brace tension yielding in Tier n_y before Δ is attained in the analysis step. Otherwise, the columns must be stiffened.

A similar analysis of the isolated column is performed for critical tier drift verification against the limit $\Delta_{max,cr}$. This criterion was used to determine the minimum number of yielding tiers but a more accurate verification must be performed at this stage to reflect more closely the actual boundary conditions and the effect of the brace horizontal unbalanced forces F_i at every tier level on the flexural deformation of the columns. The analysis model is shown in Figure 7.6b. Compared to the previous model, the horizontal supports at Tier n_y is removed such that only Tiers 3 and 4 are restrained. Forces F_i are determined with compression brace forces equal to C'_{exp} in all yielding tiers including Tier n_y as brace tension yielding has developed in that tier at the anticipated story

drift. The critical tier drift is equal to $\Delta_{y,cr} + \Delta_{inel,cr}$, where the former is given in Eq. 2 and $\Delta_{inel,cr}$ is determined from analysis of the isolated column model shown in Figure 7.6c. The analysis is again performed by applying a horizontal displacement at the column base equal to $\Delta_{inel(II)}$. The columns must be stiffened if the so-computed Δ_{cr} exceeds $\Delta_{max,cr}$. When large column stiffness is required, the engineer may consider using a cruciform section, latticed columns or a column stiffened by a vertical truss (Tremblay 2003; Mac Rae et al. 2004; Qu et al. 2015).

The same analysis procedure applies when the critical tier is the top tier. In this case, analysis steps are performed on sub-structures that track the brace yielding progression from the top (Figure 7.4b) with a first sub-structure that includes Tiers n and $n - 1$ (n is the total number of tiers). If needed, the sub-structuring technique can be performed until a complete mechanism is achieved, i.e. brace tension yielding is reached in all tiers. In this case, larger flexural strength demands are expected when the number of brace yielding tiers is significantly larger than n_y. Alternatively, the analysis can be halted if the required number of brace yielding tiers to prevent brace failure at the anticipated story drifts has been reached.

7.3.4 Stiffness analysis method (actual brace yielding sequence)

The stiffness analysis method is introduced as a more rigorous analysis to obtain the column bending moments and tier drifts under lateral seismic load. Compared to the sub-structuring method, it more closely reflects the actual nonlinear response of the frame as the sequence of brace tension yielding and column forces are determined with consideration of the actual frame properties. The method can then be used for any regular or irregular MT-BFs. In addition, tier drifts are obtained at each analysis step, allowing the engineer to better assess the influence of column stiffness on the frame response and, thereby, select the column sections that are required to achieve the desired behavior.

The stiffness analysis consists of analyzing the MT-BF columns isolated from the rest of the frame, as shown in Figure 7.9. Each column tier segment is treated as one frame element, and the stiffness matrix of the entire isolated column, S, is assembled from the element's stiffness matrices. Axial deformations are ignored in the analysis and each element has a 4 x 4 stiffness matrix to study in-plane rotations and horizontal displacements at every tier level. Once the stiffness matrix is assembled, the analysis is performed in successive steps, starting from the critical tier. In each analysis step, deformations and forces are obtained by solving the equation:

(8) $$[S]\{D\} = \{F\}$$

where D and F are the deformation and force vectors. In Figure 7.9, the stiffness matrix of one column of a 5-tiered frame is illustrated. This matrix includes 11 rows and 11 columns as there are two degrees of freedom by tier (θ and δ) except at the ground level where δ is equal to zero. The system can be reduced to 10x10 if the columns are fixed at their bases ($\theta_0 = 0$). The deformation vector includes rotations and displacements that develop at tier level after brace tension yielding has initiated in the critical tier. Hence, it is assumed that flexural column deformations before that point are small and can be neglected. Also, as was the case in the sub-structuring method, elastic frame deformations up to that point are excluded from the analysis process and must be added if total tier drifts are required. The force vector includes external moments M_i and external horizontal forces F_i at tier levels. As shown, the moments M_i are set equal to zero, as is the case in most MT-BFs. The forces F_i are obtained from the analysis, except that F_i is determined from brace forces in yielded tiers after brace tension yielding has occurred in two tiers, as explained later.

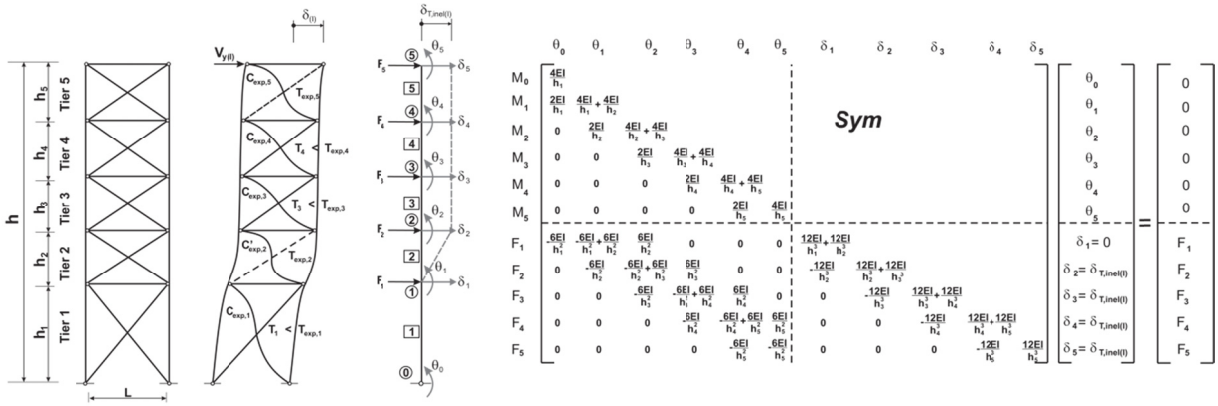

Figure 7.9: Analysis Step I: Stiffness analysis of the isolated RHS column of the 5-tiered CBF.

The system of equations shown in Figure 7.9 is the one used to initiate the analysis process (Analysis Step I) for a 5-tiered braced frame for which the critical tier is Tier 2. In this analysis step, the story drift is gradually increased as brace inelastic deformations develop in Tier 2 up to the point where brace tension yielding initiates in another tier. The analysis must be performed at this point but the story inelastic displacement $\delta_{T,inel}$ is not known yet. A trial value of $\delta_{T,inel}$ is applied to obtain brace tension forces and identify the next yielding tier. As shown in Figure 7.9,

the displacement $\delta_1 = 0$ and displacements at tier levels 2 to 5 are the same and equal to the applied story inelastic displacement $\delta_{T,inel}$ ($\delta_2 = \delta_3 = \delta_4 = \delta_5 = \delta_{T,inel}$). Using the upper 6 equations, rotations θ_0 to θ_5 can be determined for the applied $\delta_{T,inel}$. These rotations are used together with the δ_i values in the lower 5 equations to determine the forces F_i, from which column shears V_{ci} can be determined by statics. The total story shear resisted by the frame, $V_{y(I)}$, is equal to the story shear resisted by the braces and the columns in Tier 2:

$$(9) \qquad V_{y(I)} = V_2 = \left(T_{exp,2} + C'_{exp,2}\right)\cos\theta_2 + 2V_{c2}$$

and this value is used to determine the axial loads in the tension braces in all other tiers:

$$(10) \qquad T_i = \frac{V_{y(I)} - 2V_{c,i}}{\cos\theta_i} - C_{exp,i}$$

At the end of Analysis Step I, brace tension yielding will occur in the tier where T_i/T_{exp} is maximum and the displacement $\delta_{T,inel(I)}$ is adjusted so that $T_i = T_{exp}$ in that tier. Column shears and moments obtained from the analysis for this displacement are those that must be considered to verify column strength and stability in this analysis step. The column axial loads due to gravity loading plus computed brace forces are used in this verification. The tier drift in the tier(s) where brace tension yielding has been reached is also verified at the end of the analysis step. For this example, the verification is:

$$(11) \qquad \Delta_2 = \Delta_{y,2} + \frac{\left(\delta_{3(I)} - \delta_{2(I)}\right)}{h_2} \le \Delta_{max,2}$$

where $\Delta_{y,2}$ is obtained from Eq. 2. In Eq. 11, the computed tier drift is checked against the maximum allowable tier drift, Δ_{max}. At the end of the analysis step, the story drift corresponding to $\delta_{T,inel(I)}$, $\Delta_{(I)}$, is obtained from:

$$(12) \qquad \Delta_{(I)} = \frac{\delta_{T,inel(I)}}{h} + \Delta_e\left(\frac{V_{y(I)}}{V}\right)$$

If $\Delta_{(I)}$ exceeds the maximum anticipated story drift Δ, the analysis process is halted and the conditions at the anticipated story drift are obtained by repeating the analysis with an imposed displacement $\delta_{T,inel}$ given by:

$$\delta_{T,inel(I)} = h\left[\Delta - \Delta_e\left(\frac{V_{y(I)}}{V}\right)\right] \quad (13)$$

Column forces and tier drifts at this displacement are those that are used to verify the column section. The column section is adjusted as required to meet strength and stability requirements and prevent drifts from exceeding Δ_{max}. If the section is changed, the story drift Δ is recomputed and the analysis process is repeated to determine the conditions at Δ. It is noted that in the stiffness analysis method the column stiffness need not be verified to ensure brace yielding propagation, as column flexural stiffness is explicitly considered in the analysis.

If the story drift in Analysis Step I is less than the maximum anticipated story drift, the same procedure is repeated in Analysis Step II except that modifications must be made to account for the new brace yielding state. Assuming for the frame example in Figure 7.9 that brace tension yielding is triggered in Tier 5 in Analysis Step I, Analysis Step II is performed using the structure stiffness equation presented in Figure 7.10. In this case, inelastic deformations take place in both Tiers 2 and 5 and the analysis step is completed when brace tension yielding eventually initiates in either Tier 1, 3 or 4. For this analysis, $\delta_1 = 0$, $\delta_2 = \delta_3 = \delta_4$, and δ_5 corresponds to $\delta_{T,inel(II)}$. To reflect the constraint $\delta_2 = \delta_3 = \delta_4$, lines and columns of the system that correspond to δ_2 and δ_3 are merged in the line and column associated to the horizontal degree of freedom δ_4 (Rubinstein 1996). In the analysis, the total force $F_2 + F_3 + F_4$ for this common degree of freedom is determined from brace forces in yielded tiers. For this example, it is equal to the differences between story shears resisted by the braces in tiers 5 and 2, as obtained from Eq. 7 (= 0.5 ($V_{br,5} - V_{br,2}$)) with brace compression loads C equal to C'_{exp} and brace tension loads T equal to T_{exp}. The upper portion of the system of equations is solved for rotations θ_1 to θ_6 and displacement δ_4 for a given $\delta_{T,inel} > \delta_{T,inel(I)}$, and these deformations are used to solve for forces F_i using the equations presented in Figure 7.10. Column shears, story shear and brace tension forces can then be calculated and the displacement $\delta_{T,inel(II)}$ that triggers brace tension yielding in the next yielding tier can be determined as described in Analysis Step I. Additional analysis steps are performed as necessary to attain the anticipated story drift.

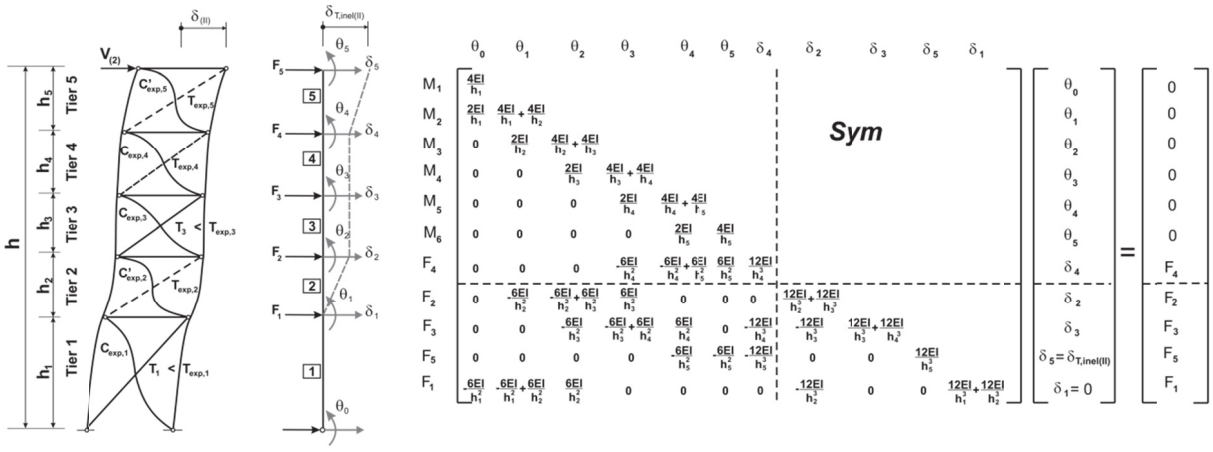

Figure 7.10: Analysis Step II: Stiffness analysis of the isolated RHS column of the 5-tiered CBF.

7.4 Design examples

Two design examples are presented to illustrate and validate the seismic analysis methods proposed for MT-BFs. The first design example presents the application of the sub-structuring technique for Frame 1 that corresponds to the 5-tiered steel SCBF studied in the first section of the article (Figure 7.2a). In the second example (Frame 2), the stiffness analysis method is applied to the same frame except that it is designed for higher seismic loads and the brace sizes in Tier 3 have been intentionally increased to create strength irregularity along the frame height (Figure 7.11b). In both examples, maximum allowable tier drift is based on brace fracture. Member design was first performed in accordance with the AISC 341-10 Seismic Provisions. As shown in Figure 7.11, the demand-to-capacity ratios for the braces (P_u / $\phi_c P_n$) are close to 1.0 in all tiers except for the oversized braces in Tier 3 of Frame 2 (P_u / $\phi_c P_n$ = 0.47). In the frames, each column must carry a factored roof dead load (1.2 + 0.2S_{DS})×D of 242 kN. The total axial compression loads in the columns due to gravity plus seismic analysis (AISC 341-10 Analysis Case 1) are 4857 and 5738 kN for Frames 1 and 2, respectively, which required W610x195 and W610x217 sections.

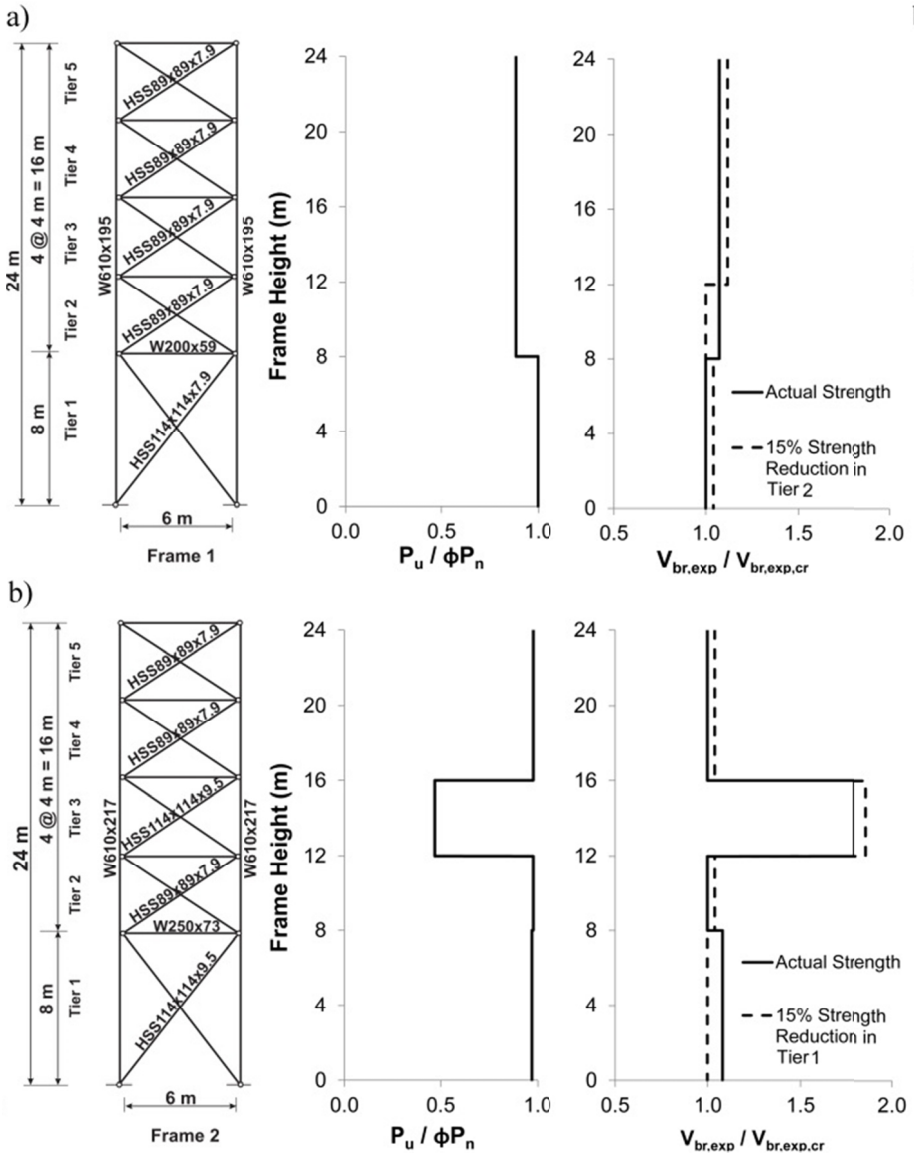

Figure 7.11: Frame configuration, brace demand-to-capacity ratios, and shear resistances for: a) Frame 1; and b) Frame 2.

7.4.1 Design Example 1

For Frame 1, the critical tier is identified by comparing the story shear resistances, $V_{br,exp}$, from Eq. 1. As shown in Figure 7.11a, Tier 1 has the lowest story shear resistance ($V_{br,exp,1}$ = 1205 kN) and is the critical tier. As discussed, the possibility of other critical tier scenarios should be also checked by reducing the brace resistances in other tiers, as shown for Tier 2 in Figure 7.11a. In this example, only critical Tier 1 scenario is presented. The sub-structuring technique is chosen for this

well-proportioned regular frame with bottom up brace tension yielding sequence consistent with the critical Tier 1 scenario. The number of yielding tiers, n_y, is determined using Eq. 2 with a maximum anticipated story drift Δ equal to the ASCE 7 design story drift, $\Delta = C_d\Delta_e/I_e$, where C_d and I_e are the deflection amplification factor and importance factor (C_d = 5 and I_e = 1). As described in Section 2, the brace failure for the critical tier is expected to occur at a tier drift $\Delta_{max,cr}$ = 1.9%. Solving Eq. 2 for Δ = 1.21%, h_{cr} = 8.0 m, V = 490 kN, and R_yF_y = 483 MPa gives h_y = 14.8 m, which means that n_y = 3 is required.

In Analysis Step I, the sub-structure includes Tier 1 and 2 and brace tension yielding is being triggered in the second tier. For this step, the maximum column bending moment of 425 kN-m occurs at Tier 1 as determined with Eq. 4. For this step, the axial compression load in that tier is equal to P_u = 4432 kN. The columns are verified for strength and stability under this combined axial force and in-plane bending moments and a W760x314 section is required. With this larger column section, the design story drift is reduced to Δ = 1.02% and h_y from Eq. 2 becomes 9.4 m, meaning that n_y = 2 and Analysis Step II is no longer required.

Column stiffness check to trigger yielding in Tier 2 is then verified. The isolated column analysis is performed with restraints specified at Tiers 1 to 5. Under the inelastic story drift $\Delta_{inel(I)}$ = 0.52%, the reaction at Tier 1 is 87 kN, which is much less than the half of the difference between V_{br2} = 1293 kN and V_{br1} = 974 kN assuming C_{exp} and C'_{exp} in the compression braces in Tiers 2 and 1, respectively. The selected column is therefore too flexible and a W360x382 section is needed to initiate brace yielding in Tier 2.

Tier drift in critical Tier 1 Δ_{cr} is also checked at Analysis Step I to ensure that flexural stiffness of that column is sufficient to limit Δ_{cr} to $\Delta_{max,cr}$ = 1.9%. The check is performed with the W760x314 columns. The drift in the critical tier is the sum of $\Delta_{y,cr}$ = 0.5% when the brace tension yielding initiates, plus $\Delta_{inel,cr}$ = 1.33% determined from the analysis of the isolated RHS column where lateral supports are assigned at Tiers 2 to 5 and horizontal unbalanced forces from brace loads in Tiers 1 and 2 assuming C'_{exp} in the compression braces in both tiers are applied at Tier 1. This leads to Δ_{cr} = 1.83%, which is lesser than the limit and the W760x314 columns are sufficient to satisfy drift requirements.

In Figure 7.12a, column bending moments and tier drifts from sub-structuring technique with the W760x314 columns are compared to those obtained from the stiffness analysis method for this frame. As shown, both methods give very similar results for both parameters. The stiffness analysis method predicts the same number of brace yielding tiers. The bending moment from sub-structuring technique are slightly larger at Tier 1 due to ignoring continuity of the columns at Tier 2 in the sub-structure used in Analysis Step I.

In this example, only one analysis step was needed; however, the situation could have been different if critical tier was shorter or the frame designed for a larger anticipated story drift. For instance, if the anticipated story drift was $\Delta = 1.5\ C_d\Delta_e/I_e$, n_y would be 4 and larger W360x463 columns would be needed to satisfy the drift requirements in the critical Tier 1.

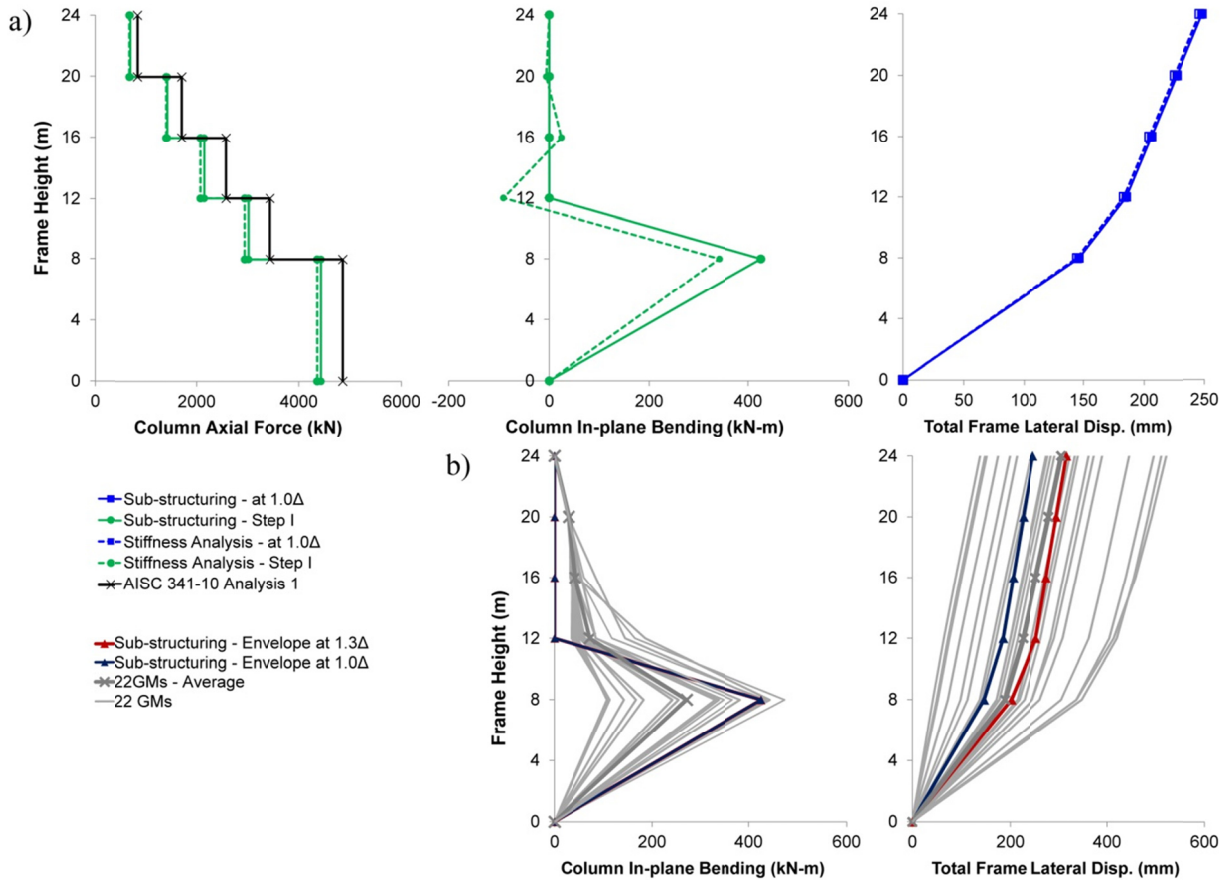

Figure 7.12: Analysis of Frame 1: a) Columns demands and frame lateral displacements; and b) NLRH analysis results for column bending and tier drift demands.

7.4.2 Design Example 2

The second design example (Frame 2) is presented using the stiffness analysis method. The configuration of the frame is shown in Figure 7.11b. For this frame, the design period is equal to 0.74 s, which gives a seismic coefficient C_s = 0.135 and a base shear V of 543 kN per frame. The design story drift is equal to Δ = 1.20% based on the initial member design. The critical tier is identified by comparing story shear resistances in Figure 7.11b. As shown, $V_{br,exp}$ is minimum and same in Tiers 2, 3, and 5. Considering the 15% reduction in brace resistances, critical Tier 1 scenario (Figure 7.11b) should be also studied. In this example, the critical Tier 2 scenario is illustrated. Using the fracture model by Tremblay et al. (2003), failure of the HSS braces in Tiers 1, 2 (or 4 or 5), and 3 are expected to occur at Δ_{max} = 2.1, 2.2, and 1.9% respectively. For Analysis Step I, the column stiffness matrix is assembled for 5 tiers, as shown in Figure 7.9. Once the stiffness equation is developed, the inelastic story drift is increased until brace tension yielding develops in Tier 5 at $\delta_{T,inel}$ = 79 mm. Column bending moments and axial loads due to gravity loading plus computed brace forces are shown in Figure 7.13a. W760x284 columns are selected to resist this combined demand at every tier. With this new column section the story drift reduces to Δ = 1.08%. Introducing the properties of the selected columns in the stiffness matrix, $\delta_{T,inel}$ = 46 mm when brace yielding initiates in Tier 5, and $\Delta_{(I)}$ from Eq. 12 becomes 170. This story drift is less than Δ, the bending moments and tier drifts are calculated at this $\Delta_{(I)}$ value. W760x284 columns are found adequate to resist these new force demand. Tier drift in yielding tier $\Delta_{inel,2}$ = 1.15% is obtained. This value is added to $\Delta_{y,2}$ = 0.5% to give Δ_2 = 1.65%. This drift does not exceed the limit and the column section is kept unchanged. Since $\Delta_{(I)}$ is smaller than Δ, frame analysis continues in Analysis Step II. The roof displacement is increased to $\delta_{T,inel}$ = 70 mm until brace tension yielding starts in Tier 4. Column bending moments and tier drifts are shown in Figure 7.13a for this step. The W760x284 section selected in the previous step is found adequate to resist combined moment and axial force demands in this step. Drifts in yielding Tiers 2 and 5 are equal to 1.1 and 1.7% respectively, which are lower than the corresponding limits. The value of $\Delta_{(II)}$ = 194 mm is smaller than Δ, requiring Analysis Step III to be performed. In this analysis step, it is found that brace tension yielding occurs in Tier 1 at $\Delta_{(III)}$ = 912 mm, which exceeds design story drift Δ. The analysis is performed at $\delta_{T,inel}$ = 135 mm which corresponds to Δ. Bending moment and axial compression force demands at this point are shown in Figure 7.13a. The W760x284 section is still

sufficient to resist the combined demands. In Tier 5, the drift is equal to $\Delta_2 = 2.70\%$, in excess of the 2.2% limit for this tier and a stiffer W360x421 column section is chosen. With this column, the story drift is 0.95% and Tier 5 drift is reduced to 2.2%, which is adequate. Drift results for Analysis Step III shown in Figure 7.13a were obtained with the W360x421 column section.

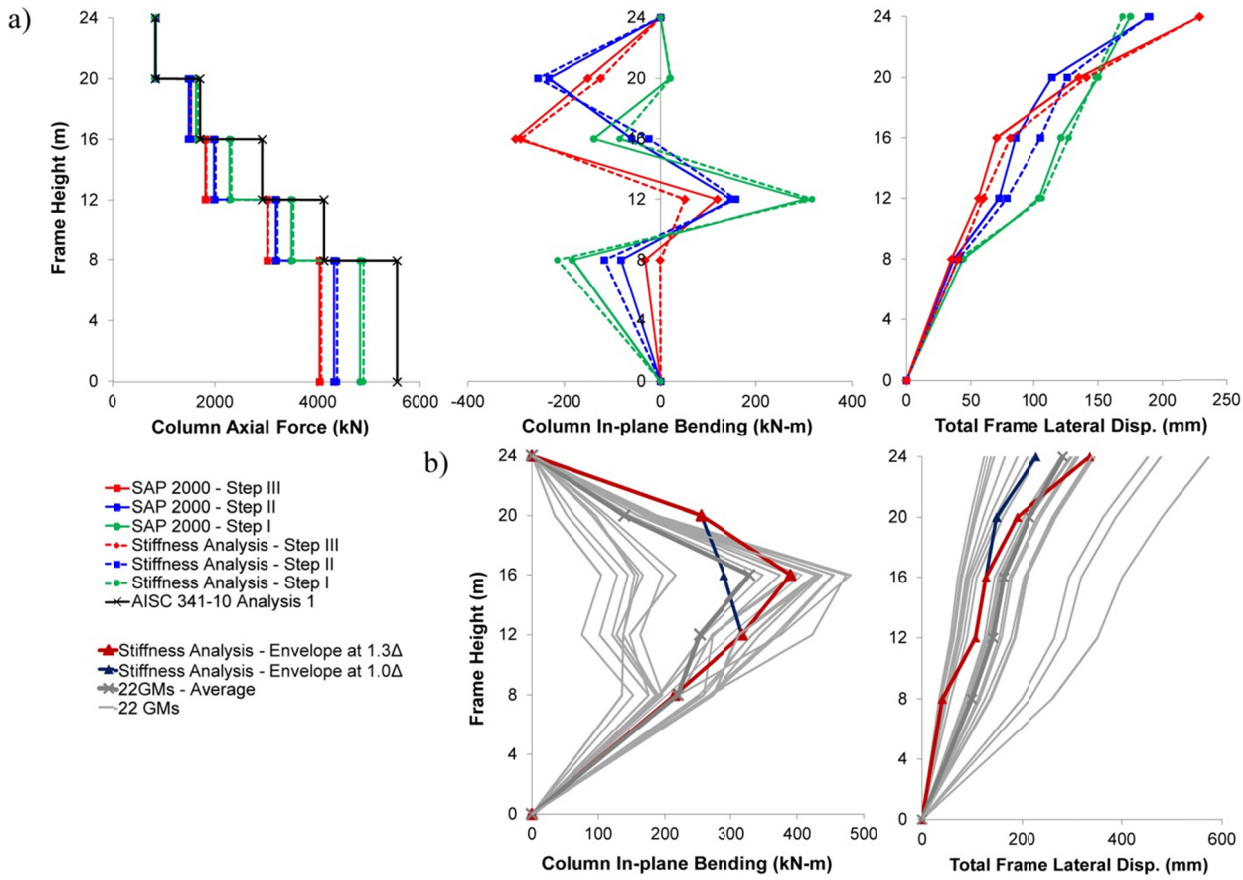

Figure 7.13: Analysis of Frame 2: a) Columns demands and frame lateral displacements; and b) NLRH analysis for column bending and tier drift demands.

For this frame, nonlinear incremental static (pushover) analysis was performed using the SAP 2000 program (CSI 2015) to verify the results obtained from stiffness analysis. The SAP 2000 analysis consists of a series of displacement controlled elastic static analyses performed on a model that was progressively modified to represent the status of the braces as the roof displacement was increased. Each analysis corresponded to each of the analysis steps of the

proposed stiffness method. In each step, the tension and compression braces were replaced by concentrated loads corresponding to their expected resistances as done in the method. The results for Analysis Steps I to III are given in Figure 7.13a. The comparison of the results indicates reliable prediction of the response by the proposed stiffness analysis method. This also shows that a computer analysis program can be used to perform the structural analysis calculations required in the proposed method.

For this frame, drift requirement controlled the size of the columns. For simplicity in the calculations, the anticipated story drift was obtained with the computed fundamental period of the structures with the upper limit ($C_u T_a$) specified in ASCE 7. In practice, the anticipated story drift could be obtained without the upper limit ($C_u T_a$), which would reduce the drift demands on the columns. Stiffness requirements on columns can also be mitigated by selecting bracing members that have a longer low-cycle fatigue life.

7.4.3 Nonlinear Response History Analyses

Nonlinear response history NLRH analysis was performed for both frame examples under the far-field record set of 22 ground motion records described earlier. The final column design was used to perform the NLRH analyses. No column buckling was observed in the analyses. The tier drifts are compared in Figs 12b and 13b for Frames 1 and 2 to those calculated using the proposed methods. For both frames, the predicted deformation patterns are similar to the NLRH analysis ones indicating that the brace tension yielding sequence was well predicted by the two proposed methods. For Frame 2, however, critical Tier 2 scenario was chosen to predict the demand, whereas critical Tier 1 scenario was also triggered in the NLRH analyses due to the small difference between story shear resistances of Tiers 1 and 2 (Figure 7.11b). In this case, the difference between the AISC expected brace strength values and the brace nonlinear response in the analysis was sufficient to overcome the difference in $V_{br,exp}$. This confirms the need to examine all plausible critical tier scenarios in the analysis. The analysis for Frame 1 was performed with the W760x314 columns, as determined from strength requirements. Similar small difference in $V_{br,exp}$ existed between Tiers 1 and 2 (Figure 7.11a); however, ground motions only triggered brace yielding in Tier 1 because the columns were too flexible, as expected from design. The analyses were redone with the required stiffer W360x382 section and brace tension yielding was observed in Tiers 1 and 2, as was also predicted.

It is noted for these two frames that the average story drift demands exceed the Δ value used in design: 1.26 Δ and 1.20 Δ for Frames 1 and 2, respectively. This was expected due to the fact that MCE level earthquake were used, whereas Δ corresponded to the design earthquake level. To show that the methods can predict frame behaviour for these larger story drifts, the analyses were redone using 1.30 Δ for both frames without changing the column sizes to still allow comparison with the NLRH analysis results. Figure 7.12b shows that an excellent agreement can be achieved for Frame 1 when a realistic story drift is used in the calculations. For Frame 2, additional drift concentrated in Tiers 4 and 5, consistent with the selected critical Tier 2 scenario, whereas the ground motions imposed larger inelastic demand in Tier 1 due to brace yielding in that tier.

For both frames, the average tier drift exceeded Δ_{max} because of the larger story drifts imposed by the ground motions. For Frame 1, this would have been predicted by performing the analysis at 1.30 Δ, and larger column sections would have been selected. For Frame 2, the larger drift in Tier 5 under 1.30 Δ assuming critical Tier 2 scenario (4.4%) would also necessitate larger columns. If the analysis is performed under 1.30 Δ with critical Tier 1 scenario, Tier 5 drift reduces to 0.5% and Tier 1 drift increases 2.2%. NLRH analysis results stand between two analysis cases corresponding to critical scenarios 1 and 2.

For Frame 1, column bending moments are compared for the W760x314 section in Figure 7.12b. In the figure, the envelopes of the absolute values are presented both for the design method and the NLRH analysis. As observed, the design predictions envelope very well the demand from the ground motions. This result was anticipated because the brace force scenarios used to determine the moments represent most possible critical conditions, which is consistent with the approach used in the current AISC Seismic Provisions for column axial loads in braced frames. For Frame 2, NLRH analysis was redone with W760x284 columns to obtain a direct comparison with the moments predicted using the stiffness analysis method with the same column section. As shown in Figure 7.13b, the predictions lie between the average and envelope values of the NLRH analysis results because Analysis Step III was performed at the anticipated story drift rather than the story drift that would trigger yielding of the next tier. In the stiffness method, column moments depend on story drift and as shown in Figure 7.13b, the moments obtained from analysis under 1.30 Δ reflect better the average moment demand from ground motions.

7.5 Conclusions

MT-BFs designed in accordance with the current AISC Seismic Provisions are prone to column buckling and brace fracture due to non-uniform distribution of drift demands along their height when responding to strong earthquake events. These two undesirable limit states must be addressed in design. Two analysis methods, the sub-structuring technique and the stiffness analysis based method, were proposed to predict seismic induced column in-plane bending moment and tier drift demands for MT-BFs with three or more bracing panels. The methods account for initiation of brace tension yielding in the critical tier and subsequent propagation of brace tension yielding in other tiers as observed in MT-BFs. Bending moments obtained from the method can be used to design the columns for strength and stability and therefore prevent column buckling. The methods also provide column stiffness requirements to minimize drift concentration such that brace failure is avoided.

In both methods, analysis steps are performed that correspond to occurrences of brace tension yielding as the story drift is increased. In each step, brace forces that represent brace buckling and yielding sequence are considered to determine the column moments and tier drifts. The sub-structuring method is a simpler method introduced for well-proportioned braced frames with uniform tier properties assuming bottom up or top down brace yielding sequence. Each analysis is performed on a simple sub-structure including the yielding tiers. The stiffness analysis method is a more rigorous procedure that predicts the progression of brace tension yielding with consideration of the actual nonlinear response of the frame. Therefore the method can be used for any regular or irregular MT-BFs. The application of the two methods was illustrated for two 5-tiered SCBF examples. The methods were validated for the two frames using nonlinear seismic response history analysis.

The seismic induced demands obtained from the analysis methods depend on the story drift considered in the analysis; therefore, a story drift consistent with the target performance should be selected. The proposed analysis method was developed for in-plane seismic demands; design requirements should be also developed for concomitant out-of-plane flexural demand.

Acknowledgments

Funding from the Natural Sciences and Engineering Research Council (NSERC) of Canada is acknowledged. The authors express their appreciation to Larry Fahnestock of the University of Illinois at Urbana-Champaign and Christopher Stoakes of the University of Iowa, as well as members of AISC Task Committee 9 – Seismic Design for their most valuable input on this topic.

References

AISC. (2010a). "*ANSI/AISC 341-10, Seismic Provisions for Structural Steel Buildings.*" American Institute of Steel Construction, Chicago, IL.

ASCE. (2010). "*ASCE/SEI 7-10*, *Minimum Design Loads for Buildings and Other Structures.*" American Society of Civil Engineers, Reston, VI.

CSA. (2014). *CSA S16-14, Design of Steel Structures*. Canadian Standards Association, Mississauga, ON.

CSI. (2015). SAP 2000 v17.2, Integrated finite element analysis and design of structures, Computers and Structure Inc., Berkeley, CA.

FEMA. (2009). *ATC 63, FEMA P695: Quantification of Building Seismic Performance Factors*." Applied Technology Council, Redwood City, CA.

Imanpour, A., and Tremblay, R. (2014). "Seismic design of steel multi-tiered braced frames: Application of incremental static analysis for design of steel multi-tiered braced frames." *Proc. Eurosteel 2014*, Naples, Italy, Paper no. 688.

Imanpour, A., Tremblay, R., Davaran A., Stoakes, C., and Fahnestock, L. (2015a). "Seismic Performance Assessment of Multi-Tiered Steel Concentrically Braced Frames Designed in Accordance with Current AISC Seismic Provisions." Submitted to *J. Struct. Eng., ASCE*.

Imanpour, A., Tremblay, R., Fahnestock, L., and Stoakes, C. (2015b). "Analysis and Design of Two-Tiered Steel Braced Frames under In-plane Seismic Demand." Submitted to *J. Struct. Eng., ASCE*.

Imanpour, A., and Tremblay, R. (2015). "Steel Multi-Tiered Concentrically Braced Frames in Canada: Seismic Design Method and Response." Submitted to *Can. J. Civ. Eng.*

MacRae, G. A., Kimura, Y., and Roeder C. (2004). "Effect of Column Stiffness on Braced Frame Seismic Behavior." *J. Struct. Eng., ASCE*, 130:3(381), 381-391.

McKenna, F. and Fenves, G.L. (2004). "*Open System for Earthquake Engineering Simulation (OpenSees).*" Pacific Earthquake Engineering Research Center (PEER), University of California, Berkeley, CA. http://opensees.berkeley.edu/.

Qu, B., Sanchez-Zamora, F., and Pollino, M. (2015). "Transforming Seismic Performance of Deficient Steel Concentrically Braced Frames through Implementation of Rocking Cores." *J. Struct. Eng., ASCE*, DOI: 10.1061/(ASCE)ST.1943-541X.0001085.

Rubinstein, M.F. (1966). *Matrix Computer Analysis of Structures, 1st ed.,* Prentice-Hall, Inc., Englewood Cliffs, NJ, 402 p.

Stoakes, C.D. and Fahnestock, L.A. (2012). "Influence of weak-axis flexural yielding on strong-axis buckling strength of wide flange columns." *Proceedings, Annual Stability Conference, SSRC,* Grapevine, Texas, April 17-20.

Stoakes, C.D., and Fahnestock, L.A. (2013). *Three-Dimensional Finite Element Simulation of the Seismic Behavior and Performance of Multi-Tier Braced Frames*, Interim report to the American Institute of Steel Construction, AISC.

Tremblay, R. (2003). "Achieving a Stable Inelastic Seismic Response for Concentrically Braced Steel Frames." *Eng. J., AISC*, 40(2), 111-129.

Tremblay, R., Archambault, M.H., and Filiatrault, A. (2003). "Seismic Performance of Concentrically Braced Steel Frames made with Rectangular Hollow Bracing Members." *J. of Struct. Eng.*, ASCE, 129, 12, 1626-1636.

Symbols

C_d	Deflection amplification factor
C_{exp}	Brace expected strength in compression
C'_{exp}	Brace expected post-buckling strength
C_s	Seismic response coefficient
C_u	Coefficient for upper limit on calculated period

D	Dead load
D	Deformation vector
E	Young's modulus
EI_c	Column flexural stiffness
F	Force vector
F_i	Horizontal resultant of the unbalanced brace loads
F_y	Yielding strength
h	Total frame height
h_{cr}	Height of the critical tier
h_i	Tier height (i = 1 to 5)
$h_{SS(i)}$	Total height of the substructure at Analysis Step i
h_y	Height over which brace tension yielding must propagate
I_e	Importance factor
K	Effective length factor
KL	Column effective length
M_{ci}	Column weak-axis bending moment at tier level (i = 1 to 5)
M_i	External moment at tier level (i = 1 to 5)
n	Total number of tiers
n_y	Minimum number of yielding tiers
P_n	Nominal compressive strength
P_u	Required axial strength
R	Response modification coefficient
R_yF_y	Expected steel yield stress
S	Stiffness matrix

S_s	Mapped MCE_R spectral response acceleration parameter at short period
S_1	Mapped MCE_R spectral response acceleration parameter at 1.0 s period
T_a	Approximate fundamental period of the building
T_{exp}	Brace expected strength in tension
T_i	Axial load in the tension brace
V	Design story shear
$V_{br,i}$	Horizontal story shears contributed by the braces in Tiers i
V_c	Column shear force
$V_{y(i)}$	Total story shear resisted by the braces and the columns in yielding tier at Analysis Step i
$V_{br,exp}$	Story shear resistance
ϕ_c	Resistance factor for compression
$\phi_c P_n$	Design axial strength
θ	Angle between the braces and horizontal plane
θ	Rotational degree of freedom at tier level
δ	Translational degree of freedom at tier level
Δ	Maximum anticipated story drift
Δ_{cr}	Drift in the critical tier
$\Delta_{(i)}$	Story drift at Analysis Step i
Δ_{inel}	Portion of the anticipated story drift that develops after brace tension yielding has initiated in the critical tier
$\Delta_{max,cr}$	Maximum allowable drift in the critical tier
$\Delta_{max,i}$	Maximum allowable drift in Tier i
$\delta_{T,inel}$	Story inelastic displacement

$\delta_{T,inel(i)}$ Story inelastic displacement at Analysis Step i corresponding to $\Delta_{(i)}$

$\Delta_{y,cr}$ Drift in the critical tier when brace tension yielding initiates in that tier

CHAPTER 8 ARTICLE 5 : SEISMIC DESIGN AND RESPONSE OF STEEL MULTI-TIERED CONCENTRICALLY BRACED FRAMES IN CANADA

Ali Imanpour[1] and Robert Tremblay[2]

[1]Ph.D. Candidate, Dept. of Civil, Geological and Mining Engineering, Polytechnique Montreal, Montreal, QC, Canada H3C 3A7. (corresponding author). E-mail: aimanpour@gmail.com

[2]Professor, Dept. of Civil, Geological and Mining Engineering, Polytechnique Montreal, Montreal, QC, Canada H3C 3A7.

The article was submitted to the *Canadian Journal of Civil Engineering* on September 15, 2015.

Abstract

This article investigates the seismic design and response of steel multi-tiered concentrically braced frames (MT-BFs) in which braces meet at columns between diaphragms. The seismic design provisions of CSA S16-14 are described and illustrated for 3-tiered Type MD (moderately ductile) and 5-tiered Type LD (limited ductile) braced frames. An analysis method is proposed to evaluate the in-plane flexural demand on columns. The seismic response of the frames is examined through nonlinear response history analysis. As assumed in design, inelastic deformations tend to concentrate in one tier over the frame height, causing non-uniform drift demands and in-plane bending moments in the columns. CSA S16 provisions predicted well the frame in-plane flexural response and result in acceptable ductility demands on the braces. An alternative seismic analysis and design approach that accounts for vertical distribution of brace tension yielding along the frame height is proposed for frames that exceed the limits prescribed in CSA S16.

Key words: Multi-tiered concentrically braced frames, Seismic response, Nonlinear analysis.

8.1 Introduction

Steel multi-tiered braced frames (MT-BFs) are braced frames that comprise two or more bracing panels stacked on top of each other between horizontal diaphragms in a building. This geometry is common in tall single-storey buildings such as industrial facilities, sport centers, airplane hangars or warehouses. An example is shown in Figure 8.1a. X-, V, Inverted V, and diagonal bracing configurations can be utilized in MT-BFs. Multi-tiered braced frames represent an economical and practical option for such buildings as they use shorter braces that are more effective in compression and more easily satisfy slenderness limits compared to braces that span over the full frame or storey height. For very tall applications, single diagonal members become impractical and a multi-tiered configuration often represents the only available solution. In seismic design, smaller braces typically lead to reduced seismic force demands on brace connections, columns, and other structural components. In MT-BFs, the columns are braced at every tier level in the plane of the frame while buckling out-of-plane can occur over the full frame or storey height. I-shaped members oriented such that strong axis bending occurs out-of-plane are therefore generally used for the columns. This arrangement is also suitable for MT-BFs located on exterior walls where the columns must resist lateral wind loads applied to the wall cladding.

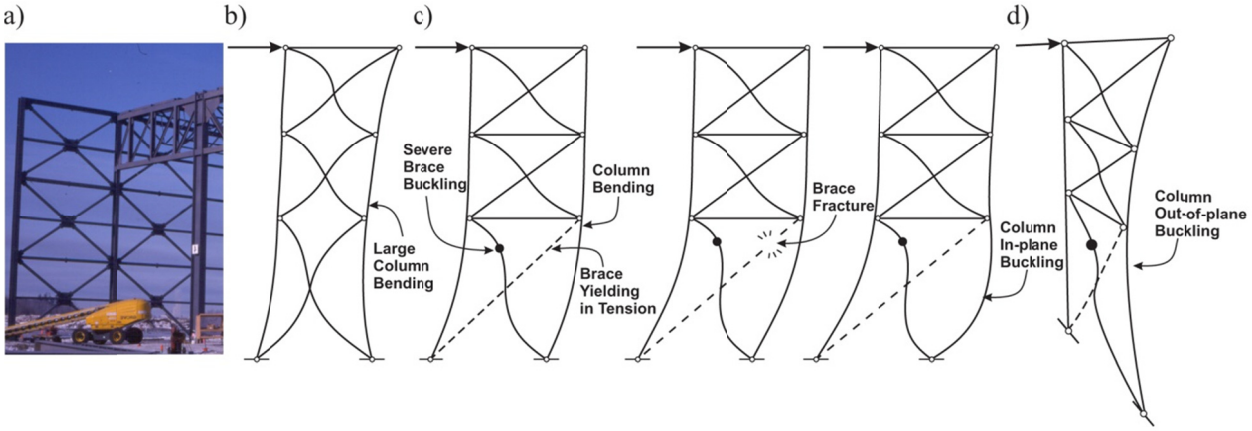

Figure 8.1: a) Three-tiered concentrically steel braced frame with X-bracing; b) Flexural demand on MT-BF columns without intermediate struts; c) Concentration of inelastic deformations in a MT-BF inducing in-plane flexural demand on columns and large inelastic demand on bracing members; d) Column out-of-plane buckling mode.

Under seismic ground motions, brace buckling in multi-tiered braced frames produces inwards unbalanced horizontal loads imposed to the columns that must be resisted by horizontal struts placed at every tier level (Figure 8.1b). Inelastic deformations in MT-BFs are also expected to concentrate in the bracing members of one tier along the frame height (Imanpour et al. 2012a, 2012b), which induces in-plane flexural demand on columns that may lead to column buckling. Drift concentration may impose excessive ductility demand on braces which can cause premature brace failure (Figure 8.1c). Brace out-of-plane buckling may also affect out-of-plane stability of the columns as shown in Figure 8.1d. Special design provisions have been introduced in CSA S16 (CSA 2014) to account for this behaviour and achieve satisfactory seismic response. This paper describes these seismic provisions and their application is illustrated for X-braced frame examples. The response of typical frames having different numbers of tiers and tier height ratios is examined through nonlinear response history analysis. An alternative design method is proposed to determine in-plane seismic demand in frames having a large number of tiers for which brace tension yielding is expected to develop in more than one tier.

8.2 CSA S16 seismic design provisions for MT-BFs

The National Building Code of Canada (NRCC 2015) defines two categories of concentrically braced steel frames that must be designed and detailed to withstand earthquake effects through stable inelastic deformations: moderately ductile (Type MD) and limited ductility (Type LD) braced frames with ductility-related force modification factors R_d equal to 3.0 and 2.0, respectively. Seismic requirements for both systems are given in Clause 27 of CSA S16 design standard for steel structures (CSA 2014). For both categories, the bracing members are designed and detailed to dissipate seismic energy by yielding in braces. Other components must resist gravity load effects plus seismic induced forces corresponding to the brace probable resistances. Two loading cases must be considered: one where the compression braces attain their probable compressive (buckling) resistance C_u and one where they reach their degraded buckled (post-buckling) resistance C'_u; in both cases, the tension braces carry forces equal to their probable yield tensile resistances T_u (Figure 8.2). The first case reflects a situation likely to occur early during an earthquake, when the tension braces reach their yield strength after the compression braces have just buckled. The second case occurs after the frame has sustained several reversed

inelastic cyclic loading. The two loading cases aimed at bounding intermediate conditions that are expected during an earthquake.

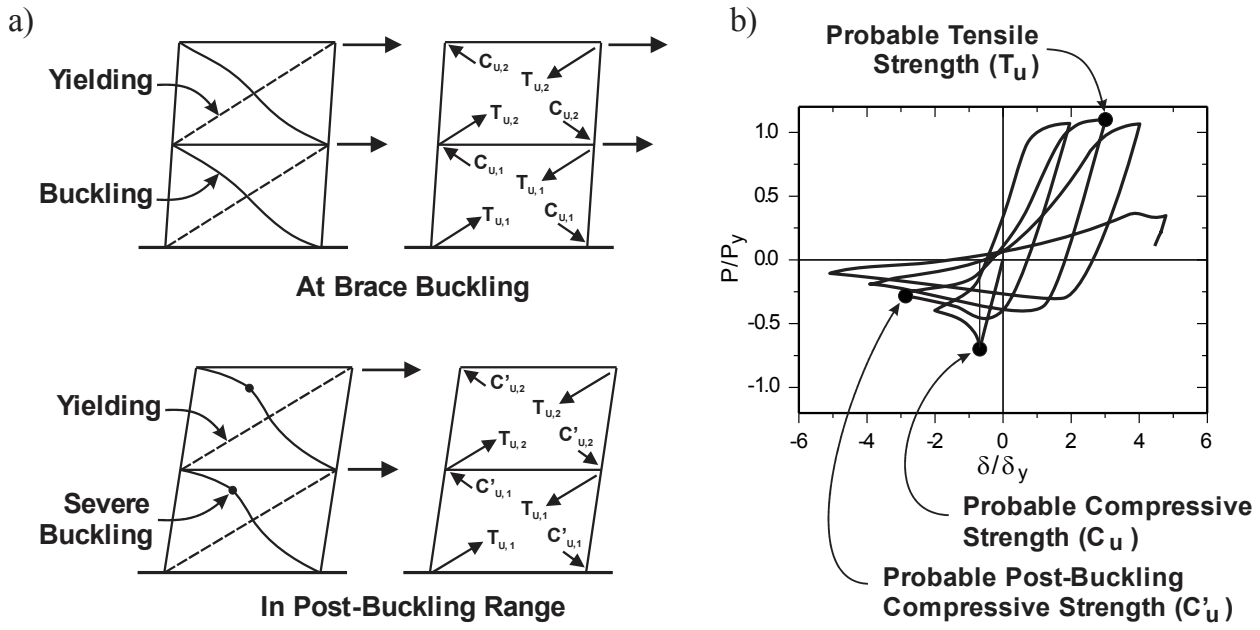

Figure 8.2: a) Brace induced loading conditions for the design of brace connections, beams, and columns of Type MD and Type LD CBFs; b) Brace hysteretic response.

In MT-BFs, braces meet at columns between horizontal diaphragms and additional requirements must be met to ensure satisfactory seismic response. As shown in Figure 8.2a, unbalanced horizontal loads are imposed to columns after buckling of the braces, when the compressive strength of the braces reduce to C'_u and larger tension develops in the tension-acting braces. This imposes high in-plane flexural demand on the columns which may compromise frame stability (Figure 8.1b), similar to the response of K-bracing, a configuration prohibited for Types MD and LD CBFs. In MT-BFs, this undesirable behaviour is mitigated by introducing horizontal struts at every tier levels that can resist the expected unbalanced brace loads. After brace buckling, lateral seismic loads are entirely resisted up to full yielding of the tension braces by the truss mechanism formed by the braces, struts and columns, rather than by flexure of the columns.

Even if struts are present, brace tension yielding in MT-BFs tends to initiate and concentrate in a critical tier where the braces offer the lowest storey shear resistance. Plastic elongation of the

braces in this critical tier results in relatively larger tier drifts, which induces in-plane flexural demand on the columns (Figure 8.1c). This behaviour is expected in all MT-BFs, even if the bracing panels and braces are well proportioned to achieve uniform storey shear resistance over the frame height because of unavoidable variations in material properties, geometrical imperfections or boundary conditions that exits between tiers of as-built MT-BFs. The columns must therefore resist the axial compression combined with the bending moments induced by the non-uniform drift pattern. Concentration of inelastic deformations in the critical tier can also impose excessive ductility demand on the bracing members in that tier which, in turn, can cause premature failure of the braces (Figure 8.1c).

Special seismic provisions for MT-BFs have been introduced for the first time in the 2009 edition of CSA S16 (CSA 2009). Struts are required at every tier level and the columns must be designed for the combined axial load and bending moment induced assuming that brace tension yielding only develops in the critical tier. All possible critical tier scenarios must be examined. To limit tier drifts and brace ductility demand, MT-BFs in CSA S16-09 were only permitted for Type LD CBFs. Additionally, concomitant notional out-of-plane transverse loads were specified at brace-to-column intersecting points equal to 10% of the axial load carried by the compression members meeting at these points. These loads aimed at providing the columns with sufficient strength to resist out-of-plane forces due to initial geometric imperfections and brace out-of-plane buckling.

Additional studies have been performed on MT-BFs designed in accordance with CSA S16-09 (Imanpour et al. 2012b; Imanpour and Tremblay 2014a). In these studies, MT-BFs having up to 5 tiers and designed as Type MD were also investigated to examine the possibility of relaxing S16 seismic provisions. The studies confirmed the in-plane flexural demand on MT-BF columns. Drift concentration in critical tiers and column flexural demands were found to generally increase when increasing the number of tiers and the R_d factor. Although more severe, the seismic response of some of the Type MD frames was found acceptable. The studies finally showed that MT-BF columns experienced out-of-plane bending moments corresponding to that induced by notional loads equal to 0.4-0.8% of the compression axial forces in the columns at brace intersecting points, significantly lower than the 10% transverse notional load specified in CSA S16-09. In 2014, MT-BF provisions were modified to reflect these recent findings: MT-BFs are permitted to be used for Type MD braced frames with 2 or 3 tiers and for Type LD braced frames

up to 5 tiers. The notional out-of-plane load has been reduced to 2% of the column axial compression load below the brace-to-column intersecting point.

8.3 Seismic design of MT-BFs

8.3.1 Prototype building and design data

A single-storey industrial building with 102 m x 48 m plan dimensions is selected for this study. The building height, h_n, is 20 m and the spacing of the exterior columns, L, is 6 m. Lateral loads in each direction are resisted by four MT-BFs, two frames per exterior wall. The building is located on a class C site in Vancouver, BC. Three braced frames are examined in this study (Figure 8.3). The design of the 3-tiered Type MD frame of Figure 8.3a is examined first. The design of the two other frames is discussed later. The design earthquake loads were determined in accordance with NBCC 2015. The importance factor, I_E is equal to 1.0 and the factors R_d and R_o are 3.0 and 1.3 respectively. The building period is equal to 1.0 s, resulting in a design spectral acceleration (S) of 0.42 g. Using the equivalent static force procedure and accounting for accidental torsion, the storey shear per braced frame, V, is 389 kN including 14 kN notional load. The design roof dead load (D) and snow load (S) are equal to 1.2 and 1.64 kPa, respectively. The gravity induced column axial load is equal P_G = 232 kN for the load combination D + E + 0.25S. For this structure, the stability coefficient is less than 0.1 and P-delta effects are ignored.

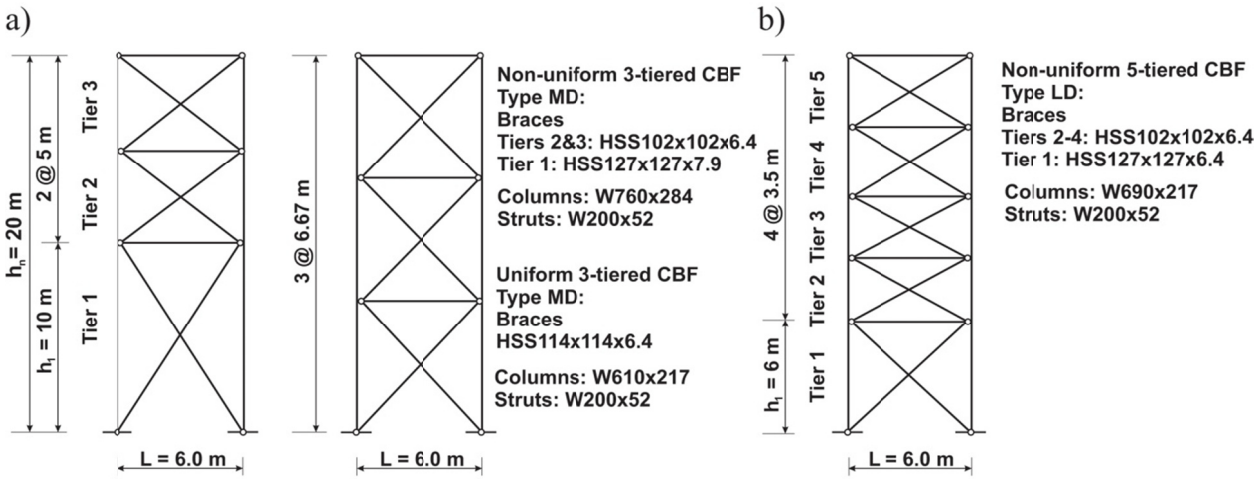

Figure 8.3: Three braced frames studied: a) Non-uniform and uniform 3-tiered Type MD CBFs; b) Non-uniform 5-tiered Type LD CBF.

8.3.2 Design of the braces

The braces in each tier are designed to resist in tension and compression the seismic storey shear, V. The resulting brace axial compression forces due to seismic and gravity loads are equal to 395 kN in Tier 1 and 259 kN in Tiers 2 and 3. The braces are designed for out-of-plane buckling in compression, assuming an effective length factor $K = 0.45$ for this X-bracing configuration. The braces were selected from ASTM A500, grade C, (F_y = 345 MPa) square HSS members satisfying CSA S16-14 brace slenderness and width-to-thickness ratios limit. The selected braces are shown in Figure 8.3a and their properties are given in Table 8.1. In the table, C_f and C_r are the brace factored compression loads and axial resistances, respectively. The probable brace tensile and compressive resistances determined with probable steel yield strength R_yF_y of 460 MPa are also given.

Table 8.1: Brace properties for the unifrom 3-tiered Type MD CBF.

Tier	HSS Braces	A mm^2	r_x mm	Kl/r	C_f kN	C_r kN	C_f / C_r	T_u kN	C_u kN	C'_u kN	V_u kN	V'_u kN
2&3	102x102x6.4	2170	38.6	91	259	326	0.80	998	479	200	1135	920
1	127x127x7.9	3390	48.3	109	395	401	0.98	1559	573	312	1097	963

8.3.3 Design of the struts

As required in CSA S16-14, horizontal struts are provided between the tiers. The most critical brace force condition for the struts is the second case of Figure 8.2a as shown in Figure 8.4a. A W200x52 is selected to resist maximum axial compression of 649 kN at Tier level 1. For uniformity, the same section is also used for the strut at Tier 2.

As discussed in the next section, the critical tier for this frame is Tier 1. If brace inelastic response is constrained to that tier, the loading condition of Figure 8.4a would not occur as the compression brace forces in Tiers 2 and 3 would remain equal to, or close to C_u = 479 kN instead of C'_u = 200 kN. This would result in a reduced axial compression of 439 kN in the strut at Tier level 1. For this frame, however, the difference in storey shear resistances between tiers is small

(less than 5% as discussed in the next section) and it is possible that the critical tier actually forms in Tier 2 or 3 due to variability in brace resistances along the frame height, which would result in strut compression forces equal to those obtained when considering C'_u in all tiers. For frames with nearly uniform storey shears, it is therefore advisable to consider the loading condition of Figure 8.4a for strut design.

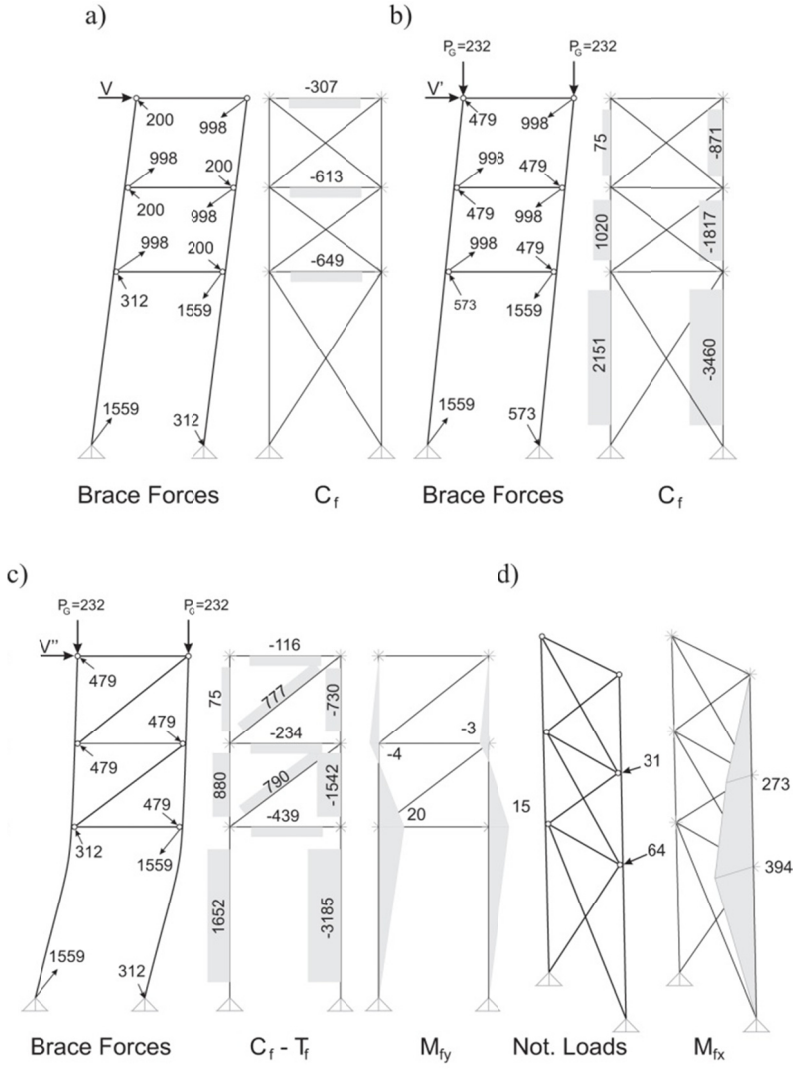

Figure 8.4: Seismic analysis of the non-uniform 3-tiered Type MD CBF: a) Axial compression in struts under loading condition with all compression braces in the post-buckling range; b) Axial column loads under gravity and brace loading condition with all compression braces at buckling; c) Axial loads and bending moments in columns from nonlinear static analysis assuming inelastic demand concentrated in Tier 1; and d) Out-of-plane bending moments due to transverse notional loads. (forces in kN, moments in kN-m)

8.3.4 Design of the columns

The building exterior columns are W shaped members continuous over the full frame height and oriented such that out-of-plane bending occurs about their strong axis. They are assumed pinned at their top and bottom ends for bending about both directions. The columns are first designed to resist the gravity loads plus the brace axial loads of the first brace force scenario of Figure 8.2a, as illustrated in Figure 8.4b. At brace buckling, the drifts are still small and bending moments in the columns can be ignored. The column segment in Tier 1 governs the design because it has the largest buckling length in the plane of the frame (10 m) and carries the highest axial compression (3460 kN). The column buckling length about strong axis is taken equal to 20 m. A W760x257 section is selected.

The column must then be verified for the additional loading condition for MT-BFs which accounts for a possible concentration of brace inelastic deformations in the critical tier. For this purpose, the critical tier is identified by comparing the horizontal storey shear resistances V_u provided by the braces when they develop their probable resistances T_u and C_u (Imanpour et al. 2012b). As shown in Table 8.1, Tier 1 is the weakest tier where brace tension yielding is expected to develop and cause inelastic tier drifts and degradation of the brace compressive strength from C_u to C'_u. The storey shear resisted by the braces in Tier 1 will therefore reduce from V_u to V'_u in Table 8.1, as determined with brace forces T_u and C'_u in that tier. This will diminish the force demand in the tension braces in the stronger Tiers 2 and 3, preventing brace tension yielding in these tiers, and subsequent frame inelastic deformations will therefore concentrate in Tier 1. The frame deformed shape and brace axial forces for this scenario are shown in Figure 8.4c. As specified in CSA S16, member forces and deformations are determined when the roof displacement reaches the anticipated deflection including inelastic effects, i.e. $\delta_{roof} = R_d R_o \delta_e / I_E$, where δ_e is the elastic roof lateral deflection under the design seismic force. For this frame, δ_e is 32 mm and δ_{roof} = 125 mm.

Column forces at this target displacement can be obtained from a nonlinear incremental static (pushover) analysis. This however requires explicit modelling of the inelastic response of the braces in tension and compression, including brace buckling and subsequent degradation of the compression strength under cyclic loading (Imanpour and Tremblay 2014b). Such models often cause convergence difficulties and are not readily available in commercially available structural

analysis programs. For MT-BF design, it is more convenient to perform a static analysis with a model in which the bracing members that have reached their probable resistances are removed and replaced by axial forces corresponding to their probable resistances. This technique is illustrated in Figure 8.4c. Braces in the critical Tier 1 are replaced by forces T_u = 1559 kN and C'_u = 312 kN. In Tiers 2 and 3, the compression braces are replaced by forces C_u = 479 kN. Truss elements are kept in the model for the tension braces in Tiers 2 and 3 as these members are still elastic. Static analysis is performed by imposing the gravity loads plus a horizontal displacement of 125 mm at the roof level. In Figure 8.4c, brace tension loads in Tiers 2 and 3 are obtained from this analysis, as well as in-plane shears and bending moments in the columns. As anticipated, tension brace loads of 790 and 777 in Tiers 2 and 3 are smaller than T_u = 998 kN. The analysis gives factored axial compression C_f = 3183 kN and in-plane (weak axis) moment M_{fy} = 15 kN-m in the bottom tier column segment under compression. Second order effects should be included in this analysis but were not included here to ease understanding the relationship between bending moments and forces.

As discussed earlier, the columns must also resist concomitant strong axis bending moments due to transverse out-of-plane notional loads. In Figure 8.4d, these loads induce a moment M_{fx} = 394 kN-m for the verification of the column segment in Tier 1. Under this loading condition, the initially selected columns must be increased to W760x284. The frame lateral deflection is influenced by the column size and the nonlinear response shown in Figure 8.4c depends on the column in-plane flexural stiffness. With the revised W760x284 columns, δ_{roof} reduces from 125 to 121 mm and the analysis is redone by imposing this roof lateral displacement. In Tier 1, C_f in the column becomes 3186 kN and M_{fy} is augmented to 17 kN-m. The moment M_{fx} remains unchanged and W760x284 section is found be adequate to resist these revised actions. The analysis also shows that the drift in critical Tier 1 is 68 mm (0.68%) when δ_{roof} is 121 mm. Although not required in S16, the engineer should verify if this drift is acceptable. In this example, the height of the critical tier is relatively high, which resulted in moderate tier drift and column in-plane demand. As discussed below, more severe situations can be encountered for other critical tier scenarios or frame geometries.

In lieu of the above static analysis, column moments can be estimated using the three-moment equation with the anticipated frame deformation pattern at the target storey displacement. In the

non-yielding tiers, the tier relative lateral deformation Δ_i when brace yielding develops in the critical tier can be obtained from:

$$\Delta_i = \Delta_{e,i}\frac{V'_{u,cr}}{V} + \frac{V'_{u,cr} - 2C_u\cos\theta_i}{\left(2EA\cos^3\theta_i\right)/L} \quad (1)$$

where θ is the angle of the braces from horizontal, E and A are the Young's modulus of elasticity and the brace cross-sectional area, respectively, $V'_{u,cr}$ is the storey shear resistance provided by the braces in the critical tier for the post-buckling brace condition, and Δ_{ei} is the tier lateral deformation under the lateral load V. The deformation of the critical tier is obtained by removing the sum of the Δ_i values of non-yielding tiers from the roof displacement δ_{roof}. The displacements at tier levels defining the frame deformation pattern are then obtained using these tier lateral deformations (Figure 8.5a). For the frame example: δ_1 = 70 mm, δ_2 = 95 mm, and $\delta_3 = \delta_{roof}$ = 121 mm. In-plane bending moments in the columns are then computed using the classical three-moment equation developed for determining bending moments in continuous beams on multiple supports subjected to relative support settlements. For a 3-tiered frame, this gives the following two equations that can be solved for M_{fy1} and M_{fy2}:

$$2M_{fy1}\left(h_1+h_2\right) + M_{fy2}h_2 = \frac{6EI_c\left(\delta_1\right)}{h_1} - \frac{6EI_c\left(\delta_2-\delta_1\right)}{h_2} \quad (2)$$

$$M_{fy1}h_2 + 2M_{fy2}\left(h_2+h_3\right) = \frac{6EI_c\left(\delta_2-\delta_1\right)}{h_2} - \frac{6EI_c\left(\delta_3-\delta_2\right)}{h_3} \quad (3)$$

In these equations, EI_c is the flexural stiffness of the column. The remaining parameters are shown in Figure 8.5a. For the frame example with the W760x284 columns and the calculated deformation pattern, the moments M_{fy1} and M_{fy2} are respectively equal to 23 and = 7 kN-m, which compares well with those obtained from the frame analysis.

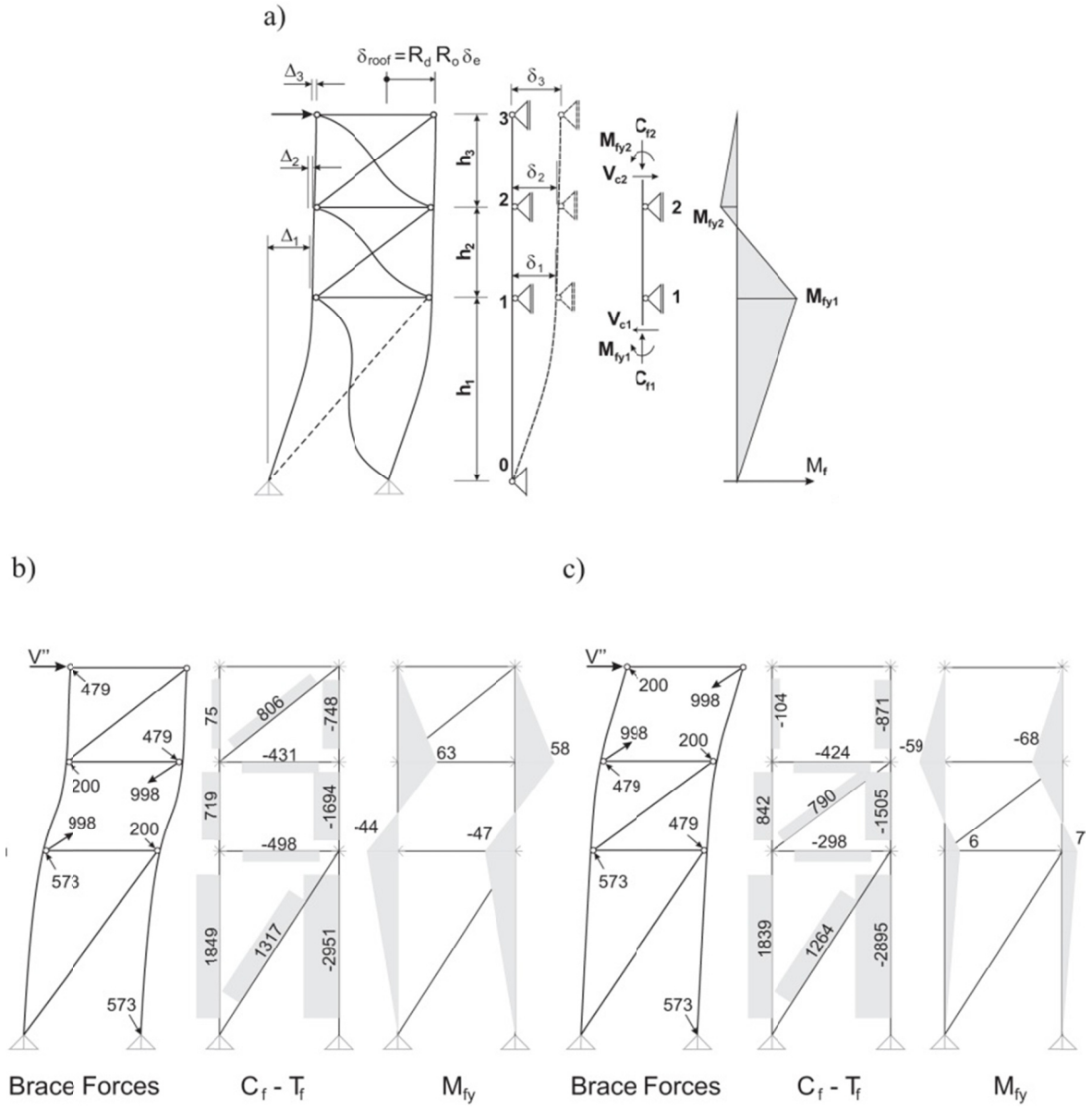

Figure 8.5: a) Calculation of the in-plane flexural demand on the column using three-moment equation; b) Nonlinear response of the non-uniform 3-tiered Type MD CBF for critical Tier 2; and c) Nonlinear response of the non-uniform 3-tiered Type MD CBF for critical Tier 3.

8.3.5 Alternative critical tier scenarios

In the previous section, column design was performed assuming critical Tier 1. In Table 8.1, V_u in Tiers 2 and 3 (1135 kN) is close to V_u in Tier 1 (1097 kN) and the critical tier could be either Tier 2 or Tier 3 when considering that the actual brace resistances in the as-built frame may differ

from the probable values in Table 8.1. Therefore, these other potential critical tier scenarios must also be investigated when verifying the columns, which can be done by slightly reducing the brace resistances in a tier until it becomes the weakest. In Figure 8.5b, results from static analysis are shown for the case where Tier 2 becomes critical by reducing the brace strengths by 5% in that tier. In the analysis, both braces in Tier 2 and the compression braces in Tiers 1 and 3 are replaced by their probable actions and a roof displacement of 121 mm is imposed together with gravity loads. The final W760x284 columns were used in the analysis. The computed forces in the tension braces in Tiers 1 and 3 do not exceed T_u in these tiers, confirming the possibility of the critical Tier 2 scenario. For this loading condition, C_f is smaller (2951 kN) in the lower column segment but the moment M_{fy} has increased from 17 to 47 kN-m when compared to critical Tier 1 scenario. The drift in Tier 2 is 0.85%, larger than in the previous scenario. Similarly, the frame response and member forces when Tier 3 is critical are presented in Figure 8.5c. These two scenarios result in larger moments M_{fy} near Tier 2 level but the axial compression is smaller in the second tier.

For this frame example, critical Tier 1 scenario controlled column design but this may not be the case for another frame and all likely critical tier scenarios must be investigated to ensure adequate seismic response. In view of the variations in brace yield strengths and brace compression strength predictions, it is suggested that alternative critical tier scenarios should be investigated when V_u in a tier is within 1.1 to 1.15 times the minimum V_u. When selecting critical tier, one may consider that: in shorter tiers, columns have relatively higher flexural stiffness and attract larger moments; column stability is generally more critical in taller tiers because of the longer in-plane buckling lengths; axial compression is maximum in bottom column segments and is typically larger when the critical tier is the bottom tier as compression braces in the other tiers resist loads equal to C_u; and braces in shorter critical tiers generally are more prone to failure because they have shorter length to accommodate frame inelastic deformations.

8.3.6 Other frame configurations

The above analysis and design approach was adopted for the 3-tiered Type MD braced frame with identical tiers and the 5-tiered Type LD irregular frame of Figure 8.3. For the 3-tiered frame, three critical tier scenarios were examined to design the columns. The critical Tier 1 scenario was the most severe. It resulted in larger moments M_{fy} (= 28 kN-m) compared to the non-uniform 3-

tiered frame because of the shorter tier height. The concomitant axial load and out-of-plane moment in Tier 1 were 3144 kN and 355 kN-m respectively. Due to shorter buckling length about weak axis (6.667 m), a smaller W610x217 column section was needed to satisfy the column strength and stability requirements. The anticipated roof deflection was δ_{roof} = 127 mm and the critical Tier 1 drift was found equal to 0.87%, larger than for the non-uniform 3-tiered frame because the frame inelastic deformations are concentrated in a shorter tier.

For the Type LD 5-tiered braced frame, a larger design seismic load V = 577 kN was used because of the lower value for R_d (= 2.0). Five critical tier scenarios were considered to obtain the in-plane bending demands and verify the columns. Column design was governed by the critical Tier 1 scenario triggered by reducing the brace strength in Tier 1 by 7%. For this case, the columns in Tier 1 had to resist the combined forces C_f = 3416 kN, M_{fy} = 15 kN-m, and M_{fx} = 612 kN-m and a W690x217 section was selected. The critical Tier 1 drift reached 0.73% with δ_{roof} = 125 mm. For this frame, a larger 1.01% drift was predicted in Tier 2 for the critical Tier 2 scenario.

8.4 Seismic response of MT-BFs

8.4.1 Numerical model and ground motions

Nonlinear Response History (NLRH) analysis was performed using the numerical model shown in Figure 8.6 to study the in-plane response of the prototype MT-BFs. The model was created using the *OpenSees* program 2.4.2 (McKenna and Fenves, 2004). In this model, columns and braces are modeled with fiber discretization of the cross-section using the force-based beam-column element. Past studies have shown that this model can reproduce adequately inelastic flexural buckling response under cyclic loading for HSS bracing members (Aguero et al. 2006; Uriz et al. 2008) and I-shaped columns (Lamarche and Tremblay 2011). The uniaxial Steel02 material model was selected to account for Baushinger effect as well as isotropic and kinematic strain hardening behaviour. The material was defined with E = 200 GPa, and yield strengths F_y of 345 MPa for the columns and struts and 460 MPa for the braces. Residual stresses were included in the model for the columns. Buckling of braces and columns was simulated by dividing each member into ten elements and using a co-rotational formulation to account for geometric nonlinearities. The braces were assigned an initial sinusoidal imperfection corresponding to their first out-of-

plane buckling mode shape with a maximum amplitude of 0.001 times the buckling lengths. For the columns, bi-directional initial sinusoidal out-of-straightness corresponding to the first in-plane and out-of-plane buckling modes was considered as shown in Figure 8.6. Defect amplitudes were set equal to $h_n/1000$ and $h_i/1000$ for out-of-plane and in-plane buckling, respectively, where h_i represents the tier heights. The columns were pinned at their bases. Nonlinear rotational springs with strength and stiffness properties representing the rotational response of the brace gusset plates under out-of-plane buckling of the braces were assigned at the ends of the continuous bracing members and discontinuous brace segments. The struts were modeled using elastic beam-column elements. Rigid elastic truss and beam-column elements were used to reproduce connection sizes.

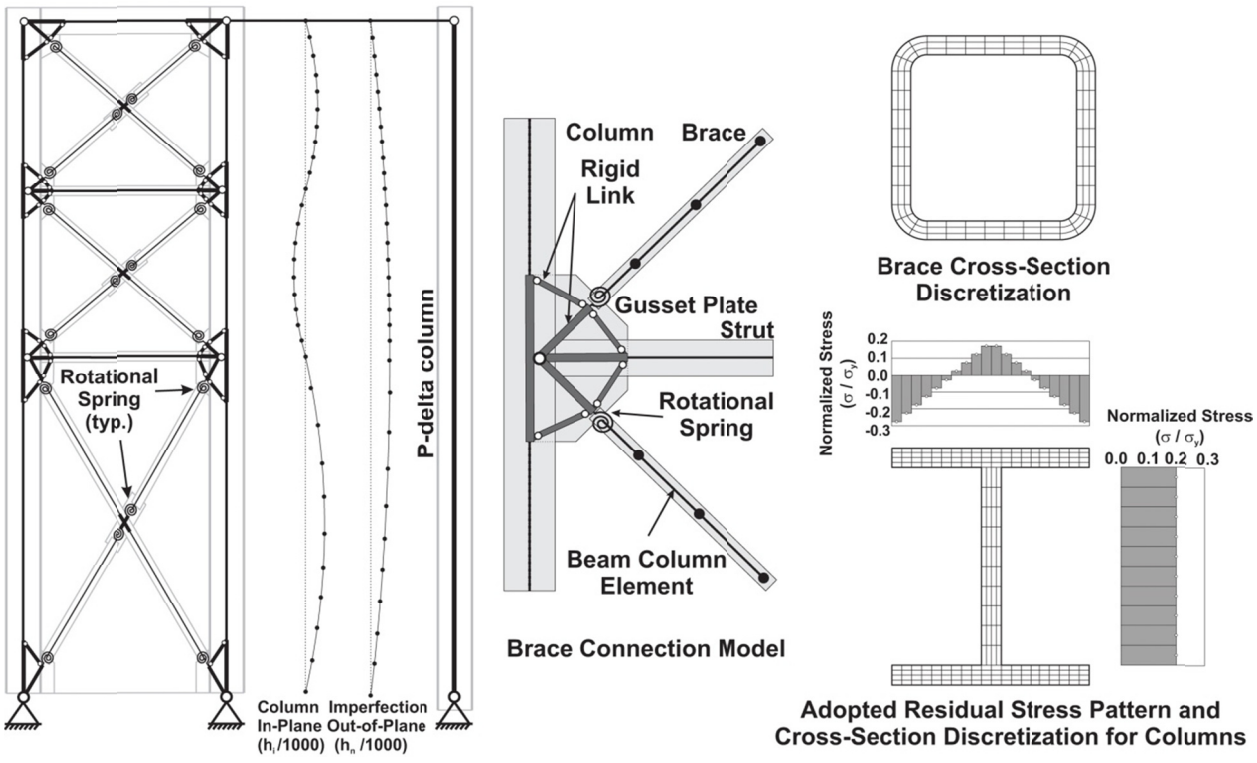

Figure 8.6: Finite element model of the 3-tiered braced frame.

Gravity loads were applied to the columns and the model also included a P-delta column represented by a co-rotational truss element that carried the remaining frame tributary gravity loads. Point

masses representing the frame tributary seismic weight were applied at top of the columns. Rayleigh mass proportional damping equal to 2% of critical in the first mode of vibration was used to model the inherent damping of the building. A group of 21 ground motions were selected and scaled to match, on average, the NBCC design spectrum for Vancouver using the method presented in Dehghani and Tremblay (2015).

8.4.2 In-Plane seismic response

The 50th (median) and 84th percentile values of peak response parameters from the 21 ground motions are presented in Table 8.2 for the three prototype structures. The 5-tieredframe is discussed at the end of the section. For the non-uniform 3-tiered Type MD frame, the NLRH analyses were performed twice: 1) with R_yF_y = 460 MPa for all braces, and 2) with 0.95 R_yF_y = 437 MPa for the braces in Tier 3 to create a critical Tier 3 scenario. In the table, the values in brackets are the results from the second analysis. For the uniform 3-tiered frame, a reduced yield strength of 437 MPa was assigned to the braces in Tier 1 to intentionally initiate brace yielding in that tier. In the three cases, the frames exhibited stable response without column buckling under any of the ground motion records. Median peak storey drifts are close to the anticipated roof drift ($R_dR_o\delta_e$). The peak drifts induced in the critical tiers are larger than the roof drifts, confirming non-uniform drift demands along frame heights and concentration of inelastic deformations in critical tiers. This behaviour is reflected by the drift ratio, which compares the maximum critical tier drift to the storey drift. The uniform 3-tiered frame experienced larger critical tier drifts than its non-uniform counterpart due to a shorter critical tier. The same observation can be made between the critical Tier 3 and critical Tier 1 scenarios for the non-uniform frame. In Table 8.2, median in-plane bending demands in the columns (M_{cy}) are also well predicted for the two 3-tiered frames. In Figure 8.7a, peak frame lateral displacement and column bending moment envelopes from the individual ground motion records are given together with median values for the non-uniform 3-tiered frame. An excellent match is observed between the median NLRH analysis results and design predictions for both critical tier scenarios.

Among the applied ground motions, those imposing larger storey drifts also induce more pronounced deformations in the critical tiers and, thereby, larger flexural demands on the columns. This trend is confirmed when comparing 84th and 50th percentile results in Table 8.2: the differences between the two sets of values are more pronounced for the critical tier drift and

tier drift ratio compared to those observed for the storey drifts. This was expected as additional frames lateral deformations induced by the more severe ground motions tend to concentrate in the critical tiers. As a result, the 84th percentile bending moments significantly exceeded the values considered in design, with NLRH/design ratios reaching 2.75, 1.84 and 2.83 for the three cases. Although column instability was not observed in the analyses, such large bending moments should probably be accounted for in design by using larger storey drifts. The proposed method was found adequate to predict this higher demand. For instance, for the non-uniform 3-tiered CBF with Tier 1 critical, the method predicts a drift and a column moment in the critical tier equal to 1.0% and 0.06 M_{py}, respectively, if the 84th percentile storey displacement obtained from NLTH analysis is used in the frame analysis. These two values match well the corresponding 84th percentile NLRH analysis results (0.93% and 0.06 M_{py}) in Table 8.2.

Table 8.2: MT-BFs studied: Statistics of peak frame response from NLRH analyses.

Frame	**Non-uniform 3-tiered Type MD CBF**		**Uniform 3-tiered Type MD CBF**		**Non-uniform 5-tiered Type LD CBF**	
Parameter	**50th**	**84th**	**50th**	**84th**	**50th**	**84th**
Total storey drift (%)	0.63 [0.63]	0.77 [0.77]	0.63	0.80	0.56	0.74
$\delta_{roof,}$NLRH / R_d R_o δ_e	1.04 [1.04]	1.27 [1.28]	1.00	1.26	0.90	1.19
Critical tier drift (%)	0.68 [0.81]	0.93 [1.19]	0.77	1.27	0.85	1.30
Critical tier drift (NLRH / design)	1.00 [0.87]	1.37 [1.28]	0.89	1.50	0.66	1.01
Drift ratio	1.06 [1.29]	1.21 [1.51]	1.19	1.58	1.48	1.77
Column moment in Tier	1[2]	1[2]	1	1	4	4
$M_{cy,NLRH}$ / M_{py}	0.03 [0.10]	0.06 [0.16]	0.06	0.15	0.10	0.22
$M_{cy\text{-}NLRH}$ / $M_{cy\text{-}design}$	1.15 [1.15]	2.75 [1.84]	1.13	2.83	0.53	1.16

The analysis of the non-uniform 5-tiered Type LD frame was performed using reduced R_yF_y = 437 MPa in Tier 5 to reproduce the critical tier scenario considered in design that induced maximum moments at Tier 4 level. As expected from the lower R_d value used in design, limited inelastic response took place in the braces; nevertheless, as indicated in Table 8.2, inelastic drifts concentrated in Tier 5 and the largest bending moments developed at Tier 4 level, as anticipated. Critical tier drifts and tier drift ratios are similar to those observed for the 3-tiered frames, which indicates that

restricting 4- and 5-tiered frames to the Type LD CBF category, as specified in CSA S16-14, is an adequate means of achieving consistent frame response for this system. In counterpart, median column flexural demands for this frame are less than predicted in design. This is because brace compressive resistances under seismic motions in the NLRH analysis did not exactly correspond to values C_u and C'_u assumed in design, and brace yielding in fact also developed in identical Tier 4, which resulted in a smoother deformation pattern and reduced column bending. This shows that, the assumption made in S16 that inelastic deformations are limited to a single tier over the storey height may lead to conservative bending moment estimates for such frames with multiple identical tiers. As discussed in the next section, this assumption may not be valid for tall MT-BFs designed for more ductile response and an alternative design method is proposed that more closely reflects the actual frame response.

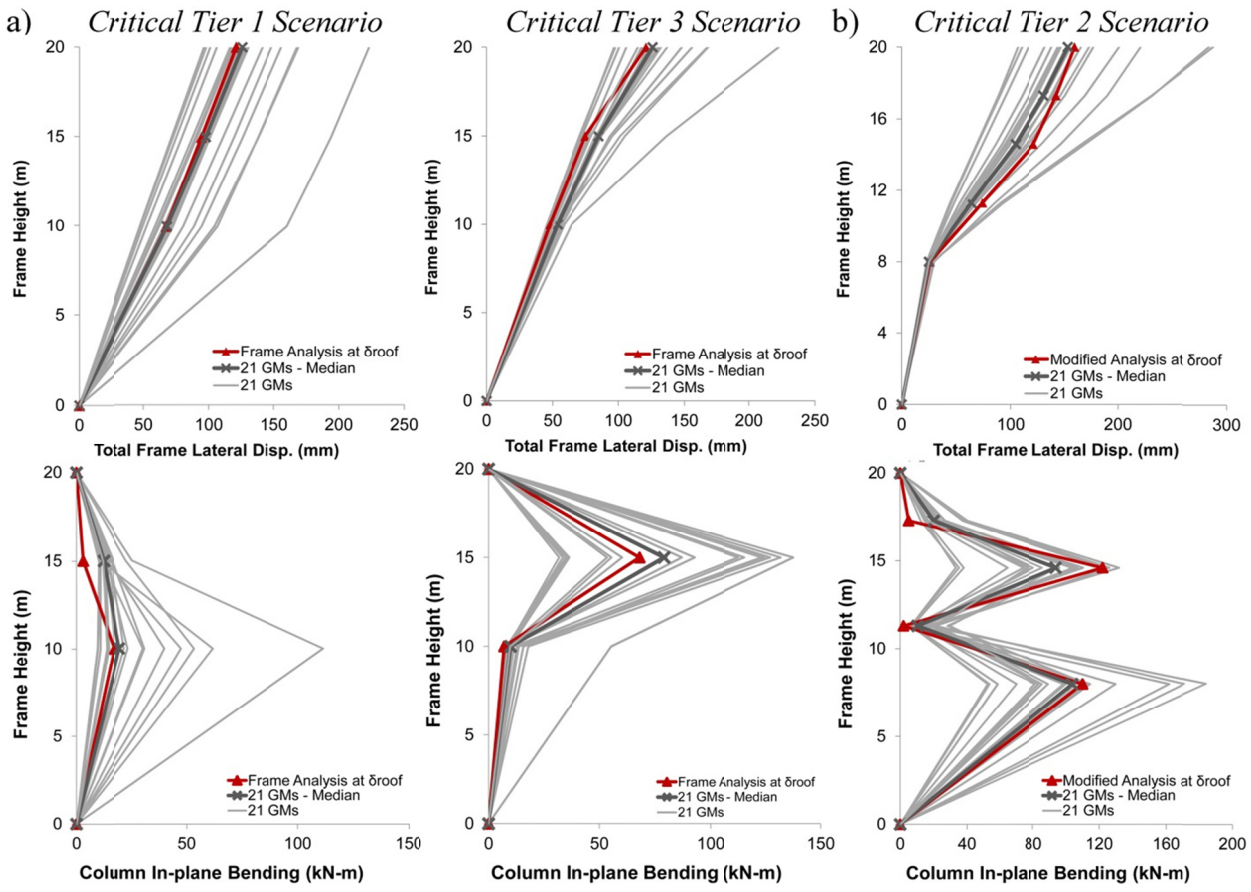

Figure 8.7: Frame lateral displacement and column in-plane bending demands for a) 3-tiered Type MD CBF; and b) 5-tiered Type MD CBF.

8.5 Alternative design method for tall type MD CBFs

In CSA S16, limits are specified on the number of tiers to prevent excessive tier drifts and brace ductility demand in MT-BFs. Taller frames may be needed for some building applications and an alternative design method is introduced in this section for such frames. The method is illustrated for the 5-tiered Type MD frame with non-uniform tier heights shown in Figure 8.8a. The frame exceeds the 3-tier limit of CSA S16-14. It is first designed in accordance with current S16 provisions assuming that brace tension yielding develops only in one tier. The design is then revised to reflect the actual frame response.

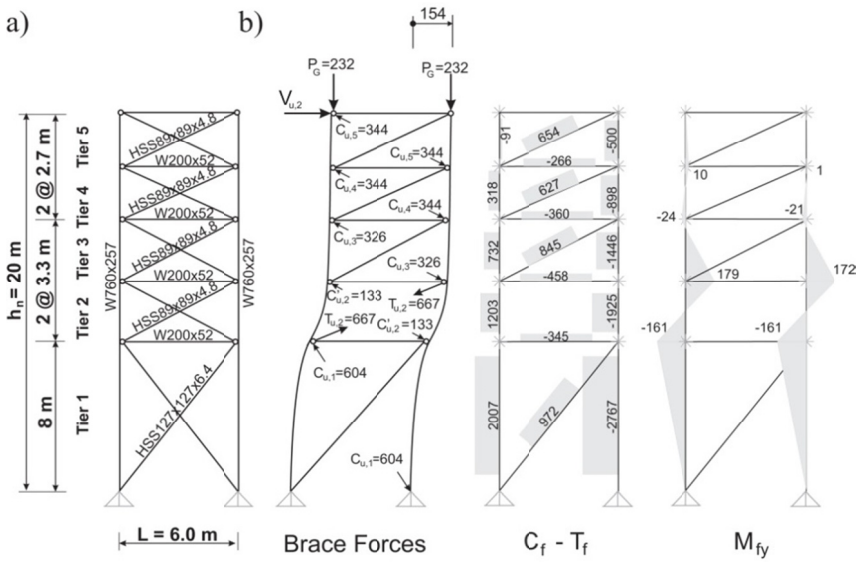

Figure 8.8: 5-tiered Type MD CBF: a) Configuration and member sizes; b) Brace forces, axial loads and bending moments from nonlinear static analysis assuming inelastic demand concentrated in Tier 2. (forces in kN, moments in kN-m, displacement in mm)

For this frame, V = 389 kN and two brace sizes are used over the frame height: HSS127x127x6.4 in Tier 1 and HSS 88.9x88.9x4.8 in Tiers 2 to 5. The resulting probable shear resistances V_u are 1127 kN for Tier 1, 870 kN for Tiers 2 and 3, and 922 kN for Tiers 4 and 5. Four critical tier scenarios (2 to 5) were therefore studied and W760x257 columns were selected based on the critical Tier 2 scenario. Final design forces for this case are shown in Figure 8.8b for δ_{roof} = 154 mm. For this brace loading scenario, Tier 2 drift reaches 1.47% and Tier 1 columns must resist the combined forces C_f = 2767 kN, M_{fx} = 515 kN-m, and M_{fy} = 161 kN-m.

As shown in Figure 8.8b, the brace axial force in Tier 3 is 845 kN, which exceeds T_u = 667 kN for HSS 88.9x88.9x4.8 braces. This indicates that brace tension yielding in that tier will also initiate before the roof displacement reaches the anticipated value, contrary to the assumption of brace yielding in only one tier implicit in the CSA S16 seismic provisions. The analysis procedure must therefore be modified to account for the expected propagation of brace yielding along the frame height as illustrated in Figure 8.9a. This is done by performing successive analysis steps corresponding to initiation of brace yielding in the frame until the anticipated storey drift is attained.

This first analysis step is performed with the initially designed W760x257 columns and the results are shown in Figure 8.9b. In this analysis, it is found that a roof drift of 120 mm is required to reach a brace tension force equal to T_u = 667 kN in Tier 3, which gives the column axial forces and bending moments shown in Figure 8.9b. Using these values together with the out-of-plane bending moments from notional loads reduced the column size to W690x217. This first analysis step is redone with this new section to obtain consistent forces and moments at brace yielding initiation in Tier 3. It is found that brace yielding occurs at a roof displacement equal to 128 mm and the W690x217 columns are sufficient to resist the corresponding demands. For the second analysis step, the tension brace in Tier 3 is removed from the model and replaced by T_u and a roof displacement equal to δ_{roof} = 160 mm predicted with the W690x217 columns is applied. As shown in Figure 8.9c, this results in brace tension forces of 605 and 498 kN in Tiers 4 and 5, less than T_u = 667 kN in these tiers, and 729 kN in Tier 1, also less than T_u = 1274 kN in that tier. This shows that no further brace yielding is expected when the frame attains the anticipated storey drift and the analysis is halted at this step. Comparing the brace tension forces to T_u in each tier reveals that brace tension yielding would occur in Tier 4 if the frame drift was to exceed $R_d R_o \delta_e$. The selected W690x217 columns are found sufficient to resist the forces induced in this second analysis step. Compared to the results shown in Figure 8.8b, column bending moments in both steps are reduced because brace yielding develops in two tiers instead of only one, which gives smaller column flexural deformations. Column axial compression forces also diminished under the more realistic brace forces considered in the modified analysis method. Drifts are expected to reach 1.47 and 1.44% in Tiers 2 and 3 respectively. At this point, if needed, the column stiffness could be increased to reduce tier drift by triggering yielding in a third tier.

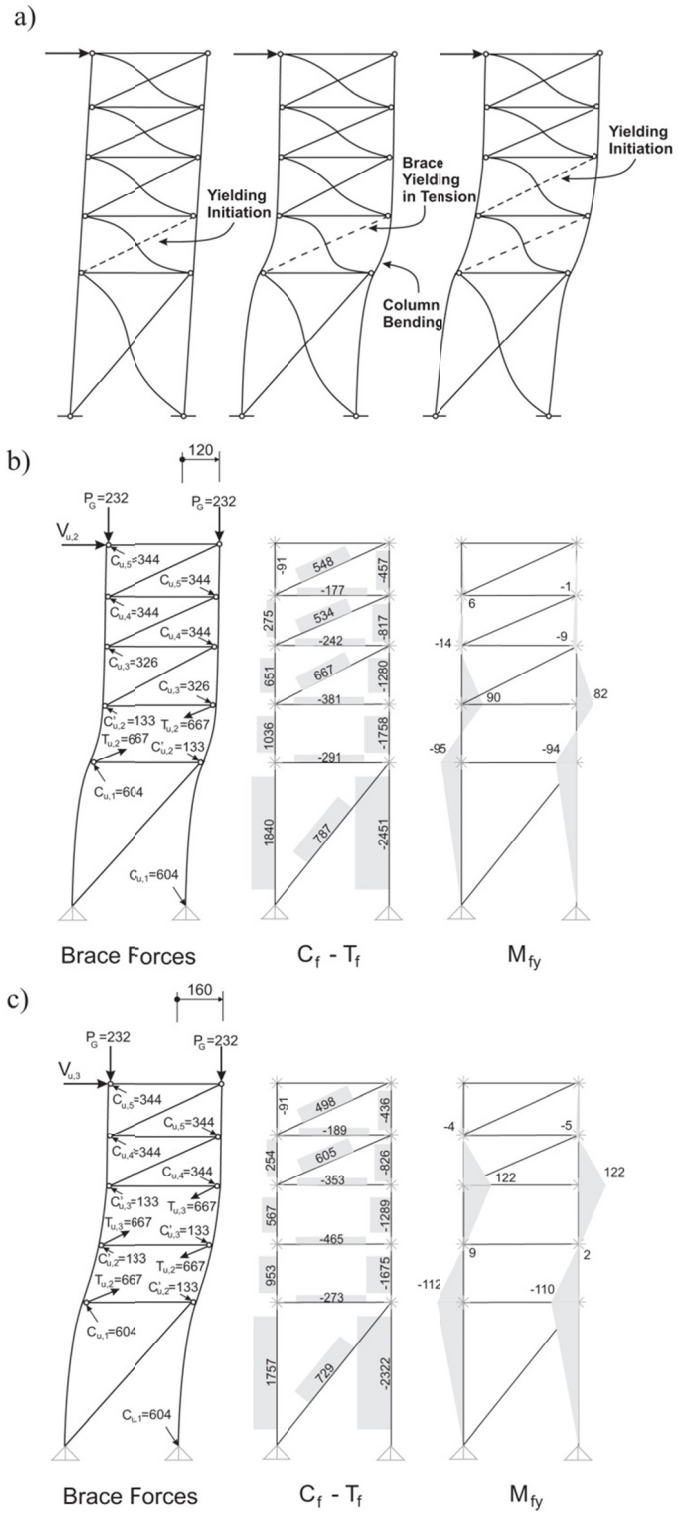

Figure 8.9: a) Progressive brace yielding for a 5-tiered CBF; b) Modified analysis for 5-tiered Type MD CBF at brace tension yielding in Tier 3 (Analysis 1); and c) Modified analysis for 5-tiered Type MD CBF at anticipated storey drift (Analysis 2). (forces in kN, moments in kN-m, displacement in mm)

NLRH analysis of this frame was performed under the same suite of ground motions and considering 5% reduction in brace yield strength in Tier 2 to replicate the governing design conditions. No column instability occurred in the analyses and statistics of the response are given in Table 8.3, including the range of values obtained in NLRH analysis. As shown, the NBCC storey drift lies between the median and 84th percentile analysis results. In Figure 8.7b, very good agreement is observed between design frame lateral deformations and median time history displacement values. As predicted in design, inelastic brace deformations distributed between Tiers 2 and 3. As also expected from the frame analysis and as was observed in the 5-tiered Type LD frame, brace tension yielding also extended to Tier 4 and even Tier 5 under the stronger ground motions, which resulted in more uniform tier drift response in the top 4 tiers. Median peak drifts in Tiers 2 and 3 are therefore smaller than obtained from frame analysis but the 84th percentile values are close to the design predictions. The ratio of NLRH analysis to design column in-plane bending demand is close 1.0 in Tiers 1 and 3, confirming the appropriateness of the modified analysis procedure for flexural demand. Lesser than expected bending demand was induced at Tier 2 level, which is attributed to the fact that brace tension yielding took place nearly simultaneously in Tiers 2 and 3 in the NLRH analysis, with less dissimilar compression brace force conditions between the two tiers compared to design assumptions. However, the good match in moments at Tiers 1 and 3 show that design conditions in fact develop when differences in brace resistances is sufficient to delay or prevent brace tension yielding in subsequent tiers.

This example shows that the proposed analysis/design method accounts for the progression of brace yielding that characterizes the seismic response of tall MT-BFs with a large number of tiers. The method results in smaller column bending moment demands compared to currentS16 method, which may translate in smaller steel tonnage. The method can also be used to control the frame response by selecting column sections required to develop the required number of yielding tiers so that tier drifts remain within acceptable limits over the frame height.

Table 8.3: Statistics of peak frame response from NLRH analyses for frame designed according to the proposed method.

Frame	**Non-uniform 5-tiered Type MD CBF**		
Parameter	**50th**	**84th**	**range**
Total storey drift (%)	0.72	0.92	(0.49 – 1.33)
$\delta_{roof,NLRH}$ / R_d R_o δ_e	0.91	1.15	(0.61 – 1.66)
Tier 3 drift (%)	1.22	1.64	(0.73 – 2.31)
Tier 3 drift (NLRH / design)	0.85	1.14	
Tier 2 drift (%)	1.16	1.44	(0.65 – 1.96)
Tier 2 drift (NLRH / design)	0.79	0.98	
Tier 1 drift (%)	0.31	0.33	(0.29 – 0.37)
Drift ratio	1.69	1.77	(1.44 – 1.80)
$M_{cy,NLRH}$ / M_{py} (Tier 3)	0.17	0.20	(0.06 – 0.24)
$M_{cy\text{-}NLRH}$ / $M_{cy\text{-}design}$ (Tier 3)	0.77	0.90	
$M_{cy,NLRH}$ / M_{py} (Tier 2)	0.02	0.04	(0.01 – 0.05)
$M_{cy\text{-}NLRH}$ / $M_{cy\text{-}design}$ (Tier 2)	0.13	0.27	
$M_{cy,NLRH}$ / M_{py} (Tier 1)	0.19	0.23	(0.09 – 0.33)
$M_{cy\text{-}NLRH}$ / $M_{cy\text{-}design}$ (Tier 1)	0.95	1.15	

8.6 Conclusions

Seismic design provisions of CSA S16 for multi-tiered braced frames were presented and illustrated for three prototype multi-tiered X-braced frames. A simple computer-based static analysis method was proposed to determine column design forces and tier drifts consistent with CSA S16. NLRH analysis was performed to examine the seismic behaviour of the prototype frames and validate CSA S16 provisions. The proposed analysis method was modified for the design of tall MT-BFs in which brace tension yielding is expected to propagate in more than one tier. A 5-tiered CBF example was used to illustrate this alternative method and the frame response was examined through NLRH analysis. The main conclusions are summarized as follows:

- The proposed computer-based analysis methods can be used to analyze and design MT-BFs with uniform or non-uniform properties and frames where brace inelastic deformations distribute in several tier.
- Response history analysis showed that frames complying with CSA S16 limitations develop brace tension yielding essentially in one tier without excessive tier drifts. The seismic induced

column in-plane flexural bending demand can be well predicted when applying CSA S16 requirements.

- The study showed that multiple critical tier scenarios, resulting in different tier drift and force demands, may develop in MT-BFs and must be considered in design.
- Seismic force and deformation demands from NLRH analysis were well predicted by the proposed analysis methods. For the frame exceeding the CSA S16 limits on number of tiers, the frame actual inelastic response, including the sequence of brace tension yielding, was properly tracked by the proposed modified method.
- Allowing brace tension yielding in more than one tier can lead to more economical column designs compared to current CSA S16 provisions.
- In-plane moment demand on the columns was found to be sensitive to the storey drifts assumed in design. Representative storey drift estimates should therefore be used to avoid underestimating moments in columns.

The proposed methods can be used as tools to control the frame response by selecting frame configuration, bracing members, and/or column sections to achieve desired seismic performance. The design procedure only addresses in-plane seismic response. Future studies should investigate the appropriateness of the current out-of-plane notional loads as specified in CSA S16 and examine column stability under coupled in-plane and out-of-plane flexural demands.

Acknowledgments

Funding from the Natural Sciences and Engineering Research Council (NSERC) of Canada is acknowledged.

References

Aguero, A., Izvernari, C., and Tremblay, R. 2006. Modelling of the Seismic Response of Concentrically Braced Steel Frames using the OpenSees Analysis Environment, Int. J. of Advanced Steel Construction, 2(3): 242–274.

CSA. 2009, 2014. CSA S16-09, CSA S16-14, Design of Steel Structures, Canadian Standards Association, Mississauga, ON.

Dehghani M., and Tremblay R. 2015. Robust Period-Independent Ground Motion Selection and Scaling for Effective Seismic Design and Assessment, Journal of Earthquake Engineering, in press.

Imanpour, A., Tremblay, R., and Davaran, A. 2012a. Seismic performance of steel concentrically braced frames with bracing members intersecting columns between floors. In Proceedings of the 7th STESSA Conference, Santiago, Chile, pp. 447–453.

Imanpour, A., Tremblay, R., and Davaran, A. 2012b. Seismic Evaluation of Multi-Panel Steel Concentrically Braced Frames. In Proceedings of the 15WCEE, Lisbon, Portugal, Paper No. 2996.

Imanpour, A., and Tremblay, R. 2014a. Seismic performance evaluation and design of multi-tiered steel concentrically braced frames. In Proceedings of the 10th National Earthquake Engineering Conf., Anchorage, AK, Paper No. 1347.

Imanpour, A., and Tremblay, R. 2014b. Seismic design of steel multi-tiered braced frames: Application of incremental static analysis for design of steel multi-tiered braced frames. In Proceedings of Eurosteel 2014, Naples, Italy, Paper No. 688.

Imanpour, A., Tremblay, R., Davaran, A., Stoakes, C., and Fahnestock, L. 2015. Seismic Performance Assessment of Multi-Tiered Steel Concentrically Braced Frames Designed in Accordance with Current AISC Seismic Provisions. Submitted to J. Struct. Eng., ASCE.

Lamarche, C.P., Tremblay, R. 2011. Seismically induced cyclic buckling of steel columns including residual-stress and strain-rate effects. J. of Constr. Steel Res., 67: 1401–1410.

McKenna, F. and Fenves, G.L. 2014. Open System for Earthquake Engineering Simulation (OpenSees). Pacific Earthquake Engineering Research Center (PEER), University of California, Berkeley, CA. (http://opensees.berkeley.edu/)

NRCC. National Building Code of Canada 2016, 14th ed. National Research Council of Canada, Ottawa, ON, 2016.

Uriz, P., Filippou, F.C., Mahin, S.A. 2008. Model for cyclic inelastic buckling for steel member. J. Struct. Eng., ASCE, 134(4): 619–628.

Symbols

A	Brace cross-sectional area
C_f	Factored compression axial load

C_r	Brace factored compression axial resistance
C_u	Probable compressive strength
C'_u	Probable post-buckling compressive strength
D	Dead load
E	Seismic load
E	Young's modulus
EI_c	Flexural stiffness of the column
F_y	Yielding strength
h_i	Tier height
h_n	Building height
I_E	Importance factor
K	Effective length factor
L	Spacing of the exterior columns
M_{cy}	Column in-plane weak-axis bending moment
M_{fyi}	Column in-plane (weak-axis) factored moment at Tier i
M_{fxi}	Column strong-axis factored moment at Tier i
M_{py}	Column weak-axis plastic moment
P_G	Gravity induced column axial loads
R_d	Ductility-related force modification factor
R_o	Overstrength force modification factor
r_x	Brace radius of gyration
R_yF_y	Probable steel yield strength
S	Snow load
S	Design spectral acceleration

T_u	Probable tensile strength
V	Design storey shear
V_u	Horizontal storey shear resistances provided by the braces when they develop their probable resistances T_u and C_u
V'_u	Horizontal storey shear resistances provided by the braces when they develop their probable resistances T_u and C'_u
$V'_{u,cr}$	Storey shear resistance provided by the braces in the critical tier for the post-buckling brace condition
δ_e	Elastic roof lateral deflection under the design seismic force V
Δ_{ei}	Tier lateral deformation under the lateral load V
δ_i	Displacements at Tier i level
Δ_i	Tier relative lateral deformation
δ_{roof}	Anticipated deflection including inelastic effects
θ	Angle of the braces from horizontal

CHAPTER 9 GENERAL DISCUSSION

In the present study, an understanding of the seismic behaviour of multi-tiered steel concentrically braced frames was developed; moreover, analysis and design strategies were proposed to address the observed deficiencies. Most findings have been presented in the articles prepared in the course of the work. However, some aspects of the seismic response and design of MT-BFs have not been discussed in the articles and are summarized in the following sections.

9.1 Buckling response of an isolated MT-BF column

As observed in the nonlinear analyses of the MT-BF columns designed in accordance with 2010 AISC Seismic Provisions (2010a), column buckling in the first tier segment occurs when two plastic hinges form along the tier height. Buckling response of isolated columns and columns part of MT-BFs is investigated in this section to understand the sequence of events leading to column buckling in MT-BFs and examine the influence of the loading conditions on the buckling mode and column strength. The *OpenSees* (McKenna and Fenves 2004) model validated against the experimental data, as introduced in Chapter 3, is used in this study. The column resistance is first compared to that obtained from the interaction equations of AISC 360-10 (2010b) and CSA S16-14 (2014). Then, the buckling response of the same column is examined assuming boundary conditions representing multi-tiered braced frame columns. Finally, an MT-BF column buckled under ground motion is discussed.

– **Isolated column study**

The buckling mode and strength of the column is compared to that of a W-shape column as defined in the current steel design standards. As shown in Figure 9.1a, the column is a W610x195 column with 6.0 m height and pinned at both ends. The column properties are given in Table 9.1. An effective length factor equal to 1.0 was adopted for both weak- and strong-axes. As shown, the compressive resistances are given in accordance with both AISC 360 and CSA S16 standards:

$$P_{n-AISC360} = F_{cr} A \qquad where\, F_{cr} = \left[0.658^{\frac{F_y}{F_e}} \right] F_y \;\; when \;\; \frac{F_y}{F_e} \le 2.25$$

(1)
$$F_{cr} = 0.877 F_e \;\; when \frac{F_y}{F_e} > 2.25$$

$$F_e = \frac{\pi^2 E}{\left(\frac{KL}{r} \right)^2}$$

(2) $$P_{n-CSA} = \frac{A F_y}{(1+\lambda^{2n})^{\frac{1}{n}}} \qquad where\, \lambda = \sqrt{\frac{F_y}{F_e}} \;\; and \;\; F_e = \frac{\pi^2 E}{\left(\frac{KL}{r} \right)^2}$$

where A is the column cross-sectional area. F_{cr}, and F_e are respectively the inelastic and elastic buckling stresses, and λ is the dimensionless slenderness parameter.

Table 9.1: Isolated W610x195 column properties.

Section	A	r_x	r_y	KL/r_x	KL/r_y	M_{px}	M_{py}	P_{nx} AISC	P_{ny} AISC	P_{nx} (CSA S16)	P_{ny} (CSA S16)
	mm²	**mm**	**mm**			**kN-m**	**kN-m**	**kN**	**kN**	**kN**	**kN**
W610x195	24900	259	75	23	80	2091	462	8260	5406	8331	4860

P-M interaction equations in the AISC and CSA standards aim at verifying the strength of a column under axial load and bending moment. For a case where flexure is about y (weak) axis and the moment is applied at one end only, the equations are:

(3) $$PM_{AISC360} = \frac{P_u}{P_n} + \frac{8}{9} \frac{B_1 M_{uy}}{M_{ny}}$$

where P_u is the required column axial strength, M_{uy} is the column weak-axis required flexural strength, and M_{ny} is the column weak-axis nominal flexural strength. B_1 is the multiplier for *P*-δ effects and defined as follows:

$$(4) \qquad B_1 = \frac{C_m}{1 - P_u / P_{e1}} \geq 1.0 \ \textit{where} \ C_m = 0.6 + 0.4\left(M_1 / M_2\right)$$

where C_m is the equivalent moment coefficient, M_1 and M_2, calculated from a first-order analysis, are the smaller and larger moments, respectively, at the ends of the column segment in each tier. M_1 / M_2 is taken equal to zero as the column in this study is pinned at the base, which gives C_m = 0.6. P_{e1} is elastic buckling strength of the column in the plane of bending (weak-axis) and equal to $F_e A$ assuming K =1.0.

$$(5) \qquad PM_{CSA\ S16} = \frac{P_u}{P_n} + \frac{\beta U_{1y} M_{uy}}{M_{ny}}$$

where β is a weak axis bending coefficient , and U_{1y} is the factor to account for moment gradient as well as second-order effects of axial force acting on the deformed member and defined similar to B_1 except that no upper limit is considered in CSA S16. For the isolated column study presented here, U_{1y} is set to 1.0. In Eq. 5, M_{uy}/M_{ny} is taken equal to 1.0 for the values of the axial forces $P_u / P_n < 0.15$.

The AISC and CSA interaction equations are plotted in Figure 9.1e for the column studied. As shown, both equations give very similar results, except for low axial load level in which case the Canadian equation results in greater moment capacity.

Strength predicted by these interaction curves are compared to the predictions obtained using the column *OpenSees* model. Details of the model are the same as presented in the validation study (Section 3.2.2) except that the column height is set to 6.0 m and the nominal yield strength of 345 MPa is assigned to the steel material. Additionally, the column is pinned at both ends and an initial in-plane out-of-straightness corresponding to the column first buckling mode with maximum amplitude of 1/1000 of the height is assigned in the model. The loading conditions were modified, as will be discussed next.

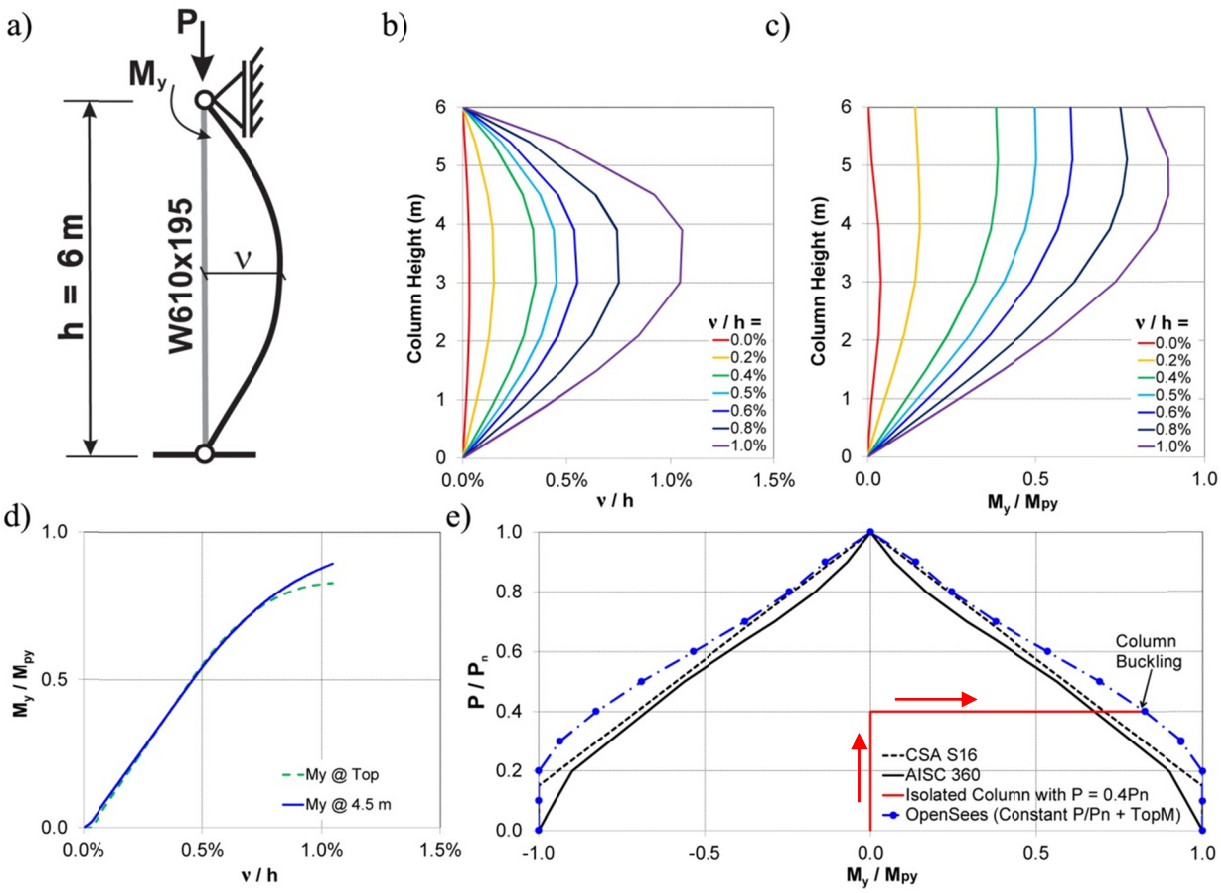

Figure 9.1: Weak-axis flexural buckling response of an isolated pinned-pinned W610x195 column from pushover analysis under $P = 0.4P_n$ and end moment M_y: a) Configuration and loading; b) Lateral displacement variation along the height; c) Weak-axis bending demand variation along the height; d) Weak-axis bending demand history; and e) Column P-M_y interaction demand vs capacity.

For the first analysis, a constant P/P_n value was used, with P_n equal to P_{ny} from the AISC 360-10. A moment was gradually applied at one end up to column buckling, as illustrated in Figure 9.1a. The evolution of the column deflected shape and in-plane moment, M_y, are plotted in Figures 9.1b and 9.1c for the case $P/P_n = 0.4$. In the plots, ν is the column lateral deflection at its mid-height. As shown, the moment acting in the column between the end supports gradually increases to eventually exceed the applied end moment due to P-δ effects. A plastic hinge formed at the point of maximum intermediate moment (4.5 m), which resulted in buckling of the column. The moments that produce such column buckling for various P/P_n ratios are compared to the AISC

and CSA interaction equations in Figure 9.1e. As shown, column buckling generally occurred as predicted by the code interaction equations for the higher axial load levels; however, code equations underestimate the moment capacities obtained from *OpenSees* for lower axial loads. This can be attributed to the fact that the code equations do not reflect the actual higher *P-M* interaction strength available for weak-axis bending.

A second loading condition that more closely reflects the conditions in MT-BFs was then applied to the *OpenSeees* column model: the column was subjected to a constant axial load plus a weak-axis rotation θ that was applied at the column top end and gradually increased until flexural buckling occurred about weak axis (Figure 9.2a). This loading is expected in a MT-BF with critical Tier 2 for which column buckling develops in the first tier. The column response as the end rotation is increased for an axial load equal to 40% of P_{ny} is illustrated in Figures 9.2b and 9.2c. The first plastic hinge formed near the column mid-height at $\nu / h = 1.3\%$. Beyond this point, as the end rotation kept increasing, the moment at the top end of the column started to reduce and eventually reversed to maintain the equilibrium of the column in its deformed configuration. A second plastic hinge eventually formed at the column top end when the moment reached the flexural capacity of the column at that location. With these two plastic hinges, column flexural buckling developed at $\nu / h = 5.3\%$. In Figure 9.2e, the evolution of the moment at the column top end under 0.4 P_n is plotted in the *P-M* interaction diagram. Before reversal, the moment is positive and it reverses to negative values when approaching buckling. In the figure, the curves showing the points of column buckling are also plotted, as obtained by repeating the *OpenSees* analysis for various P/P_n ratios. The buckling interaction curve is very similar to the one obtained when *P* and *M* were applied to the column (Figure 9.1), i.e. with *OpenSees* results matching code predictions for the higher axial load levels and giving higher moment capacities for lower axial loads. In fact, the buckling interaction curves from the two *OpenSees* analyses, the one where *P* and *M* were applied and the one where *P* and θ were applied are nearly identical. However, for the latter, the column buckling occurred after moment reversal at the top end of the column.

The buckling interaction curve was also obtained from *OpenSees* analysis of the column in which a constant $M_y / \underline{M}_{py}$ was first applied at the column top end and downward axial displacement was then gradually increased up to buckling. That interaction curve is plotted in Figure 10.2e; it corresponds very well to the interaction curve obtained from the *OpenSees* analysis of the column subjected to constant $P / \underline{P}_n$ while increasing the end rotation.

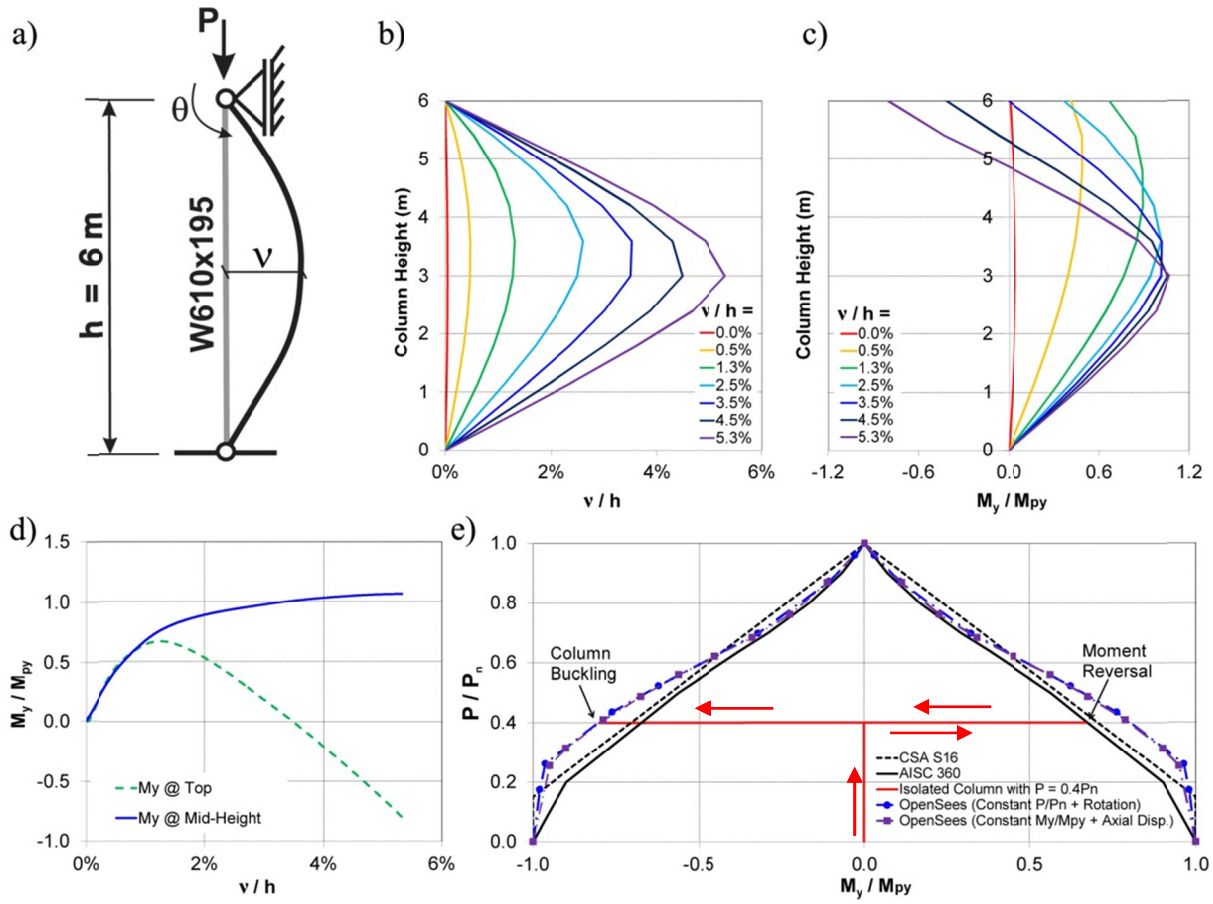

Figure 9.2: Weak-axis flexural buckling response of an isolated pinned-pinned W610x195 column from pushover analysis under $P = 0.4P_n$ and end rotation θ: a) Configuration and loading; b) Lateral displacement variation along the height; c) Weak-axis bending demand variation along the height; d) Weak-axis bending history; and e) Column P-M_y interaction demand vs capacity.

In MT-BFs with critical Tier 1, column buckling develops as a result of increasing bending moments that are induced by non-uniform tier drifts along the frame height, rather than by increasing end rotations. This loading scenario may affect the buckling sequence of MT-BF columns and results in a different strength compared to what is assumed in the AISC 360 or CSA S16 equations. Thus, the buckling response of the isolated column was studied under an increasing drift as observed in these MT-BFs.

Figure 9.3 shows the results for the buckling analysis of an isolated column, more closely simulating the MT-BF conditions. A 6 m tall W610x195 column pinned at its base and fixed at its upper end was first subjected to an axial compression load equal to 40% of its predicted axial

compression strength P = 2162 kN (KL = 6.0 m) and weak axis bending demand was then induced in the column by imposing a gradually increasing lateral displacement at the top end of the column (Figure 9.3a). As shown in Figures 9.3b and 9.3c, the moment is slightly larger at the mid-height of the column due to the P-δ effects induced by the axial compression load. The combination of the first order and second order effects led to plastic hinging forming at the column mid-height at a storey drift of approximately 5.3% h. After the plastic hinge is formed, the flexural rigidity of the column was reduced and the moment at the top end of the column started to reduce to maintain equilibrium as plastic rotation developed in the plastic hinge. The moment at the top eventually changed sign upon increasing further the drift, similar to the situation when end rotation was gradually applied. Column buckling developed at a storey drift of 13.3% h following the formation of a second plastic hinge at the top end of the column when the flexural capacity of the column was attained at this location.

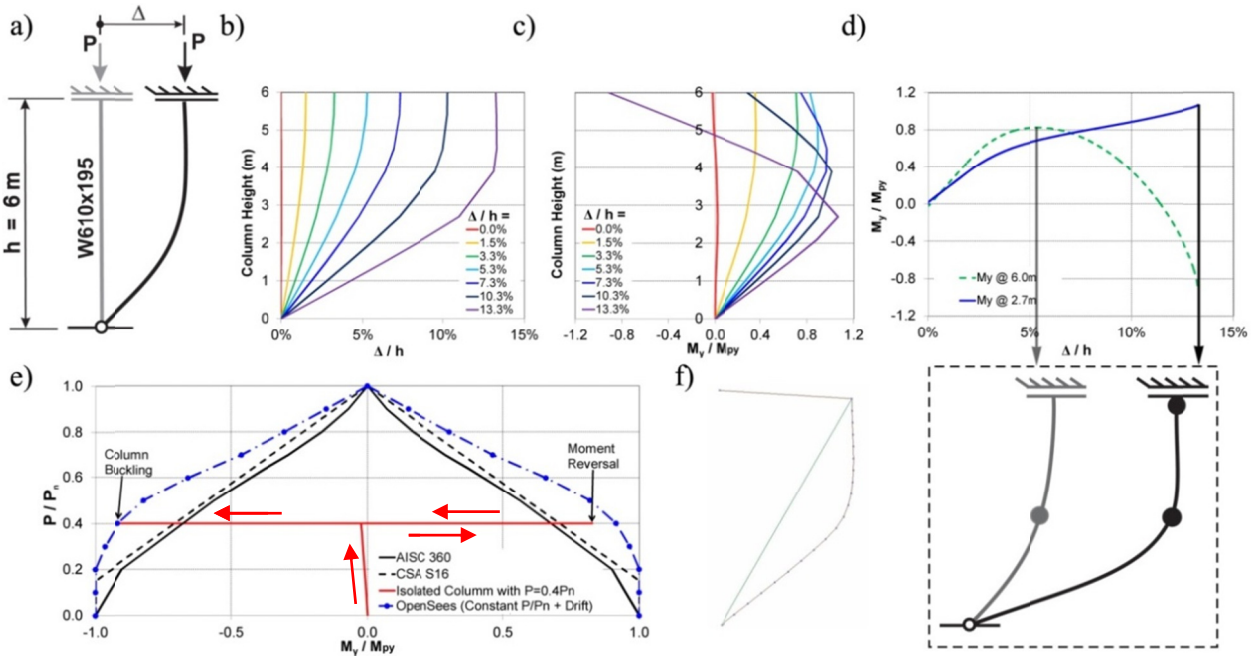

Figure 9.3: Weak-axis flexural buckling response of an isolated W610x195 column from pushover analysis under $P = 0.4P_n$ and lateral displacement Δ: a) Configuration and loading; b) Lateral displacement variation along the height; c) Weak-axis bending demand variation along the height; d) Weak-axis bending demand history; e) Column P-M_y interaction demand vs capacity; and f) Deformed shape from *OpenSees* at buckling initiation.

In Figure 9.3e, the P-M_y interaction is illustrated for this column. The combined P-M_y history at the column top is compared to the AISC and CSA S16 interaction curves. In this figure, the interaction curve obtained from *OpenSees* is also plotted; this curve was obtained from the buckling analysis of the column shown in Figure 9.3a under various axial loads by gradually increasing the drift. For the case studied, buckling occurred when the demand exceeds the AISC and CSA predicted capacities and reached the predicted capacity of the column from the *OpenSees* simulations. This suggests that the code equations provide conservative strength predictions. The buckling shape of the column from *OpenSees* is shown in Figure 9.3f.

Detail of the response for the same loading condition but under a higher axial compression load equal to 80% of the column predicted axial compression strength P = 4324 kN is given in Figure 9.4. A similar response was observed for this case; however, buckling occurred at a drift of 4.4% h, much smaller than in the previous case with an axial load of 40% P_{ny} in Figure 9.3c. The reason is attributed to the larger axial compression load carried by the column, which resulted in larger P-δ effects that induced higher bending moments at intermediate locations along the column height. Under the higher axial load, the first plastic hinge formed along the height of the column at a storey drift of 2.5% h (Figure 9.4f), also much smaller than 5.3% h observed in the previous case. As in the previous case, column buckling occurred at a top moment larger than predicted by AISC and CSA interaction curves (Figure 9.4e).

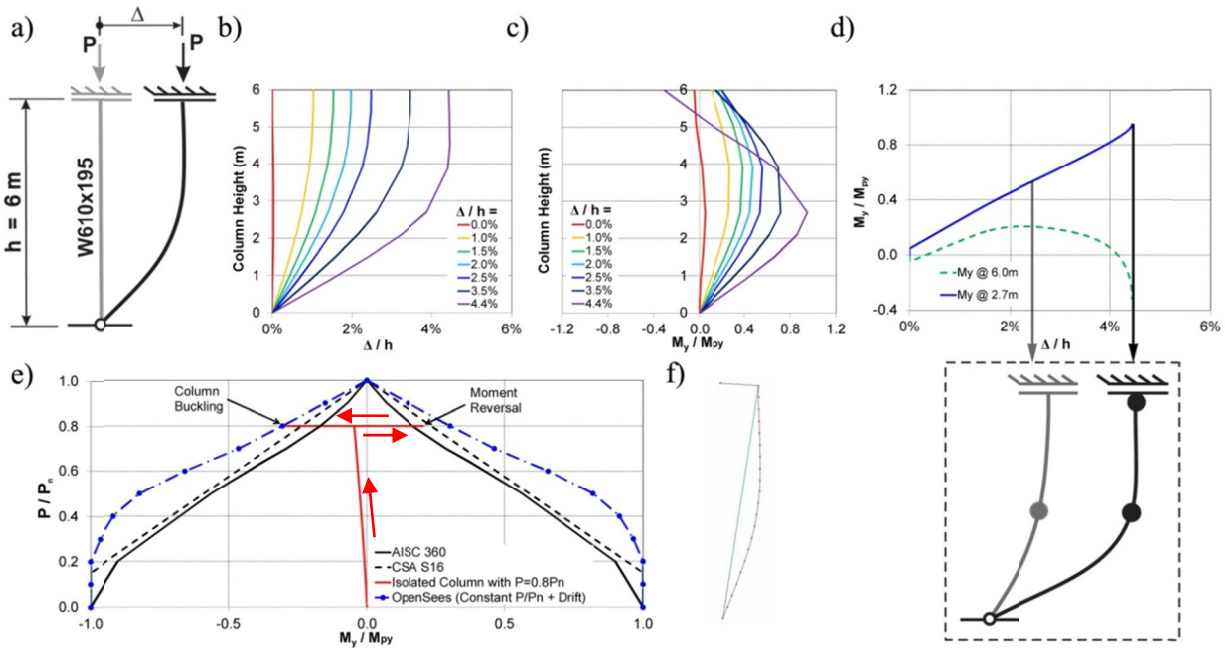

Figure 9.4: Weak-axis flexural buckling response of an isolated W610x195 column from pushover analysis under $P = 0.8P_n$ and lateral displacement Δ: a) Configuration and loading; b) Lateral displacement variation along the height; c) Weak-axis bending demand variation along the height; d) Weak-axis bending demand history; e) Column P-M_y interaction demand vs capacity; and f) Deformed shape from *OpenSees* at buckling initiation.

– **Buckling response of a MT-BF column**

The buckling response of a first tier column part of an MT-BF is presented to illustrate the sequence of events leading column buckling in a real MT-BF under a ground motion. For this study, the 4-tiered braced frame presented in Section 3.2.3 (Figure 3.5) was selected. For this frame, the lateral displacements at Tier 1 and RHS column bending demands obtained from the NLRH analysis are shown in Figures 9.5b and 9.5c. The results are plotted between t = 16.4 s, when the buckling initiates, and 17.0 s, when the flexural buckling completely developed in Tier 1 column. As shown in these figures, the moment is much larger at the mid-height of the column due to the P-δ effects induced by the high axial compression load, as was the case for the isolated column of Figure 9.4. Similar to the buckling response observed for the isolated columns subjected to axial compression and drift, the combination of the first order and second order effects led to plastic hinging forming at the column mid-height at t = 16.66 s. After the plastic hinge formed, the

flexural rigidity of the column was reduced and the moment at top end of the column started to diminish and eventually reverse to maintain equilibrium of the column in its deformed configuration, as the plastic rotation develops in the first plastic hinge at the mid-height of the column. Column buckling developed at t = 16.7 by forming the second plastic hinge at the top end of the column because the column does not have enough flexural capacity to maintain equilibrium.

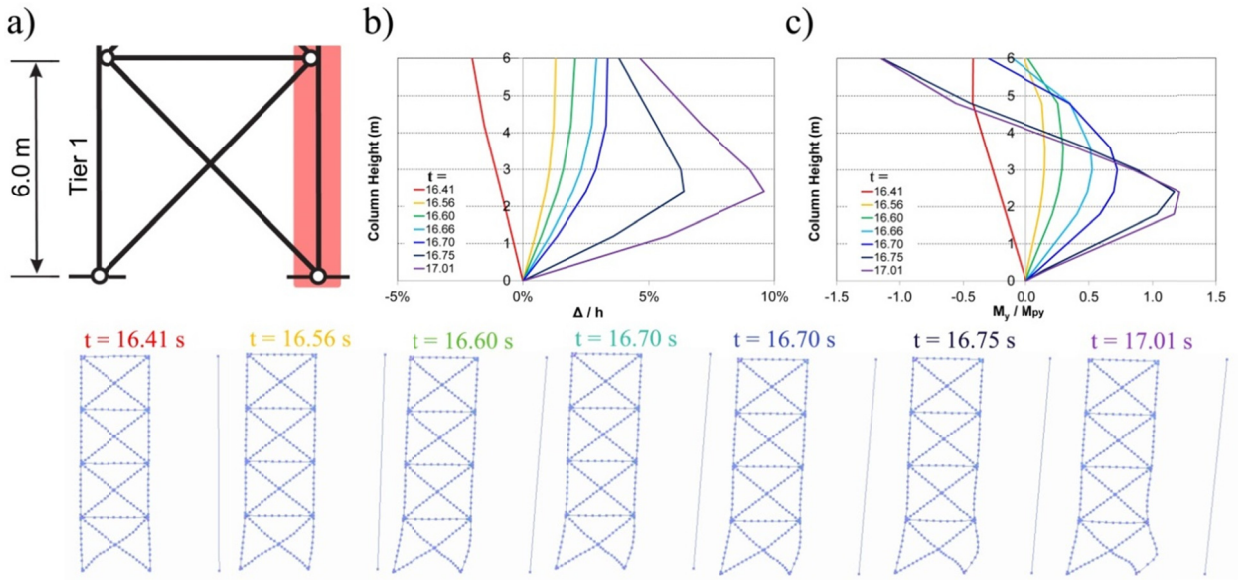

Figure 9.5: NLRH analysis of the 4-tiered CBF under 1992 Landers, Yermo Fire Station record; a) Tier 1 configuration; b) Lateral displacement variation along the height of Tier 1; c) Weak-axis bending demand variation along the height of the RHS column.

– **Conclusive remarks**

This study has led to three key conclusions on the buckling response of MT-BF columns:

1) Contrary to the case in which a column is subjected to increasing end moments for which buckling occurs after one plastic hinge has formed near the column mid-height, columns under increasing end rotation or relative transverse displacement, cases similar to the situation in MT-BFs, requires the formation of two plastic hinges along the height to develop flexural buckling, one near the column mid-height and one at the top end. The second plastic hinges forms after reversal of the moment at the top end of the column;

2) Column flexural buckling is significantly affected by the second order effect, which reduces the column ductility capacity under the axial compression load; and

3) Column weak-axis flexural buckling under gradually increasing end rotation or tier drift is conservatively predicted by the AISC 360 and CSA S16 interaction equations.

In view of the column design in MT-BFs as proposed in this study, column strength and stability is verified for the axial forces and the bending moments at top of the column. However, the isolated column study (Figures 9.3 and 9.4) showed that the moment at the column mid-height may be higher than the moment at the column top due to geometric nonlinearities, which means that verifying the column for the design axial force and bending demand at tier level may not prevent the formation of a plastic hinge at the column mid-height. Future research is needed to verify the adequacy of the current AISC and CSA interaction equations for this failure mode. In particular, the equations or values assigned to the B_1 or U_1 coefficients should be revisited.

9.2 Column out-of-plane buckling in MT-BFs

In previous chapters, the instability mode that was observed for MT-BFs designed in accordance with the U.S. standards occurred by flexural buckling in the plane of the frame. This buckling mode was discussed in Section 9.1 of this chapter. The results of NonLinear Response History (NLRH) analyses showed that column instability also included out-of-plane flexural buckling over the full frame height as shown in Figure 9.6 for a 4-tiered CBF under 1979 Imperial Valley – Delta record. The column out-of-plane buckling was triggered after the first plastic hinge completely formed at the column mid-height in the bottom tier. Since the column is pinned at both ends for rotation in out of the plane of the frame, the formation of the first plastic hinge, even if column plastic hinging develops about its weak axis, combined with out-of-plane imperfections, brace out-of-plane forces due to column out-of-plane imperfections, and plastic hinging in gusset plates due to brace buckling, is sufficient to develop out-of-plane buckling of the column. This indicates that preventing column plastic hinging due to in-plane flexural demand, by applying the design method proposed in this study, will most likely also prevent column out-of-plane buckling. This was confirmed by evaluating the seismic response of the MT-BFs designed for the combined axial force and in-plane bending demands as no out-of-plane buckling occurred in the analysis. However, out-of-plane moments induced by brace out-of-plane

forces due to column out-of-plane imperfections and plastic hinging in gusset plates due to brace buckling should be considered as acting simultaneously with the in-plane bending moment in design. Also, there is concern that current column interaction equations, in which plastic moment capacities are allowed to be used, may not address properly the possibility of coupled buckling under combined axial force and biaxial bending moments (Stoakes and Fahnestock 2013). Additional research is needed to examine the observed coupled buckling due to combined axial loads and plastic hinging under in-plane flexural demand.

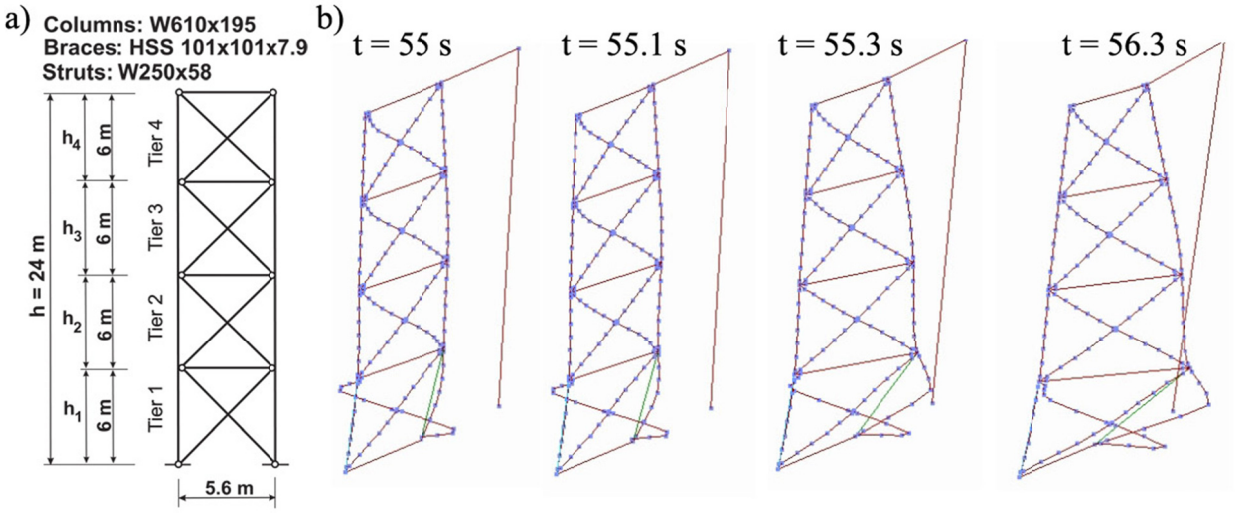

Figure 9.6: a) 4-tiered braced frame; b) Deformed shape at incipient collapse under 1979 Imperial Valley Delta record.

The results of the 3D finite element study showed that column buckling in MT-BFs may also involve torsional deformation, especially in the cases where the combined in-plane and out-of-plane deformations are maximum at the same location (Stoakes and Fahnestock 2013). This situation is shown for the RHS column of a 2-tiered braced frame in Figure 9.7. Initial studies showed that this response resulted from yielding of a corner of one of the flanges of the column under combined axial loads, in-plane flexural demands, and limited out-of-plane bending moment. Additional three-dimensional finite element analysis should be performed to further investigate flexural-torsional buckling mode if larger out-of-plane flexural demand exists. Furthermore, the efficiency of column bracing to prevent torsional buckling of the columns

should be investigated. In this study, a strut-to-column connection detail was proposed to achieve such behaviour. Design requirements should be developed for this bracing.

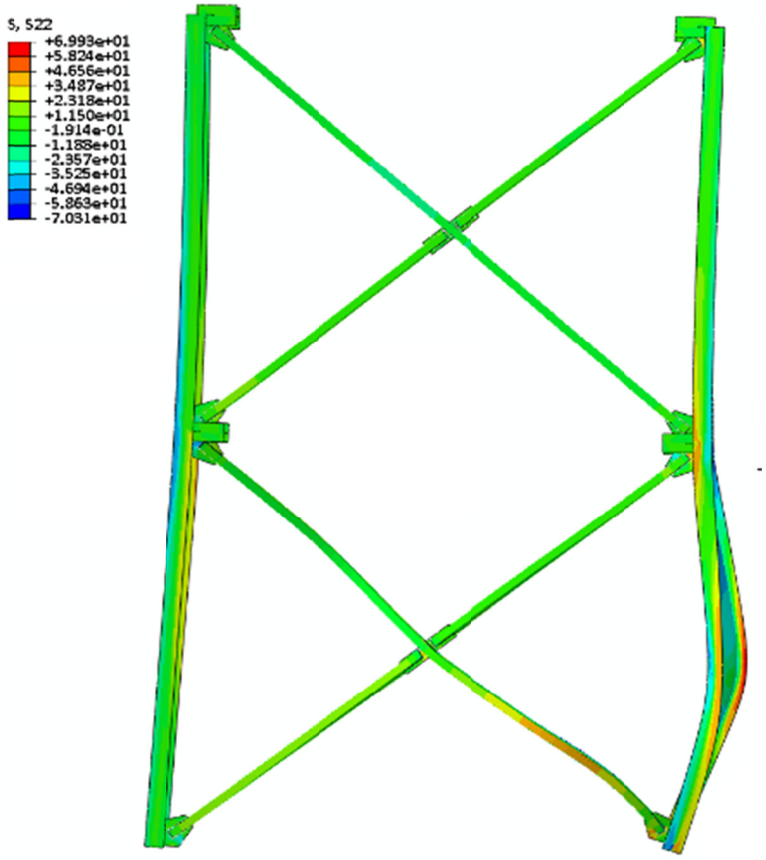

Figure 9.7: A 2-tiered CBF deformed shape at incipient collapse under 1979 Imperial Valley Delta record (Imanpour et al. 2015a).

9.3 Critical tier scenarios

In the proposed design methods, column forces and tier drifts depend on the position of the critical tier and subsequent propagation of brace yielding. Thus, all plausible critical tier scenarios should be considered in a design. This means that more than one critical tier scenario may need to be examined in a design. The method proposed to identify the critical tier was based on the code expected brace strengths when braces reach their tension and compression resistances in the tier. However, code expected strengths represent upper bound resistance estimates and that actual brace strengths may actually differ from these values due to unavoidable variations in material properties

(yield strength and strain hardening), cross-sectional areas, strain rate effects, member imperfections and boundary conditions. Therefore, design engineers should consider reduction in brace resistances in selected critical tiers by a given margin representative of the expected variability in brace strength. Alternatively, brace resistance can be increased in non-critical tiers.

This reduction is necessary for uniform frames where all tiers have identical heights and brace sizes. To illustrate the possibility of various critical tier scenarios, a uniform 5-tiered shown in Figure 9.8a was selected and designed in accordance with the 2010 AISC Seismic Provisions. The member sizes are given in this figure. For this frame, a reduction of 20% in brace yield strength was considered in any tier and NLRH analysis was performed five times under 1994 Northridge Beverly Hills - Mulhol record. Tier drift history is shown in Figure 9.8b for all possible critical tier scenarios (Tier 1 to 5). As shown, most inelastic frame deformations develop in the tier with reduced brace strengths. For the cases in which the critical tiers are intermediate ones, limited yielding also occurs in the adjacent tiers. These results confirm the need to examine all plausible critical tier scenarios in the analysis.

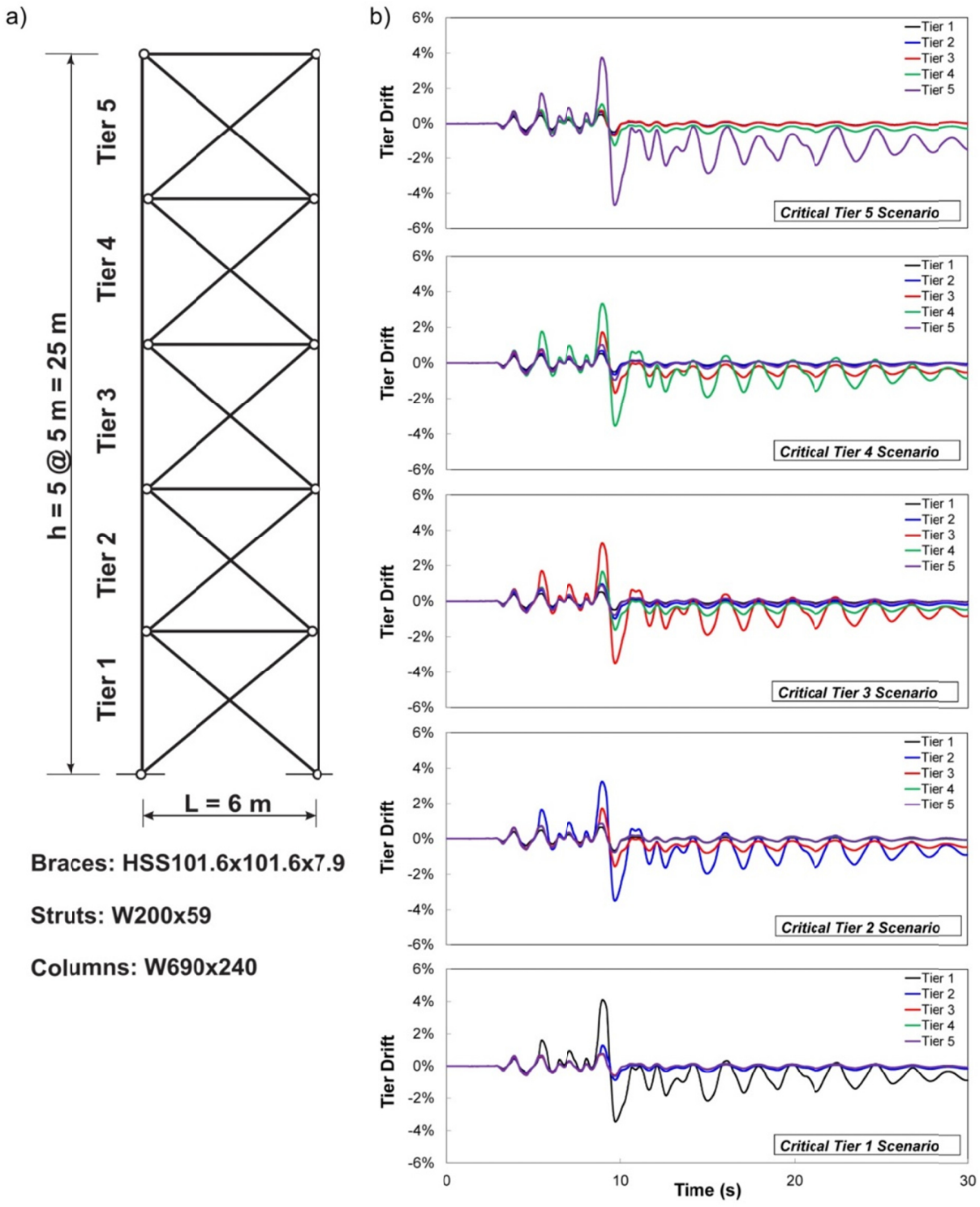

Figure 9.8: a) Frame configuration and member sizes; b) Tier drifts for the five critical tier scenarios.

9.4 Improvement of the prediction of the column bending demand

In the proposed design methods, column bending demands depend on the evolution of the brace post-buckling strength in tiers contributing to frame inelastic response. However, brace compression resistance at buckling and post-buckling ranges were considered in the design to determine the bending demands. The results of the NLRH analysis of the prototype frames, when tension yielding is triggered, showed that the actual brace forces in the compression braces are different than the assumed values; brace force in the critical tier is higher than the assumed brace post-buckling resistance, whereas brace force in the yielding tier is less than brace buckling resistance, as it degrades after first buckling. In the proposed design methods, this actual brace loading condition typically leads to lower column bending demands. Table 9.2 shows the brace forces and the maximum column bending demand computed in design stage and the median of the brace forces from the nonlinear response history analysis for a 2-tiered braced frame when brace tension yielding is initiated in non-critical Tier 1. For this frame, if the actual brace force values were used to determine the column bending moment, the moment would reduce by 42% which can affect the required steel tonnage for the braced frame columns.

Table 9.2: Calculation of the column in-plane bending moment for a 2-tiered braced frame.

Tier	**Tier condition**	**Compression brace force assumed in design kN**	**Max. column bending in design kN-m**	**Compression brace force from NLRH analysis kN**	**Column bending from modified brace forces kN-m**	**Moment reduction (%)**
2	Critical	$C'_{exp} = 129$	430	$1.64\ C'_{exp} = 211$	249	42
1	Yielding	$C_{exp} = 576$		$0.79\ C_{exp} = 455$		

Reduced compression brace forces can be therefore adopted in the design procedure to obtain more realistic design forces for the columns and an economical column design. The reduction factor for the column bending moment can be determined from NLRH analysis of MT-BFs with various geometrical configurations, seismicity levels, bracing configurations, brace sections, brace connections, etc. This modification may also be considered when determining column axial forces, especially for the taller frames with a large number of tiers for which column axial forces

are significantly affected when assuming the actual compression brace forces. The determination of appropriate brace load reduction factors was out of scope of this thesis and could be the topic of further investigations.

9.5 Additional design considerations

The application of the proposed design methods always leads to larger column sizes compared to the methods where columns are designed to carry axial loads only. However, design engineers can select more effective frame geometries and/or brace sizes to minimize the unbalanced brace forces imposed on the columns and achieve more economical designs. The following considerations could be adopted in design to reduce in-plane bending demands on MT-BF columns:

- **Using less critical frame geometries**

Column bending demands can be reduced by selecting more appropriate tier heights. Figure 9.9a shows three configurations of a 2-tiered braced frame designed for a seismic base shear of 428 kN. For all the frames, HSS 101.6x101.6x7.9 and HSS 88.9x88.9x6.4 were selected in Tiers 1 and 2, respectively, to carry the seismic base shear. Note that these braces represent the most economical design for all the frames. Critical tiers are respectively 2, 2, and 1 for Frames 1 to 3 as obtained by comparing expected storey shear resistances $V_{br,exp}$ in the two tiers in Figure 9.9b. Figure 9.9c shows the column in-plane bending demands computed based on the proposed design method for the three frames. For this example, the column bending demand reduces from 496 kN-m (in Frame 1) to 334 kN-m (in Frame 2) by increasing the height of Tier 1 by only 0.5 m. This corresponds to 33% reduction in the column bending moment, which may reduce the column sizes in design. The lower column bending demands in Frame 2 is due to the smaller difference between the expected storey shear resistances provided by the braces $V_{br,exp}$ in the critical Tier 2 and yielding Tier 1 as shown in Figure 9.9b. One should also consider the effect of having different in-plane column buckling length on column design when adjusting tier heights. The reason is that maximum axial force generally occurs in the bottom tier column segment and selecting a taller height for Tier 1 may lead to larger columns.

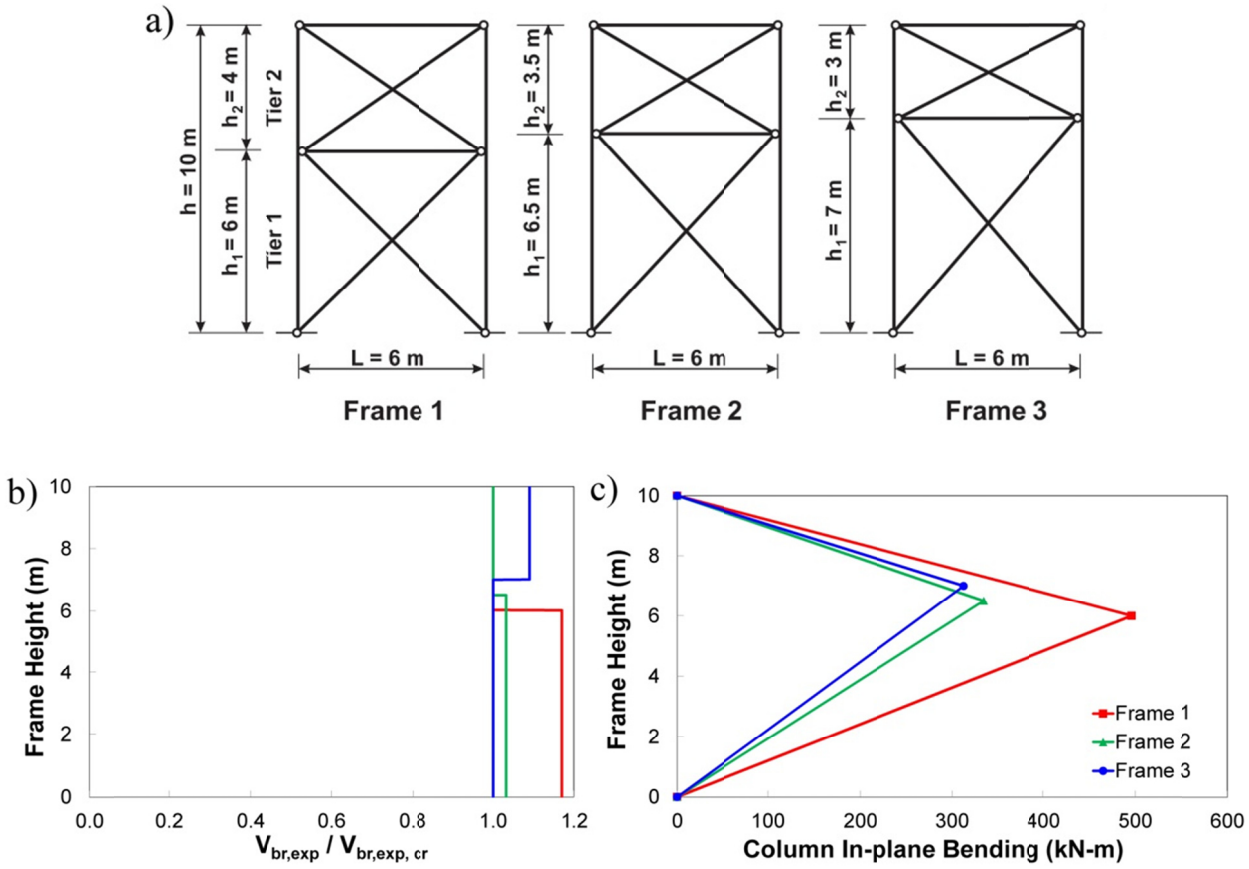

Figure 9.9: a) Frame configurations; b) Expected storey shear resistances provided by braces; and c) Column in-plane bending moments.

– **Tightly sizing the braces**

Tightly sizing the braces can contribute to reducing the unbalanced brace force resistances and, as a result, in-plane flexural bending demands on the columns. To illustrate the effect of brace sizes on the column bending demand, the larger HSS 101.6x101.6x7.9 braces were used in both tiers for the three frames shown in Figure 9.9a. The demand-to-capacity ratios (P_u / $\phi_c P_n$) and the story shear resistances ($V_{br,exp}$) are shown in Figures 9.10a and 9.10b. As shown, smaller P_u / $\phi_c P_n$ ratios are obtained for the oversized braces in Tier 2 of all the frames, which results in larger $V_{br,exp}$ values in that tier. The column bending demands were recalculated based on the new brace resistances and plotted in Figure 9.10c. As shown, the demands have significantly increased for all of the frames.

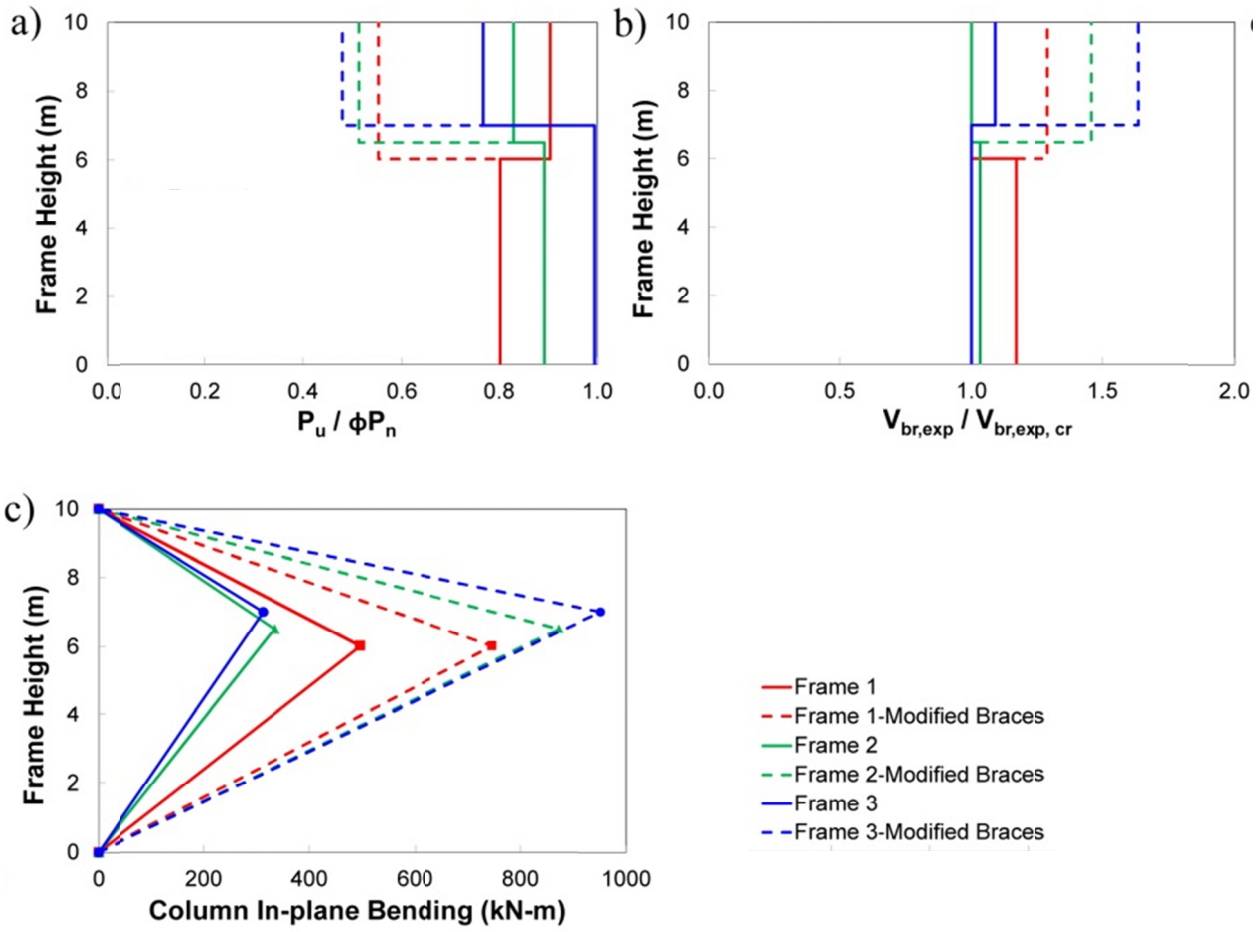

Figure 9.10: a) Brace demand-to-capacity ratios; b) Expected storey shear resistances provided by braces; and c) Column in-plane bending moments.

– **Using braces having higher resistance to low-cycle fatigue**

Past experimental studies on steel braces showed that using slender braces and/or braces with smaller width-to-thickness ratio increases the resistance to low-cycle fatigue fracture of Hollow Square Section (HSS) braces (Tremblay et al. 2003; Fell 2009). For instance, Figure 9.11 shows the influence of the brace slenderness on the fracture life of Rectangular Hollow Section (RHS) braces. For a given brace, increasing the overall slenderness requires sections with smaller radius of gyration which, for HSS braces commonly used in MT-BFs, means smaller cross-section dimensions and, thereby, smaller width-to-thickness ratios. Resistance to low-cycle fatigue is then also increased from a reduced width-to-thickness ratios when using more slender HSS braces. Selecting slender bracing members in MT-BFs could be a good solution when tier drifts control the

design of the columns. For instance, for *KL* = 3500 mm, HSS 114x114x8.0 (b/t = 12.5; *KL*/*r* = 81) and HSS 102x102x9.5 (*b*/*t* = 8.5; *KL*/r = 94) both can resist P_u = 500 kN. Although the former is more effective structurally (2% less steel), using the brace fracture model by Tremblay et al. (2003), it is expected that the 114x114x8.0 will fail at a tier drift of approximately 1.91% whereas fracture of the second is expected to occur at a tier drift equal to 2.37%. However, when adopting this approach, one should consider that a more slender brace will typically have a larger cross-sectional area and, consequently, will induce higher axial loads in the braced frame columns.

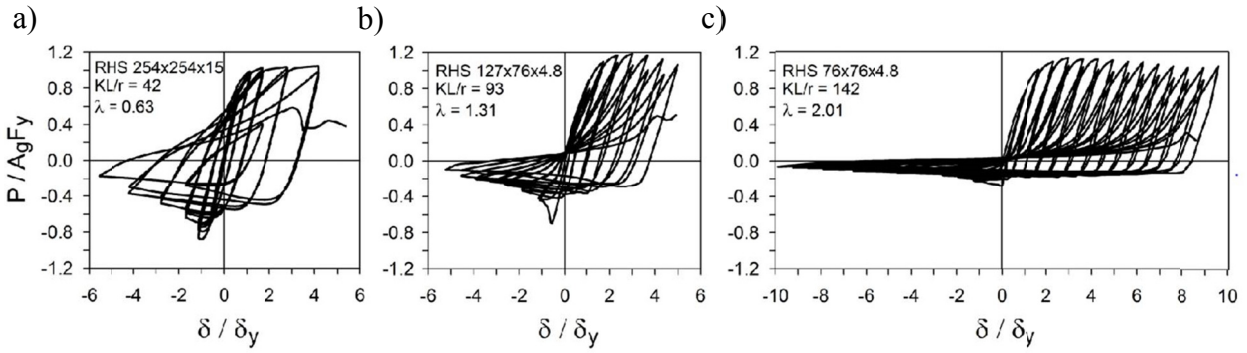

Figure 9.11: Influence of brace effective slenderness ratio on hysteretic response: a) *Kl*/*r* = 42; b) *Kl*/*r* = 93; and c) *Kl*/*r* = 142 (Ziemian 2010).

– **Using braces from the same heat for fabrication**

If possible, it would be preferable to use the braces from the same heat to reduce the uncertainties in the brace resistances, which would contribute to lower unbalanced brace loads and, thereby, in-plane bending demands on the columns.

– **Using alternative column sections**

More effective column cross sections such as built-up cruciform sections made of welded W-shapes or tubular sections can be used instead of commonly used W-shapes oriented such that weak-axis bending develops in-plane. The application of doubly symmetric members would result in higher in-plane flexural strength and stiffness which, in turn, would contribute to reducing the structure costs. Additionally, W-shape members can be oriented such that in-plane bending demands expected in MT-BF columns induce bending moment about their strong axis. This

orientation can also lead to an economical column design provided that out-of-plane bending demands induced by wind loads do not require a larger column section. To illustrate the influence of the selection of a column section, the columns of Frame 1 shown in Figure 9.9 were designed first with W-shape columns oriented such that seismic in-plane demands induce weak-axis bending. Then, two alternative column designs are proposed: 1) W-shape columns bent about their strong axis in the plane of the frame; and 2) cruciform columns. Results for each design are summarized in Table 9.3, which include design forces, column sections, and required steel tonnage for the studied cases. As shown, the application of W-shaped section oriented such that in-plane bending develops about its strong axis results in the most economical design compared to the other design alternatives. Reduction in steel tonnage with a built-up cruciform section is comparable to the case where W-shape columns oriented in strong-axis are used. However, using built-up sections would generally involve additional efforts and costs for fabrication of the columns compared to rolled members.

Table 9.3: Application of alternative column sections in a 2-tiered braced frame.

Column design	**Section**	**Nominal flexural strength, M_n (kN-m)**	**Nominal compressive strength, P_n (kN)**	**Available in-plane flexural stiffness, EI (kN-m^2)**	**Column Steel tonnage (t)**
W-shape (Weak-Axis)	W360x421	1549	14656	119800	8.42
W-shape (Strong-Axis)	W610x195	1975	2451	334000	3.90
Built-up Cruciform	CW530x101	1042	8008	128580	4.04

9.6 Additional MT-BF design examples

Two methods were proposed in Chapter 7 to analyze MT-BFs with three or more tiers. Two design examples were presented in that chapter to illustrate and validate sub-structuring technique (Design Example 1) and stiffness analysis method (Design Example 2). In this section, four additional design examples (Design Examples 3 to 6) are presented and the proposed methods are used to determine the column force demands and tier drifts. Design Examples 3 and 4 were analyzed based on the sub-structuring technique and stiffness analysis based method was used to analyze the braced frames in Design Examples 5 and 6. NLRH analysis was then performed and the results (envelopes of the absolute values) were compared to the anticipated seismic demands.

– **Design Example 3**

Design Example 3 presents the application of the sub-structuring technique for the 5-tiered steel SCBF shown in Figure 9.12. This frame is the same as the frame studied in Design Example 1 (Chapter 7). Loadings and initial design was presented in Chapter 7. In Design Example 1, bottom up brace tension yielding scenario was selected assuming critical Tier 1. However, as discussed, the possibility of other critical tier scenarios should be also checked by reducing the brace resistances in other tiers. By considering a 15% reduction in brace yielding strength in Tier 5, the story shear resistance in that tier reduces to $V_{br,exp,5}$ = 1152 kN which is the lowest and Tier 5 becomes the critical. The sub-structuring technique with top down brace tension yielding sequence can then be used to analyze the frame. In this example, maximum allowable tier drift is based on brace fracture. The brace failure for the critical tier is expected to occur at a tier drift $\Delta_{max,cr}$ = 2.2%. The number of yielding tiers, n_y, is determined using Eq. 2 (presented in Chapter 7) with a maximum anticipated story drift Δ = 1.21% as determined in Design Example 1. Solving Eq. 2 for Δ, the height of the critical tier, h_{cr} = 4.0 m, seismic base shear, V = 490 kN, and brace expected yield stress R_yF_y = 483 MPa gives h_y = 9.5 m, which means that n_y = 3 is required. Two analysis steps are performed to initiate brace tension yielding in Tiers 4 and 3 respectively. Column in-plane bending demands together with the axial loads are used to design the columns at each analysis step. A W760x257 is selected to resist the demands. The flexural stiffness of the selected columns is verified to ensure initiation of brace tension yielding in the three yielding tiers and to limit drift in the critical Tier 5. Larger W360x421 columns are required to satisfy these requirements.

In Figure 9.12, column bending moments from sub-structuring technique with W760x257 columns are compared to the results from NLRH analysis of a frame with the same column section. In the figure, the envelopes of the absolute values from both the design method and the NLRH analysis are presented. The comparison of the anticipated demands and analysis results indicates that the sub-structuring method conservatively predicts column demands in Tiers 3 and 4. The reason is associated to the brace force scenarios used to determine the moments. These forces represent extreme brace compressive force scenarios; however, less critical brace force conditions occurred under the ground motions and led to lesser unbalanced storey shear forces in

the columns. This is a good example where refined design brace forces would improve the prediction of the column bending demand.

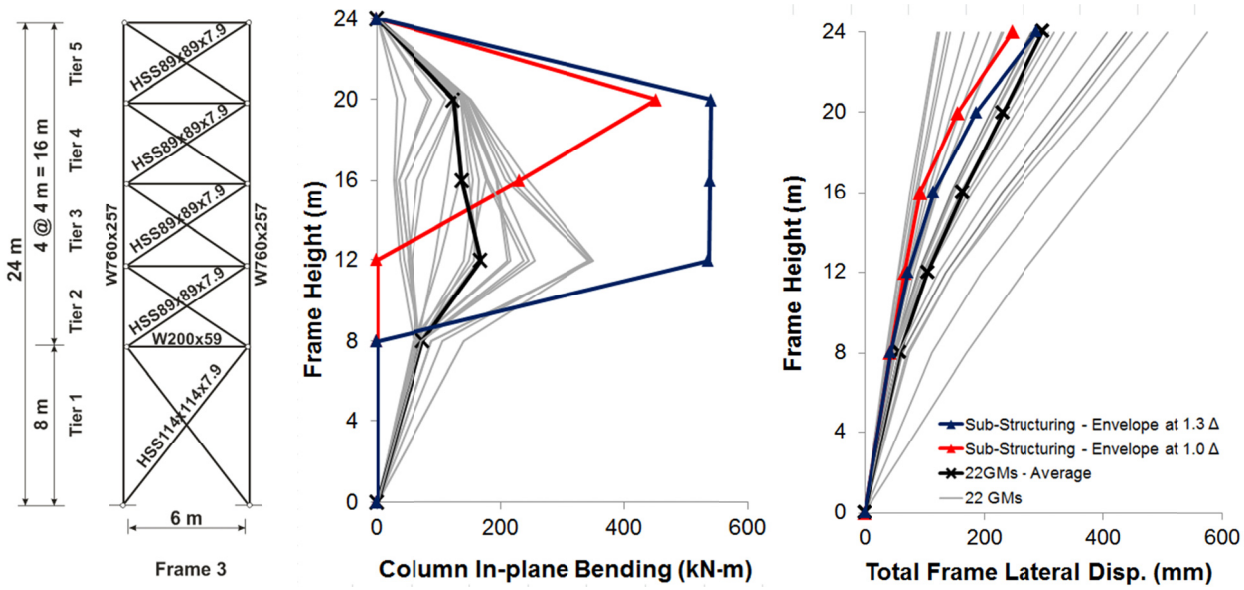

Figure 9.12: Design Example 3: Column bending and tier drift demands from NLRH analysis vs. anticipated values from sub-structuring technique.

As it can be seen in Figure 9.12, the design bending moments obtained based on brace yielding limited to Tiers 3 to 5. In the ground motion, yielding also occurred in Tier 2 because the average story drift demands exceeded the Δ value used in design and reach 1.3 Δ. This was expected due to the fact that MCE level earthquake were used, whereas Δ corresponded to the design earthquake level. If the analysis is redone with 1.3 Δ, $n_y = 4$ and yielding will also develop in Tier 2. The moment predicted based on 1.3 Δ is shown in Figure 9.12. These results confirm that a realistic storey drift must be used to predict column bending demands for MCE level.

NLRH analysis was redone with the final W360x421 columns to verify the prediction of tier drifts. Figure 9.12 shows frame lateral displacement from sub-structuring technique compared to those obtained from the NLRH analysis. The predicted deformation patterns using Δ reflects brace tension yielding in upper three tiers whereas the analysis assuming 1.3 Δ gives a closer deformation pattern compared to the NLRH analysis results.

– **Design Example 4**

In this example, the frame of Design Example 3 is redesigned with W-shape braces (Frame 4) instead of HSS members. Bracing members are oriented such that out-of-plane buckling occurs about their weak axis. Frame configuration and member sizes are shown in Figure 9.13. Tier 1 has the lowest story shear resistance ($V_{br,exp,1}$ = 1185 kN) compared to the other tiers ($V_{br,exp,2\text{-}5}$ = 1438 kN), so that Tier 1 is the critical tier. The sub-structuring technique is chosen for this well-proportioned frame with bottom up brace tension yielding sequence starting in Tier 1. In this example, maximum allowable tier drift is set to 1.5% in all the tiers to comply with the target performance assumed for the structure. Also, an anticipated story drift equal to 1.5 Δ = 1.49% is considered. The number of yielding tiers, n_y, with 1.5 Δ, h_{cr} = 8.0 m, V = 490 kN, and R_yF_y = 380 MPa is h_y = 17 m, which means that n_y = 4 is required. W690x384 is selected to satisfy the strength requirements. With this larger column, 1.5 Δ is reduced to 1.19% and the number of yielding tiers becomes equal to 2. For this two yielding tier condition, stiffer W360x551 columns are required to initiate brace tension yielding in the two tiers and limit the drift in critical Tier 1 to 1.5%.

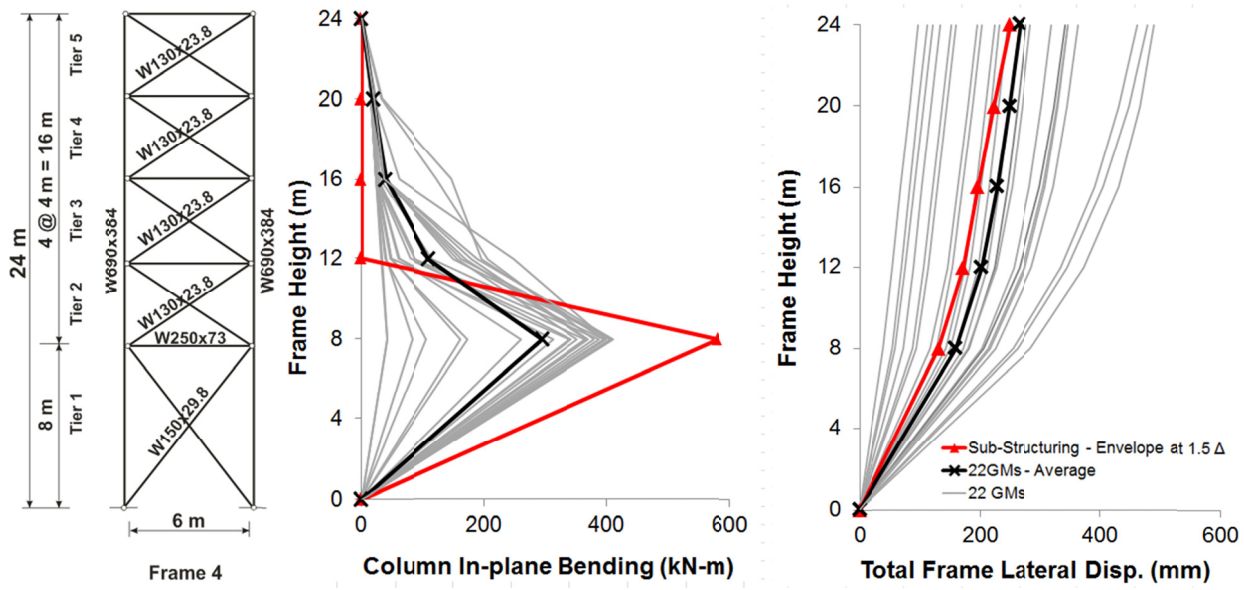

Figure 9.13: Design Example 4: Column bending and tier drift demands from NLRH analysis vs. anticipated values from sub-structuring technique.

Figure 9.13 shows the results of the NLRH analysis and the anticipated values obtained from the sub-structuring technique for the column bending demands (with W690x384 columns) and tier drifts (with W360x551 columns). An excellent match was observed between the anticipated values and analysis results for both column bending demands and frame deformations. Note that with the larger W360x551 columns, the number of yielding tiers remained equal to 2 and column bending demands and design predictions remained unchanged as shown in Figure 9.14.

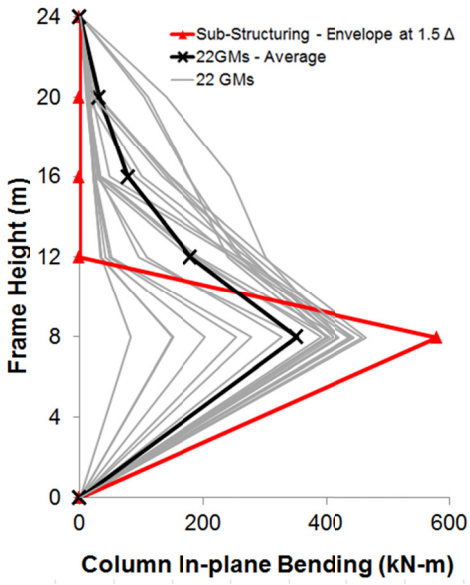

Figure 9.14: Design Example 4: Column bending demands from NLRH analysis vs. anticipated values from sub-structuring technique with W360x551 columns.

– **Design Example 5**

A 5-tiered steel SCBF shown in Figure 9.15 is selected (Frame 5). This frame is a uniform well-proportioned frame and can be analyzed using either sub-structuring or stiffness analysis methods. In this example, stiffness analysis method is used to analyze the frame. Frame loadings are the same as Frame 2 presented in Design Example 2 (Chapter 7). The frame is designed for a seismic base shear of 543 kN. Initial member design was performed in accordance with 2010 AISC Seismic Provisions. W690x240 was selected for the columns. The brace and strut sizes are shown in Figure 9.15. Comparing expected shear resistances of the braces in tiers indicates that all the tiers can be critical ($V_{br,exp,1\text{-}5}$ = 1483 kN). Therefore, five critical tier scenarios should be

examined to determine the column demands and tier drifts. In this example, only critical Tier 1 scenario is presented assuming 5% reduction in yielding strength of the braces in that tier. As discussed, the other critical tier scenarios should be also examined by reducing the brace resistances in those other tiers. Two analysis steps are required to reach the anticipated story drift $\Delta = 1.11\%$. The first step is performed to initiate brace tension yielding in Tier 2 and the second step corresponds to the frame response at roof displacement equal to Δ. A W840x329 column section is selected to resist combined axial force and bending moment demands in Tier 1. Column flexural stiffness is then verified to limit tier drifts to a maximum allowable tier drift based on brace fracture. Using the fracture model by Tremblay et al. (2003) for rectangular HSS braces, failure of the HSS 114x114x7.9 braces in yielding tiers is expected to occur at a tier drift of approximately 1.9%. Larger W360x421 columns are then chosen to limit drift in critical Tier 1 to 1.9%.

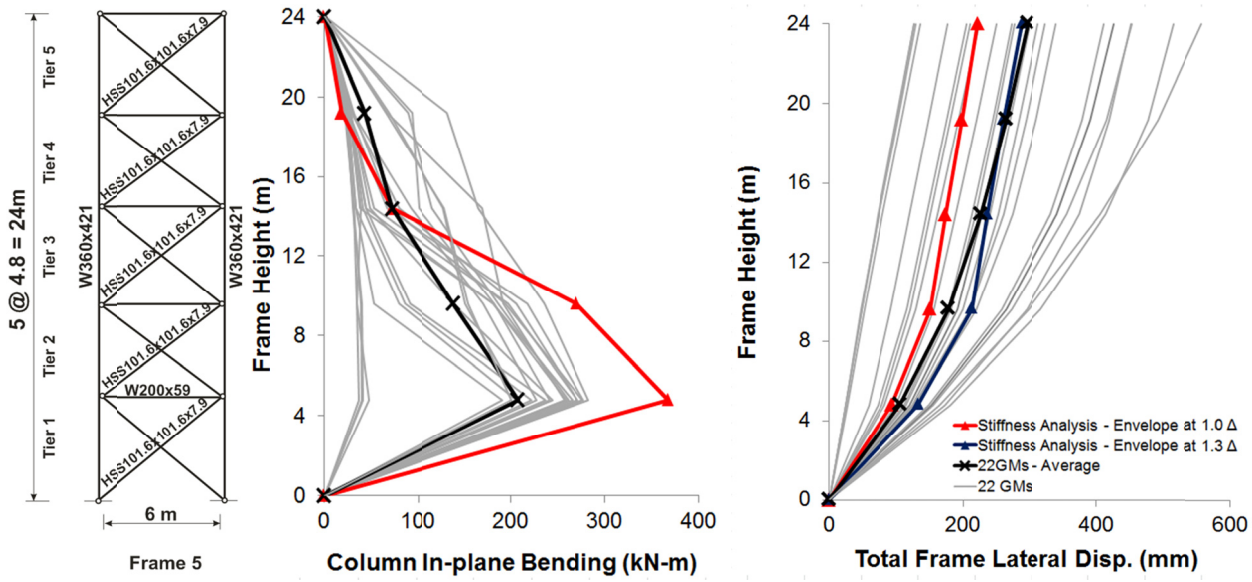

Figure 9.15: Design Example 5: Column bending and tier drift demands from NLRH analysis vs. anticipated values from stiffness analysis method.

The final W360x421 columns are used to perform the NLRH analysis. Column in-plane bending demands are shown in Figure 9.15. Envelope of the column bending from NLRH analyses are compared to those calculated using the proposed stiffness analysis method. As observed, the

design predictions envelope very well the demand from the ground motions. Column bending demand at Tier 1 obtained from stiffness analysis method is higher than the average value of the analysis results; the reason is that the difference between the story shear resistances in identical Tiers 1 and 2 is lesser under the ground motions compared to that assumed in design because the brace force scenarios used to determine the moments represent most possible critical conditions. The tier drifts are compared in Figure 9.15 to those calculated using the stiffness analysis method. The predicted deformation patterns are similar to the NLRH analysis ones indicating that the brace tension yielding sequence is well predicted by the proposed method. The average story drift demands exceed the Δ value used in design: 1.3 Δ. The stiffness analysis was redone using 1.30 Δ without changing the column sizes to still allow comparison with the NLRH analysis results. Figure 9.15 shows that an excellent agreement can be achieved when a realistic story drift is used in the calculations.

– **Design Example 6**

In this example, the stiffness analysis method is used to analyze Frame 6 shown in Figure 9.16. The configuration and loadings of this frame are the same as Frame 5 except that W-shaped members are used for the braces. Initial member design was performed in accordance with 2010 AISC Seismic Provisions. W690x240 was selected for the columns. The brace and strut sizes are shown in Figure 9.16. The brace sizes in Tiers 2 and 4 have been intentionally increased to create strength irregularity along the frame height ($V_{br,exp,1}$ = 1289 kN vs. $V_{br,exp,2}$ = 2223 kN). Therefore, Tiers 1, 3, and 5 are potential critical tiers for this frame. In this example, the critical Tier 1 scenario is examined by reducing brace yielding strength in that tier by 5%. The other potential critical tier scenarios should be also checked by reducing the brace resistances in Tiers 3 and 5. These scenarios are not studied here. For this frame, tier drifts are limited to a maximum allowable tier drift corresponding to brace fracture. Based on the results of experimental study on W-shape braces (Fell et al. 2009, Tsai et al. 2010), a maximum allowable tier drift of 2.5% is assumed in all the tiers. Also, an anticipated story drift equal to 1.5 Δ = 1.41% is considered in design. Two analysis steps are required to reach the anticipated story drift. The first step is performed to initiate brace tension yielding in Tier 5 and the second step corresponds to the frame response at roof displacement equal to 1.5 Δ. A W920x420 column section is selected to resist combined axial

force and bending moment demands obtained from the Analysis Steps I and II. The flexural stiffness of the selected column is sufficient to limit the tier drifts to maximum allowable tier drift.

Column bending demands obtained from NLRH analysis are compared to the design predictions in Figure 9.16. An excellent match is observed between the average of NLRH analysis results and the prediction by stiffness analysis method. The comparison between the design prediction and NLRH analysis result for tier drifts (Figure 9.16) shows that propagation of brace yielding is appropriately predicted; additionally, frame inelastic deformations are distributed in Tiers 1 and 5 as expected in design.

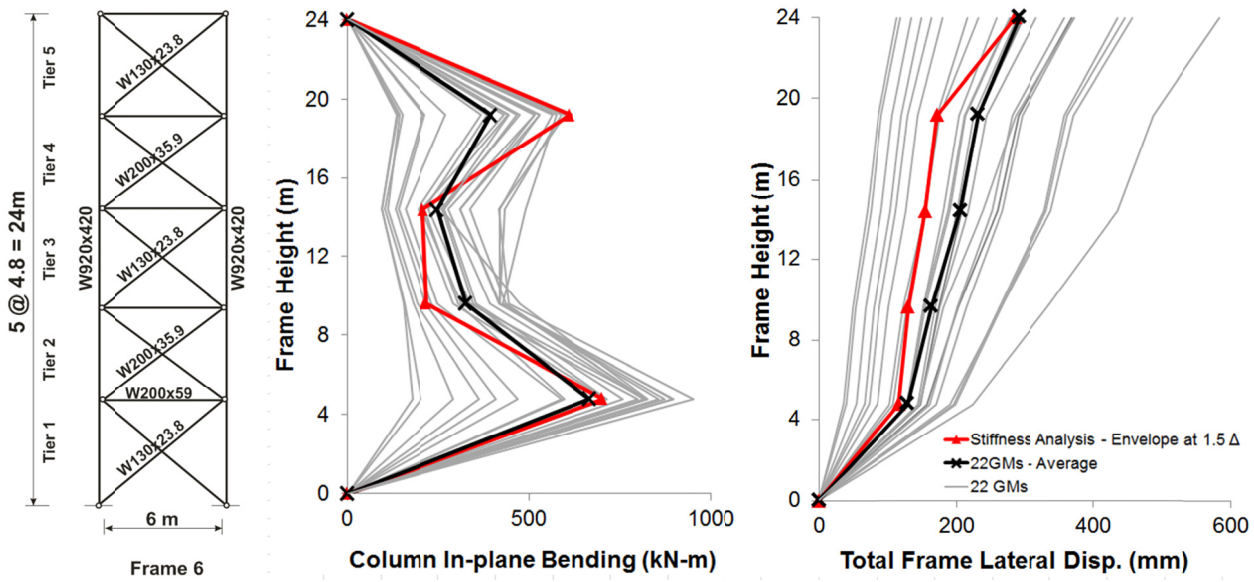

Figure 9.16: Design Example 6: Column bending and tier drift demands from NLRH analysis vs. anticipated values from stiffness analysis method.

CHAPTER 10 CONCLUSIONS AND RECOMMENDATIONS

10.1 General

In this chapter, the main findings and conclusions of the study are summarized and the areas that need further examination are introduced. Within the context of seismic response and design of steel multi-tiered braced frames (MT-BFs), this Ph.D. dissertation had two main objectives: 1) Assessment of the seismic response of MT-BFs; and 2) Development of seismic analysis and design methods for MT-BFs. The primary original contributions of this thesis work are:

- Development of computationally efficient numerical models for steel MT-BFs
- Improvement of the CSA S16 Canadian steel design standard concerning the special design requirements for Type LD and Type MD MT-BFs
- Development of analysis and design tool for tall Type MD concentrically braced frames for in-plane seismic demand in the context of CSA S16
- Development of analysis methods and design guidelines for multi-tiered special concentrically braced frames for in-plane seismic demand in the framework of the AISC Seismic Provisions
- Development of a hybrid simulation model for MT-BFs

This chapter reviews the main conclusions of the articles presented, together with a preliminary study on the hybrid testing program. Furthermore, recommendations for future investigations are presented based on the discussion of the results in Chapter 9.

10.2 Summary and conclusions

Steel Multi-tiered Braced Frames are used to resist lateral loads in tall single-storey structures such as industrial buildings, sport facilities, convention centers, airplane hangars or warehouse buildings. They consist of two or more bracing panels that are stacked between the ground and roof levels. MT-BF generally represents a more practical and cost-effective solution when excessively long bracing members extending from the foundations to the roof level are required to brace the full building height in such structures. For seismic applications, brace lengths and

sizes are reduced significantly, which eases satisfying the slenderness limits specified in the seismic provisions. Horizontal struts are also employed between the tiers to resist the unbalanced brace force induced due to the brace buckling in the adjacent tiers. MT-BF columns are typically I-shaped that are oriented such that strong axis bending takes place out-of-plane. The columns can be considered as laterally braced in the plane of the frame at every tier level, which also contributes to reducing the steel tonnage. However, out-of-plane buckling develops over full frame height as MT-BF columns are unbraced in out-of-plane direction. Adjacent gravity columns located along MT-BF lines can be laterally braced for in-plane buckling by adding horizontal struts at tier levels between the braced frame and gravity load carrying system.

For a seismic design of MT-BFs in Canada, special seismic provisions were introduced in the CSA S16 Canadian steel design standard. According to these requirements, struts are required at every tier level and the columns must be designed for the combined axial load and seismic induced bending moment, assuming that brace yielding in tension develops in one tier only. In the U.S., no seismic design provision have been adopted for the design of this framing configuration in the 2010 AISC Seismic Provisions and MT-BFs are classified as K-type braced frames not permitted for Special and Ordinary Concentrically Braced Frames (SCBFs and OCBFs). In view of the fact that struts in MT-BFs creates to a more robust seismic lateral load path compared to K-braced frames, there was a motivation to better understand the seismic response of MT-BFs and develop design provisions for that system. In particular, essential differences between multi-tiered and multi-storey braced frames raise questions about the application of the current seismic design guidelines developed for single bracing panels between adjacent levels to braced frames with multiple bracing panels stacked between floors.

Limited studies performed on MT-BFs, before the introduction of the CSA S16-09 requirements, had showed that inelastic frame deformations tend to concentrate in the weaker tier which imposes in-plane bending demands on MT-BF columns. These studies had also confirmed that drift concentration in the critical tier may cause brace low-cycle fatigue fracture and/or column buckling. MT-BFs are extensively used in North America for single storey industrial steel buildings. This extensive use, however, had not been accompanied by an adequate research effort to fully understand their seismic response and rationalize their design. Thus, addressing unanswered questions including the need for special seismic design requirements in the U.S. and

the adequacy of the current seismic provisions for MT-BFs in Canada were the main motivations of this study.

The first objective pursued in this study was to examine the seismic response of MT-BFs designed in accordance with the CSA S16-14 and 2010 AISC Seismic Provisions. For Canadian applications, seismic response evaluation was performed to assess the adequacy of the current design requirements specified for MT-BFs and to verify if improved design provisions were required. For the frames designed in accordance with the U.S. design standards, seismic evaluation aimed at verifying the necessity of developing new seismic design requirements for MT-BFs. The second objective of this study was to develop and present seismic analysis and design strategies for MT-BFs consistent with the current North American design provisions. The study was limited to single-storey buildings with steel braced frames.

A preliminary study was performed on prototype MT-BFs designed in accordance with CSA S16-09. The prototype frames included Type LD and MD frames with 2-, 3- and 4-tiers. The special requirements specified in this standard for MT-BFs were considered in design. A fiber-based numerical model of the frame was developed using the *OpenSees* program (McKenna and Fenves 2004) to perform nonlinear analyses on the prototype frames. The model included the columns, struts, bracing members, and springs. A simple connection detail was considered in the model to simulate the brace-to-column connections. The results confirmed that brace tension yielding develops in the critical tier only, which prevents further distribution of inelastic response in other tiers. It was also shown that this behaviour imposes in-plane seismic flexural demand on the columns. That demand was found to be appropriately predicted following the CSA S16-09 requirements. Furthermore, the analysis results showed that the performance of Type MD MT-BFs is adequate for frames with a limited number of tiers. Also, the concentration of lateral displacements along the frame height did not induce significant out-of-plane bending moments in the columns. These results were used to improve CSA S16 requirements in 2014: MT-BFs are now permitted to be used for Type MD braced frames with 2 or 3 tiers and for Type LD braced frames up to 5 tiers. The notional out-of-plane transverse load has also been reduced to 2% of the factored axial compression load in the column below the brace-to-column intersecting point.

After the initial investigation, a series of X-braced frames was designed according to the 2010 AISC Seismic Provisions. The 3-Dimentional fiber-based model of the frame created in the

preliminary study was used with improvements to more realistically account for the rigidity of the connections in the frame response. For this purpose, the brace-to-column connection model was refined to reproduce connection size, taking into consideration the influence of the gusset plate. The model was validated against 3D finite element models. It was shown that the fiber-based model could appropriately capture tier drift concentration and column buckling in MT-BFs. Additionally, the model was used for a wide range of frames for the U.S. and it was found to be a computationally efficient tool to perform such an extensive parametric study. In view of the larger *R* values in the U.S. design, concentration of inelastic brace deformations was more pronounced compared to the similar Canadian applications. Such higher concentration also induced larger in-plane bending demands in the columns. The in-plane bending moments together with the high axial compression loads in the columns resulted in flexural yielding and plastic hinge forming in the columns which, in turn, led to column instability in several of the cases studied. For these cases, column buckling was the dominant failure mode. It developed in flexure about the weak axis in the plane of the frame. Complete plastic hinge formation associated with in-plane buckling also triggered out-of-plane buckling response of the column over the full frame height due to the lack of lateral support at the tier level(s). Column torsional movement was also observed for a 2-tiered CBF after column buckling initiation. It was demonstrated that column buckling is more likely to occur over the first tier height when the critical tier is located at the bottom of the frame, where axial load demand on the column is maximum. This response confirmed that brace-strut assemblies can provide a sufficient in-plane lateral bracing to the columns even if the braces respond in the nonlinear range. Additionally, it was found that the excessive drift demands developed in the weaker tier reach a level that could lead to low-cycle fatigue fracture of the bracing members. Eventually, the necessity of developing new design provisions to address this undesirable behaviour and achieve satisfactory seismic response for this framing configuration was verified.

Several alternative braced frame systems with no specific requirements were examined as potential solutions to improve the seismic response of MT-SCBFs. The strategies include the use of higher design seismic loads, the application of fixed base condition, and using Buckling Restrained Bracing (BRB) members instead of conventional braces. The results revealed that increased design seismic load did not have significant beneficial effects on the flexural demand imposed on the columns and the occurrence of column buckling failure; however, the application

of a fixed base condition resulted in less critical conditions for the stability of the columns in the bottom tier. A satisfactory response with more uniform drift demand and smaller column bending moments were observed when using BRBs.

A seismic analysis and design method consistent with the 2010 AISC Seismic Provisions was first proposed for two-tiered special concentrically braced frames for in-plane seismic demand. In this method, the tier where brace inelastic demand is expected to initiate and concentrate is identified as the critical tier. Then column in-plane bending moment due to uneven brace inelastic response is determined. That column demand depends on the differences in storey shear resistance that develops between tiers when the bracing members are at buckling and in the post-buckling ranges. Minimum in-plane flexural strength is needed for the columns to compensate for this unbalance in storey shear resistance and prevent buckling failure of the columns. The columns are then designed to resist the in-plane flexural moments together with the axial loads. Furthermore, the columns must possess sufficient in-plane flexural stiffness to control the maximum drift in the critical tier and prevent excessive inelastic demand at the anticipated storey drift. For this purpose, drift in the critical tier is estimated when the braces respond in inelastic range. The proposed design procedure was validated using nonlinear incremental static (pushover) and dynamic analyses performed on a prototype frame using the fiber-based numerical model. It was confirmed that this new procedure prevents column buckling and distributes frame inelastic deformations between the two tiers.

A preliminary seismic analysis and design method was then developed for in-plane seismic demand in the framework of the 2010 AISC Seismic Provisions for uniform MT-BFs with more than two tiers assuming a brace yielding sequence from the bottom or top tier. In this method, the critical tier is first identified and the column shear forces and bending moments are determined taking into account the continuity of the columns over the frame height for an assumed yielding tier. This method was first used for isolated braced frames. The application of the method was then extended to frames where the gravity columns located on the same braced line are involved in the resistance of seismic in-plane bending moments imposed on the MT-BF columns. The study was performed for a prototype 4-tiered SCBF. In this method, in-plane bending moments are distributed between braced frame and gravity columns in proportion to their relative flexural stiffness. Three different design approaches were proposed to design the braced frame and gravity columns. The numerical model developed for MT-BF was expanded to simulate the

gravity load carrying system. The seismic behaviour of the prototype frames were then evaluated using nonlinear analyses. It was demonstrated that seismic demands on the bracing members and braced frame columns are effectively reduced when mobilizing the gravity columns for lateral resistance. Also, in-plane bending moments are distributed between the gravity and braced frame columns with respect to their flexural stiffness, as predicted at the design stage. The nonlinear analyses and column cost estimation showed that the design approach, where both braced frame and gravity columns are designed to resist their respective share of the flexural demand, results in an adequate seismic response and cost-effective strategy. It was also found that the approach where gravity columns are selected first without consideration of seismic effects, braced frame columns are designed to carry their share of bending moments, and the initially selected gravity columns are verified for the seismic induced bending moments using their expected strengths, also results in an acceptable seismic response.

For braced frames with three or more tiers, the preliminary analysis and design method was refined to obtain two more comprehensive methods in line with the 2010 AISC Seismic Provisions. The proposed methods are the sub-structuring technique and the stiffness analysis method. Both methods were developed to estimate column flexural demands and tier drifts. The methods account for the initiation of brace tension yielding in the critical tier and subsequent propagation of brace tension yielding in other tiers. In both methods, analysis steps are performed that correspond to occurrences of brace tension yielding as the storey drift increases. In each step, brace forces that represent brace buckling and yielding sequence are considered to determine the demands. The columns are verified for the combined bending moment and axial load and modified as necessary to prevent buckling. The methods also provide minimum column stiffness requirements to ensure subsequent brace yielding initiation and minimize drift concentration at the anticipated storey drift. The sub-structuring technique is limited to well-proportioned braced frames with uniform tier properties, assuming that yielding initiates in the top or bottom tier. In this method, each analysis is performed on a simple sub-structure including the yielding tiers. The stiffness analysis based method is more rigorous and accounts for the actual frame nonlinear response and can therefore be applied to both regular and irregular MT-BF configurations. In this method, the stiffness matrix of one of the MT-BF columns is assembled and solved for external concentrated forces corresponding to horizontal unbalanced brace forces at tier levels. The application of the methods was illustrated for two 5-tiered SCBF examples in Chapter 7. Additional

cases were also presented in Chapter 10. The methods were validated using nonlinear response history analysis. A very good match was found between the analysis results and design predictions.

In view of the lack of sufficient guidelines in the 2010 AISC Seismic Provisions for the seismic design of multi-panel braced frames and the popularity of this framing configuration in the U.S., the analysis and design methods proposed for two- and multi-tiered frames provide design engineers with useful tools to achieve a safe and reliable structural design on the one hand, and enhance the overall state of knowledge of MT-BFs for researchers and code developers on the other hand.

For Canadian applications, a complementary study was performed based on the findings of the initial work performed at the beginning of the research. The complementary study resulted in a computer-based static analysis technique to analyze MT-BFs assuming that brace tension yielding develops in one tier only, consistent with the CSA S16-14 assumptions. In this technique, yielding and buckled braces are replaced by concentrated loads corresponding to their probable axial resistances. Prototype frames were designed using the proposed technique and nonlinear response history analysis was performed to examine their seismic response. The results showed that the seismic provisions of CSA S16 reflect well the observed response and the proposed analysis technique leads to good prediction of in-plane bending demands in the columns. For the Type MD frames exceeding the CSA S16-14 limits, the assumption of yielding being limited to only one tier may not hold for all cases. An alternative design method using the same computer-based analysis technique was then developed to account for distribution of the brace tension yielding along the frame height. Design and analysis of prototype frame showed that the proposed method can appropriately predict brace tension yielding sequence as well as column force demands; additionally, the proposed method generally offers more economical column design compared to CSA S16-14 provisions. The knowledge gained in this study represents supportive information that can be used to improve the CSA S16 design provisions in the future, especially for taller ductile multi-tiered braced frames. Design engineers can also apply the proposed procedure in their day-to-day practice as a simple and efficient tool to design of wide range of buildings with the multi-tier configuration.

To complement the assessment of the column buckling response, a hybrid test program was initiated for MT-BF columns using the Multi-Directional Hybrid Testing System (MDHTS) recently installed at the Structural Engineering Laboratory of Polytechnique Montréal. The hybrid testing includes a steel W-shape column specimen part of an MT-BF (the physical sub-structure) and the rest of the frame simulated in the *OpenSees* program (the numerical sub-structure). A computational model was developed for hybrid simulation of the MT-BFs. The main features, components and capacity of the MDHTS were reviewed. The 3D finite element analyses of the system were performed to evaluate the local and global behaviour of the systems' components under critical loading cases expected in the experimental program. The results showed that the test setup is capable of providing the expected boundary conditions within acceptable error margin. A test matrix was also developed for MT-BF columns. In this test program, a group of MT-BFs were designed in accordance with the Canadian and the U.S. design standards and the experimental specimens were selected such that they cover a wide range of the columns used in these frames. Preliminary cyclic testing revealed the presence of frictional forces in the testing machine that must be considered in the hybrid simulation. Friction compensation techniques were developed using an *OpenSees* model of the MDHTS and models programmed in Simulink. It was found that the Simulink model in which the friction forces developing in each of the actuator swivels is needed to properly represent the test apparatus response. At the time of writing, the implementation of the hybrid controller system for the MDHTS had not been completed. It is expected the techniques developed in this thesis will be used to perform the proposed MT-BF column test program when the testing machine becomes operational.

10.3 Recommendations

In this dissertation, the seismic response of MT-BFs was presented by focusing on the stability of columns. Seismic design methods were proposed to estimate column in-plane flexural demand and tier drifts in order to prevent column instability and minimize concentration of drift. An MT-BF hybrid testing program was also developed. The results of this study raised additional questions regarding the seismic response of steel MT-BFs that should be addressed in future research. The study also identified aspects of MT-BF seismic design that need further investigation. These issues and aspects are summarized below:

- Physical tests of a full frame assembly are needed to confirm the inelastic behaviour of MT-BFs as was predicted by the numerical analyses, and to validate the adequacy of the proposed design methods.
- In this study, a biaxial buckling mode, which involves in-plane and out-of-plane deformations, was observed for MT-BF columns under in-plane seismic demand. The analysis by Stoakes and Fahnestock (2013) also showed that the out-of-plane buckling of the column in MT-BFs can be affected by flexural yielding due to the in-plane demands. Thus, additional three-dimensional finite element analysis should be performed to further investigate column stability considering coupled in-plane and out-of-plane demands. Also, the appropriateness of the current column interaction equations to address this coupled buckling response under combined axial loads and biaxial bending demands should be verified.
- The buckling response of MT-BF columns subjected to concomitant out-of-plane bending moments due to gravity loads (e.g. moment frames, crane supporting structures) or out-of-plane lateral loads should be investigated.
- The buckling failure of the columns as obtained in the numerical simulations should be validated through experimental programs to confirm the unsatisfactory performance of MT-BFs as observed in this study and to provide sufficient data regarding the nonlinear behaviour of W-shape columns in MT-BFs. In particular, the observed sequence of bending moments leading to development of column buckling and the biaxial buckling mode should be examined.
- The results of the analyses showed that the column in-plane bending demands can be reduced if actual brace forces are considered in design instead of expected brace resistance values specified in the codes. The determination of appropriate brace load reduction factors was out of scope of this thesis and could be the topic of future investigations.
- In the analyses, limited out-of-plane bending demand was observed on the MT-BF columns as a result of brace out-of-plane forces due to column out-of-plane imperfections, plastic hinging in gusset plates due to brace buckling, and column initial geometric imperfections. The observed demands are significantly less than that obtained by applying the notional transverse loads specified by CSA S16-14. Further investigation is needed to predict actual

out-of-plane bending demand of the MT-BF columns and evaluate the influential parameters. Also, column design requirements should be developed for this concomitant out-of-plane flexural demand.

- This study covered multi-tiered concentrically braced frames. Only preliminary studies were performed for MT-BRBFs and MT-OCBFs for the U.S. applications. Design provisions also need to be developed for multi-tiered eccentrically brace frames, MT-BRBFs, and, for the U.S. applications, MT-OCBFs.
- The study was limited to single-storey buildings. Additional research is needed to investigate the seismic response of MT-BFs in multi-storey structures and propose complementary design provisions as necessary.
- Studies should be performed to examine if the use of moment-resisting connections between struts and columns could be beneficial to inelastic seismic response of MT-BFs.

BIBLIOGRAPHY

Agarwal, K.M., and Stafiej, A.P. (1980). "Calculation of Effective Lengths of Stepped Columns." *Eng. J. AISC,* 15(4), 96–105.

Aguero, A., Izvernari, C., and Tremblay, R. (2006). "Modelling of the Seismic Response of Concentrically Braced Steel Frames using the OpenSees Analysis Environment", *Int. J. of Advanced Steel Construction*, 2(3), 242–274.

Auger, K. (2015). Personal communication.

AISC. (2010a). *ANSI/AISC 341-10, Seismic Provisions for Structural Steel Buildings*, American Institute of Steel Construction, Chicago, IL.

AISC. (2010b). *ANSI/AISC 360-10, Specifications for Structural Steel Buildings*, American Institute of Steel Construction, Chicago, IL.

Anderson, J.P., and Woodward, J.H. (1972). "Calculation of Effective Lengths and Effective Slenderness Ratios of Stepped Columns." *Eng. J. AISC,* 7(4), 157–166.

Aoki, K., Fukuyama, K., Okumoto, H., Ukai, K., Taga, K. (1998). "Design of a High Rise Building Using Unbonded Braces with Varying Cross Section." *J. Constr. Steel Res.,* 6, 139–144, (in Japanese).

Archambault, M.H. (1995). "*Étude du comportement séismique des contreventements ductiles en X avec profiles tubulaires en acier*." EPM/GCS-1995-09, Department of Civil Engineering, École Polytechnique, Montréal, QC.

ASCE. (2005, 2010). *SEI/ASCE 7-05, SEI/ASCE 7-10, Minimum Design Loads for Buildings and Other Structures*, American Society of Civil Engineers.

Balazadeh Minouei, Y. (2015). Personal communication.

Bendapudi, K.V. (1994). "Practical Approaches in Mill Building Columns Subjected to Heavy Crane Loads." *Eng. J. AISC*, 31(4), 125–140.

Bertero, V.V., Uang, C.M., Llopiz, C.R., and Igarashi, K. (1989)."Earthquake simulator testing of concentric braced dual system." *J. Struct. Eng., ASCE*, 115(8), 1877–1894.

Calabrese, A., Almeida, J. P., and Pinho, R. (2010). "Numerical issues in distributed inelasticity modelling of RC frame elements for seismic analysis." *J. Earthq. Eng.*, 14(1), 38–68.

CEN (2004), *Eurocode 8 – Design Provisions for Earthquake Resistant Structures, EN-1998-1:2004,* E, Comite Europeen de Normalization, Brussels, Belgium.

Chen, C.H., Lai, J.W., and Mahin, S. (2008). "Seismic Performance Assessment of Concentrically Braced Steel Frame Buildings" *The 14 World Conference on Earthquake Engineering*, Beijing, China.

CSA. (2001, 2009, 2014). CSA S16-09, CSA S16-14, *Design of Steel Structures*, Canadian Standards Association, Mississauga, ON.

Dalal, S.T. (1969). "Some non-conventional cases of coumn design." *Eng. J. AISC*, 6(1), 28–39.

D'Aniello, M., La Manna Ambrosino, G., Portioli, F., and Landolfo, R. (2013). "Modelling aspects of the seismic response of steel concentric braced frames." *Steel and Composite Structures*, 15(5), 539–566.

Davaran, A. (2001). "Effective length factor for discontinuous X-bracing systems." *J. of Eng. Mechanics*, 127(2), 106–112.

Davaran, A., and Hoveidae, N. (2009). "Effect of mid-connection detail on the behavior of x-bracing systems." *J. Constr. Steel Res.*, 65(4), 985–990.

Davaran, A., Gélinas, A., and Tremblay, R. (2015). "Inelastic Buckling Analysis of Steel X-Bracing with Bolted Single Shear Lap Connections." *J. Struct. Eng.*, *ASCE*, 141(8), 04014204.

El-Tayem, A.A., and Goel, S.C. (1986). "Effective Length Factor for Design of X-Bracing Systems." *Eng. J. AISC,* 23, 41–45.

Fell, B.V., Kanvinde, A.M., Deierlein, G.G., and Myers, A.T. (2009). "Experimental Investigation of Inelastic Cyclic Buckling and Fracture of Steel Braces." *J. Struct. Eng., ASCE*, 135(1), 19–32.

Flores, F.X., Charney, F.A., and Lopez-Garcia, D. (2014). "Influence of the gravity framing system on the collapse performance of special steel moment frames." *J. Constr. Steel Res.*, 101, 351–362.

Fogarty, J., and El-Tawil, S. (2013). “Collapse behavior of steel columns under lateral loading.” *ASCE Structures Congress*, Pittsburgh, PA, 2848–2859.

Fogarty, J., Yossef, N., and El-Tawil, S. (2013). “Collapse resistance of locally damaged steel columns.” *J. Constr. Steel Res.*, 82, 195–202.

Fraser, D.J. (1987). “The in-plane stability of a frame containing pin-based stepped columns.” *Proc. Int. Conf. all Steel and Aluminium Structures*, Cardiff. UK.

Fraser, D.J. (1989). “Uniform Pin-Based Crane Columns, Effective Length.” *Eng. J. AISC*, 26(2), 61–65.

Fraser, D.J. (1990). “The In-Plane Stability of a Frame Containing Pin-Based Stepped Column.” *Eng. J. AISC*, 27(2), 49–53.

Fraser, D.J., Bridge, R.Q. (1990). “Buckling of Stepped Crane Columns.” *J. Constr. Steel Res.,* 16, 23–38.

Fukuta, T., Nishiyama, I., Yamanouchi, H., and Kato, B. (1989). “Seismic performance of steel frames with inverted V braces.” *J. Struct. Eng.*, 115(8), 2016–2028.

Galambos, T.V., and Ketter, R.L. (1958). *Columns Under Combined Bending and Thrust,* Fritz Engineering Laboratory Report 205A.21, Bethlehem, Pennsylvania.

Hsiao, P.C., Lehman, D.E., and Roeder, C.W. (2012). “Improved analytical model for special concentrically braced frames.” *J. Constr. Steel Res*., 73, 80–94.

Hsiao, P.C., Lehman, D.E., and Roeder, C.W. (2013). “A model to simulate special concentrically braced frames beyond brace fracture.” *Earthquake Eng. And Struct. Dynamics*, 42, 183–200.

Huang, H.C. (1968). “Determination of Slenderness Ratios for Desing of Heavy Mill Building Stepped Columns.” *Iron and Steel Engineer*, 123–134.

Imanpour, A., Tremblay, R., and Davaran, A. (2012a). “Seismic performance of steel concentrically braced frames with bracing members intersecting columns between floors.” Proc., *7th STESSA Conference*, Santiago, Chile, 447–453.

Imanpour, A., and Tremblay, R. (2012). "Analytical Assessment of Stability of Unbraced Column in Two Panel Concentrically Braced Frames." *3rd International Structural Specialty Conference*, Edmonton, Alberta, Canada, Paper No. 1218.

Imanpour, A., Tremblay, R., and Davaran, A. (2012a). "Seismic Evaluation of Multi-Panel Steel Concentrically Braced Frames." *15WCEE*, Lisbon, Portugal, Paper No. 2996.

Imanpour, A., Stoakes, C., Tremblay, R., Fahnestock, L., and Davaran, A. (2013). "Seismic Stability Response of Columns in Multi-Tiered Braced Steel Frames for Industrial Applications." *ASCE Structures Congress*, Pittsburgh, PA, 2650–2661.

Imanpour, A., Tremblay, R., Davaran, A. (2014a). "A New Seismic Design Method for Steel Multi-Tiered Braced Frames." *ASCE Structures Congress*, Boston, MA, 2707–2720.

Imanpour, A., and Tremblay, R. (2014a). "Seismic performance evaluation and design of multi-tiered steel concentrically braced frames." *Proc., 10th National Earthquake Engineering Conf.*, Anchorage, AK, Paper No. 1347.

Imanpour, A., and Tremblay, R. (2014b). "Seismic design of steel multi-tiered braced frames: Application of incremental static analysis for design of steel multi-tiered braced frames." *Proc., Eurosteel 2014*, Naples, Italy, Paper No. 688.

Imanpour, A., Auger, K., Tremblay, R. (2014b) "Seismic Design of Multi-Tiered Steel Braced Frames including the Contribution from Gravity Columns." *Proc., 12th International Conference on Computational Structures Technology*, Civil-Comp Press, Stirlingshire, UK, Paper No. 53. doi:10.4203/ccp.106.53

Imanpour, A., Tremblay, R., Davaran, A., Stoakes, C., and Fahnestock, L. (2015a). "Seismic Performance Assessment of Multi-Tiered Steel Concentrically Braced Frames Designed in Accordance with Current AISC Seismic Provisions." Submitted to *J. Struct. Eng., ASCE*.

Imanpour, A., Tremblay, R., Fahnestock, L., and Stoakes, C. (2015b). "Analysis and Design of Two-Tiered Steel Braced Frames for Enhanced In-plane Seismic Response." Submitted to *J. Struct. Eng., ASCE*.

Imanpour, A., Auger, K., Tremblay, R. (2015c). "Seismic design and performance of multi-tiered steel braced frames including the contribution from gravity columns under in-plane seismic demand." Submitted to *J. Advances in Engineering Software*.

Imanpour, A., and Tremblay, R., (2015a). "Analysis Methods for the Design of Special Concentrically Braced Frames with Three and More Tiers for In-Plane Seismic Demand." Submitted to *J. Struct. Eng., ASCE*.

Imanpour, A., and Tremblay, R., (2015b). "Seismic Design and Response of Steel Multi-Tiered Concentrically Braced Frames in Canada." Submitted to *Can. J. Civ. Eng*.

Jain, A.K., Goel, S.C., and Hanson, R.D. (1980). "Hysteretic cycles of axially loaded steel members." *J. Struct. Div. ASCE*, 106(8), 1777–1795.

Kanvinde, A.M. (2014). Personal communication.

Kahn, L.F., and Hanson, R.D. (1976). "Inelastic cycles of axially loaded steel members." *J. Struct. Div. ASCE*, 102(5), 947–959.

Krawinkler, H., and Gupta, A. (1998). "Story drift demands for steel moment-resisting frame structures." Proc., *6th U.S. Nat. Conf. on Earthquake Engineering*, Seattle, WA.

Lacerte, M. and Tremblay, R. (2006). "Making Use of the Brace Overstrength to Improve the Seismic Response of Multistory Split-X Concentrically Braced Steel Frames", *Can. J. Civ. Eng.*, 33, 1005–1021.

Lai, J.W., and Mahin, S. (2014) "Steel Concentrically Braced Frames using Tubular Structural Sections as Bracing Members: Design, Full-Scale Testing and Numerical Simulation." *Int. J. of Steel Struct.*, 14(1), 43–58.

Lay, M.G. (1973). "Effective lengths of crane columns." *Steel Const. Australian Institute of Steel Construction*, 7(2), 9–19.

Lamarche, C.P., Tremblay, R., (2011). "Seismically induced cyclic buckling of steel columns including residual-stress and strain-rate effects." *J. of Constr. Steel Res.*, 67, 1401–1410.

Lee, S., and Goel, S.C. (1987). *Seismic behavior of hollow and concrete-filled square tubular bracing members*, Research Rep. No.UMCE 87-11, Univ. of Michigan, Ann Arbor, MI.

Lee, D.Y., Subhash, C.G., and Stojadinovic, B. (2008a). "Exposed Column-Base Plate Connections Bending About Weak Axis: I. Numerical Parametric Study." *International Journal of Steel Structures*, 8, 11–27.

Lee, D.Y., Subhash, C.G., and Stojadinovic, B. (2008b). "Exposed Column-Base Plate Connections Bending about Weak Axis: II. Experimental Study." *Int. J. of Steel Struct.*, 8, 29–41.

Lui, E.M., and Sun, M.Q. (1995). "Effective Length of Uniform and Stepped Crane Columns." *Eng. J. AISC*, 32(2), 98–106.

MathWorks (2012). *MATLAB: The Language of Technical Computing*, The MathWorks, Inc., Natick, MA.

McKenna, F., and Fenves, G.L. (2004). "*Open System for Earthquake Engineering Simulation (OpenSees)*." Pacific Earthquake Engineering Research Center (PEER), University of California, Berkeley, CA. http://opensees.berkeley.edu/.

Menegotto, M., and Pinto, P.E. (1973). "Method of analysis for cyclically loaded reinforced concrete plane frames including changes in geometry and non-elastic behavior of elements under combined normal force and bending." *Proc., IABSE Symposium on Resistance and Ultimate Deformability of Structures Acted on by Well Defined Repeated Loads*, 15–22.

Moghaddam, H., Hajirasouliha, I., and Doostan, A. (2005). "Optimum seismic design of concentrically braced steel frames: concepts and design procedures." *J. Constr. Steel Res.*, 61, 151–166.

Moore, W.E. (1986). "A Programmable Solution for Stepped Crane Columns." *Eng. J. AISC*, 21(2), 55–58.

MTS (2015). *Civil engineering testing solution,* http://www.mts.com.

Myers, A.T., Kanvinde, A.M., Deierlein, G.G., and Fell, B.V. (2009). "Effect of weld details on the ductility of steel column baseplate connections." *J. Constr. Steel Res.*, 65, 1366–1373.

Newell, J., and Uang, C.M. (2006). *Cyclic behavior of steel columns with combined high axial load and drift demand,* Rep. No. SSRP-06/22, Dept. of Structural Engineering, Univ. of California, San Diego, La Jolla, CA.

NRCC. (2010). *National Building Code of Canada 2010, 13th ed.*, National Research Council of Canada, Ottawa, ON.

OpenFresco (2012). *Open Framework for Experimental Setup and Control*, http://openfresco.neesforge.nees.org.

Palmer, K.D., Roeder, C.W., Lehman, D.E., Okazaki, T., Shield, C.K., Powell, J. (2012). "Concentric X-braced frames with HSS bracing." *Int. J. of Steel Struct.,* 12(3), 443–459.

Peng, B.H.H., MacRae, G.A., Walpole, A.R., Moss, P., Dhakal, R., and Clifton, C. (2008). "Plastic hinge location in columns of steel frames subjected to seismic actions." *Bulletin of the New Zealand Scociety for Earthquake Engineering*, 41(1).

Picard, A., and Beaulieu, D. (1987). "Design of diagonal cross bracings, Part 1:Theoretical study." *Eng J Am Inst Steel Constr*, 24(3), 122–126.

Pollino, M., Sabzehzar, S., Qu, B., and Mosqueda, G. (2013). "Research Needs for Seismic Rehabilitation of Sub-standard Buildings using Stiff Rocking Cores." *ASCE Structures Congress*, Pittsburgh, PA, 1683–1693.

Popov, E.P., and Black, R.G. (1981). "Steel struts under severe cyclic loadings." *J. Struct. Eng.*, 107(9), 1857–1881.

Qu, B., Sanchez-Zamora, F., and Pollino, M. (2014). "Transforming Seismic Performance of Deficient Steel Concentrically Braced Frames through Implementation of Rocking Cores." *J. Struct. Eng.*, DOI: 10.1061/(ASCE)ST.1943-541X.0001085.

Richards, P.W. (2009). "Seismic Column Demands in Ductile Braced Frames." *J. Struct. Eng., ASCE*, 135(1), 33–41.

Roeder, C.W., Lehman, D.E., Clark, K., Powell, J., Yoo, J.H, Tsai, K.C., Lin, C.H., and Wei, C.Y. (2011). "Influence of Gusset Plate Connection and Braces on the Seismic Performance of X-Braced Frames." *Earthquake Eng. And Struct. Dynamics*, 40(4), 355–374.

Sabelli, R., and Hohbach, D. (1999). "Design of cross-braced frames for predictable buckling behavior." *J. Struct. Eng., ASCE*, 125(6), 703–703.

Schellenberg, A. (2008). *Advanced Implementation of Hybrid Simulation*, Ph.D. Thesis, Dep. of Civil and Environmental Engineering, Univ. of California, Berkeley, CA.

Scot, M.H., and Fenves, G.L. (2006). "Plastic Hinge Integration methods for Force-Based Beam-Column Elements." *J. Struct. Eng., ASCE*, 132(2), 244–252.

Segal, F., Levy, R., and Rutenberg. A. (1994). "Design of Imperfect Cross-Bracings." *J. of Eng. Mech., ASCE*, 120(5), 1057–1075.

Shaback, J.B. (2001). *Behaviour of square HSS braces with end connections under reversed cyclic axial loading,* Master's thesis, Univ. of Calgary, Calgary, AL., Canada.

Simão, P.D., Girão Coelho, A.M., and Bijlaard, F.S.K. (2012). "Stability design of crane columns in mill buildings." *Engineering Structures*, 42, 51–82.

Simulia (2011). *Abaqus FEA*, www.simulia.com.

Spacone, E., Filippou, F.C., and Taucer, F.F. (1996). "Fiber beam-column model for nonlinear analysis of R/C frames, part I: Formulation." *Earthquake Eng. And Struct. Dynamics*, 25(7), 711–725.

Stoakes, C.D., and Fahnestock, L.A. (2012). "Influence of weak-axis flexural yielding on strong-axis buckling strength of wide flange columns." *Proc., Annual Stability Conference, SSRC*, Grapevine, Texas, April 17–20.

Stoakes, C.D., and Fahnestock, L.A. (2013). *Three-Dimensional Finite Element Simulation of the Seismic Behavior and Performance of Multi-Tier Braced Frames*, Interim report to the American Institute of Steel Construction, AISC.

Stoman, S.H. (1988). "Stability Criteria for X-Bracing Systems." J. of Eng. Mech., ASCE, 114, 1426–1434.

Stoman, S.H. (1989). "Effective length spectra for cross bracings." *J. Struct. Eng., ASCE*, 115, 3112–3122.

Tang, X., Goel, S.C. (1987). "*Seismic analysis and design considerations of braced steel structures*." UMCE 87-4 Report, Department of Civil Engineering, University of Michigan, Ann Arbor, MI.

Tremblay, R. and Stiemer, S.F. (1994). "Back-up Stiffness for Improving the Stability of Multi-storey Braced Frames under Seismic Loading." *Proc. 1994 SSRC Annual Techn. Session*, Bethlehem, PA, 311–325.

Trembaly, R., Timler, P., Bruneau, M., Filiatrault, A. (1995). "Performance of steel structures during the 1994 Northridge earthquake." *Can. J. Civ. Eng.*, 22, 338–360.

Tremblay, R., Bruneau, M., Nakashima, M., Prion, H.G.L., Filiatrault, A., DeVall, R. (1996). "Seismic design of steel buildings: lessons from the 1995 Hyogoken–Nanbu earthquake." *Can. J. Civ. Eng.*, 23, 727–756.

Tremblay, R., Robert, N. and Filiatrault, A. (1997). "Tension-Only Bracing: a Viable Earthquake-Resistant System for Low-rise Steel Buildings?" *Proc. SDSS '97 5th Intern. Colloquium on Stability and Ductility of Steel Structures*, Nagoya, Japan, 2, 1163–1170.

Tremblay, R. (2000). "Influence of Brace Slenderness on the Seismic Response of Concentrically Braced Steel Frames." *Behavior of Steel Structures in Seismic Area, Proc., STESSA 2000 Conference*, Edited by Mazzolani and R. Tremblay, Montreal, Canada, August, 527–534.

Tremblay, R. (2001). "Seismic Behavior and Design of Concentrically Braced Steel Frames." *Eng. J. AISC*, 38(3), 148–166.

Tremblay, R. (2002). "Inelastic seismic response of steel bracing members." *J. Constr. Steel Res.,* 58(5-8), 665–701.

Tremblay, R. (2003). "Achieving a stable inelastic seismic response for multi-story concentrically braced steel frames." *Eng. J. AISC,* 40(2), 111–129.

Tremblay, R., Archambault, M.H., and Filiatrault, A. (2003). "Seismic response of concentrically braced steel frames made with rectangular hollow bracing members. *J. Struct. Eng., ASCE*, 129(12), 1626–1636.

Tremblay, R., and Merzouq, S., (2004). "Dual buckling restrained braced steel frames for enhanced seismic response." *Proc., Passive Control Symp*., Tokyo Institute of Technology, Yokohama, Japan.

Tremblay, R. (2008). "Influence of brace slenderness on the fracture life of rectangular tubular steel bracing members subjected to seismic inelastic loading." *ASCE Structures Congress*, Vancouver, BC, Canada.

Tsai, C.Y., Tsai, K.C., Lin, C.H., Wei, C.Y., Wang, K.J., Yu, Y.J., and Wu, A.C. (2010). "Cyclic responses of three two-story seismic concentrically braced frames." *Front. Archil. Civ. Eng. China*, 4, 287–330.

Tsai, C.Y., Tsai, K.C., Lin, P.C., Ao, W.H., Roeder, C.W., Mahin, S.A., Lin, C.H., Yu, Y.J., Wang, K.J., Wu, A.C. (2013). "Seismic design and hybrid tests of a full-scale three-story concentrically braced frame using in-plane buckling braces." *Earthquake Spectra,* 29(3), 1043–1067.

Uetani, K., and Tagawa, H. (1998). "Criteria for suppression of deformation concentration of building frames under severe earthquakes." *Eng. J. AISC,* 20(4-6), 372–383.

Uriz, P. (2005). *Towards Earthquake Resistant Design of Concentrically Braced Steel Structures*, Ph.D. Thesis. Dept. of Civil and Environmental Engineering, Univ. of California, Berkeley, CA.

Uriz, P., and Mahin, S.A. (2008). *Towards earthquake resistant design of concentrically braced steel structures*, PEER 2008/08, Pacific Earthquake Engineering Research Center, University of California, Berkeley, CA.

Uriz, P., Filippou, F.C., Mahin, S.A. (2008). "Model for cyclic inelastic buckling for steel member." *J. Struct. Eng., ASCE*, 134(4), 619–28.

Wada, A., Qu, Z., Ito, H., Motoyui, S., Sakata, H., and Kasai, K. (2009). "Seismic Retrofit Using Rocking Walls and Steel Dampers." *ATC & SEI Conference on Improving the Seismic Performance of Existing Buildings and Other Structures, ASCE*.

Wakabayashi, M., Matsui, C., Minami, K., and Mitani, I. (1974). "Inelastic behavior of full-scale steel frames with and without bracings." *Building Disaster Prevention Research Institute*, Kyoto University, 24(216), 1–23.

Wakabayashi, M., Nakamura, T., and Yoshida, N. (1977). "Experimental studies on the elastic–plastic behavior of braced frames under repeated horizontal loading." *Building Disaster Prevention Research Institute*, Kyoto University, 27(251), 121–154.

Wang, D.Q., and Boresi, A.P. (1992). "Theoretical study of stability criteria for X-bracing systems." *J. of Eng. Mech., ASCE*, 118, 1357–1364.

Wijesundara, K.K., Nascimbene, R., and Rassati, G.A. (2014). "Modeling of different bracing configurations in multi-storey concentrically braced frames using a fiber-beam based approach." *J. Constr. Steel Res.*, 101, 426–436.

Yang, F., and Mahin, S.A. (2008). *Limiting Net Section Fracture in Slotted Tube Braces*, Steel Tips Series, Structural Steel Education Council, Moraga, CA.

Ziemian, R. (2010). *Guide to Stability Design Criteria for Metal Structures*, John Wiley & Sons, Inc., Hoboken, New Jersey.

APPENDICES

APPENDIX A – DEVELOPMENT OF AN MT-BF HYBRID TESTING PROGRAM

A1. General

An experimental program for cyclic and hybrid testing of columns part of CBFs and MT-BFs started in the fall 2014 at the Structural Engineering Laboratory of Polytechnique Montréal. The author was involved in this activity to develop a hybrid testing program for MT-BFs. In this appendix, the main objectives of the test program, the test setup, the column test matrix, the preliminary column testing, and the hybrid simulation development are presented.

A2. Objectives

As large-scale physical tests offer a robust method to assess the behaviour of steel structures under earthquake loading, an experimental program including the hybrid simulation of the MT-BFs was developed to: 1) implement hybrid simulation using MDHTS, 2) generate physical test data on MT-BF columns, and 3) verify the buckling response observed in the numerical study.

A3. Multi-Directional Hybrid Testing System

A3.1. Features

The Multi-Directional Hybrid Testing System (MDHTS) shown in Figure A.1 is an advanced large structural testing system specially designed to impose any combination of loads and deformations to the test specimen along 6 DOFs using a sophisticated control system. The system can be used to study the response of various structural components subjected to gravity and/or seismic loading effects by performing multi-axis static, quasi-static cyclic, pseudo-dynamic, or hybrid tests. Different end conditions including pinned, fixed, or semi-rigid condition can be reproduced using the movable upper platen of the system. The control system is capable of controlling the upper platen by specifying three translational and three rotational Degree-OF-Freedoms (DOFs) of the control point (on the upper platen) in either load- or displacement-controlled or combination of these two modes.

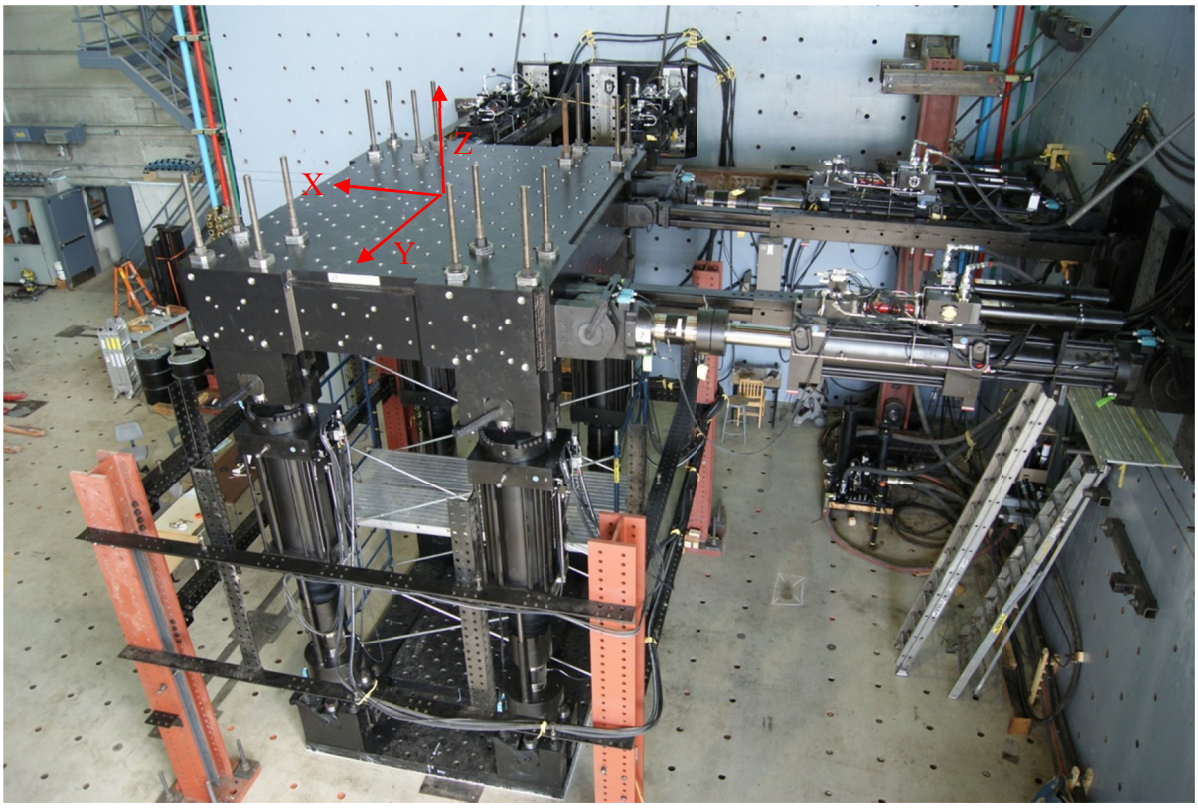

Figure A.1: Multi-Directional Hybrid Testing System at Polytechnique Montréal.

The MDHTS is capable of:

- applying complex multi-directional loading histories to the test specimens via control of the upper platen;
- reproducing different top end conditions;
- testing large-scale structural components such as building columns;
- loading in load- or displacement-controlled mode or combination of these two modes at any of the six DOFs;
- collecting applied loads as well as 3-Dimentional (3D) positional information using global and local displacement coordinates; and
- performing hybrid simulations.

A3.2. Components

As shown in Figure A.2, the MDHTS is attached to the L-shaped strong wall through four horizontal actuators and to the strong floor using four vertical actuators. The base attachment platen consists of a 140 mm thick steel plate (lower platen). The height of the vertical actuators can be increased using spacers, which accommodates specimens with total height varying between 4.0 and 8.0 m. The main components of the MDHTS are summarized as follows:

- Four 1800 kN, ± 300 mm stroke vertical actuators (Figure A.2);
- Four 1000 kN, ± 375 mm stroke horizontal actuators (Figure A.2);
- Upper and lower steel platens with 625 and 140 mm thicknesses respectively (Figure A.2);
- 12-Channels MTS Flextest 200 (494) Multi-Directional Controller;
- Hydraulic Control and Configuration (HCC) System; and
- Data Acquisition System (DAQ).

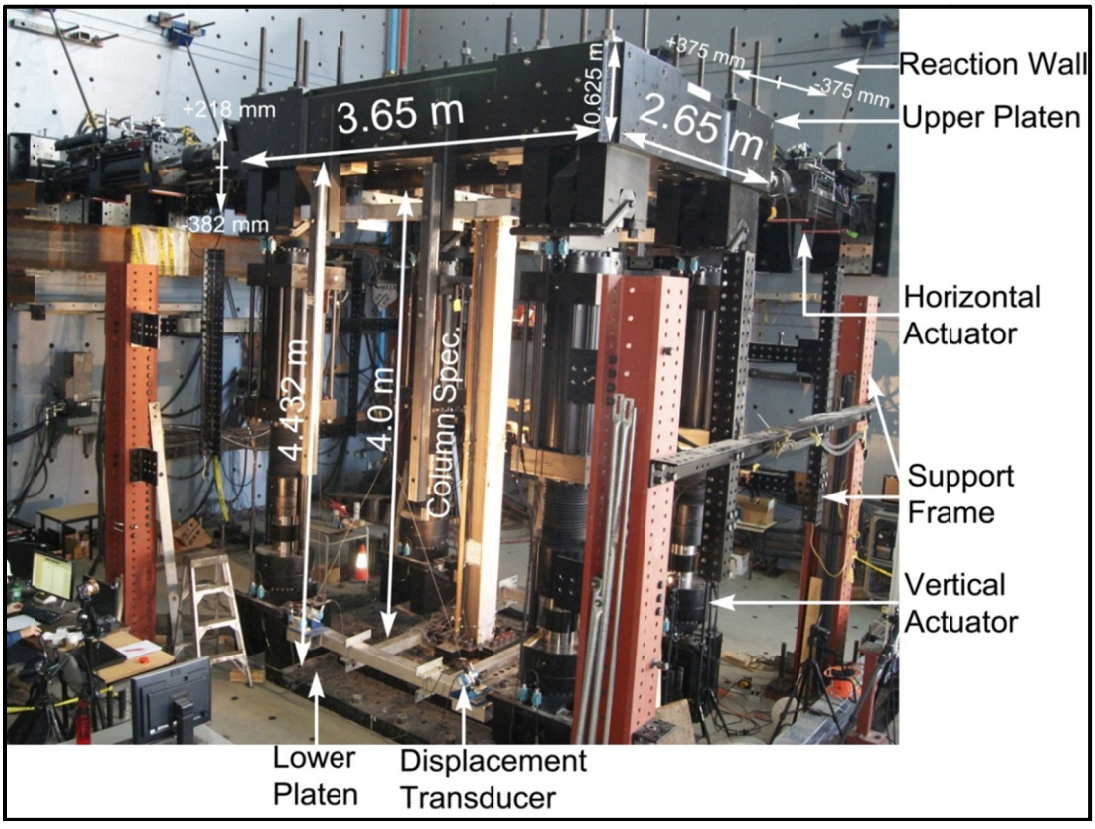

Figure A.2: Components of Multi-Directional Hybrid Testing System.

A3.3. Capacity

Total translational and rotational capacities of the MDHTS can be obtained based on the force and stroke capacities of each actuator. Table A.1 gives the total translational capacity of the system in each DOF.

Table A.1: Translational capacity of the MDHTS.

Plane	**Vertical**	**Vertical**	**Horizontal**	**Horizontal**
Axis	**Z**	**Z**	**X & Y**	**X & Y**
Force (kN)	± 7200		± 2000	
Displacement (mm)		± 300		± 375

The rotational capacity of the MDHTS is presented in Table A.2 about three axes of rotation. The moments and rotations were calculated assuming that the specimen is centered in the machine. Moment capacities are given in ranges as the horizontal actuators can be at their lowest or highest levels.

Table A.2: Rotational capacity of the MDHTS.

Plane	**Vertical**	**Vertical**	**Horizontal**
Axis	**X-X**	**Y-Y**	**Z-Z**
Moment (kN-m)	±19980 to ±28980	±16380 to ±25380	±5000
Rotation (radian)	± 0.122	± 0.122	± 0.122

A4. Finite element analysis

3D finite element model of the MDHTS was created in the *Abaqus* program (Simulia 2011) with eight-node solid elements. The concrete strong floor of the laboratory was included in the model. The actuators were not considered in this model; they were replaced by concentrated loads acting in the directions of their longitudinal axes. The column specimen was also included in the model. This model was analyzed, under various critical loading conditions representing the loading protocol developed for the column specimens, to verify the stress levels in the connection plates, bolts, lower and upper platens. Furthermore, the influence of the connecting plate and/or bolt slip

on the stiffness and buckling load of the column specimens was determined. Figures A.3a and A.3b show the finite element model of the machine and column bottom connection, respectively.

a)

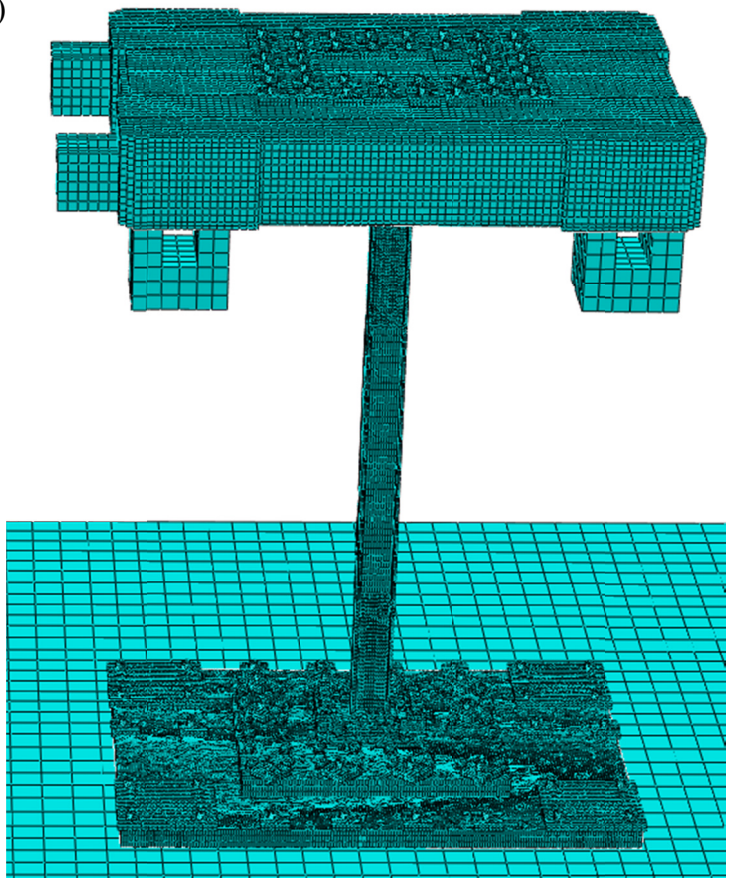

b)

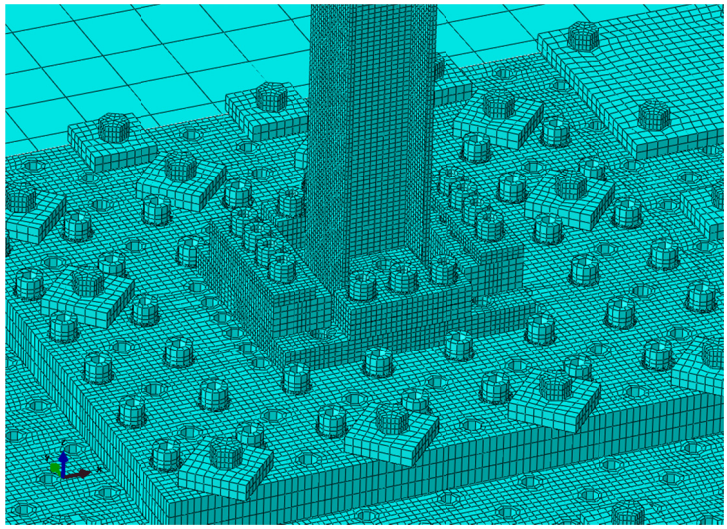

Figure A.3: a) Finite element model of MDHTS; and b) Column end connection to the lower platen.

Several worst-case loading conditions were studied to check the stresses in the system. Figure A.4 shows one of these conditions, where the upper platen was pushed up to a lateral displacement corresponding to the storey drift of 12%. Strong axis bending was selected because of larger uplift and overturning moments induced in the platens. Elastic material properties were assigned to the column. Von Mises stresses did not exceed the yielding stress in any one of the bolts, anchors, connecting plates, or platens.

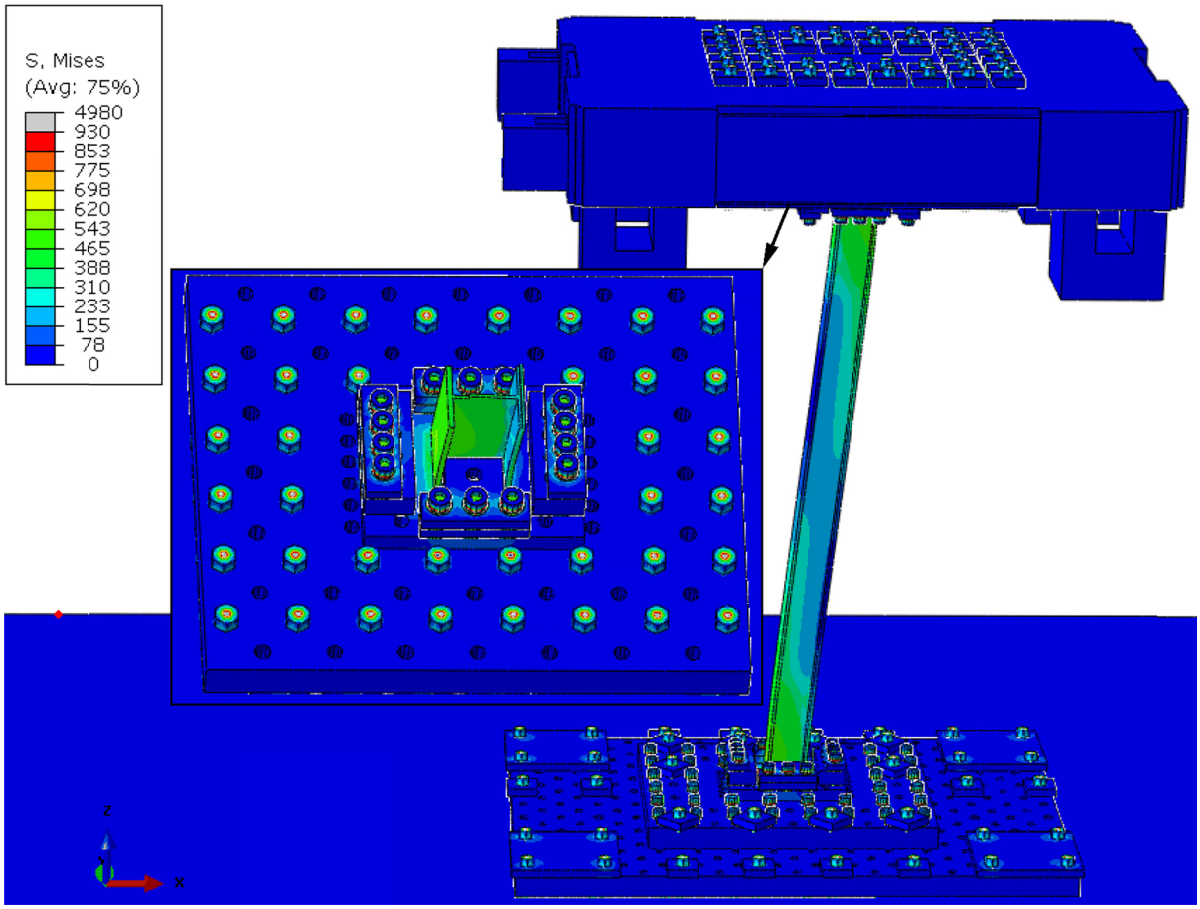

Figure A.4: Von Mises stress in the platens induced under storey drift of 12% in strong axis of the column (MPa).

Column buckling was also studied for the weak-axis flexural buckling mode to ensure that the test results would be promising. For this analysis, elastic properties were assigned to the column specimen. Figure A.5a shows the buckled shape of the column when the upper platen was loaded

toward the lower platen in a displacement controlled analysis. A comparison (Figure A.5b) was made between the theoretical value and finite element analysis results for the elastic buckling load of the column specimen to verify if the connecting plates can provide sufficient fixity for the specimen. The effective length factor of the column specimen was obtained equal to 0.53, which is 6% less than the ideal fixed-fixed condition. A 6% reduction was also observed for the axial stiffness when comparing it to the theoretical value (Figure A.5c).

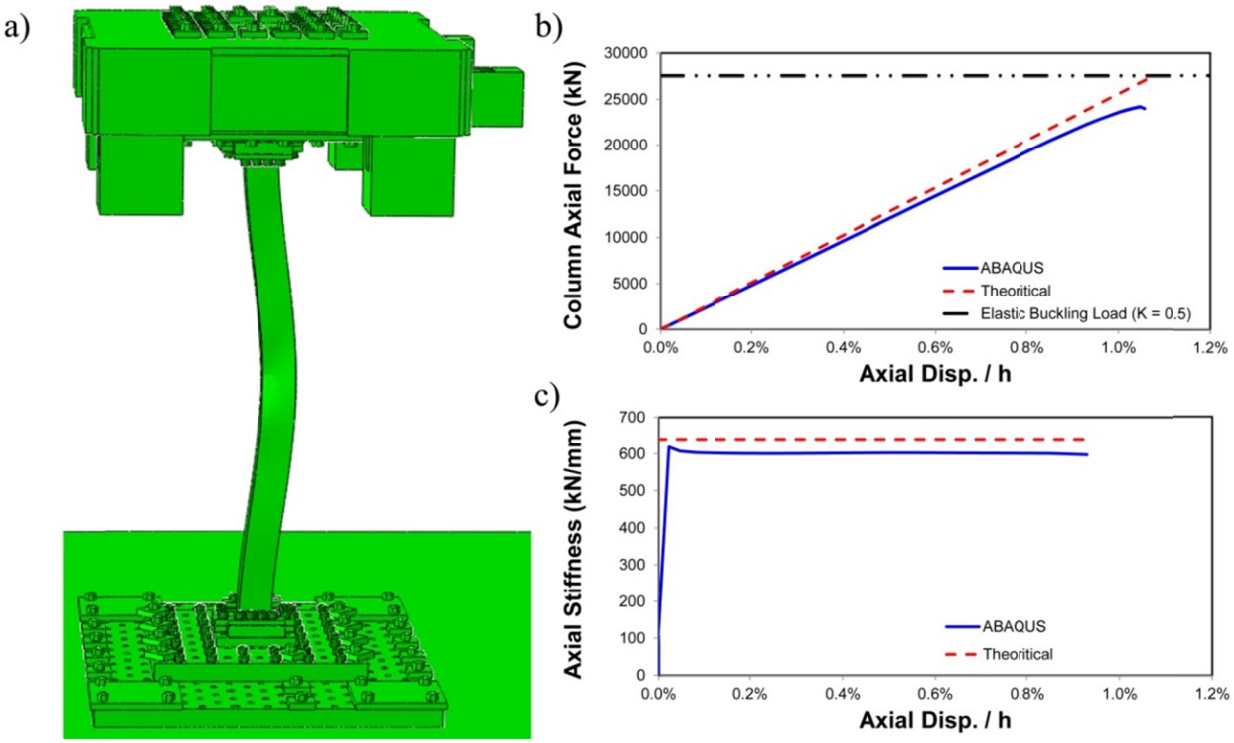

Figure A.5: Axial displacement analysis: a) Buckled column in the MDHTS; and b) Column axial force-axial displacement; and c) Elastic axial stiffness of the column (*h* is the column height equal to 4000 mm).

In order to verify the flexural stiffness of the column specimen in the MDHTS, a pushover analysis was performed by applying a lateral displacement to the upper platen. The weak-axis bending was considered and inelastic material properties were assigned to the specimen. Figure A.6 shows the result for this analysis. The comparison between the lateral stiffness and theoretical stiffness of the

column including shear and flexural deformations indicates 10% lower stiffness for the column in the MDHTS, which is attributed to the deformations of the bolts and the connecting plates.

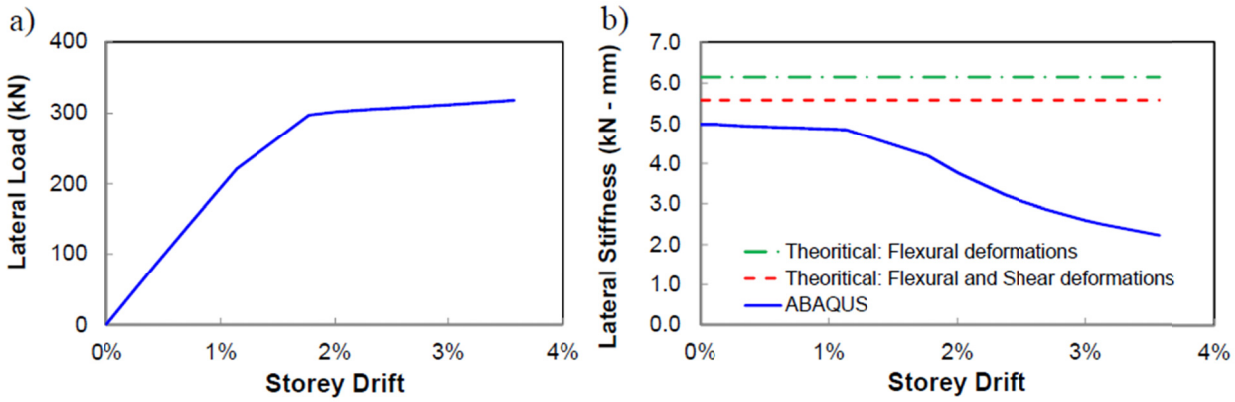

Figure A.6: Lateral displacement analysis: a) Column lateral force-storey drift; and b) Column lateral stiffness-storey drift.

A5. Column test matrix

Design of the test specimens was performed by studying a group of multi-tiered CBFs ranging between 2- and 6-tiers. In total, 135 and 90 MT-BFs were designed in accordance with the CSA S16-09 provisions (2009) and the AISC Seismic Provisions (2010), respectively, by changing the number of tiers, frame height, tier height ratio, and frame ductility. Then, W-shaped sections that are commonly used for the columns were identified and scaled down such that the scaled columns have the minimum standard deviation when comparing their overall slenderness (KL/r) and width-to-thickness (b/t_f, h/t_w) ratios to those of unscaled members. Figure A.7 shows the MT-BF columns as a function of the flange width (b) and depth (d). The W250x101 and W610x195 column specimens were selected for this test program, because they were representative of the most frequent MT-BF columns with square and deep sections respectively (Figure A.7). Both sections meet the requirements of width-to-thickness ratio for seismic design and are in Class 1 according to the requirements of CSA S16 (2014) and highly ductile categories according to the AISC Seismic Provisions, respectively. Also, these columns satisfy the limitation of the test setup as discussed earlier in this appendix. The test matrix of the W250x101 column specimens is shown in Table A.3. Fourteen identical W250x101 columns made of ASTM A992 steel with nominal yield stress F_y =

345 MPa were selected for the preliminary test program. The specimens are 4000 mm tall and represent the first storey column of CBF buildings or the first/second tier column of 2-tiered CBFs. The test matrix for the deep W610x195 sections has not been developed yet.

Table A.3: Column test matrix.

Test	Type	End condition	Axial Loading	Lateral Loading
CS1	Monotonic	Fixed-Fixed	Displacement	
CS2	Cyclic	Pinned-Fixed	Force	Displacement in weak-axis
CS3	Cyclic	Pinned-Fixed	Force	Displacement plus rotation in strong-axis
CS4	Cyclic	Pinned-Fixed	Force	Displacement plus rotation in weak-axis
CS5	Cyclic	Fixed-Fixed	Force	Displacement in weak-axis
CS6	Cyclic	Fixed-Fixed	Force	Displacement in weak-axis
CS7	Seismic	Pinned-Fixed	Force from NLRH analysis	Displacement and rotation in strong-axis from NLRH analysis
CS8	Seismic	Pinned-Fixed	Displacement from NLRH analysis	Displacement and rotation in weak-axis from NLRH analysis
CS9 & CS10	Seismic	Pinned-Fixed	Displacement from NLRH analysis	Displacement and rotation in strong-axis from NLRH analysis
CS11 – CS14	Hybrid	Pinned-Fixed		

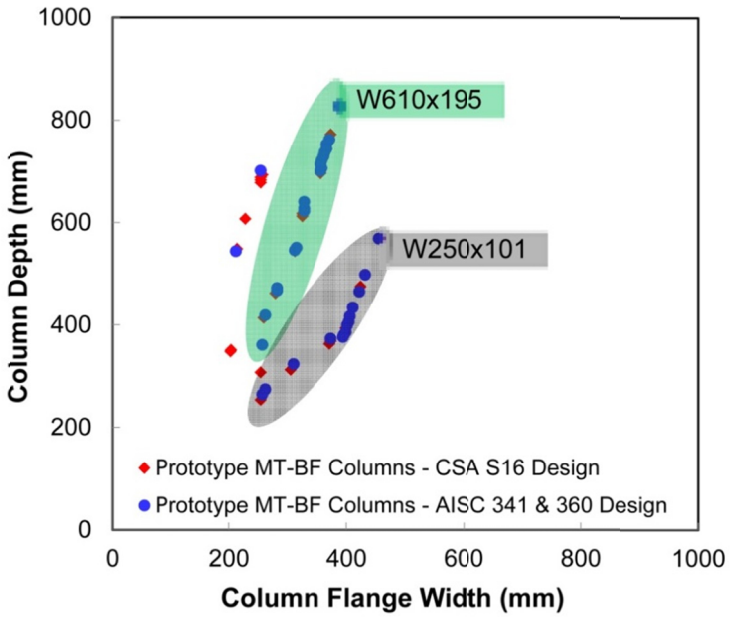

Figure A.7: Variation of prototype MT-BF columns with depth and flange width.

For the preliminary W250x101 column test program (smaller specimens), column base plates were designed to provide the complete fixity. A 76 mm thick base plate was considered at each end of the specimen. Column web and flanges were fillet welded to the base plate (Lee et al. 2008a, 2008b; Myers et al. 2009; Kanvinde 2014). The specimens were attached to the top and bottom platens of the test setup with 14 high-strength bolts per base plate.

A6. Preliminary column testing

As of now, eight specimens of Table A.3 including CS1 to CS8 have been tested under monotonic and cyclic loadings. Buckling response of the steel W-shape columns was studied in this testing program. The test specimens were also used to initiate the MDHTS and evaluate several aspects of the testing machine including the test setup and the controller system. Evaluation of the test results for the specimens tested under monotonic or cyclic loadings showed that the measured forces were always larger than the expected forces under the applied displacements or rotations. Figure A.8a shows the test specimen CS6. For this test, a fixed axial force of 4146 kN (0.9 P_n) was applied to the specimen at the beginning of the test and maintained during the cyclic displacements corresponding to the loading protocol specified for prequalification of beam-to-column connections in Appendix K of the AISC Seismic Provisions. The column bucked in the displacement cycle of 2% storey drift (Figure A.8b). The measured lateral force-lateral displacement (for the weak-axis direction) and the numerical prediction are plotted in Figure A.8c. In the figure, the results of the last cycle were removed from the plot to ease comparison between the forces. The large differences observed between the forces in the two plots are attributed to the frictional forces that developed in the system, which increased the value of the measured forces.

As shown in Figure A.8c, the development of the frictional force is approximately similar in negative and positive directions of the applied displacements. Additionally, the friction forces are independent of the amplitude of the displacement applied to the specimen.

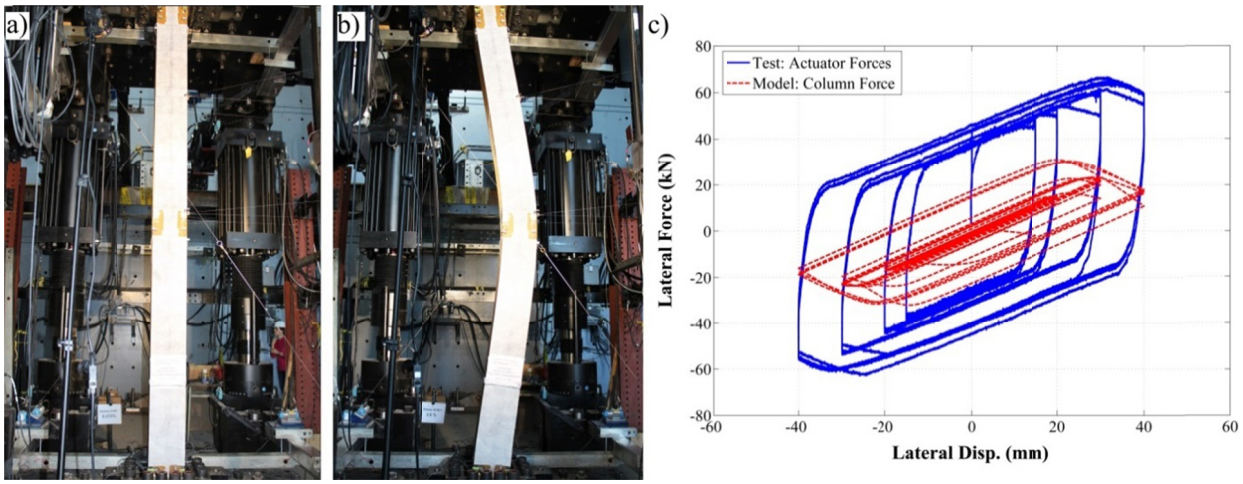

Figure A.8: Test specimen CS6: a) Specimen before the test; b) Buckled shape; and c) Comparison of the measured forces from the test and column force from the *OpenSees* prediction.

A7. Development of MT-BF hybrid testing

The computational model of the MT-BF created in the *OpenSees* program (McKenna and Fenves 2004) was modified to include the experimental element representing the column specimen in the laboratory. The *OpenFresco* program (OpenFresco 2012) was used as a middleware to connect the computational model of the frame to the physical sub-structure (the column specimen). Purely numerical hybrid simulations were performed to ensure that the physical substructure is correctly linked to the computational model. In these analyses, the column specimen was simulated using the MTS 793 Software and MTS Simulation Interface (CSI) (MTS 2015) with elastic properties. The analysis results were compared to those obtained from numerical *OpenSees* models to ensure that the physical substructure is correctly linked to the computational model. The selection of the numerical integrator and the integration time step for the hybrid simulation was also verified through these analyses. Figure A.9 compares the history of results between the numerical analysis and purely numerical hybrid simulation for a 2-tiered CBF designed based on 2010 AISC Seismic Provisions. As shown, the purely numerical hybrid simulation provides results that are identical to the numerical response history analysis. Larger residual deformations developed in the numerical model because column buckling is not captured by the purely numerical hybrid simulation with an elastic experimental element.

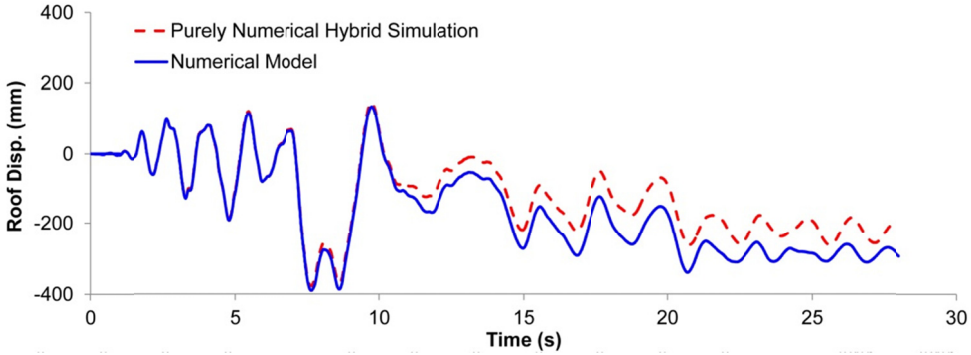

Figure A.9: Roof displacement from the nonlinear response history analysis of the numerical model and purely numerical hybrid simulation model for a 2-tierd CBF under 1971 San Fernando LA - Hollywood Stor record.

The hybrid simulation was then performed in the laboratory with the actual experimental specimen. A schematic diagram of the hybrid simulation loop is shown in Figure A.10 for a 2-tierd concentrically braced frame. As shown, frictional forces developed in the system add to the test specimen resistance and increase the measured forces sent to the finite element model as feedback signals. The increased force feedbacks then lead to produce deformations, in the numerical model, not consistent with the deformed shape state of the physical specimen. This would cause unrealistic displacement commands generated for the next step of the analysis, because the internal forces in the physical specimen do not match the measured forces. This inconsistency in the command and feedback signals should be properly addressed when performing hybrid simulation with the MDHTS. One solution to this problem is to compensate for the friction forces during the hybrid simulation. For this purpose, friction forces should be first estimated and then a suitable friction compensation model should be introduced between the MDHTS controller and the numerical model.

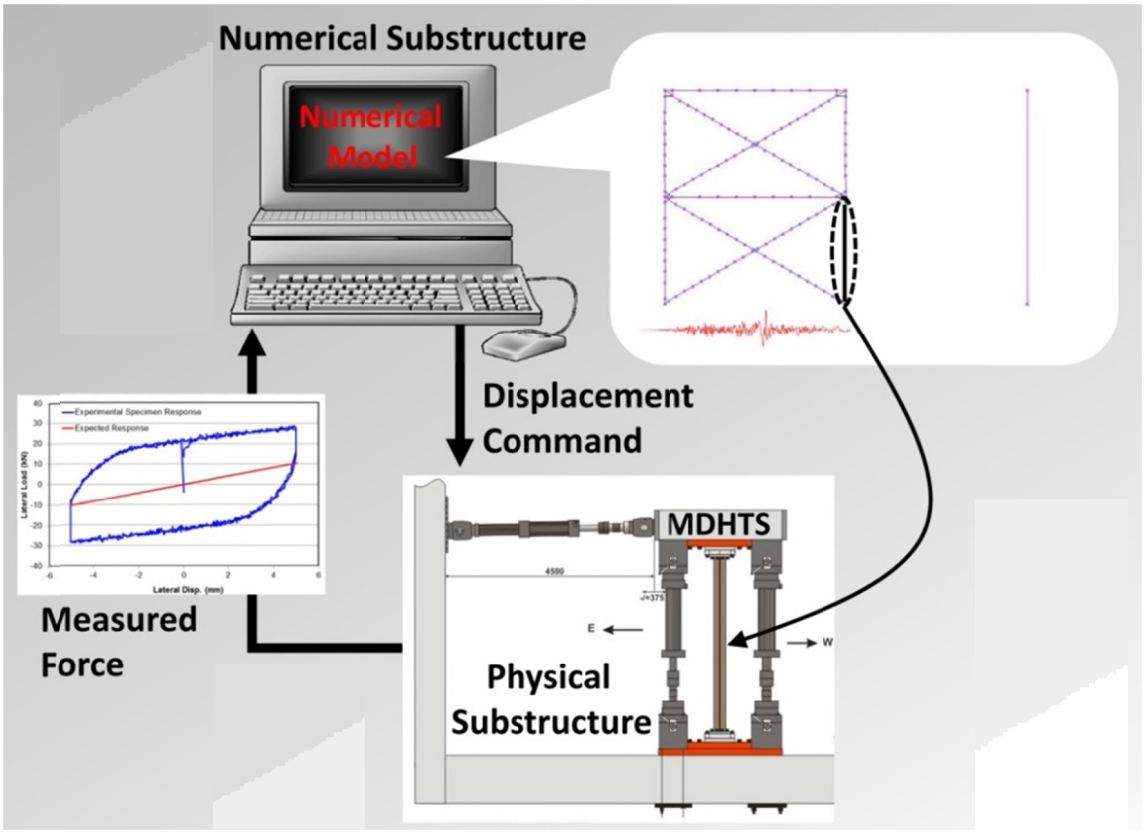

Figure A.10: Schematic diagram of the hybrid simulation loop using the MDHTS.

Friction was characterized by running cyclic tests with different levels of column axial forces in all DOFs. Applied axial forces ranged between –2500 kN and +2500 kN with an interval of 500 kN. The tests were performed in the displacement-controlled mode. Figure A.11 shows the lateral forces measured by the system controller at X-axis when the cyclic displacement is applied in the same direction for various levels of axial forces. The expected response of the specimen is also shown in these plots to highlight the friction forces generated in the system. These results indicate that the friction force depends on the level of axial force applied in the specimen. Additionally, the friction force is not identical to the axial forces in tension and compression. A similar response was observed for the other DOFs.

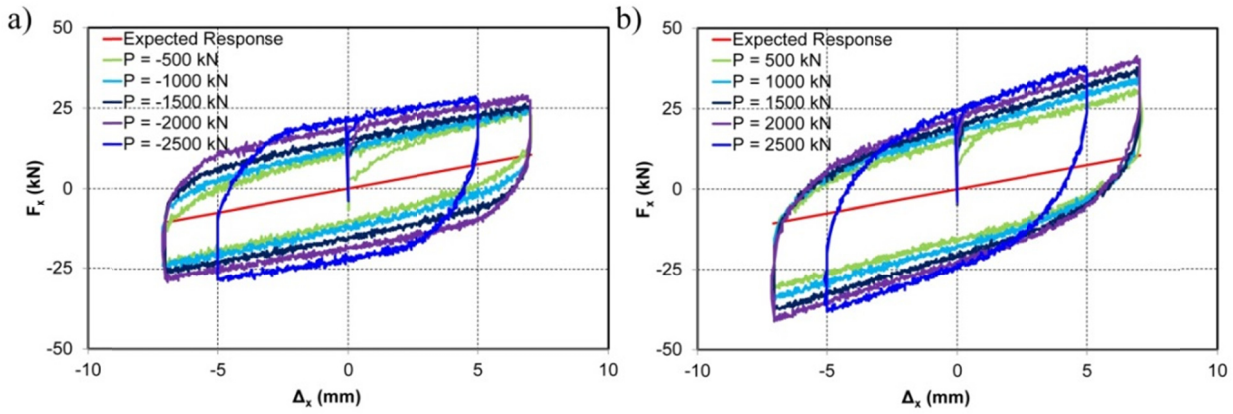

Figure A.11: Measured forces in X-axis by varying axial forces: a) in compression; and b) in tension.

Hence, for a given displacement or rotation, the friction force was estimated along the corresponding DOF by removing the expected force of the specimen from the measured values. Figure A.12 gives the results of forces generated in X and Y-axes, and the moment generated about Y-axis when an axial compression force equal to 500 kN is applied. As shown in the plots, the hysteretic of the friction response represents an elastic-perfectly plastic behaviour under the cyclic loadings. This means that the maximum force values in Figure A.12 can be used to reproduce the friction force using any elastic-perfectly plastic material model. Linear interpolation was adopted for axial load levels expected in the column tests (P > 2500 kN and P < -2500 kN) but that were not covered in the friction tests. Figure A.13 shows the variation of the maximum friction force against the applied axial load in the specimen.

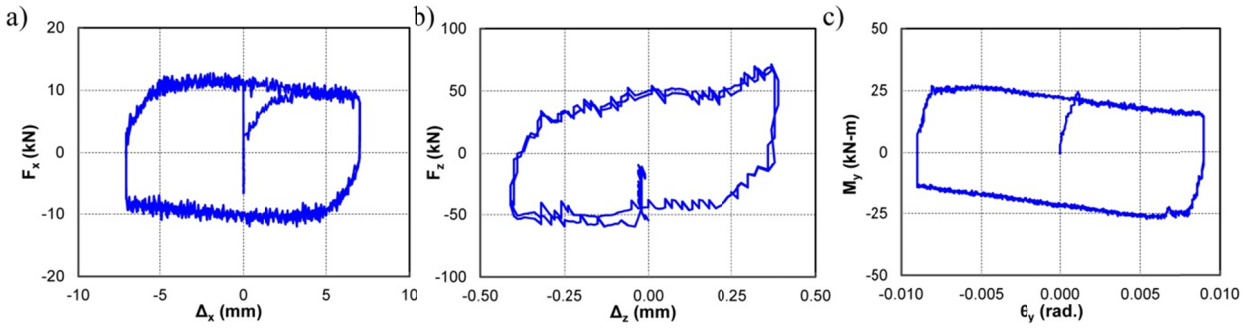

Figure A.12: Friction force generated in MDHTS under axial compression force of 500 kN: a) Shear force-lateral displacement in X-axis; b) Axial force-axial displacement in Z-axis; and c) Moment-rotation about Y-axis.

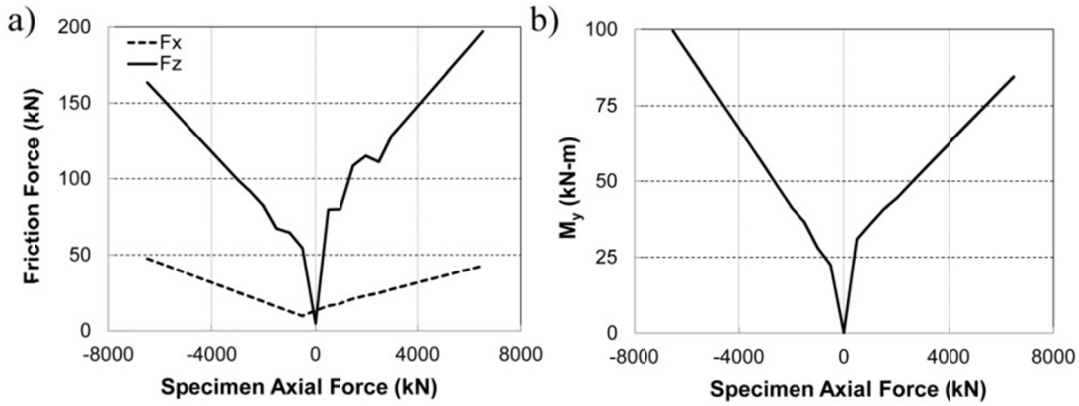

FigureA.13: Variation of friction force with applied axial force: a) Shear force in X-axis and axial force in Z-axis; and b) Moment about Y-axis.

In the next step, a 3D fiber element model of the MDHTS was programmed in the *OpenSees* program to compensate for the friction force for the hybrid simulation. As shown in Figure A.14, the model includes elasticBeamColumn elements for vertical and horizontal actuators, elasticBeamColumn elements with rigid properties to connect the actuators to the upper platen, and springs to connect the actuators to the rigid elements, strong wall or strong floor. These springs were modeled using zeroLength elements and represent the actuator swivels. The actuators were considered fixed at their ends facing the strong wall or strong floor. The upper platen was modeled using elasticBeamColumn elements with rigid properties. The flexural stiffness of actuators elements was obtained from the hysteretic of the friction force by approximately connecting the negative and positive plateaus. For these elements, a negligible value was assigned for the axial and torsional stiffness. For the zeroLength elements, rigid properties were assumed for the torsional, shear and axial stiffness, whereas elastic-perfectly plastic material was assigned to two rotational DOFs. The flexural strength and stiffness assigned to this material was obtained by transforming the friction resistance and stiffness (from hysteretic response shown in Figure A.12) to flexural moments and stiffness in the swivels by means of the virtual work principle. For instance, the friction force generated in the system due to the applied displacement in Y-axis results in flexural moments about X-axis in the swivels of the vertical actuators.

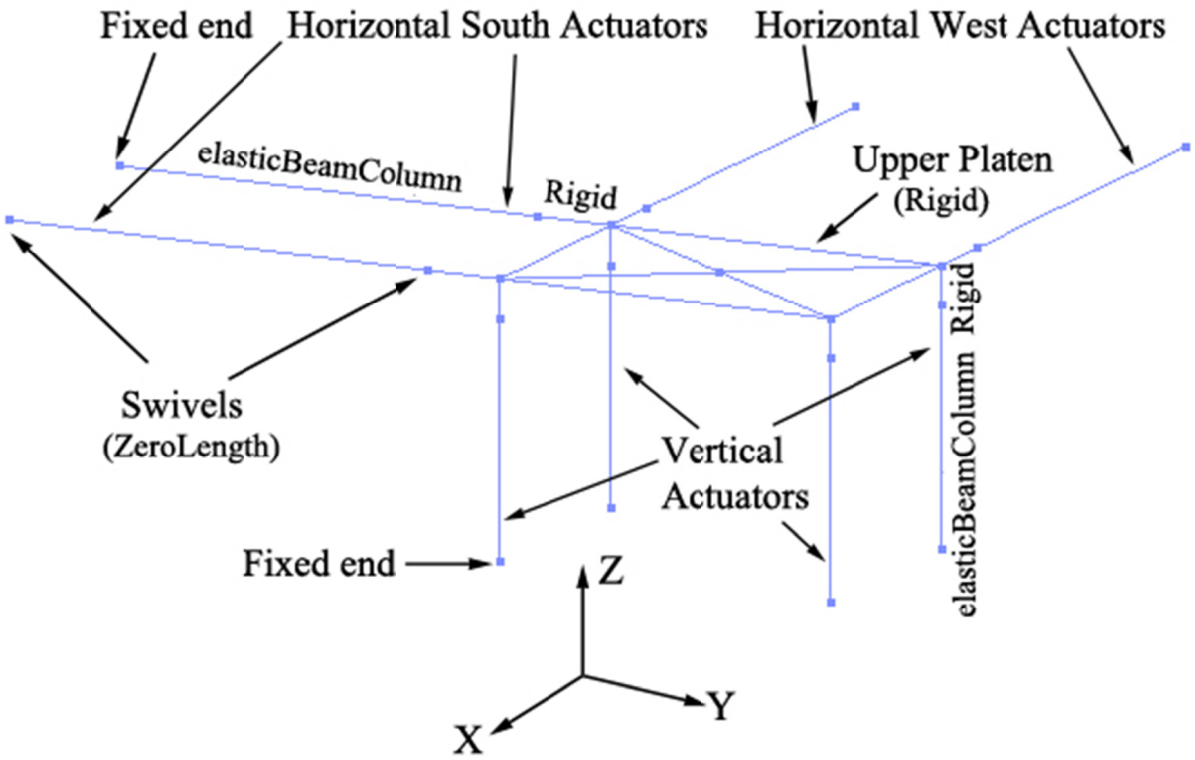

Figure A.14: Numerical model of the MDHTS in *OpenSees*.

A calibration study was then performed on the model. Cyclic displacements were applied in the *OpenSees* model with zero axial force. The resultants of the actuator reactions were compared against the test results. Figure A.15 illustrates comparisons for the shear force in X-axis, axial force in Z-axis, and moment about Y-axis. The results showed that the model can properly reproduce the friction in the system.

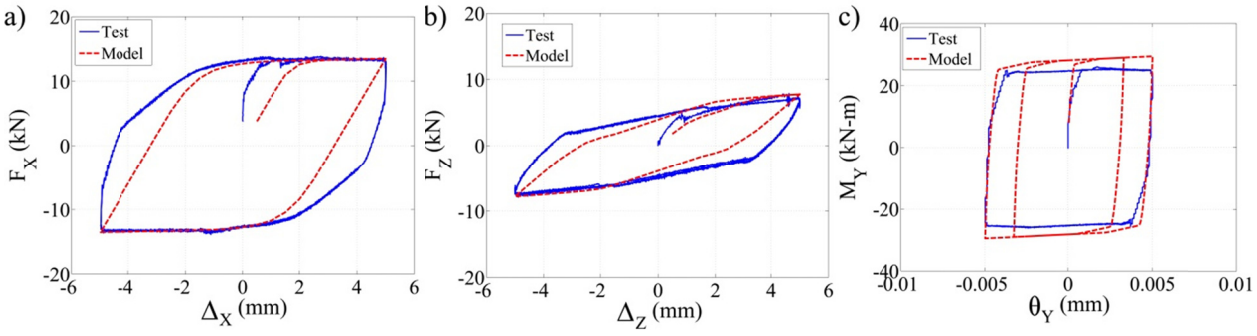

Figure A.15: Friction force generated in MDHTS: a) Shear force-lateral displacement in X-axis; b) Axial force-axial displacement in Z-axis; and c) Moment-rotation about Y-axis.

Once the friction force is determined and the numerical model of the MDHTS is created, several approaches were examined to compensate for the friction forces in the hybrid simulation. These approaches are summarized as follows:

- The numerical model of the MDHTS was included in the computational model of the sub-structure. In the model, the center of the upper platen (the MDHTS control point) was constrained to the displacements and rotations of the top of the experimental element in the numerical sub-structure. By applying seismic loading in the model, actuator swivels rotate to accommodate the movement of the upper platen and result in generating reaction forces in the MDHTS model. However, it was found that the additional forces generated by the machine model were added to the feedback signal received by the experimental element. Further investigation of this strategy was halted after analyzing the data obtained from the hybrid simulations.
- A friction compensator model was programed in Mathworks Simulink (MathWorks 2012) using the Steel02 material base code of *OpenSees* which reproduces the hysteretic response of the friction force in the direction of interest. This model is included in the xPC Target Hybrid Controller (Schellenberg 2008) as shown in Figure A.16. In the model, the feedback signals are used as input for the friction model. In the model, the force feedbacks are corrected by removing the friction force for a given displacement command at each DOF. Three approaches were studied to reproduce the friction force in the Simulink model:
    - Displacements and rotations of the upper platen (displacement feedbacks) were imported in the model and shear forces and moments were produced to correct the feedback signals. The main disadvantage of this model was that the friction forces are reproduced from displacements and rotations of the upper platen and not generated from the rotations of the swivels where the friction is basically developed. This results in ignoring the interaction between the translational and rotational DOFs, meaning that a unit rotation of the upper platen in X-axis can produce shear forces and moments in all 6DOFs which were not considered in this approach.
    - To overcome the limitations of the previous approach, rotations of the swivels were calculated at a given displacement feedback using the geometry of the system. The

rotations were then used to generate moments in the swivels. These moments were then transformed to the shear forces and moments representing the friction forces.

- In the third approach, a series of material model as a function of the axial load was employed in the *OpenSees* model of the MDHTS. The model was then analyzed under the expected axial force, displacement, and rotation demands to generate a library of the friction force data. These results were then used as input for the Simulink model such that appropriate friction forces are selected from the library for a given set of axial load, displacement and rotation applied on the specimen.

The verification and refinement of last two approaches are the subject of an ongoing research study at Polytechnique Montréal.

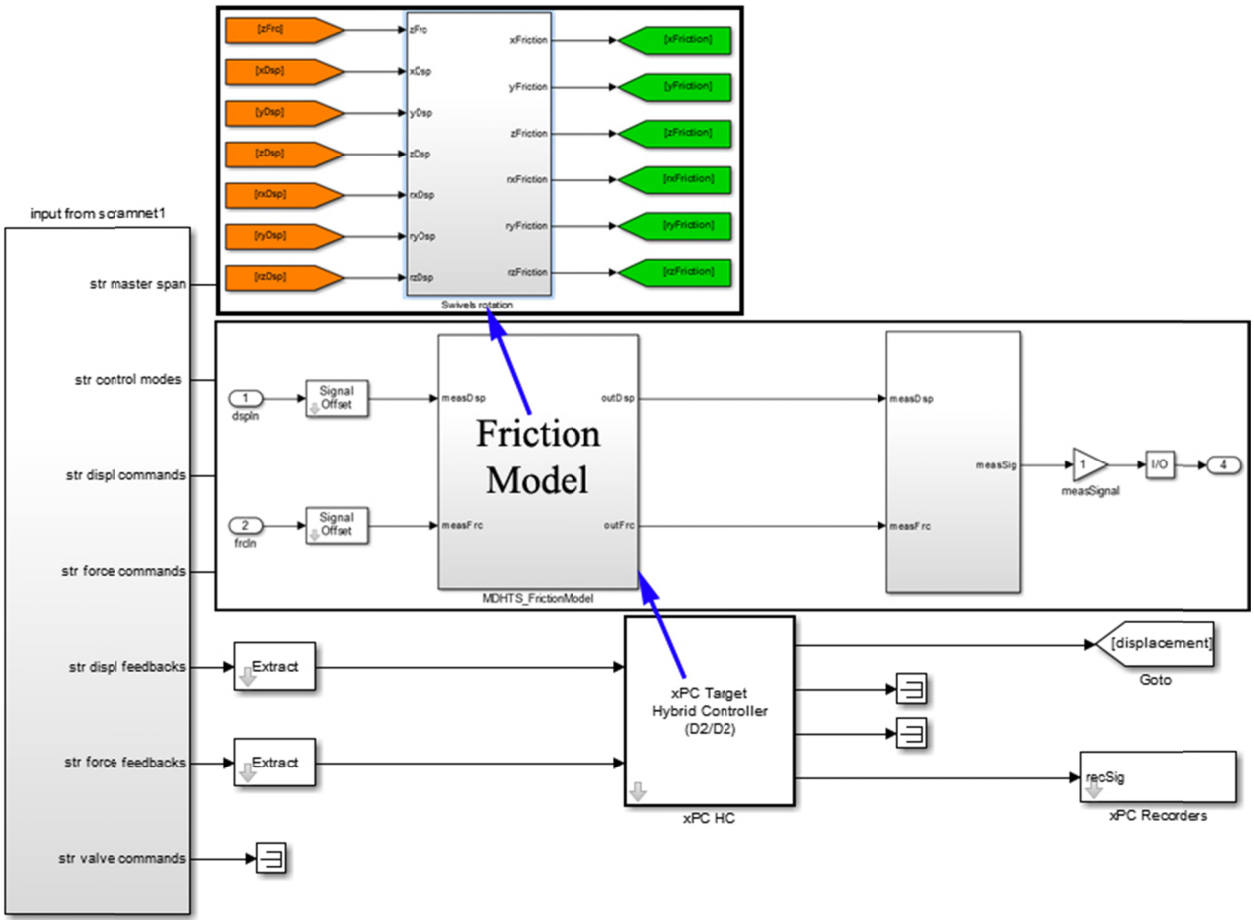

Figure A.16: Simulink model for numerical simulation of friction for hybrid simulation.

A8. Conclusions

A hybrid testing program was developed for MT-BFs using new MDHTS at Polytechnique Montréal. This program is expected to evaluate the seismic behaviour of MT-BFs focusing on the column buckling response. The columns are subjected to axial force and weak axis/biaxial bending moments. The main features, components and capacity of the MDHTS were reviewed. The 3D finite element analyses of the system were performed to evaluate the local and global behaviour of the systems' components under critical loading cases expected in the experimental program. The results showed that the test setup is capable of providing the expected boundary conditions within the acceptable error margin. The column test matrix was presented. In this test program, a group of MT-BFs were designed in accordance with the Canadian and the U.S. design standards and the experimental specimens, W250x101 and W610x195 columns, were selected such that they cover a wide range of the columns used in these frames. The computational model for the hybrid testing of MT-BFs was developed. The hybrid testing includes a steel W-shape as column part of an MT-BF (the physical sub-structure) and the rest of the frame simulated in the *OpenSees* program (the numerical sub-structure). The *OpenFresco* program was used as a middleware to connect the computational model of the frame to the physical sub-structure. Purely numerical hybrid simulations were successfully performed using the hybrid simulation model. The analysis results verified that the physical substructure is correctly linked to the computational model. Preliminary testing revealed the presence of frictional forces developed in the MDHTS. The main challenge expected in the hybrid simulation was the consideration and treatment of those frictional forces. The forces were identified for each DOF. It was found that the friction force depends on the amount of the axial load applied on the specimen. In order to reproduce the friction force, an *OpenSees* model of the MDHTS was developed where an elastic-perfectly plastic material was assigned to the spring elements representing the actuator swivels. The model was capable of reproducing the friction force measured in the system. Four approaches were examined to address the friction force using an *OpenSees* model of the MDHTS and models programmed in Simulink. In the Simulink model, the Steel02 material base code of *OpenSees* was introduced to generate the friction force. It was found that the approaches that use displacements and rotations of the upper platen as input data did not compensate for the friction force. However, the Simulink model in which the friction forces' developing in each of the actuator swivels is needed to properly represent the test apparatus response. This approach is being extensively investigated in an ongoing research program.

APPENDIX B – DETERMINATION OF THE MINIMUM NUMBER OF YIELDING TIERS IN SUB-STRUCTURING TECHNIQUE

In the sub-structuring technique proposed in Chapter 7, the minimum number of yielding tiers, n_y, dictates the number of analysis steps. An equation was proposed to determine the height h_y over which brace tension yielding must propagate to limit critical tier drift, Δ_{cr}. In this appendix, detailed derivation of this equation is illustrated. The elastic-beam theory was used by integrating twice the bending moment, M. The 5-tiered braced frame of Figure 7.6a is shown again in Figure B.1a. To obtain critical tier drift for a roof displacement corresponding to Δ_{inel} (the portion of the anticipated story drift that develops after brace tension yielding has initiated in the critical tier), the equation of the elastic curve should be first defined. The isolated column used to obtain the critical tier drift is shown in Figure B.1b. The relationship between the internal moment and column lateral deformation, ν, due to the lateral load P is a second-order differential equation as follows:

$$\text{(B1)} \qquad \frac{d^2\nu}{dx^2} = \frac{M}{EI}$$

where EI is the flexural stiffness of the column for weak-axis bending.

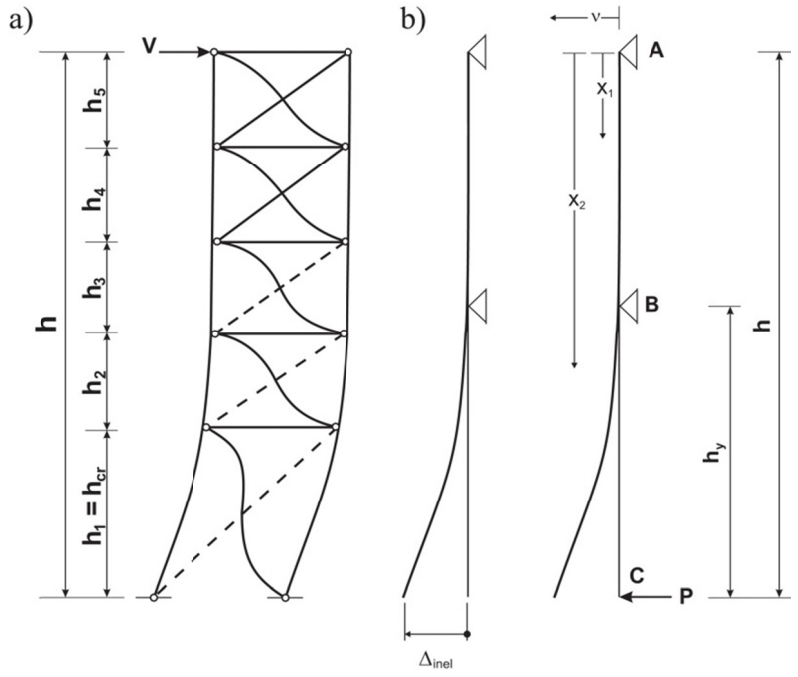

Figure B.1: a) Frame deformed shape in the sub-structuring technique for bottom up brace yielding sequence; and b) Deformed shape assumed to obtain critical tier drift.

Applying this equation for $0 \le x_1 \le h\text{-}h_y$ and $h\text{-}h_y \le x_2 \le h$ and integrating twice yield:

$$\text{for } x_1: \quad \frac{d^2\nu}{dx^2} = -\frac{M_1}{EI}$$

$$\frac{d^2\nu}{dx^2} = -\frac{1}{EI}\left[\frac{Ph_y}{h-h_y}x_1\right]$$

$$\frac{d\nu}{dx} = -\frac{1}{EI}\left[\frac{Ph_y}{h-h_y}\frac{x_1^2}{2} + A_1\right] \tag{B2}$$

$$\nu = -\frac{1}{EI}\left[\frac{Ph_y}{h-h_y}\frac{x_1^3}{6} + A_1x_1 + A_2\right]$$

$$\text{for } x_2: \quad \frac{d^2\nu}{dx^2} = -\frac{M_2}{EI}$$

$$\frac{d^2\nu}{dx^2} = -\frac{1}{EI}\left[P\left(x_2 - h\right)\right]$$

$$\frac{d\nu}{dx} = -\frac{1}{EI}\left[P\frac{x_2^2}{2} - Phx_2 + A_3\right] \tag{B3}$$

$$\nu = -\frac{1}{EI}\left[P\frac{x_2^3}{6} - Ph\frac{x_2^2}{2} + A_3x_2 + A_4\right]$$

The four constant of integration are determined using three conditions and one continuity equation as follows:

$$\begin{aligned}
&\nu_1\left(x_1 = 0\right) = 0\\
&\nu_1\left(x_1 = h - h_y\right) = 0\\
&\nu_2\left(x_2 = h - h_y\right) = 0\\
&\nu_1'\left(x_1 = h - h_y\right) = \nu_2'\left(x_2 = h - h_y\right)
\end{aligned} \tag{B4}$$

Applying the equations of B4 and solving for four constants give:

$$A_1 = \frac{Ph_y\left(h-h_y\right)}{6}$$

$$A_2 = 0$$

(B5)
$$A_3 = \frac{P\left(h-h_y\right)\left(3h+h_y\right)}{6}$$

$$A_4 = -\frac{Ph\left(h-h_y\right)^2}{6}$$

Once the constants of Eqs. B2 and B3 are known, lateral displacement of the isolated column can be expressed as a function of x:

(B6)
$$for\ x_1: \qquad \nu = -\frac{1}{EI}\left[\frac{Ph_y}{h-h_y}\frac{x_1^3}{6}+\frac{Ph_y\left(h-h_y\right)}{6}x_1\right]$$

$$for\ x_2: \qquad \nu = -\frac{1}{EI}\left[P\frac{x_2^3}{6}-Ph\frac{x_2^2}{2}+\frac{P\left(h-h_y\right)\left(3h+h_y\right)}{6}x_2-\frac{Ph\left(h-h_y\right)^2}{6}\right]$$

Lateral displacement of the isolated column at bottom end ($x_2 = h$) and at critical Tier 1 ($x_2 = h - h_{cr}$) can be determined using the Eq. B6 for x_2:

(B7)
$$\nu\left(x_2=h\right)=\frac{Phh_y^2}{3EI}$$

(B8)
$$\nu\left(x_2=h-h_{cr}\right)=\frac{P}{6EI}\left[\left(h-h_y\right)\left(3h+h_y\right)\left(h-h_{cr}\right)-\left(h-h_{cr}\right)^2\left(2h+h_{cr}\right)-h\left(h-h_y\right)^2\right]$$

Substituting Eq. B7 into Eq. B8 gives:

(B9)
$$\nu\left(x_2=h-h_{cr}\right)=\frac{\nu\left(x_2=h\right)}{2hh_y^2}\left[\left(h-h_y\right)\left(3h+h_y\right)\left(h-h_{cr}\right)-\left(h-h_{cr}\right)^2\left(2h+h_{cr}\right)-h\left(h-h_y\right)^2\right]$$

Defining inelastic portion of the anticipated story drift $\Delta_{inel} = \nu\ (x_2 = h) / h$ and inelastic portion of the critical tier drift that develops after brace tension yielding has initiated in that tier $\Delta_{cr,inel} = [\ \nu\ (x_2 = h) - \nu\ (x_2 = h - h_{cr})] / h_{cr}$, Eq. B9 can be rewritten as follows:

$$\text{(B10)} \quad \Delta_{cr,inel} = \Delta_{inel}\left(\frac{h}{h_{cr}}\right)\left[1-\frac{\left(h-h_{cr}\right)^2\left(2h+h_{cr}\right)-\left(h-h_y\right)\left(3h+h_y\right)\left(h-h_{cr}\right)+h\left(h-h_y\right)^2}{2hh_y^2}\right]$$

Drift in the critical tier when brace tension yielding initiates in that tier, $\Delta_{y,cr}$, can be obtained from brace elongation in tension:

$$\text{(B11)} \quad \Delta_{y,cr} = \frac{R_y F_y}{E \sin\theta \cos\theta}$$

where R_yF_y and E are the expected brace yielding strength and Young's modulus of elasticity. θ is the angle between the braces and horizontal plane.

Adding $\Delta_{y,cr}$ to $\Delta_{cr,inel}$ in Eq. B10 and reordering the parameters results in the total drift in the critical tier:

$$\text{(B12)} \quad \Delta_{cr} = \Delta_{y,cr} + \Delta_{inel}\left(\frac{h}{h_{cr}}\right)\left[1-\frac{h_y\left(h-h_y\right)\left(h_y-h_{cr}\right)+1.5\,h_{cr}\left(h_y-h_{cr}\right)^2+\left(h_y-h_{cr}\right)^3}{hh_y^2}\right]$$